

Towards a Total Synthesis of Peloruside A
and
The Preparation of Selected Inositol Derivatives

by

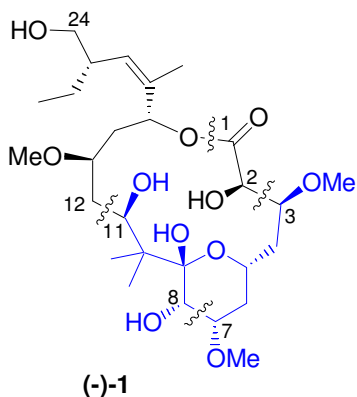
Sylvia Myrna Baars

A thesis
submitted to the Victoria University of Wellington
in fulfilment of the
requirements for the degree of
Doctor of Philosophy
in Chemistry

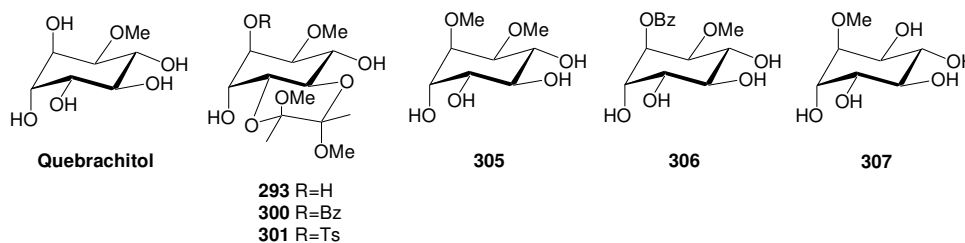
Victoria University of Wellington
2005

Abstract

This thesis covers two broad areas of work under the general theme of the synthesis of bioactive and/or synthetically useful compounds based on natural products or deriving from the chiral pool.



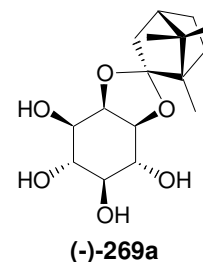
Chapters one, two and three focus on the marine secondary metabolite peloruside A (**1**), which has been shown to stabilise microtubules during mitosis and hence cause apoptosis (cell death) in a similar manner to the very successful anticancer drug Taxol®. A synthetic program with the aim of devising a total synthesis was initiated at Victoria University of Wellington after peloruside A's discovery in 1999. Four synthetic disconnects were identified in the retrosynthetic analysis of peloruside A: to give the C-1 to C-2 fragment; the C-3 to C-7 fragment; the C-8 to C-11 fragments; and the C-12 to C-24 fragment. The C-7 to C-8 bond was to be formed via an asymmetric aldol reaction to give the pyranose ring fragment (highlighted in blue). In this thesis, the synthesis of the C-3 to C-7 fragment is described. Aldol reactions with the C-8 to C-11 ketone have been investigated, and subsequent progress towards the assembly of the pyranose ring fragment is presented.



Chapters four, five, six and seven describe the preparation of selected synthetically and biologically useful derivatives of the commercially available inositols, quebrachitol (*L-chiro*-inositol-2-methyl ether) and *myo*-inositol. The butane di-acetal (BDA) derivatives **293**, **300**, and **301** (as well as acetylated and methylated derivatives thereof) were prepared during work directed towards the

synthesis of the inositol core of a phosphatidylinositol manno-oligosaccharide (PIM-6) isolated from *Mycobacterium bovis* and *M. smegmatis*. Quebrachitol derivatives **305**, **306** and **307** were prepared and subsequently tested against *myo*-inositol (the optimal competitor) in biological uptake assays of the microorganisms, *Candida albicans* and *Leishmania donovani*. For both microorganisms, the mono- and di-*O*-methylated *L-chiro*-inositol derivatives **307** and **305**, as well as quebrachitol, gave significant inhibition results, with P values from $P < 0.001$ to $P < 0.05$ for paired-sample t-test analyses, i.e. 99.9% to 95% confidence for significant inhibition, respectively. The benzoylated derivative **306** did not induce any inhibition of *myo*-inositol uptake.

Myo-inositol is the most abundant of the inositols in nature and is readily available. However, as it is a meso compound, one of the key challenges in the use of *myo*-inositol as a synthetic precursor is an efficient resolution method. The formation of *myo*-inositol camphanylidene acetal **269a** is one successful solution, and work done in an



attempt to better understand the selectivity of the reaction is reported here. Also, process development work was done to adapt the preparation so that it was suitable for scale-up, and a subsequent large scale synthesis of the acetal was undertaken. Previously unpublished X-ray crystal structures were obtained for **269a** and for two of the diastereomeric impurities of the reaction.

Acknowledgements

I would like to thank the following people for helping to make my PhD a memorable experience. There have been rewarding times and challenging times over the years since 2001 when I arrived in Wellington, and the following people (along with many others) have all contributed to making good memories of my time as a PhD student:

John Hoberg, my supervisor at VUW. Thankyou for always believing in my abilities, and for your guidance in chemistry, and general optimism in life. I hope we will meet again in the future, in some corner of the globe.

Andy Falshaw, supervisor of the work done at IRL, and dedicated thesis editor and ‘mentor’ in the final stages of the PhD. Thankyou so much!

The members and associates of the ‘Hoberg group’ over the years – Laine, Rhys, Darren, Ying, James, Maria, Wayne, Andreas, Emma, Paul, and especially Anna and Shivali, and Bridget, with whom I shared a two-woman lab for a good part of three years. I couldn’t have had a better lab partner and have now got a lifelong friend.

The staff at VUW, especially Oleg, Teresa, Sally, and Bill.

The people I worked with at IRL, especially Tony Davidson, Graeme Gainsford (X-ray crystallography), and Graham Caygill (calorimetry).

Andreas Seyfang (for biological testing of quebrachitol derivatives)

My long-time friends Katherine (Kat), Jo, and Kirsten (Kirkstone).

My Mum and Dad - of course! - for their love and support over the years and for generally being great, and to my sister Margo and brothers Erik and Dylan.

And finally, to my husband John (Davidson). Thankyou for being patient and for your understanding and support over the last few years. Thanks for being your wonderful self. Now let’s drink that bottle of champagne!!

Table of Contents

Abstract.....	ii
Acknowledgements.....	iv
Table of Contents.....	v
List of Figures.....	ix
List of Reaction Schemes.....	xi
List of Tables.....	xiv
List of Abbreviations.....	xv

Chapter One: Peloruside A: an Antimitotic Natural Product

1.1 Introduction.....	1
The history of cancer diagnosis and treatment.....	2
1.2 Cancer treatment.....	3
1.3 Antimitotic chemotherapeutic agents.....	5
Tubulin and the cell cycle.....	5
Natural products as antimitotic agents.....	8
1.4 Peloruside A.....	11
Biochemistry of peloruside A.....	12
1.5 Strategy for the synthesis of peloruside A.....	14
Synthesis of the C-3 to C-11 fragment.....	15
Synthesis of the C-12 to C-24 fragment.....	20
Introduction of the C-1 to C-2 fragment.....	22
Final assembly and macrolactonisation strategy.....	22
1.6 Peloruside A in the synthetic organic chemistry literature.....	24
1.7 The eight retrosynthetic strategies – summary and final comment.....	40

Chapter Two: Synthesis of the C-3 to C-7 Fragment of Peloruside A

2.1 Racemic synthesis of the C-3 to C-7 fragment.....	42
2.1.1 Strategy one.....	42
2.1.2 Strategy two.....	43
Adventures with ozonolysis.....	48
Deprotection trial.....	51

Summary.....	52
2.2 Enantioselective synthesis.....	53
2.2.1 Strategy one.....	53
2.2.2 Strategy two.....	53
2.2.3 Strategy three.....	54
2.3 Summary.....	59

Chapter Three: Towards the C-3 to C-11 Pyranose Ring Fragment

3.1 Preparation of the C-8 to C-11 ketone, 7 , on large scale.....	60
3.2 Model aldol reactions of the <i>gem</i> -dimethyl ketone fragment, 7	62
3.2.1 Lithium enolates - LDA and LiTMP.....	62
3.2.2 Mukaiyama aldol reactions.....	66
3.2.3 Boron-mediated aldol reactions.....	68
3.3 Aldol reactions between ketone 7 and the C-3 to C-7 fragment.....	70
3.4 Elaboration of the LDA aldol products.....	74
3.4.1 Initial cyclisation attempt and subsequent strategy modification.....	75
3.4.2 Methylations.....	77
3.5 Fragment 188 , a variant of <i>gem</i> -dimethyl ketone 7	78
3.5.1 Aldol reaction of 188 and subsequent hydroxyl protection	78
3.5.2 Selective cleavage of the MOM ether.....	79
3.5.3 Deprotection and Cyclisation of the tris-MOM-ether 190	80
3.6 Discussion, conclusions and future work.....	82

Chapter Four: The Inositols; Isomers, Biology and Functionalisation

4.1 The inositols.....	87
4.2 Biological significance of the inositols.....	89
4.2.1 Inositol phospholipids and cell signalling processes.....	90
4.2.2 Glycosylphosphatidylinositol.....	93
4.2.3 Lipoglycan cell surface structures related to GPIs.....	95
4.3 Synthetic plan for the 1L- <i>myo</i> -inositol core of the PIM-6 molecule.....	97
4.4 Quebrachitol as a synthetic precursor from the chiral pool.....	99
4.4.1 Quebrachitol.....	99
4.4.2 Quebrachitol as a synthetic precursor.....	100

Inositols and inositol derivatives.....	100
<i>Myo</i> -inositol phosphates and related structures.....	101
4.5 The formation of chiral <i>myo</i> -inositol derivatives.....	102
4.5.1 <i>Myo</i> -inositol.....	102
4.5.2 The preparation of chiral <i>myo</i> -inositol derivatives	102
Synthesis from natural <i>myo</i> -inositol derivatives.....	103
Synthesis from carbohydrates using the Ferrier rearrangement.....	104
Synthesis from bromobenzene (the Hudlicky route).....	104
Chiral chromatography.....	105
Enzymatic resolution.....	105
Formation and separation of diastereomers.....	106
4.6 Chapters Six and Seven of this thesis.....	113

Chapter Five: Functionalisation of Quebrachitol

5.1 Preparation of quebrachitol dicyclohexylidene acetal.....	114
5.2 Further protection of quebrachitol dicyclohexylidene acetal.....	116
5.3 Demethylation of 278 and 211	117
5.4 Mono-acetylation of the diol 282	122
5.5 Butane diacetal derivatives.....	125
5.6 Synthesis of quebrachitol derivatives for uptake inhibition assays.....	134
5.7 Biological testing of the derivatives.....	139

Chapter Six: Variations and Improvements on the *myo*-Inositol

Camphanylidene Acetal Procedure

6.1 <i>Myo</i> -inositol camphanylidene acetal and variations thereof.....	142
6.1.1 Introduction.....	142
6.1.2 Synthesis of a C-10 substituted camphor analogue.....	144
6.1.3 Fenchone.....	145
6.1.4 Norcamphor.....	147
6.2 Process development for <i>myo</i> -inositol camphanylidene acetal	149
6.2.1 Oxidation of (-)-borneol to give (-)-L-camphor.....	151
Calorimetric analysis of the oxidation.....	152
6.2.2 Preparation of L-camphor di-methyl acetal	156

6.2.3 <i>Myo</i> -inositol camphanylidene acetal formation.....	157
Reaction solvent.....	158
Equilibration step.....	159
6.2.4 Improved crystallisation procedure.....	160
6.2.5 Summary and conclusions.....	164

Chapter Seven: *Myo*-inositol Camphanylidene acetal Scaleup Campaign

7.1 Work and procedure in the scaleup laboratory.....	166
Equipment available in LT9.....	166
The <i>myo</i> -inositol camphanylidene acetal campaign.....	167
7.2 Stage 1 – Oxidation of (-)-Borneol.....	170
7.3 Stage 2 - Camphor di-methyl acetal.....	172
7.4 Stage 3 – 1-D- <i>Myo</i> -inositol-1,2-L-camphanylidene acetal.....	174
7.5 Crystallisation of <i>myo</i> -inositol camphanylidene acetals.....	178
Analysis of the products of the crystallisation sequence.....	184
Back to the crystallisation story.....	188
Mass balance analysis.....	190
Hydrolysis of the camphanylidene acetals.....	192
Interconversion of diastereomers.....	193
7.6 Conclusions.....	194

Chapter Eight: Experimental

8.1 General.....	197
8.2 Experimental for chapter two.....	197
8.3 Experimental for chapter three.....	209
8.4 Experimental for chapter five.....	220
8.5 Experimental for chapter six.....	231
8.6 Experimental for chapter seven.....	234
References.....	238

List of Figures

Figure 1.1. The marine natural product, peloruside A.....	1
Figure 1.2. Schematic diagram of the cell cycle.....	6
Figure 1.3. Microtubule formation from α and β tubulin.....	7
Figure 1.4. Selected compounds that promote tubulin depolymerisation.....	8
Figure 1.5. Selected compounds that promote tubulin polymerisation.....	9
Figure 1.6. Structures of mycalamides A and B, and of pateamine.....	11
Figure 1.7. The sodium borohydride reduction product of peloruside A.....	13
Figure 1.8. Summary of the retrosynthetic strategies adopted by various groups.....	40
Figure 2.1. ^1H NMR spectrum of aldehyde 13 , with (insets) portion of the ^1H NMR spectra of 160 and 161	58
Figure 3.1. Peloruside A, with the retrosynthesis of the C-3 to C-11 fragment..	60
Figure 3.2. The four possible isomeric products, and chair conformations resulting from hydrogen-bonding.....	64
Figure 3.3. ^1H NMR spectrum of 170b with (inset) the spectrum of 170a	65
Figure 3.4. Model for selectivity of the TiCl_4 catalysed aldol reaction of 169 ...	67
Figure 3.5. Enolate 7a with π -stacking of two aromatic groups.....	83
Figure 3.6. Pagenkopf's C-12 to C-8 fragment, 131 , fragment 7 , enolate 7a	84
Figure 4.1. The nine isomeric inositols.....	88
Figure 4.2. Some naturally occurring inositol derivatives.....	89
Figure 4.3. Signal transduction mechanisms.....	90
Figure 4.4. Structure of the GPI anchor of <i>Trypanosoma brucei</i>	93
Figure 4.5. General structure of a GPI.....	94
Figure 4.6. PIM-6 isolated from <i>Mycobacterium bovis</i> and <i>M. smegmatis</i>	96
Figure 4.7. Inositols and inositol derivatives prepared from L-quebrachitol.....	101
Figure 4.8. Examples of <i>myo</i> -inositol phosphates and analogues	101
Figure 4.9. <i>Myo</i> -inositol... ..	102
Figure 4.10. Sources of chiral <i>myo</i> -inositol derivatives.....	103
Figure 5.1. ^1H NMR spectrum of 293	129
Figure 5.2. ^1H NMR spectrum of 304	132
Figure 5.3. ^{13}C NMR spectrum of 304	133

Figure 5.4. ^{13}C NMR spectrum of 306	137
Figure 5.5. Graphical presentation of the results of the uptake assays in <i>C. albicans</i> and <i>L. donovani</i>	141
Figure 6.1. The four possible diastereomers of 269 , and the major steric interactions found in (-)- 269a	143
Figure 6.2. Analogues of camphor for preparation of <i>myo</i> -inositol camphanylidene acetal analogues.....	144
Figure 6.3. The four diastereomeric <i>myo</i> -inositol nor-camphanylidene acetals that are possible from one of the enantiomers of nor-camphor.....	149
Figure 6.4. Crystal structure of (-)- 269a	164
Figure 7.1. The author with the L-camphor filter cake.....	170
Figure 7.2. The table-top Buchner filter and 20 L transfer skids.....	171
Figure 7.3. The L-camphor in the 50 L flask of the Buchi rotary evaporator. ...	172
Figure 7.4. The 50 L reactor containing the <i>myo</i> -inositol camphanylidene acetal in CHCl_3 , MeOH and H_2O at the end of the equilibration step.....	176
Figure 7.5. The four diastereomers of camphanylidene acetal 269	177
Figure 7.6. ^{13}C NMR spectrum of the desired camphor acetal, (-)- 269a	179
Figure 7.7. ^{13}C NMR of crude product, containing (-)- 269a , 269b-d and <i>myo</i> -inositol.....	180
Figure 7.8. Crystallisation flow chart.....	181
Figure 7.9. Comparison of the percentage composition of the crude product, the first crystallisation product, and the first mother liquors.....	183
Figure 7.10. ^1H NMR spectra of (-)- 269a , and of the co-crystals of 269b and 269c , in d_6 -DMSO.....	185
Figure 7.11. ^1H NMR spectra of <i>myo</i> -inositol, and of a sample that contains all four diastereomers including 269d , and <i>myo</i> -inositol, in d_6 -DMSO.....	186
Figure 7.12. X-ray crystal structure of 269b	187
Figure 7.13. X-ray crystal structure of 269c	188
Figure 7.14. Composition of the slurry of the fourth mother liquors.....	189
Figure 7.15. Percentage composition of each of the parts of the mass balance...	191
Figure 7.16. Composition of the slurry of the first mother liquors.....	192

List of Reaction Schemes

Scheme 1.1. Retrosynthetic analysis of peloruside A.....	14
Scheme 1.2. Synthesis of aldehyde 13 via asymmetric allyl boration.....	15
Scheme 1.3. Grignard reaction synthesis of 13	16
Scheme 1.4. Nitrogen containing ring fragment.....	16
Scheme 1.5. Initially proposed route from malonaldehyde bis(dimethyl acetal)	17
Scheme 1.6. Synthesis of 13 via Blaise reaction.....	17
Scheme 1.7. Synthesis of the C-8 to C-11 ketone 7	17
Scheme 1.8. Postulated formation of <i>E</i> and <i>Z</i> enolates of ketone 7	18
Scheme 1.9. Formation of <i>anti</i> aldol products with ketones similar to 7	19
Scheme 1.10. Chelation control of the aldehyde attack to form 28	19
Scheme 1.11. Alternative route to pyranose ring with correct stereochemistry..	20
Scheme 1.12. Synthesis of C-12 to C-24 fragment, and coupling to a model for the C-3 to C-11 fragment.....	21
Scheme 1.13. Introduction of the C-1 to C-2 fragment.....	22
Scheme 1.14. Final assembly and macrolactonisation strategy.....	23
Scheme 1.15. Paterson, Di Francesco and Kühn's retrosynthesis.....	24
Scheme 1.16. Synthesis of fragment 47 and model aldol reaction.....	25
Scheme 1.17. Synthesis of 48 and model aldol reaction with acetone.	26
Scheme 1.18. Synthesis of the C-12 to C-24 fragment according to Paterson...	27
Scheme 1.19. Model aldol reaction and Evans-Tishchenko reduction.....	27
Scheme 1.0. De Brabander's retrosynthetic analysis of peloruside A.....	28
Scheme 1.21. Synthesis of fragment 68a	29
Scheme 1.22. Synthesis of the key intermediate 77	29
Scheme 1.23. De Brabander's assembly of the complete carbon skeleton.....	30
Scheme 1.24. Final transformations.....	30
Scheme 1.25. Ghosh and Kim's retrosynthesis.....	31
Scheme 1.26. Ghosh and Kim's synthesis of the C-1 to C-9 fragment	32
Scheme 1.27. Ghosh and Kim's synthesis of the C-10 to C-24 fragment.....	33
Scheme 1.28. Taylor and Jin's partial synthesis of the C-8 to C-19 fragment...	34
Scheme 1.29. Gurjar et al.'s retrosynthetic analysis of peloruside A.....	35
Scheme 1.30. Liu and Zhou' retrosynthesis.....	36

Scheme 1.31. Synthesis of fragment 113	36
Scheme 1.32. Synthesis of fragment 114 and LDA coupling to 113	37
Scheme 1.33. Pagenkopf et al.'s retrosynthesis of peloruside A.....	38
Scheme 1.34. Synthesis of the C-1 to C-7 fragment, 128	39
Scheme 1.35. Synthesis of an analogue of the C-8 to C-12 fragment.....	39
Scheme 1.36. Aldol reaction to form C-7 to C-8 bond and further elaboration..	40
Scheme 2.1. Route to the C-3 to C-7 fragment from 21	42
Scheme 2.2. Planned Grignard reaction synthesis of C-3 to C-11 fragment.....	43
Scheme 2.3. Hydrolysis and isomerization of the Grignard product.....	44
Scheme 2.4. Alternative protection reactions of 3-hydroxypropionitrile.....	46
Scheme 2.5. Racemic synthesis, final version.....	47
Scheme 2.6. Ozonolysis of 149 , showing the formation of by-product 152	50
Scheme 2.7. Proposed route to key fragment 13 employing a Blaise reaction...	54
Scheme 2.8. Enantioselective synthesis of the C-3 to C-7 fragment.....	55
Scheme 2.9. Preparation of (+)- <i>B</i> -allyldiisopinocampheylborane ((+)- 11)	56
Scheme 3.1. Synthesis of <i>gem</i> -dimethyl ketone fragment 7	61
Scheme 3.2. Aldol reaction of 7 with benzaldehyde to give 170	63
Scheme 3.3. Preparation and NOE analysis of trimethylsilyl enol ether 169	66
Scheme 3.4. Formation of <i>anti</i> - aldol product (racemic) 171b with Cy_2BCl	69
Scheme 3.5. Initial aldol reactions between ketone 7 and racemic 140	70
Scheme 3.6. Aldol reaction with fragment (<i>S</i>)- 13	71
Scheme 3.7. Elimination of aldehyde 13 to give by-product 176	72
Scheme 3.8. Aldol reaction with (<i>S</i>)- 160	72
Scheme 3.9. Formation of eliminated aldol product 179 with $\text{Ti}(\text{OiPr})_4$	73
Scheme 3.10. Modified strategy for pyranose ring formation.....	74
Scheme 3.11. Product of deprotection of 28	75
Scheme 3.12. Pd/C deprotection of TES and Bn groups of aldol product 28	76
Scheme 3.13. Modified new strategy.....	76
Scheme 3.14. Attempted methylation of 178	77
Scheme 3.15. Origin of byproduct 187	77
Scheme 3.16. Aldol reaction of 188 and subsequent acetylation.....	79
Scheme 3.17. Deprotection of MOM ethers of 190 , and further elaboration.....	81
Scheme 3.18. Byproduct 194 , and proposed mechanism of formation.....	82

Scheme 3.19. Aldol reactions between 7 , 169 and aldehyde (S)- 198	83
Scheme 4.1. Planned synthesis of suitably protected inositol core for PIM-6....	98
Scheme 4.2. Synthesis of 228 and 229 from naturally occurring phytic acid.....	103
Scheme 4.3. Synthesis of 1-D-6-deoxy- <i>myo</i> -inositol via Ferrier rearrangement.	104
Scheme 4.4. Synthesis of a <i>myo</i> -inositol derivative from bromobenzene.....	105
Scheme 4.5. Example of enzyme-mediated esterification.....	106
Scheme 4.6. Example of enzymatic hydrolysis.....	106
Scheme 4.7. Resolution by formation and separation of diastereomers.....	107
Scheme 4.8. Use of a menthyl carbonate derivative.....	107
Scheme 4.9. Camphanate ester example.	108
Scheme 4.10. Derivatisation of <i>myo</i> -inositol orthoacetate as camphanate ester...	108
Scheme 4.11. From the first total synthesis of the <i>T. brucei</i> VSG GPI.....	109
Scheme 4.12. Resolution using bis-dihydropyran reagent.....	109
Scheme 4.13. Resolution using an improved bis(dihydropyran) reagent.....	110
Scheme 4.14. Formation of diastereomers with acetyl mandelic acid.....	110
Scheme 4.15. Use of menthoxyacetylchloride in diastereomer formation.....	111
Scheme 4.16. Use of acetyl mandelic acid chloride in diastereomer formation..	111
Scheme 4.17. Formation of <i>myo</i> -inositol camphanylidene acetals.....	112
Scheme 4.18. Synthesis of D-Ins(1,4,5) <i>P</i> ₃ from (+)- 269a	113
Scheme 5.1. Preparation of 274 under Dean-Stark conditions.....	114
Scheme 5.2. Synthesis of 1L-1,2:3,4-di- <i>O</i> -cyclohexylidene-5- <i>O</i> -methyl- <i>chiro</i> - inositol 274 and 1L-1,2- <i>O</i> -cyclohexylidene-5- <i>O</i> -methyl- <i>chiro</i> -inositol 276	115
Scheme 5.3. Preparation of derivatives 277 , 278 and 211 from 274	116
Scheme 5.4. Cleavage of <i>trans</i> -cyclohexylidene moiety and demethylation.....	117
Scheme 5.5. Formation of the diol 282 by demethylation of 274	119
Scheme 5.6. Likely mechanism of migration of cyclohexylidene groups.....	121
Scheme 5.7. Monoacetylation of inositol derivative 282	122
Scheme 5.8. Proposed transition states for the monoacetylation reaction.....	123
Scheme 5.9. Monoacetylation reaction applied to non-symmetrical diol 282	123
Scheme 5.10. Formation of the axial acetyl product 289 via transition state I ...	124
Scheme 5.11. Attempted protection of the diequatorial diol of 276 with BDA.	126
Scheme 5.12. Attempts to protect O-3 and O-4 of 292 as a cyclic acetal.	127
Scheme 5.13. Per-methylation and deprotection of the BDA product.....	128

Scheme 5.14. Acetylation of the BDA derivative 293	128
Scheme 5.15. Preparation of a trimethoxy derivative.....	130
Scheme 5.16. BDA derivative from demethylated compound.....	131
Scheme 5.17. The derivatives prepared for the enzyme inhibition study.....	134
Scheme 5.18. Synthesis of 1L-1,2-di- <i>O</i> -methyl- <i>chiro</i> -inositol.....	135
Scheme 5.19. Synthesis of 1L-1- <i>O</i> -benzoyl-2- <i>O</i> -methyl- <i>chiro</i> -inositol.....	135
Scheme 5.20. Preparation of 1L-1- <i>O</i> -methyl- <i>chiro</i> -inositol.....	138
Scheme 6.1. Formation of (-)- 269a	143
Scheme 6.2. Planned synthesis of a camphor analogue.....	145
Scheme 6.3. Attempts to prepare a fenchone acetal of <i>myo</i> -inositol.....	147
Scheme 6.5. Formation of <i>myo</i> -inositol norcamphanylidene acetal	147
Scheme 6.6. The synthesis of 1-D- <i>myo</i> -inositol-1,2-L-camphanylidene acetal, proposed for process development and scale up.....	150
Scheme 7.1. Planned scale up campaign, showing the expected yields.....	167
Scheme 7.2. Acid-catalysed interconversion between (-)- 269a and 269b	194

List of Tables

Table 2.1. Selective deprotection of the TES group of 140 , 148 and 73	52
Table 3.1. Results of aldol reactions of 7 and 169 with benzaldehyde.....	62
Table 3.2. Attempts at selective cleavage of the MOM ether group of 158	80
Table 5.1. Conditions and results of attempted demethylations.....	118
Table 5.2. Conditions and results of demethylations of 274	120
Table 5.3. Results of the uptake assays in <i>C. albicans</i> and <i>L. donovani</i>	140
Table 6.1. Formation of dimethyl acetal 321 from fenchone	145
Table 6.2. Estimated cost of in-house synthesis of ca. 5.6 kg of L-camphor.....	152
Table 6.3. Alternative crystallisation procedure – small scale trials.....	162
Table 6.4. Alternative crystallisation procedure – larger scale trials.....	163
Table 6.5. Volumes (mL/g) used in the <i>myo</i> -inositol camphanylidene acetal preparation before and after process development	165
Table 7.1. Materials required for the scaleup preparation of (-)- 269a	169
Table 7.2. Mass balance over all parts of the crystallisation sequence	190

List of Abbreviations

[α]	specific rotation (units, (deg.mL)/(g.dm))
Ac	acetyl
AD-mix- α	commercial reagent mixture for Asymmetric Dihydroxylation
ATR	adiabatic temperature rise
aq	aqueous
BDA	butane di-acetal (protecting group)
BINOL	binaphthol
Bn	benzyl (C ₆ H ₅ CH ₂)
BnCl	benzyl chloride
Bz	benzoyl
°C	degrees Celsius
calcd	calculated
cm ⁻¹	wavenumber(s)
COSY	correlation spectroscopy
c_p	specific heat capacity at constant P
Cy	cyclohexylidene
δ	chemical shift in ppm downfield from trimethylsilane
d	doublet (spectral)
de	diastereomeric excess
(DHQ)PHN	dihydroquinine 9- <i>O</i> -(9'-phenanthryl) ether
(DHQ) ₂ PYR	dihydroquinine 2,5-diphenyl-4,6-pyrimidinediyl diether
(DHQ) ₂ PHAL	dihydroquinine 1,4-phthalazinediyl diether
DIBAL-H	diisobutylaluminium hydride
DMAP	4-(<i>N,N</i> -dimethylamino)pyridine
DMF	<i>N,N</i> -dimethyl formamide
DMS	dimethyl sulphide
DMSO	dimethyl sulfoxide
dr	diastereometric ratio
E1 _{CB}	unimolecular elimination – conjugate base
ee	enantiomeric excess
ED ₅₀	dose that is effective in 50% of subjects
ESMS	electrospray mass spectrometry
Et	ethyl (CH ₃ CH ₂)
g	gram(s)

GC	gas chromatography
h	hour(s)
<i>H</i>	specific enthalpy
HMPA	hexamethylphosphoric triamide
HPLC	high performance liquid chromatography
Hz	hertz
IC ₅₀	concentration required for 50% inhibition (of biological effect)
Ipc	isopinocampheyl
<i>i</i> Pr	isopropyl
IR	infrared
<i>J</i>	coupling constant (in NMR spectroscopy)
L	litre(s)
LAH	lithium aluminium hydride
LD ₅₀	dose that is lethal in 50% of test subjects
LDA	lithium diisopropylamide
LHMDS	lithium hexamethyldisilazide
lit.	literature
LiTMP	lithium 2,2,6,6-tetramethylpiperidide
μ	micro
m	multiplet (spectal); mass
M	molar (moles per litre)
Me	methyl (CH ₃)
mol	mole(s); molecular (as in mol weight)
MOM	methoxy methyl
mp	melting point
Ms	methanesulfonyl (mesyl)
MTSR	maximum temperature of the synthesis reaction (as written)
<i>m/z</i>	mass to charge ratio
NMR	nuclear magnetic resonance
NOE	nuclear overhauser effect
PCC	pyridinium chlorochromate
PDC	pyridinium dichromate
Ph	phenyl (C ₆ H ₅)
PMB	<i>para</i> -methoxy benzyl
PMBCl	<i>para</i> -methoxy benzyl chloride
Pr	propyl
py	pyridine

q	quartet (spectral)
R_f	retention factor (in chromatography)
RT	room temperature
Σ	sum
s	singlet (spectral)
S_N1	unimolecular nucleophilic substitution
S_N2	bimolecular nucleophilic substitution
<i>t</i> Bu	<i>tert</i> -butyl
TBDMS	<i>tert</i> -butyl dimethyl silyl
TBDPS	<i>tert</i> -butyl diphenyl silyl
TES	triethyl silyl
TESCl	triethyl silyl chloride
Tf	trifluoromethanesulphonyl (triflyl)
THF	tetrahydrofuran
THP	tetrahydropyran
TLC	thin layer chromatography
TMS	trimethylsilyl
Ts	<i>para</i> -toluenesulfonyl (tosyl)
TS	transition state
UV	ultraviolet
W	Watt

Peloruside A: an Antimitotic Natural Product

This chapter introduces the marine natural product peloruside A,¹ **1** (figure 1.1), as a potential player in the fight against cancer. A brief introduction to the diseases collectively known as cancer and the treatments currently available will be given. Peloruside A is a potential chemotherapeutic agent which causes programmed cell death (apoptosis) through stabilisation of microtubules in the cell cytoskeleton. Hence, an overview of the cell cycle and the importance of microtubules will be given, to explain the biochemistry of peloruside A, and

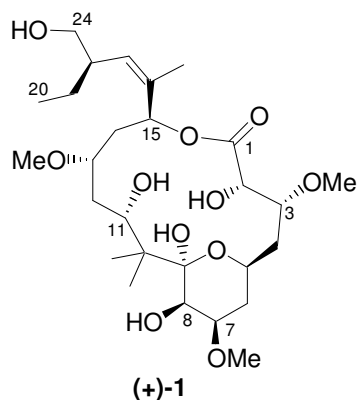


Figure 1.1. The marine natural product, peloruside A.

of other natural products that have also been found to interfere with microtubule dynamics. The retrosynthetic plan for peloruside A that is the basis of the work described in chapters two and three will then be described. Finally, a summary will be given of the relevant work published by other groups working towards a total synthesis of peloruside A since the initial reports of its biochemical potential, in 2000.

1.1 Introduction

In New Zealand, approximately one quarter of all human deaths are caused by cancer. There were a total of 16,790 new cancer registrations in 1999 alone, and 7,647 cancer-related deaths in that year.² Most of those deaths (95.1% in 2000) were of people aged 45 or over,³ but cancer affects people of all ages. Although it is estimated that about one of every three people who get cancer in New Zealand are cured, New Zealand's mortality rate due to cancer (298.3 per 100,000 population in 1999)² is still high by international standards. The most

common cancer in New Zealand males is prostate cancer, while cancer of the lung is their leading cause of cancer-related death. For New Zealand females, breast cancer has the highest incidence (28%) and is the biggest killer (18% of female cancer deaths in 1999).² Other common cancers for both sexes are large bowel cancer and melanoma.

The history of cancer diagnosis and treatment

Although cancer is sometimes thought of as a ‘modern day’ disease, its diagnosis and treatment has a long history.² Evidence of cancer has been found in Egyptian mummies from ca. 3000 BC, and papyruses dated at ca. 1600 BC describe cancer treatments. These included cutting out the tumour with a knife or red hot irons, the treatment of stomach cancer with boiled barley and dates, and the treatment of uterine cancer with the application of a concoction of fresh dates and pig’s brains. Mummies of pre-Columbian Incas of Peru have also been found that show evidence of cancer.

The Greek ‘father of medicine’ Hippocrates (ca. 300 BC), named a range of lumps, bumps and tumours as *carcinos* or *carcinoma*. It was believed that the carcinoma had spreading roots – like the legs of a crab, and they were believed to be caused by too much ‘black bile’ in the body. The Greeks and the Romans (ca. 50 AD) both found that tumours could sometimes be successfully removed by surgery and cauterisation, but also that surgery could aggravate the tumour’s spread. Through the next 1000 years, a wide variety of remedies were used – caustic pastes (often containing arsenic), blood-letting, dietary modifications, herbs, powder of crab, and other charms and potions – but little further progress was made in the understanding of cancer until ca. 1500 AD. Around that date, the practise of autopsy became more widespread, with a concomitant understanding of internal cancers. By the mid-1600’s, medical technology was rapidly improving. Microscopes were invented, and major advances made in the understanding of circulation, cells, and the lymphatic system. The 1700’s heralded the first identification of causes for some cancers, such as snuff being related to cancer in the nose, and soot to cancer in chimney sweeps. From 1840 – 1900 AD, hundreds more carcinogenic materials were identified. Improved

diagnosis methods and pathology techniques were matched by continual improvement in surgery, with crucial discoveries made in the anaesthetics and antibiotics areas. In 1895, X-rays were discovered, and radium was isolated in 1898. This led to the development in the early 1900's of radiotherapy as a viable cancer treatment. This is still one of the major weapons in the fight against cancer. Chemotherapy began to emerge as a treatment from about 1945 onwards, after observations during the Second World War that soldiers who were exposed to sulphur mustard suffered from lower white blood cell counts. This led to the use of nitrogen mustard (a similar but less toxic agent) to treat patients with high white blood cell counts (lymphoid leukaemia) and lymphomas.

1.2 Cancer treatment

It is now widely understood that cancer is, in fact, not one but many different diseases. What all have in common is that the normal growth of the body's cells has become disrupted, resulting in out-of control cell division, and often (but not necessarily), resultant growth of a cell mass or tumour. Once a tumour is established, it is possible for abnormal cells to break away and travel through the blood or lymph system to form secondary tumours (also called metastases) elsewhere in the body. The many different cancer types fall into three main categories:²

- Carcinomas, cancers that occur in the lining of the body's external and internal surfaces, e.g. the skin, mouth, bowel.
- Sarcomas, which form in the body's tissues, e.g. muscles and bones.
- Leukaemias and lymphomas – the cancers of the bone marrow and lymph glands (often do not produce tumours – 'regional' cancers).

The treatment of all these types of cancer involves medical procedures to destroy, modify, control or remove the cancer tissue. The primary goal is to remove all traces of abnormal cells and prevent recurrence of the cancer, but in some cases, treatment becomes the prevention of spreading, or finally palliative treatment – to relieve symptoms if all reasonable curative methods have been

exhausted. Peloruside A is a potential chemotherapeutic agent, which specifically acts on tubulin,^{4,5,6} and therefore this area will be elaborated in the next section. However, a brief overview of the cancer treatments that are in use today⁷ is given in the following paragraphs.

Surgery, radiation therapy and chemotherapy are the three main avenues of attack in cancer treatment. In fact, it is uncommon for a cancer to be treated by one method alone. *Combination therapy* can achieve a greater likelihood of cure, and also help minimise the damage to healthy organs and tissues. For example, surgery is often followed up with radiation therapy and/or chemotherapy to remove any remaining traces of cancer cells. Or, chemotherapy can be used to shrink a tumour, making it easier to surgically remove. Some chemotherapy drugs can make certain cancer cells more susceptible to radiation.

Surgery is the oldest form of cancer treatment, and the techniques and methods used today are extremely varied and advanced. Curative cancer surgery attempts to completely remove localised tumours, or reduce the size of a tumour to increase the effectiveness of follow-up radiation or chemotherapy. Surgery may also be done as a diagnostic procedure, to relieve pain or to repair deformities caused by curative surgery (e.g., breast reconstruction surgery following a mastectomy). In *radiation therapy* treatment, X-rays, gamma rays, and other sources of radiation are used to kill cancer cells by breaking up molecules and causing reactions that damage living cells – sometimes they are immediately destroyed, sometimes they are damaged (eg DNA damage) and the cell's ability to divide is affected. Modern technology can produce high-energy beams of radiation with great accuracy – thereby minimising the exposure of healthy tissue to the damaging rays. Two types of treatment are used – external beam radiation (teletherapy) and internal therapy (brachytherapy), where a radioactive source is placed inside the body close to the tumour. *Chemotherapy* is a systemic method of cancer treatment. This means that the drugs will reach most parts of the body, and therefore chemotherapy is very useful where cancer has already spread, or for tumours that cannot be reached surgically. The drugs may be administered orally, by injection into muscle or under the skin, into a

vein, or sometimes into the spinal fluid. For some cancers, such as Hodgkin's disease, leukaemia, and testicular cancer, chemotherapy alone can effect a cure.

There are also a number of newer techniques available, as well as a host of 'alternatives' to conventional therapies (eg, acupuncture, prayer, etc). Cancers in tissues that require hormones to develop, such as breast and prostate, may respond to ***hormonal therapy*** – the administration or withdrawal of hormones, or interference with hormone function. Rarely used on their own, hormone treatments are often used to prevent or delay recurrence of a cancer after treatment with other methods. ***Biological therapy*** is a relatively new approach for cancer treatment. Also known as immunotherapy, the aim is to stimulate the body's immune system to fight the abnormal cancerous cells.

1.3 Antimitotic chemotherapeutic agents

Tubulin and the cell cycle

In order to understand the mode of action of the antimitotic class of compounds that peloruside A belongs to, an understanding of the eukaryotic cell cycle, and the role that tubulin plays in the cell is required.

The cell cycle (shown in figure 1.2 overleaf) is the series of changes a cell goes through from the time it is first formed until its division into two daughter cells in the process called mitosis. Hence, mitosis (also known as the M-phase of the cell cycle) is both the beginning and end of the cycle. Mitosis is followed by the G-1 (Gap 1), S and G-2 (Gap 2) phases. These are collectively known as the interphase, and in healthy tissues, the duration of the three is relatively constant in different tissues. Chromosome replication happens during the S-phase of the interphase, in readiness for the process of mitosis, which will be discussed in more detail shortly.

Microtubules constitute one of the major components of the cytoskeleton – the transparent web of filamentous protein networks that dynamically

organise the interior of eukaryotic cells. They are involved in many essential cell processes, providing both structural and transport functions.^{8,9} They rigidify the cell, and they translocate vesicles, organelles, and chromosomes (through special attachment proteins).⁸ In conjunction with other proteins, they can form more complex structures such as cilia and flagella, which aid cell movement.

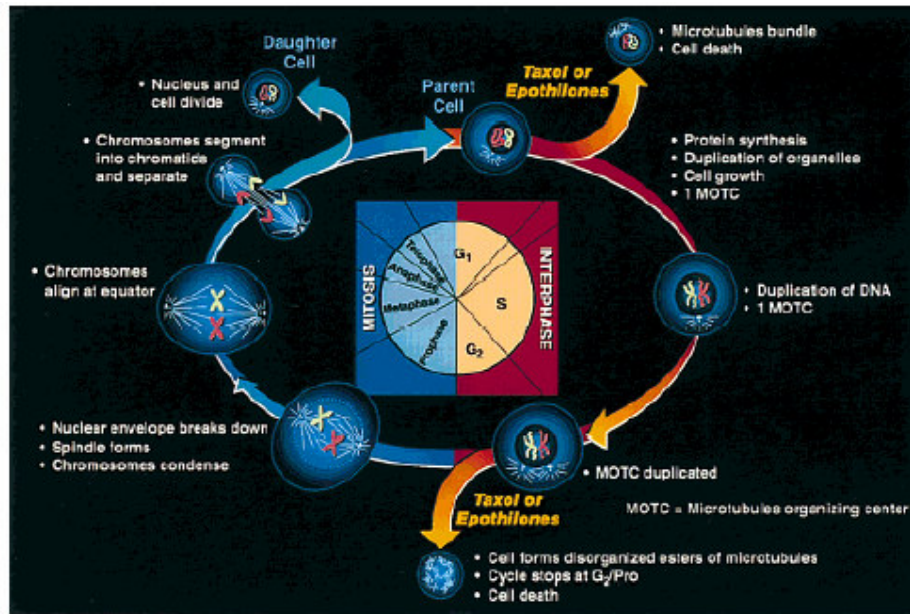


Figure 1.2. Schematic diagram of the cell cycle, including the inhibition of mitosis by Taxol® and the epothilones.⁸

Microtubules are also a major component of the mitotic spindle, and hence play a crucial role in mitosis. During mitosis, the cell undergoes dramatic structural change as it passes through the steps prophase, metaphase, anaphase, and telophase. As the prophase begins, the cytoskeletal microtubule network ‘melts’ at the centre, and two dipolar spindle-shaped networks originating from two centrosomes at opposite ends of the cell are formed. The chromosomes then align along the spindles (metaphase). During anaphase, the chromosomes move to two opposite ends of the cell, literally pulled toward the two poles by the shortening of microtubules. Each of the newly emerging daughter cells has received a complete set of genes, and the final cell division can then occur. During mitosis, the rate at which microtubules grow and disassemble increases by 20- to 100- fold relative to the rate during the interphase. These enhanced

microtubule dynamics make the cell susceptible to agents that can interact with tubulin and suppress microtubule dynamics. In particular, the metaphase to anaphase transition is very sensitive to such compounds, for example Taxol® and the epothilones (figure 1.2).

The structural subunit of the microtubule is the $\alpha\beta$ tubulin heterodimer, itself composed of two tubulin monomers (figure 1.3). The α and β tubulins share 40% amino acid sequence identity,¹⁰ and their compact structures are basically

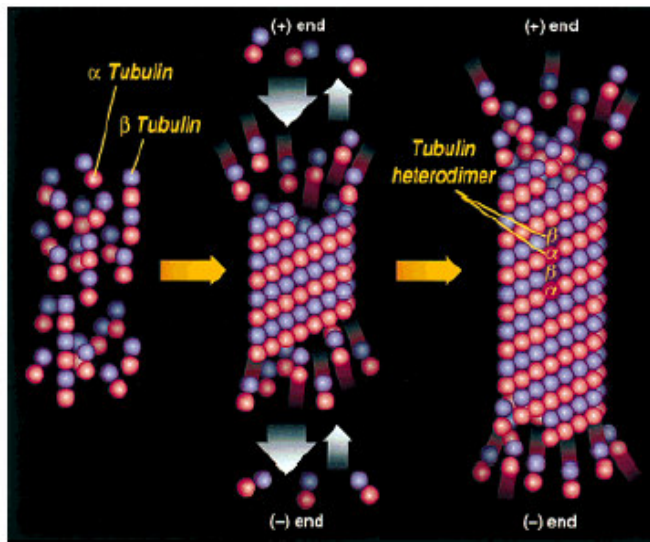


Figure 1.3. Microtubule formation from α and β tubulin.⁸

identical; comprising a core of two β -sheets surrounded by α -helices.¹⁰ In the presence of Mg^{2+} , guanosine triphosphate (GTP) and microtubule-associated proteins (MAPs), a nucleation process takes place in which the preformed heterodimers assemble to form microtubules.¹¹

Linear polymers called protofilaments form first, and when thirteen of these have aligned they self-assemble to form microtubules approximately 24 nm in diameter, and up to several μm in length.⁸ The microtubule may be elongated (or disassembled) from both ends, although the two ends are not identical. Labelled the (+) and (-) ends, the (+) end tends to grow faster. Although the half-life of tubulin is nearly 24 hours at 37 °C, the half-life of any given microtubule may be only about 10 minutes. This reflects the constant state of flux that microtubules exhibit to meet the needs of the cell. Regulatory processes within the cell control the growth rate of the microtubules, exerted by adding (for growth) or hydrolysing (for shrinkage) GTP on the ends of the microtubule.^{8,11}

Natural products as antimitotic agents

There are two broad categories of antimitotic compounds. The first of these contains compounds that, at appropriate concentrations, inhibit the formation of spindle microtubules, diverting tubulin into other types of aggregates.^{8,12(b)} They can also cause existing microtubules to depolymerise.^{8,12(b)} The well-established chemotherapeutic agents colchicine,¹³ podophyllotoxin,¹⁴ vinblastine,¹² and vincristine¹² (figure 1.4) belong to this group. It also includes compounds such as rhizoxin,¹⁵ the bacterial metabolite RPR112378,¹⁶ (figure 1.4) and a number of other natural products. These compounds have been found to interact with tubulin in a variety of ways. For example, colchicine first binds to free tubulin and the formed complexes are then incorporated into microtubules,^{12(b)} while vinblastine binds with high affinity to the ends of already formed microtubules.¹²

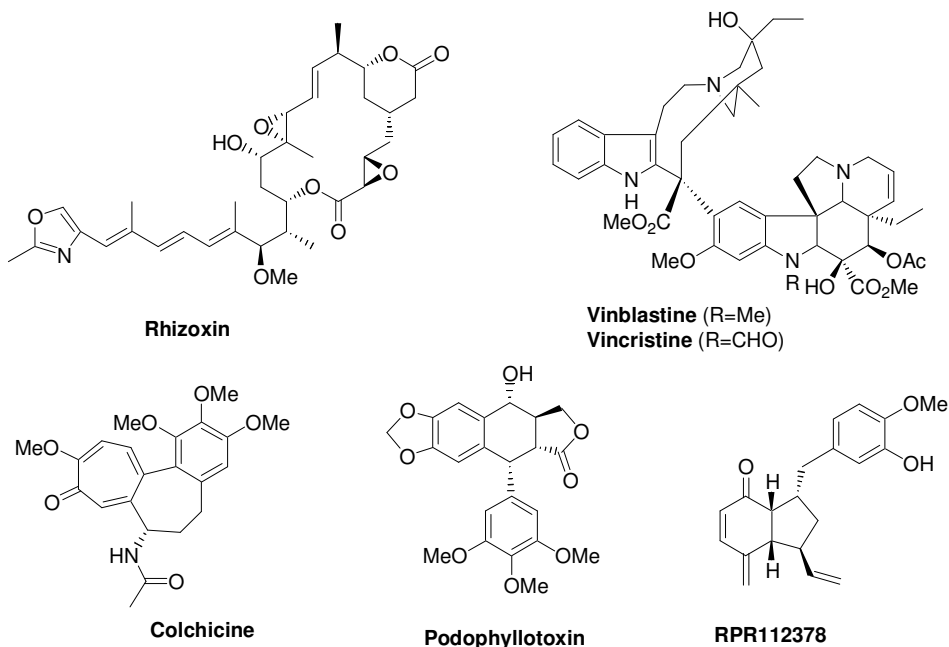


Figure 1.4. Selected compounds that promote tubulin depolymerisation.

The most successful clinically used tubulin binding agent however, has the opposite effect on microtubule dynamics. The diterpene Taxol® (paclitaxel, figure 1.5 overleaf) was isolated from extracts of the Pacific Yew tree in 1971,¹⁷ and developed as a drug by Bristol-Meyers Squibb in the 1990's. Taxol® is currently available in over 60 countries. The semi-synthetic derivative taxotere

(docetaxel), developed by Rhone-Poulenc Rorer,¹⁸ has more recently also been approved for clinical use. Both drugs are indicated primarily for the treatment of solid tumours such as those commonly found in cases of breast and ovarian cancer, and Taxol® still holds a major market share in that area.

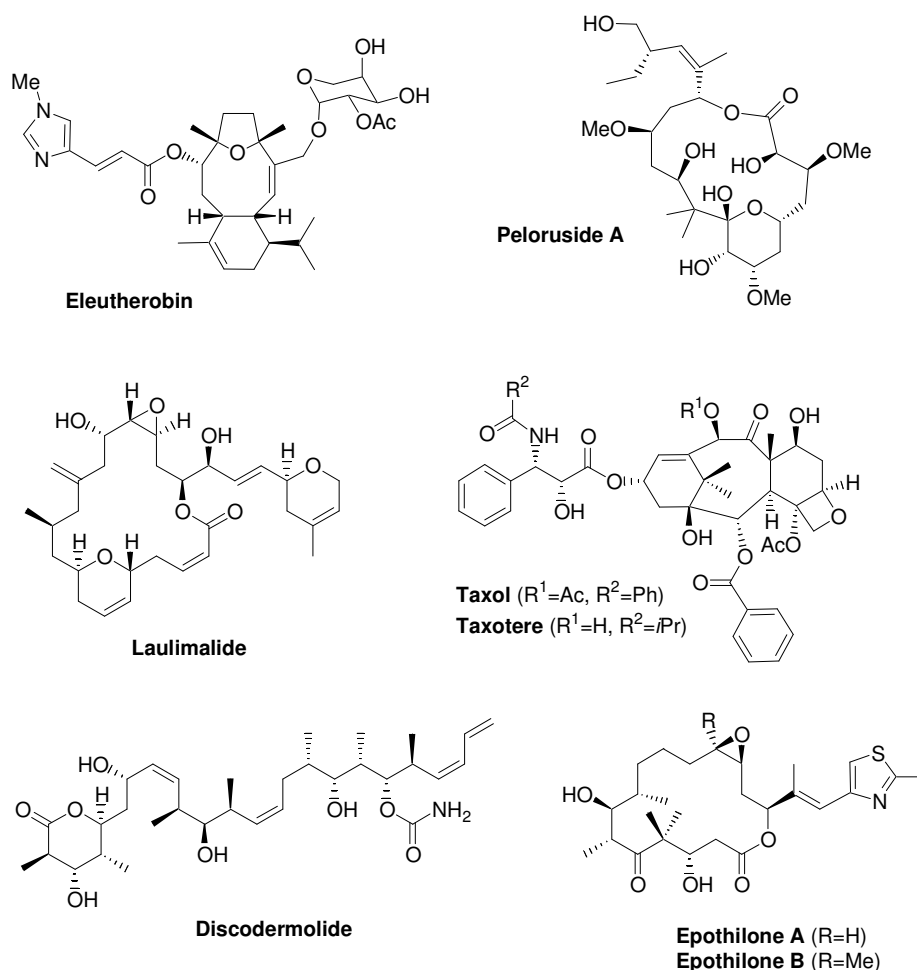


Figure 1.5. Selected compounds that promote tubulin polymerisation and microtubule stabilisation.

Unlike the tubulin-destabilising drugs that preceded it, Taxol® had the unique effect of *stabilising* microtubules. It was found to promote both the formation of abnormal mitotic spindles and mitotic arrest, and thereby initiate apoptosis.¹⁹ Induction of apoptosis is generally associated with G2/M arrest, with cells accumulating at that stage of the cell cycle and cell death occurring as a direct result of the abnormal spindle growth and suppression of microtubule dynamics.²⁰ It has also been shown that in some instances the cell may pass

through the M phase and arrest at the G1 stage;²¹ the mechanism by which this happens remains unclear.

Taxol® and its relatives were, for more than fifteen years, the only known compounds to exhibit this mode of action. They have been joined more recently however, by a number of new compounds. The epothilones A and B (figure 1.5) were discovered by a German group in the late 1980's.²² They were isolated from culture extracts of a strain of the cellulose-degrading myxobacterium *Sorangium cellulosum*, first found in soil collected from the banks of the Zambezi River in southern Africa. Scientists at Merck also, independently, isolated the compounds,²³ and subsequently included them in a high-throughput screening program to discover Taxol®-like tubulin polymerisation agents. Their only hit, among tens of thousands of compounds, were the epothilones A and B. Significantly, they were shown to compete with Taxol® for the same binding site,^{23,24} and gave rise to microscopic pictures of stabilised microtubules and damaged cells essentially identical to those obtained with Taxol®.²³ Furthermore, epothilones A and B were shown to be more potent killers of tumour cells in a number of cell lines, particularly in some multiple-drug resistant ones.^{23,24} Epothilone B was identified as being too toxic for use as an anticancer drug, but aza-epothilone B (the lactam analogue) is currently in phase II clinical trials.²⁵

A computer-assisted structure analysis indicated that (+)-discodermolide (figure 1.5), isolated from the sponge *Discodermia dissoluta*,²⁶ should act as an antimitotic compound.²⁷ This prediction was confirmed, with discodermolide-treated cells accumulating at the G2/M phase. Marked rearrangement of the microtubule cytoskeleton, including extensive microtubule bundling, was observed in discodermolide-treated breast cancer cells, and discodermolide was shown to be ten-fold more active at inducing microtubule rearrangement or assembly than Taxol®.²⁷ More recently, eleutherobin,²⁸ sarcodictyin A,²⁹ and laulimalide³⁰ (figure 1.5) have been added to the list of cytotoxic tubulin-stabilising natural compounds.

1.4 Peloruside A

Peloruside A was isolated by West and Northcote¹ in 1999, from samples of the marine sponge *Mycale hentschelli* collected in Pelorus Sound on the north coast of the South Island of New Zealand. Sponges of the *Mycale* genus are a rich source of bioactive secondary metabolites, and *M. hentschelli* had already yielded the antiviral and antitumour agents mycalamide A and B and the immunosuppressant pateamine (figure 1.6). The mycalamides were originally isolated from samples collected in Otago Harbour on the southeast coast of the South Island,^{31,32} while pateamine was first identified in samples from Thompson Sound on the southwest coast of the same.³³ Interestingly, no mycalamides were detected in the Thompson Sound samples, but the sponges growing in Pelorus Sound contained mycalamide A, pateamine and peloruside A.

The isolation of peloruside A involved methanolic extraction of a 170 g (wet weight) sample of the sponge and subsequent fractionation on polymeric reverse-phase chromatographic material. NMR-guided separation was used to isolate 3.0 mg of peloruside A, 10.6 mg of mycalamide A and 11.7 mg of pateamine (figure 1.6). In the first report, the relative structure of peloruside A was elucidated through a variety of high-field NMR experiments.¹ The structure shown in figure 1.1 ((+)-**1**) is the natural enantiomer, although the opposite enantiomer was shown in the first publication. It was not until de Brabander's group published the total synthesis of (-)-**1**,³⁴ and it was shown to have a negative optical rotation (the opposite sign to that reported for the dextrorotatory natural isolate) that the absolute stereochemistry of peloruside A was known.

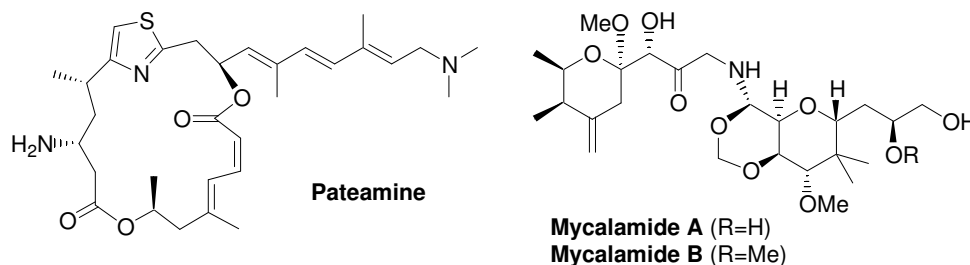


Figure 1.6. Structures of mycalamides A and B, and of pateamine.

Biochemistry of Peloruside A

Peloruside A has shown effects remarkably similar to those of paclitaxel in cell lines and with purified tubulin.⁴ After two-day exposures to either peloruside A or paclitaxel at 100 nM concentration, human lung adenocarcinoma H441 cells showed multiple micronuclei, which increased upon longer exposures. Microtubule fibre bundles and multiple asters (the centres of the spindles formed during metaphase), and large 'rod-like' fibres were observed to form. These observations are consistent with those seen for other microtubule-stabilising agents, including discodermolide and the epothilones.

Treatment of the H441 cell line with 1 μ M peloruside A or paclitaxel induced partial cell cycle arrest at the G2/M phase; peloruside A having a somewhat less marked effect than paclitaxel. However, Western blot analysis of another cellular assay, following the shift from depolymerised to polymerised tubulin, indicated that peloruside A could be slightly more efficient than paclitaxel at inducing microtubule polymerisation. At 100 nM concentration of peloruside A, the conversion was essentially complete approximately 30 minutes after addition, and for paclitaxel at the same concentration, at approximately 35 minutes after addition.⁴

With purified tubulin (free of GTP or microtubule-associated proteins), peloruside A induced polymerisation at 10 μ M concentration. Long, straight microtubules analogous to those formed with paclitaxel were seen to form at 37 °C. Only sparse microtubules were observed in the absence of the drug.⁴

The cytotoxicity of peloruside A has been tested in a number of cell lines, including the H441 cell line (as discussed above), the myeloid leukaemic cell line HL-60, the nontransformed murine myeloid cell line 32D, and 32D cells transformed with *ras* and *bcr/abl* oncogenes. The toxicities were comparable to those of other microtubule stabilising agents, with IC₅₀ values ranging from 4 nM to 15 nM. Interestingly, the sodium borohydride reduction product of peloruside A, **2** (figure 1.7, overleaf) is 30-fold less cytotoxic than peloruside A.⁵

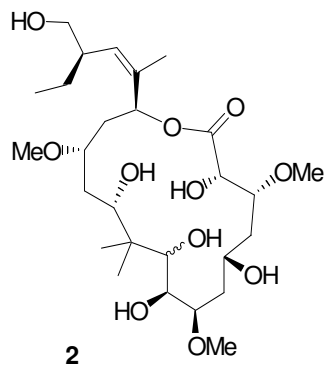


Figure 1.7. The NaBH_4 reduction product of (+)-1.

Compound **2** did not cause significant microtubule polymerisation in cell assays where peloruside A itself did.

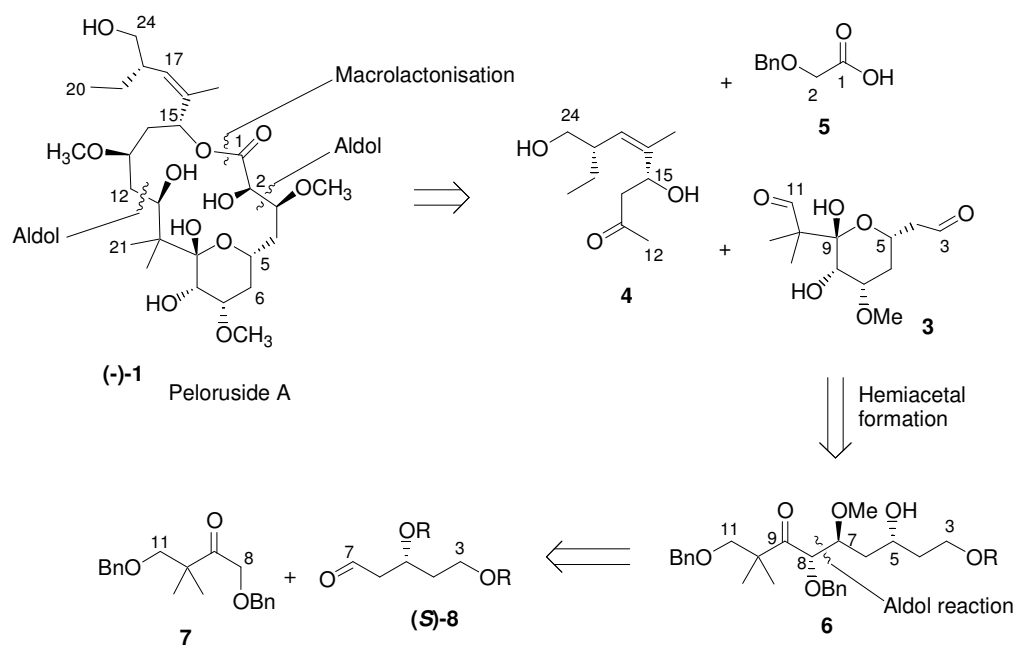
The unique structure and properties of peloruside A may convey benefits over the widely used chemotherapeutic agent paclitaxel. Paclitaxel is lipophilic (has low aqueous solubility), and therefore is administered to the patient dissolved in polyoxyethylated castor oil (Cremophor EL).

This substance contributes to paclitaxel's undesirable side effects, including hypersensitivity reactions. Moreover, paclitaxel's hydrophobicity contributes to the development of multiple-drug resistance (MDR), a phenotype that cells can develop which results in the efflux of a broad range of organic compounds (including paclitaxel) from the cell. This phenotype has generally been associated with over-expression of the P-glycoprotein efflux pump (P-gp),³⁵ but also occurs as a result of mutation of the paclitaxel binding site on β -tubulin.³⁶ Whichever mechanism is the cause, the effect is that cancers become resistant to paclitaxel. It is therefore important to identify drugs that have similar pharmacological properties to paclitaxel, but which are active in the MDR cell lines, and also which do not induce the MDR phenotype to develop in the first place. Peloruside A is considerably less lipophilic than paclitaxel, which suggests it should be both easier to administer, and active in MDR cell lines.⁴ Indeed, it has been shown that peloruside A is less susceptible than paclitaxel to MDR arising from overexpression of the P-gp pump.⁶ Peloruside A's action was furthermore not affected at all in cell lines with mutations that affect the taxoid binding site on β -tubulin.⁶ These observations were similar to those obtained for laulimalide, which had been shown to bind to a different site to paclitaxel.³⁰ It was also found that laulimalide can displace peloruside A bound to microtubules, and hence it was concluded that they may compete for the same or overlapping binding sites.⁶ The binding properties of peloruside A (and laulimalide) are therefore distinctly different from other microtubule stabilising agents such as paclitaxel, the epothilones and discodermolide. Importantly, this suggests that

they may become very useful chemotherapeutic agents against tumour cells that have developed the MDR phenotype.

1.5 Strategy for the Synthesis of Peloruside A

The retrosynthetic analysis of peloruside A that formed the basis of the work described in this thesis is presented in scheme 1.1. Three disconnections were envisioned to give three main building blocks: the pyranose ring fragment **3**, the side chain and remainder of the macrocycle fragment **4**, and the two-carbon fragment **5** as commercially available benzyloxy acetic acid.



Scheme 1.1. Retrosynthetic analysis of peloruside A.

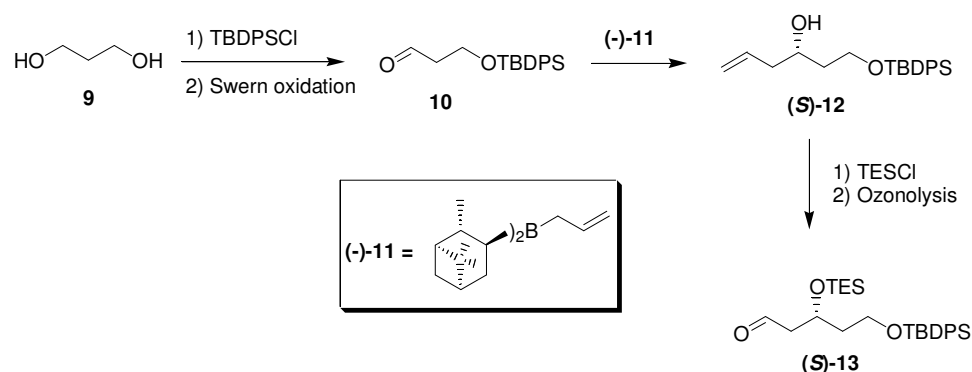
The key C-3 to C-11ⁱ pyranose ring fragment was further disconnected to give **7** and **8**; a diastereoselective aldol reaction between a suitably protected aldehyde **8** and an enolate formed from the *gem*-dimethyl ketone fragment **7** was

ⁱ Throughout chapters one, two and three, the numbering of fragments relates to the numbering of peloruside A itself (rather than the IUPAC numbering of individual fragments).

planned. The preparation of **8**ⁱⁱ and the assembly of the C-3 to C-11 fragment fall within the scope of this thesis. For completeness, however, progress that has been made towards the synthesis of all of the fragments will be outlined here in this introductory chapter, along with strategies for assembly of the building blocks and final elaboration to give peloruside A.

Synthesis of the C-3 to C-11 fragment

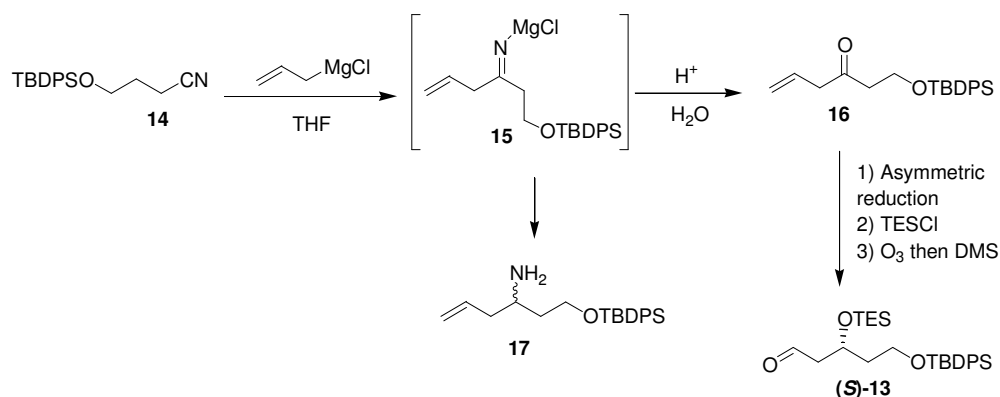
The C-3 to C-11 fragment was to be synthesised by an aldol reaction between **7** (C-8 to C-11) and a version of synthon **8** (C-3 to C-7), such as **13**, containing TES and TBDPS protecting groups. The latter is available via the synthesis shown in scheme 1.2. The starting aldehyde **10** is prepared from commercially available 1,3-propane diol (**9**) via monosilylation and Swern oxidation. Either enantiomer of alcohol **12** is then available from the well-established asymmetric allyl boration procedure developed by Brown and co-workers.³⁷ Use of (+)-*B*-allyldiisopinocampheylborane (prepared from (-)- α -pinene)^{38,39} yields the alcohol with the *R*- configuration, and use of the reagent prepared from (+)- α -pinene yields the alcohol with the *S*- configuration.⁴⁰ The resulting alcohol is then protected with a protecting group such as TES, and then cleavage of the double bond via ozonolysis followed by a reductive workup, yields the aldehyde.⁴⁰



Scheme 1.2. Synthesis of aldehyde **13** via asymmetric allyl boration procedure.

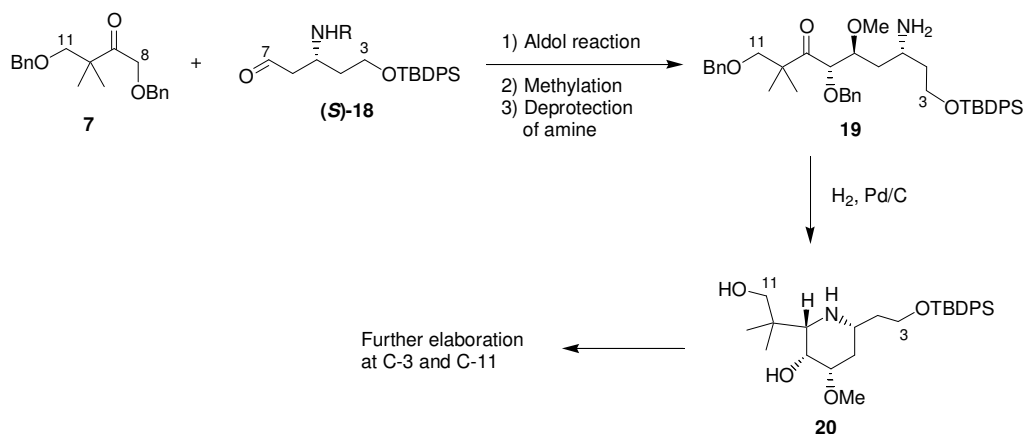
ⁱⁱ Both (*R*)-**8** and (*S*)-**8** were prepared during the course of this PhD. When the stereochemistry of peloruside A was established by De Brabander *et al.*,³⁴ it was shown to be opposite to that shown in scheme 1.1. Hence the synthetic strategy changed accordingly.

An alternative and more versatile preparation of analogues of **8** was also proposed, starting with a suitably protected derivative of 3-hydroxypropionitrile such as **14** (scheme 1.3). A Grignard reaction with allylmagnesium chloride would yield the intermediate imine **15**. This could then be hydrolysed to give the ketone **16**, followed by asymmetric reduction,^{41,42,43} protection, and ozonolysis to yield the desired aldehyde.



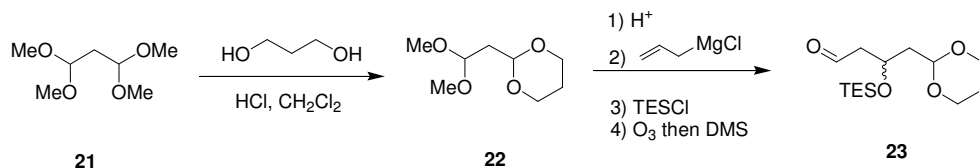
Scheme 1.3. Grignard reaction synthesis of **13**.

Alternatively, the intermediate **15** could be converted to the amine **17**,³⁷ or **17** could be prepared by addition of chirally modified allylboron reagent directly to **14**,⁴⁴ allowing entry into a nitrogen-containing analogue of peloruside A. The amine would need to be protected while the rest of the ring system was installed (scheme 1.4). It was envisioned that, upon deprotection to give **19**, the amine would cyclise onto the ketone at C-9 to form an imine, which would be reduced to give **20**, a nitrogen-containing analogue of fragment **3**.



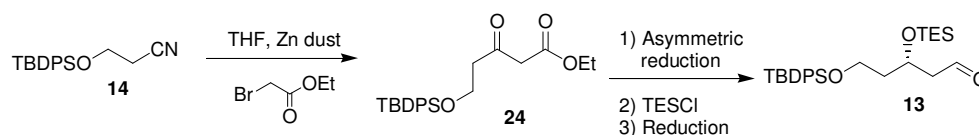
Scheme 1.4. Nitrogen containing ring fragment.

There are a number of other potential synthetic routes to suitable analogues of fragment **8**. Malonaldehyde bis(dimethyl acetal) (**21**) was proposed early on as a potentially useful starting material (scheme 1.5). The mixed acetal **22** could be prepared and one aldehyde group then selectively deprotected,⁴⁵ ready for either a Grignard reaction⁴⁶ or the boron-mediated allylation described above.



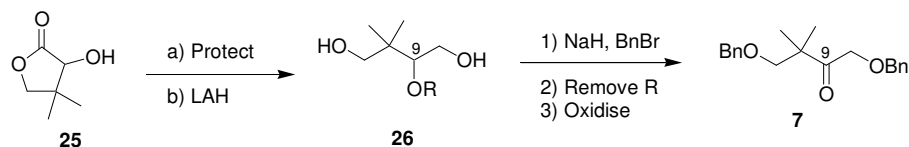
Scheme 1.5. Initially proposed route from malonaldehyde bis(dimethyl acetal).

The nitrile **14** could also be used in a Blaise reaction⁴⁷ with ethyl bromoacetate and zinc dust, followed by asymmetric reduction, protection and reduction of the ester to give the desired aldehyde **13** (scheme 1.6).



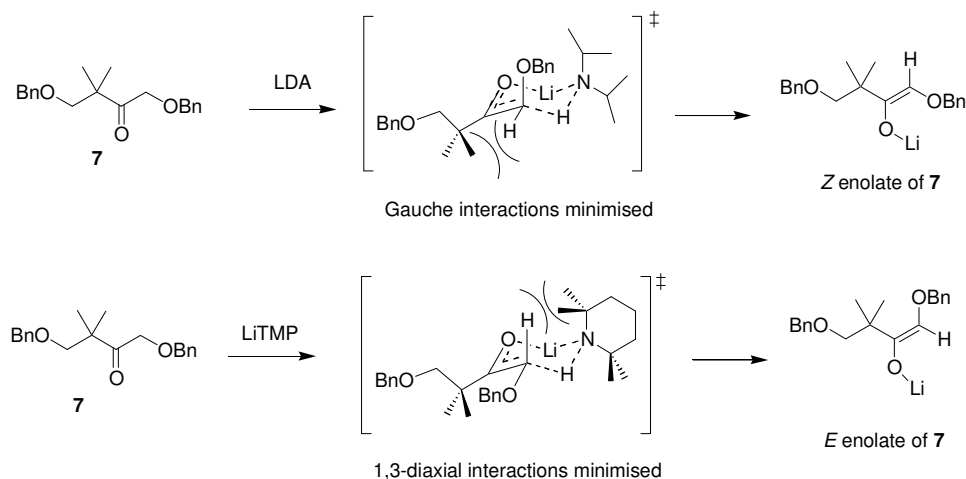
Scheme 1.6. Proposed synthesis of **13** via a Blaise reaction.

The synthesis of the C-8 to C-11 ketone⁴⁸ **7** started from the commercially available pantolactone, **25** (scheme 1.7). Protection of **25** was followed by reductive ring opening to give the diol, **26**. The two primary hydroxyl groups were then converted to their benzyl ethers. Subsequent liberation and oxidation of the hydroxyl group at C-9 yields the ketone fragment **7** as required. The use of benzyl ethers was preferred due to literature precedent for the formation of benzyloxy enolates,⁴⁹ and the ease with which they can be selectively removed fitted well within the overall synthetic plan.



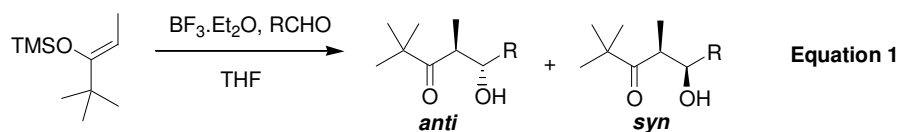
Scheme 1.7. Synthesis of the C-8 to C-11 ketone, **7**.

In order to obtain the desired stereochemical relationship between the methoxyl and hydroxyl substituents at C-7 and C-8 of peloruside A, the formation of an *anti* aldol product is required from the aldol reaction between **7** and **8**. If the classic Zimmerman-Traxler (cyclic six-membered transition state) model for the aldol⁵⁰ reaction is invoked, the *E* enolate of **7** was required to achieve this aim. It was anticipated that the use of LDA would provide the *Z* enolate of **7**, minimising the steric interaction between the gem-dimethyl groups and the OBn substituent at C-8 (figure 1.8). However, use of the more sterically hindered base LiTMP may, due to increased 1,3-diaxial interaction, force the OBn substituent to adopt an equatorial position as the enolate is formed, hence providing the *E* enolate.⁵¹



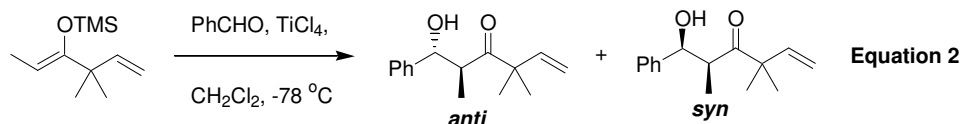
Scheme 1.8. Postulated formation of *E* and *Z* enolates of ketone **7**.

Alternatively, Mukaiyama-type aldol reactions have been shown, since their introduction in the 1970's,⁵² to be widely useful. Trimethylsilyl enol ethers of ketones similar to **7** have been shown to give *anti* aldol products upon reaction with various aldehydes, for example in equation 1, scheme 1.9 where the Lewis acid $\text{BF}_3 \cdot \text{OEt}_2$ gave excellent yield and diastereoselectivities.⁵³ In the same publication, TiCl_4 was also used, to give similar diastereoselectivities but slightly lower yields (53% and 65% for $\text{R}=\text{Ph}$ and $\text{R}=\text{iPr}$). Another example where TiCl_4 was used as the Lewis acid is shown in equation 2, scheme 1.9.⁵⁴



R=Ph, 95% yield, >95:5 anti:syn

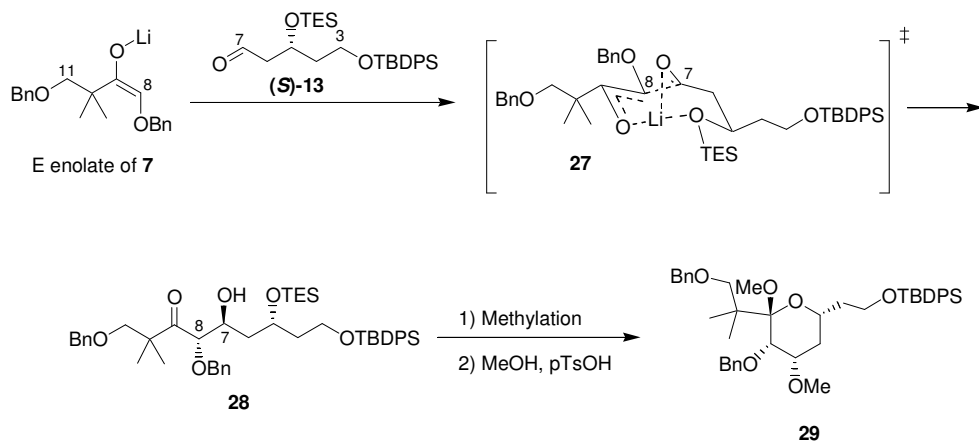
R=ⁱPr, 84% yield, >95:5 anti:syn



63% yield, >97:3 anti:syn

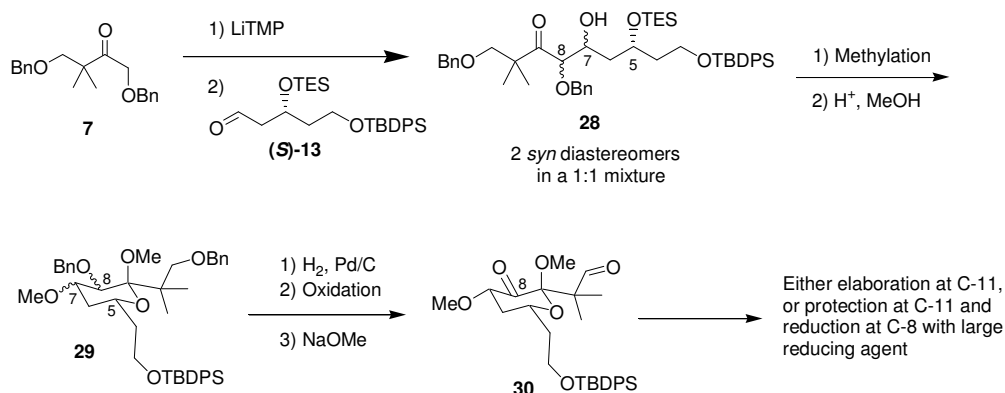
Scheme 1.9. Formation of *anti* aldol products with ketones similar to **7**.

Once an *E* enolate of **7** has been formed, the next challenge will be to control the facial selectivity of the attack on the approaching aldehyde, **13**. It has been reported that useful chelation control can be achieved using lithium enolates,⁵⁵ such as the LiTMP discussed above. In this case, it is anticipated that the lithium enolate will chelate to the aldehyde moiety, coordinating to both the aldehyde oxygen and the OTES substituent. In the transition state **27** (depicted in scheme 1.10), both the gem-dimethyl substituent of **7** and the alkyl chain of the aldehyde fragment adopt equatorial positions. Because the stereochemistry at C-5 (OTES substituent) is fixed, and because of the crowded nature of the transition state, only one conformation is favourable and attack at the '*re*' face of the aldehyde is preferred. Hence, the anticipated *anti* aldol product **28** also has the correct 1,3-*anti* relationship between C-5 and C-7.



Scheme 1.10. Chelation control of the aldehyde attack to form **28**.

Should establishing a stereoselective aldol reaction prove unsuccessful, an alternative approach to setting the stereochemistry around the ring has also been proposed (scheme 1.11). In this case, the aldol product **28** would have undefined stereochemistry at C-7 and C-8. After methylation and cyclisation of this molecule to give acetal **29**, the benzyl protecting groups would be removed and the resulting hydroxyl groups then oxidised. The methoxy at C-7 can then be epimerised, using for example sodium methoxide in methanol, to the more thermodynamically favourable equatorial conformation (**30**).⁵⁶ Elaboration at C-11 could then proceed, and at a later stage in the synthesis, the ketone at C-8 would be selectively reduced with a reducing agent such as NaBH₄³⁴ to give the axial hydroxyl group.

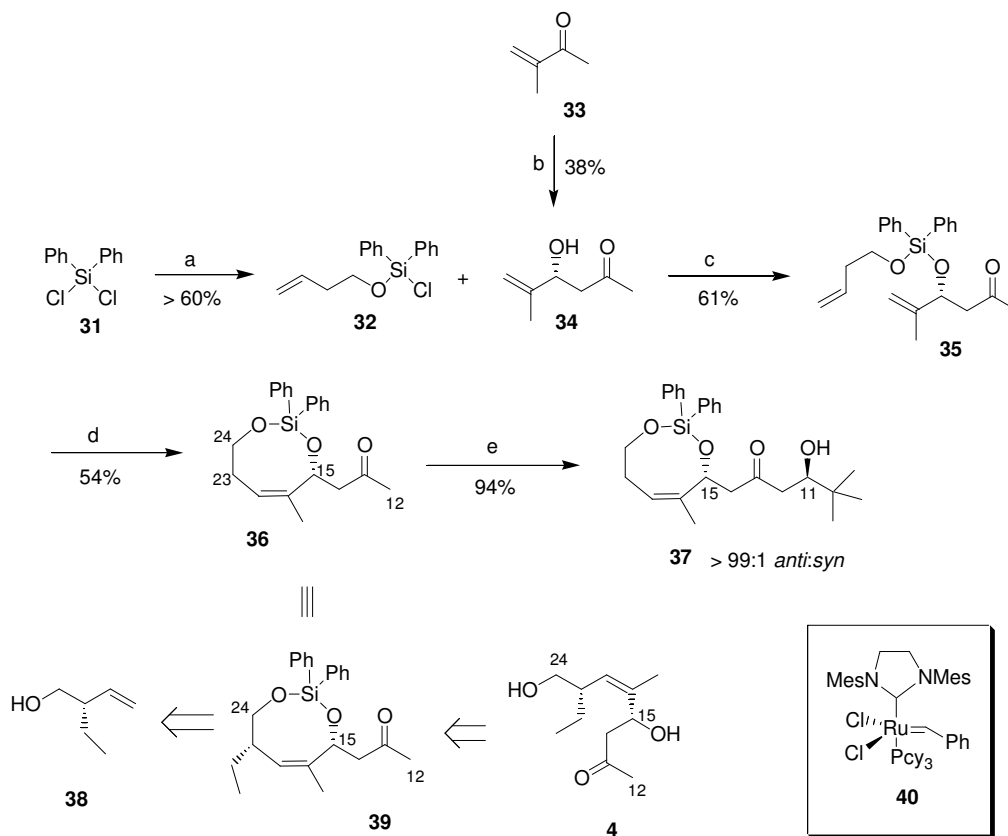


Scheme 1.11. Alternative route to pyranose ring with correct stereochemistry.

Synthesis of the C-12 to C-24 fragment

A successful strategy for the synthesis of the C-12 to C-24 fragment **4** has been developed by Dr. Bridget Stocker,^{48,57} albeit without the ethyl group in place (scheme 1.12). Cyclic compound **36** is equivalent to **39**, a protected analogue of the desired fragment **4**, however the silyl protecting group was found to be crucial to the subsequent aldol reaction to form the C-11 to C-12 bond with good stereoselectivity, and hence will not be removed until later in the synthesis. Although the ethyl group at C-23 had not yet been introduced, the use of (*S*)-2-ethyl-3-butenol (**38**) in place of 3-butenol in step (a), scheme 1.12 would allow

access to the requisite fragment **39** (equivalent to **36**). Both (*R*)- and (*S*)-2-ethyl-3-butenol are available in one step using a Zr-catalysed ethyl-magnesium of 2,5-dihydrofuran.⁵⁸

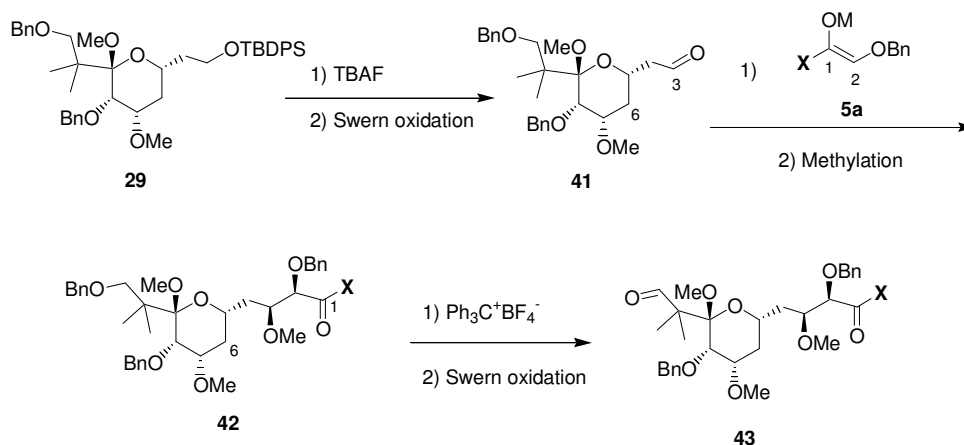


Scheme 1.12. Synthesis of C-12 to C-24 fragment, and coupling to a model for the C-3 to C-11 fragment. Reagents: (a) 3-butenol, Et₃N, CH₂Cl₂, reflux; (b) acetone, DMSO, 20% L-proline, RT, overnight; (c) Et₃N, CH₂Cl₂, 0 °C - RT; (d) 10 mol% **40**, CH₂Cl₂; (e) (-)-Ipc₂BCl, Et₂O, Et₃N, 0 °C then pivaldehyde, -78 °C 3 h, and -20 °C, 10 h.

Aldol reaction studies were undertaken^{48,57} using pivaldehyde as a model for the C-3 to C-11 fragment in reactions with **36** (scheme 1.12). In order to set the desired stereochemistry at C-11, a 1,5-*anti* relationship is required between C-11 and C-15. Interaction between the enolate and the remote phenyl-silyl substituents was found to provide the desired 1,5-*anti* induction. A number of boron reagents were employed successfully, with the (-)-Ipc₂BCl mediated aldol reaction giving the best yield for the compounds shown in scheme 1.12. The model aldol reaction between **36** and pivaldehyde proceeded to yield **37** in 94% yield and >99:1 ratio of 1,5-*anti*:1,5-*syn* aldol products.

Introduction of the C-1 to C-2 fragment

The C-1 to C-2 fragment is available commercially as benzyloxyacetic acid. It is proposed that a diastereoselective aldol reaction (scheme 1.13) between **41** and the enolate of a derivative of the benzyloxyacetic acid (**5a**), will give the desired π -facial selectivity. Based on literature precedent, the use of a chiral auxiliary (X) such as Evan's oxazolidinone⁵⁹ should afford the desired selectivity. Methylation of the resulting alcohol (to give **42**) and deprotection of the primary benzyl group using triphenylmethyl tetrafluoroborate⁶⁰ followed by Swern oxidation⁶¹ will give the C-1 to C-11 fragment **43**, ready to undergo the aldol reaction with the C-12 to C-24 fragment as discussed above.

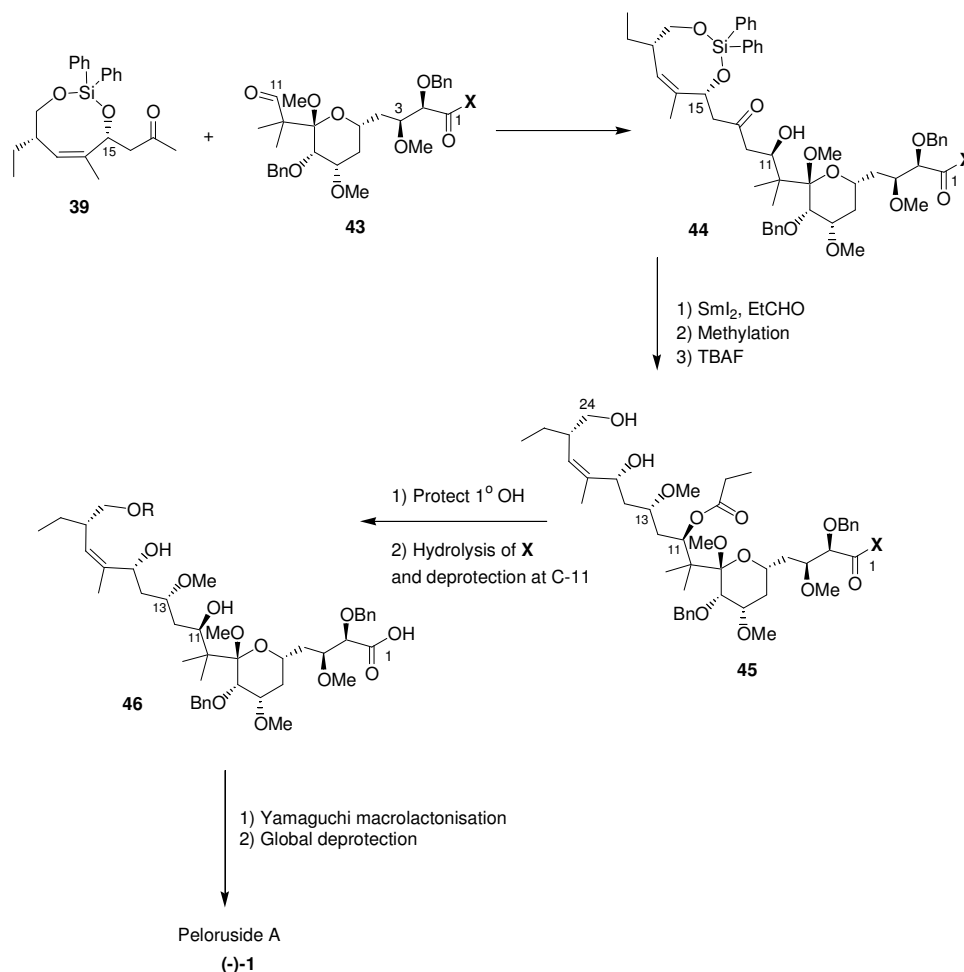


Scheme 1.13. Introduction of the C-1 to C-2 fragment.

Final assembly and macrolactonisation strategy

The final assembly strategy is depicted in scheme 1.14. First, an asymmetric aldol reaction as developed by Dr. Stocker between **39** and **43** will set the 1,5-*anti* relationship between C-11 and C-15. At this point the complete carbon skeleton of peloruside A is in place. Then, an Evans-Tischenko reduction⁶² of **44** with samarium iodide in propanal will set the final undefined stereocentre at C-13, and protect the C-11 hydroxyl group as the propanoyl ester. Methylation of the resulting hydroxyl group and subsequent deprotection of the *bis*-silyl ether, gives intermediate **45**. In order to ensure that the final

macrolactonisation is selective for the 16-membered macrocycle, the primary hydroxyl group at C-24 will be protected. Deprotection of the propanoyl ester and hydrolysis of the chiral auxiliary 'X' to form the intermediate **46**, will be required before the final macrolactonisation, which will be attempted under Yamaguchi esterification conditions.⁶³ It is possible that the 12-membered macrocycle will also form, and depending on the result of this reaction, the C-11 hydroxyl group may need to be suitably reprotected before macrolactonisation (the propanoyl ester group would not be suitable as the conditions for its removal might also cleave the ester in the macrocycle). Finally, removal of the remaining protecting groups will reveal the target molecule, peloruside A ((-)-**1**).



Scheme 1.14. Final assembly and macrolactonisation strategy.

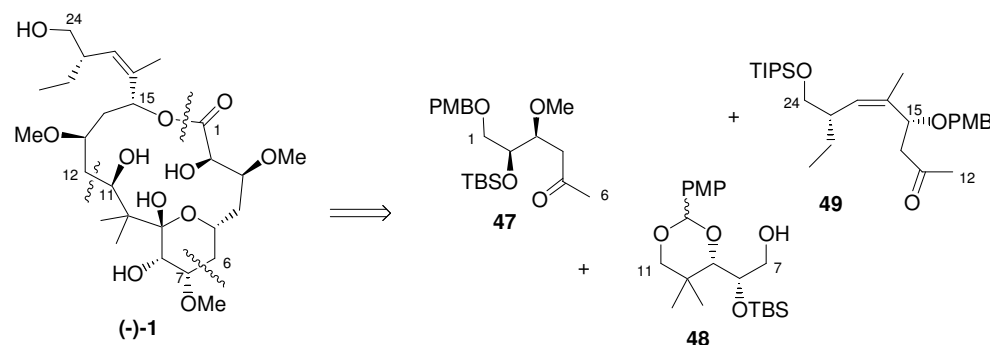
The synthetic strategy described above is convergent and seems efficient and flexible. There are many points where modifications could be made to

overcome the inevitable problems that will be encountered during the synthesis. Due to its convergent nature, it also provides ample opportunity for analogue synthesis in the future. Although the total synthesis was not achieved during the course of this PhD, it is hoped that this synthetic plan will eventually contribute to a successful total synthesis and, perhaps even more significantly, to a fruitful analogue search.

1.6 Peloruside A in the Synthetic Organic Chemistry Literature

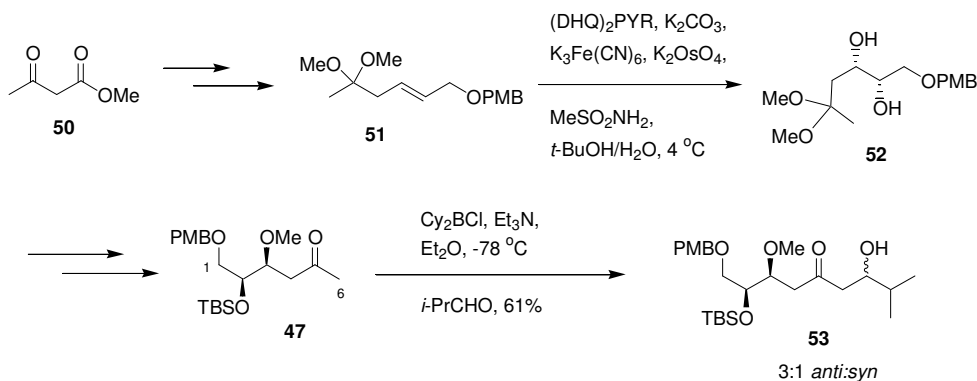
The clinical potential of peloruside A, as well as the synthetic challenges inherent in the structure, have made it an appealing target for a number of organic chemistry groups around the world. In this section, the reported synthesis and partial syntheses that have appeared to date will be discussed.

The first partial synthesis of peloruside A was reported in 2003 by Paterson, Di Francesco and Kühn from Cambridge University.⁶⁴ Their retrosynthetic strategy is shown in scheme 1.15; three major disconnections were identified to give three synthetic target fragments of similar complexity: C-12 to C-24, C-7 to C-11, and C-1 to C-6. The asymmetric syntheses of all three fragments were reported, along with boron-mediated aldol reaction studies directed towards the assembly of the complete carbon skeleton. They envisioned assembly of a fully protected complete carbon skeleton followed by macro-lactonisation, and finally deprotection which would induce hemiacetal formation and hence yield peloruside A.



Scheme 1.15. Paterson, Di Francesco and Kühn's retrosynthesis.

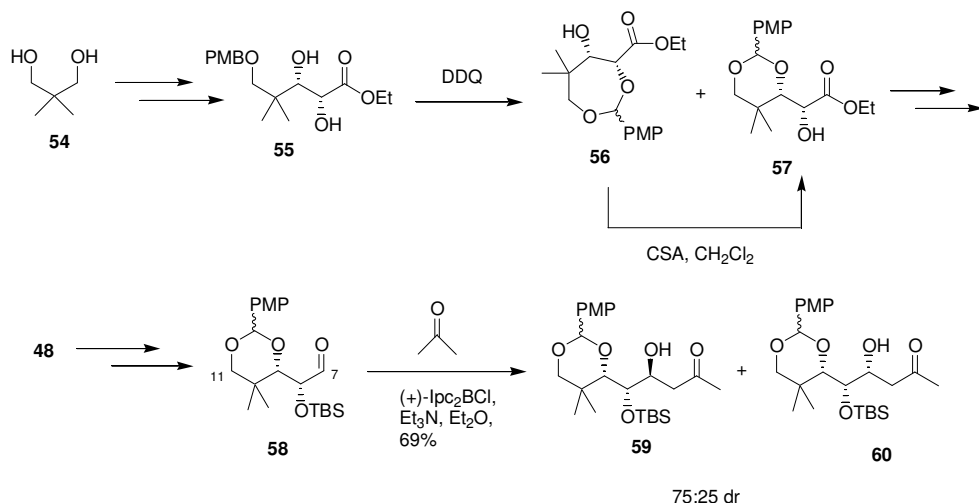
Paterson's synthesis of fragment **47** (C-1 to C-6) commenced with methyl acetoacetate **50**, affording the desired **47** after 11 steps. Sharpless asymmetric dihydroxylation was used to install the desired stereochemistry at C-2 and C-3; with an extensive screening of ligands carried out to optimise the yield and ee of the reaction. Using AD-mix- α containing (DHQ)₂PHAL, 54% ee was obtained; using the ligand (DHQ)₂PYR, 84% ee was obtained. With **47** in hand, it was found that a Cy₂BCl mediated aldol reaction between **47** and the model substrate isobutyraldehyde resulted in the desired 1,5-anti relationship between C-7 and C-3, albeit with a moderate diastereomeric ratio of 3:1.



Scheme 1.16. Synthesis of fragment **47** and model aldol reaction.

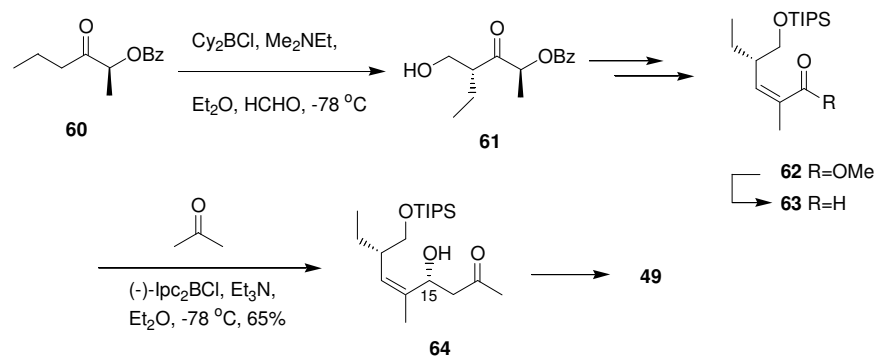
The synthesis of the C-7 to C-11 fragment **48** (scheme 1.17) was achieved in eight steps from neopentylglycol (**54**). Horner-Wadsworth-Emmons homologation and Sharpless asymmetric dihydroxylation (this time using (DHQ)PHN ligand to achieve 95% yield and 96% ee for this step) were followed by an oxidative cyclisation step in which two PMP acetals, **56** and **57** were formed. Fortuitously, it was found that the crude product mixture could be subjected to equilibrating conditions (CSA, CH₂Cl₂) to afford solely the more thermodynamically stable **57**. Silylation and DIBAL reduction gave the required fragment **48**. Subsequent Dess-Martin oxidation gave the aldehyde **58**, and with that fragment in hand, further model aldol reaction studies were conducted, also directed towards the formation of the C-6 to C-7 bond as above. Low diastereoselectivities, and even excess of the undesired product **60**, were observed with a range of boron-mediated aldol reactions, with only (+)-Ipc₂BCl

resulting in a reasonable excess of the desired diastereomer **59**. However, it was anticipated that the analogous aldol reaction with fragment **47** should result in a higher selectivity than was observed with the model substrate, acetone.



Scheme 1.17. Synthesis of **48** and model aldol reaction with acetone.

Finally, Paterson's synthesis of the C-12 to C-24 fragment **49** (scheme 1.18) commenced with the (*S*)-lactate derived ketone, **60**. The stereochemistry of the ethyl side chain was introduced (with 92:8 dr) by a Cy₂BCl mediated aldol reaction with formaldehyde to give **61**. This was followed by silyl ether formation, reduction, benzoate hydrolysis and glycol cleavage using Pb(OAc)₄ to give an aldehyde. This aldehyde was subjected to the Still-Gennari variation of Horner-Wadsworth-Emmons coupling to give exclusively the desired (*Z*)-enoate **62**. Then, after conversion to **63**, another boron-mediated aldol reaction was

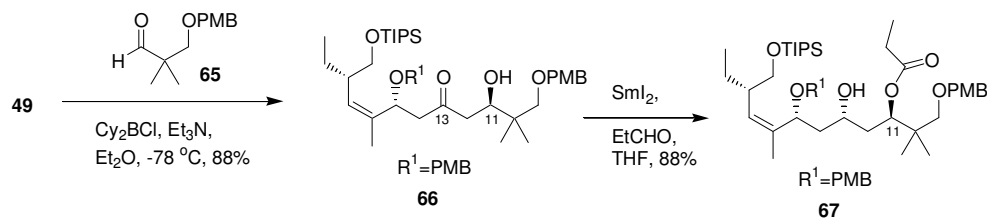


Scheme 1.18. Synthesis of the C-12 to C-24 fragment according to Paterson.

conducted. Using (-)-Ipc₂BCl, **64** was formed, setting the requisite stereochemistry at C-15 (a 83:17 dr was obtained). The resulting hydroxyl group was converted to a PMB ether to give the desired fragment **49**.

The similarity between fragment **49** and the C-12 to C-24 fragment **4** proposed in this thesis is noteworthy. Paterson's fragment is synthesised in ten linear steps with an overall yield of 18%; the equivalent fragment **4** (albeit without the ethyl group present) has been synthesised in four linear steps with an overall yield of 33%.

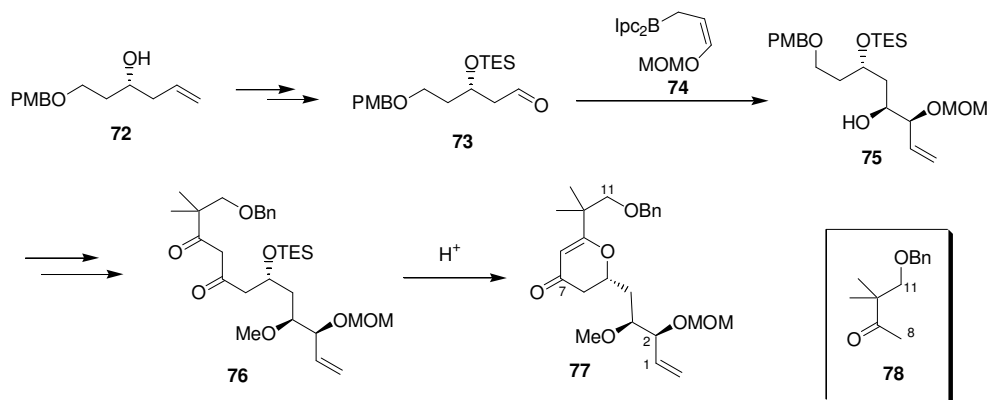
Aldol reactions of fragment **49**, directed towards the formation of the C-11 to C-12 bond, were carried out using model substrate **65** (scheme 1.19). As expected (based on previous work by Paterson's group) the reaction with Cy₂BCl/NEt₃ resulted in excellent levels of remote 1,5-anti induction to give **66** in 88% yield (>95:5 dr), thereby setting the correct stereochemistry at C-11. This induction relied upon the presence of the PMB group at the β position in **65**. Again, this strategy is comparable to the one proposed in this thesis, in which the cyclic silyl tether is responsible for the 1,5-anti induction (refer section 1.5).



Scheme 1.19. Model aldol reaction and subsequent Evans-Tishchenko reduction.

Paterson's publication also reported a successful SmI₂-catalysed Evans-Tishchenko reduction of compound **66** to give **67** (scheme 1.19), effectively providing the C-9 to C-24 subunit of peloruside A. This provides further precedence for the analogous reduction proposed in this thesis. No follow-up publication has yet appeared from Paterson's group reporting the successful assembly of the three reported fragments to give unnatural peloruside A.

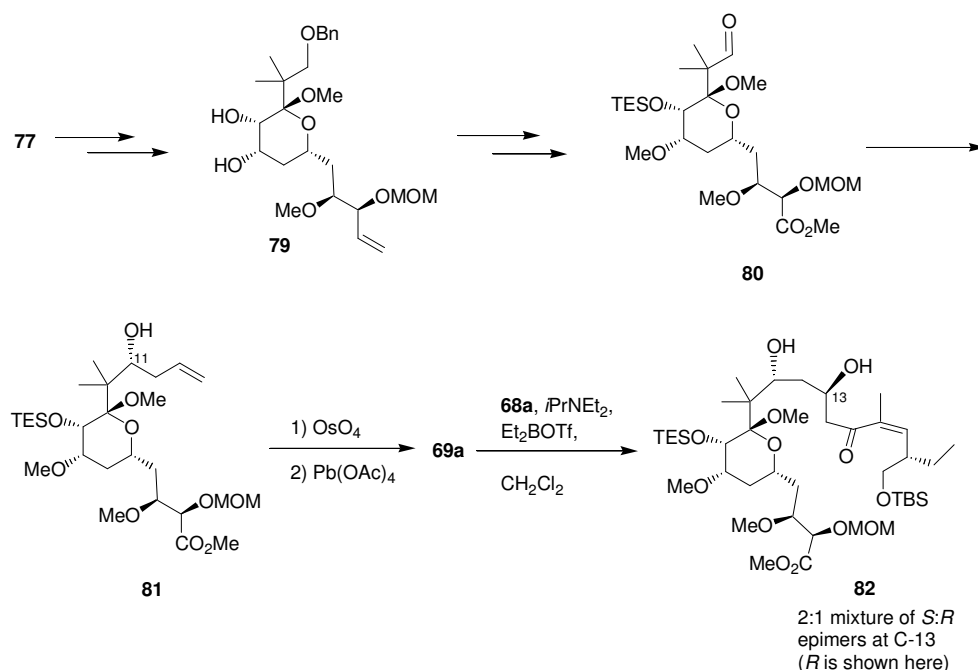
Synthesis of the second, substantially more complex C-1 to C-13 fragment **69a** began with alcohol **72** (scheme 1.22), which was protected and then dihydroxylated with catalytic OsO₄. The diol was then subjected to Pb(OAc)₄-assisted cleavage to yield the aldehyde **73**, which when treated with (Z)-alkoxyallylborane **74** at low temperature, produced the desired homoallylic alcohol **75**, setting the desired stereochemistry at C-2 and C-3. A further 5-step sequence (methylation, removal of PMB, oxidation, an aldol reaction with the lithium enolate derived from **78**, and oxidation) gave **76**, which upon stirring in an acidic toluene solution was transformed into the dihydropyranone **77**.



Scheme 1.22. Synthesis of the key intermediate **77**.

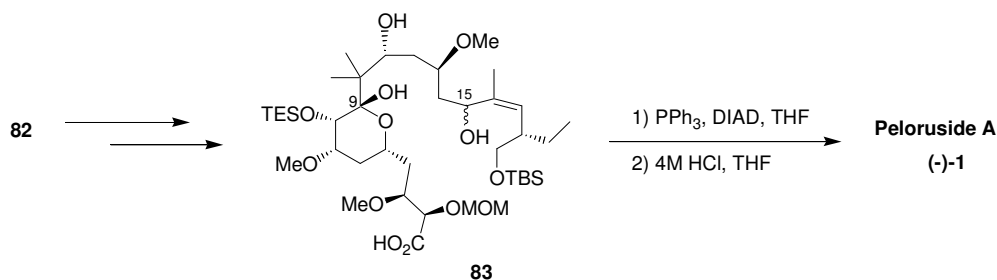
Intermediate **77** was thus the key starting point for setting the crucial stereochemistry around the ring. Luche reduction at C-7, followed by hydroxyl-directed epoxidation and in-situ methanolysis, gave the glycoside **79** in 72% yield from **77** (scheme 1.23). Further, the hydroxyl groups were protected, then the double bond oxidatively transformed to a carboxylic acid and treated with diazomethane, forming the methyl ester. Debenzylation and oxidation followed to give aldehyde **80**, ready for the introduction of the final two-carbon unit. Although the sterically crowded **80** proved resistant to nucleophilic addition, formation of a single diastereomer **81** was achieved with allyldiethylborane.

Numerous difficulties were encountered when **81** was protected at the C-11 alcohol and then further advanced through the synthesis. Therefore it was



Scheme 1.23. De Brabander's assembly of the complete carbon skeleton.

decided to attempt the assembly of peloruside A without further protection at C-11. Dihydroxylation and subsequent Pb(OAc)_4 -assisted cleavage again gave the aldehyde **69a** (a specifically protected analogue of **69**), which was coupled with the enolborinate derived from **68a**, in 87% yield, as a separable mixture of C-13 epimers in a 2:1 ratio. This rather modest selectivity was welcomed in light of the difficulties experienced previously, and at this point the complete carbon skeleton of peloruside A was in place.

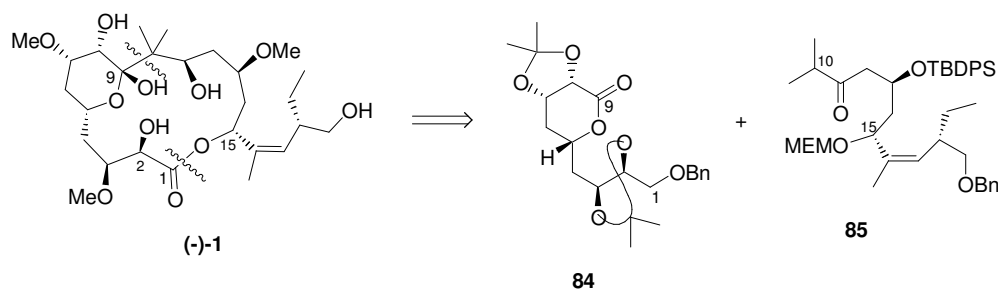


Scheme 1.24. Final transformations in de Brabander's total synthesis of (-)-1.

Methylation of the resulting hydroxyl group was accompanied by unexpected hydrolysis at C-9 to yield a hemiacetal. This was not reprotected, but carried through the next transformations: asymmetric reduction at C-15 using $\text{H}_3\text{B.SMe}_2$ and either (*S*)- or (*R*)-*B*-Me-oxazaborolidine, followed by liberation of

the carboxylic acid, to give either enantiomer of **83** (scheme 1.24), and then Mitsunobu-type macrolactonisation. Remarkably, it was found that the same lactone was produced, regardless of the stereochemistry at C-15. It was speculated that the geometric constraints of the macrocycle directed the mechanism of the reaction, so that the cyclisation occurred via either an acyloxyphosphonium intermediate (with retention of configuration) or via the more familiar alkoxyphosphonium intermediate (with inversion).

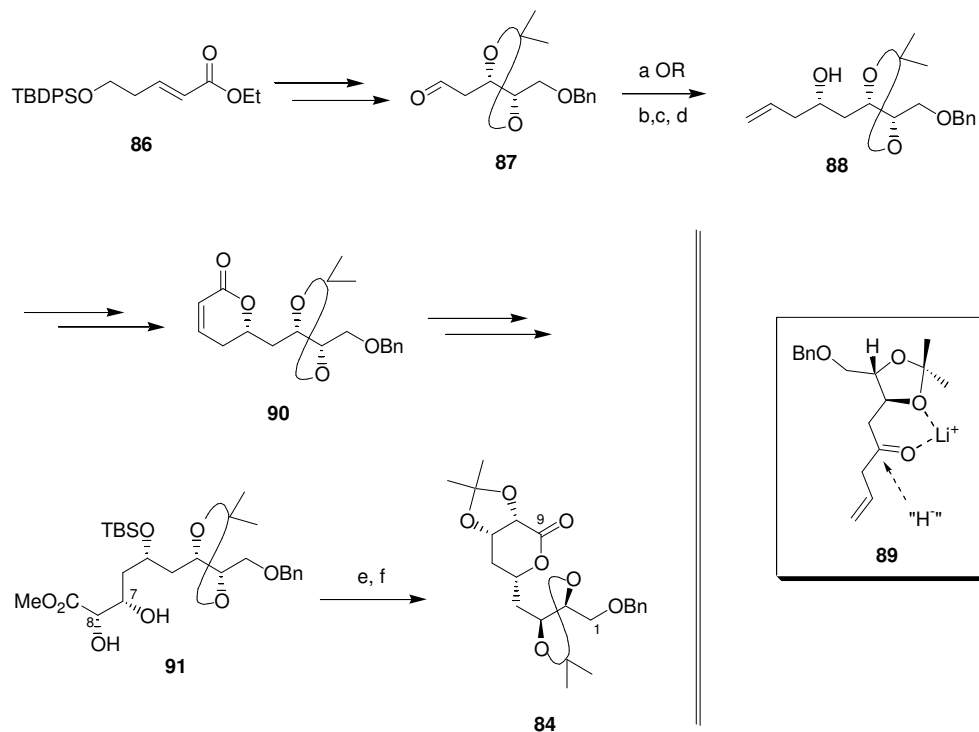
Shortly thereafter, two separate papers by Ghosh and Kim appeared reporting the partial syntheses of the C-1 to C-9⁶⁵ and the C-10 to C-24⁶⁶ fragments of peloruside A. Their retrosynthesis is shown in scheme 1.25.



Scheme 1.25. Ghosh and Kim's retrosynthesis.

The synthesis of the C-1 to C-9 fragment **84** (scheme 1.26) commenced with the α,β -unsaturated ester **86** (available from literature procedures) which was converted to aldehyde **87** via a six-step process including a Sharpless asymmetric dihydroxylation. This was then converted to allyl alcohol **88** via either the asymmetric allylation procedure developed by Brown and co-workers, or by a procedure involving treatment of the aldehyde **87** with allylmagnesium bromide, then oxidation and subsequent asymmetric reduction using LAH in the presence of LiI. The latter route gave the desired alcohol diastereoselectively (91:1 ratio) in 87% yield. The selectivity of this reduction was rationalised by a chelation-controlled transition state model in which lithium chelates to the ketone oxygen and attack is to the less hindered face of the carbonyl (**89**, scheme 1.26). The alcohol **88** is then esterified with acryloyl chloride and subjected to ring-closing metathesis to provide the lactone **90**. The lactone was converted to the

open-chain molecule^{iv} by saponification before Sharpless asymmetric dihydroxylation was employed to set the desired stereochemistry at C-7 and C-8. The resultant **91** is suitable for reaction with the C-10 to C-24 fragment, but was also further elaborated to give **84**, which allowed NOESY experiments to confirm that the desired stereochemistry had been achieved.

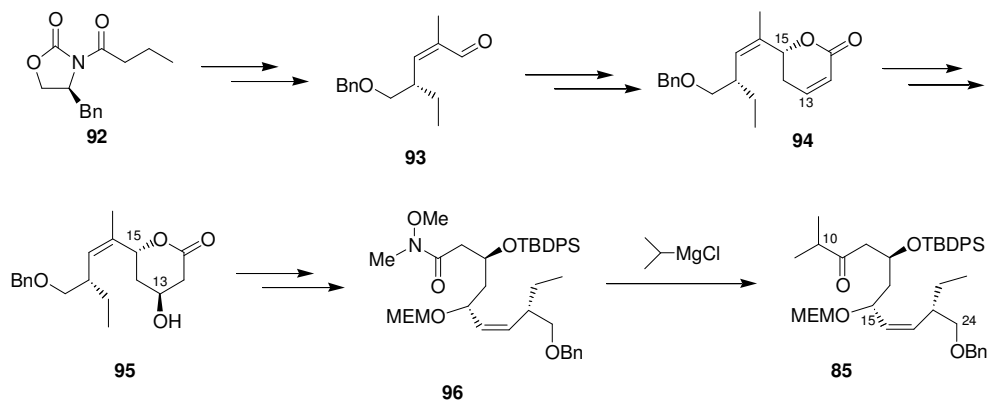


Scheme 1.26. Ghosh and Kim's synthesis of the C-1 to C-9 fragment of peloruside A. Reagents and conditions: a) allylB((-)-Ipc)₂, THF, -78 °C, 3 h (71%); b) allylMgBr, Et₂O, 0 °C, 1 h (74%); c) Dess-Martin periodinane, NaHCO₃, CH₂Cl₂, 23 °C, 2 h; d) LAH, LiI, Et₂O, -78 °C, 30 min (87%); e) *n*Bu₄N⁺F⁻, THF, 23 °C, 3 h; f) Me₂C(OMe)₂, PPTS (cat.) Me₂CO, 23 °C, 24 h (63% over 2 steps).

Their synthesis of the C-10 to C-24 segment **85** (scheme 1.27) began with the asymmetric alkylation of chiral imide **92** with benzyloxymethyl chloride (Evan's procedure). A five-step sequence including a Horner-Wadsworth-Emmons reaction (giving the tri-substituted *Z*-olefin in >99:1 selectivity) gave the aldehyde **93**, which was subjected to Brown's asymmetric allylboration with CH₂=CHCH₂B[(+)-Ipc]₂ to set the desired stereochemistry at C-15. Then, esterification and ring-closing methathesis using Grubb's first generation catalyst gave the lactone **94**. The correct stereochemistry was then introduced at C-13 by

^{iv} Dihydroxylation of **90** did not proceed even under forcing conditions.

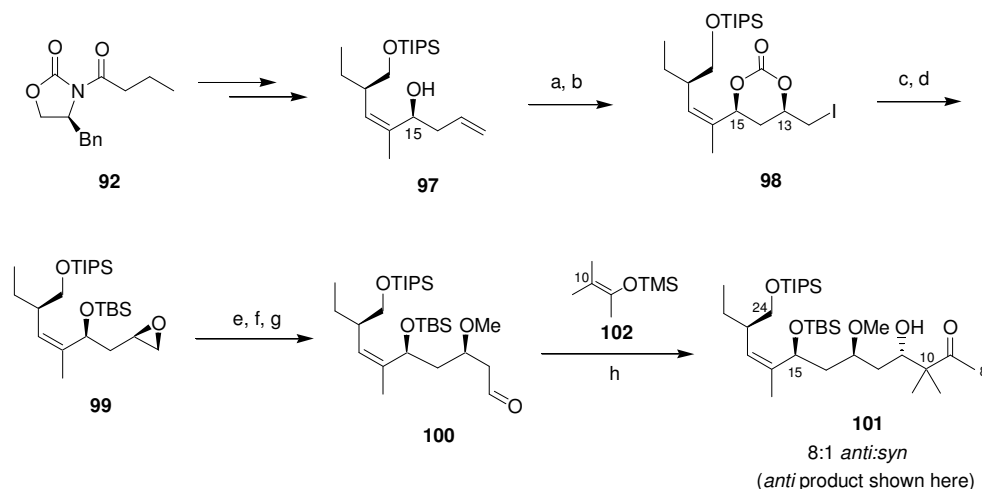
formation of a single epoxide by nucleophilic epoxidation with alkaline hydrogen peroxide, and subsequent treatment with diphenyldiselenide and sodium borohydride in 2-propanol. Hydroxylactone **95** was formed in quantitative yield, and the hydroxyl group protected with TBDPSCl. Direct opening of the lactone with isopropyl magnesium chloride proved elusive, and hence the final transformations were effected by reaction with *N,O*-dimethylhydroxylamine hydrochloride in the presence of trimethylaluminium in CH₂Cl₂, followed by protection with MEMCl to furnish the Weinreb amide **96**. Treatment of **96** with excess isopropyl magnesium chloride gave **85**, the C-10 to C-24 fragment of peloruside A.



Scheme 1.27. Ghosh and Kim's synthesis of the C-10 to C-24 fragment.

The next partial synthesis to be reported was of the C-8 to C-24 fragment **101** (scheme 1.28), by Taylor and Jin.⁶⁷ This was the first report of a synthesis of a fragment of peloruside A with the natural stereochemistry. Their synthesis began in a very similar fashion to that of Ghosh and Kim for the C-10 to C-24 fragment above, starting with the oxazolidinone **92**. A stereoselective alkylation with BOMCl in the presence of TiCl₄, a Still-Gennari olefination (providing exclusively the desired *Z*-trisubstituted alkene), and Brown's asymmetric allylation (setting the desired stereochemistry at C-15) were the key features of the nine-step approach to the intermediate **97**.

The 1,3-*syn* relationship between C-15 and C-13 was then established using an iodine-induced carbonate cyclisation reaction. After BOC-protection of



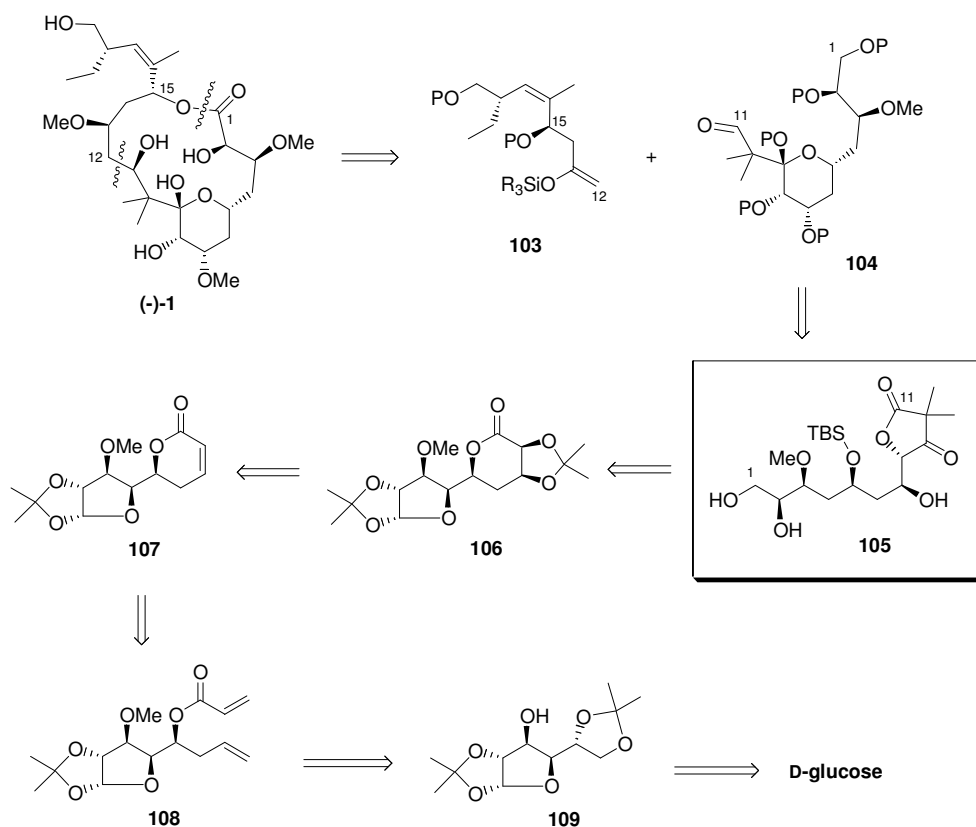
Scheme 1.28. Taylor and Jin's partial synthesis of the C-8 to C-24 fragment of peloruside A. Reagents and conditions: a) Boc-ON, 91%; b) NIS, CH₃CN, 92%; c) K₂CO₃, MeOH, 86%; d) TBDMSCl, imidazole, 92%; e) 1,3-dithiane, *n*BuLi, 85%; f) KO^tBu, MeI, 78%; g) MeI, CH₃CN/H₂O, 90%; h) **102**, BF₃·OEt₂, CH₂Cl₂, -78 °C, 91%.

97, treatment with *N*-iodosuccinimide was found to regioselectively form the six-membered carbonate **98** in excellent yield. Treatment with basic methanol and protection gave the *syn*-epoxy ether **99**, and the epoxide was then opened with the lithium anion of dithiane. After methylation, the hydrolysis of the dithiane gave aldehyde **100**. Finally, the gem-dimethyl portion of peloruside A was introduced by Mukaiyama aldol reaction of **100** with **102** in the presence of boron trifluoride etherate. Although an achiral Lewis acid was used, the reaction proceeded in a diastereomeric ratio of 8:1, providing as the major product the *anti* aldol product **101**, representing the C-8 to C-24 fragment of peloruside A.

Taylor and Jin also noted the structural and conformational similarities between peloruside A and the epothilones, derived from NMR and computer modelling analysis. The possibility that peloruside A and the epothilones may have overlapping pharmacophores was noted, although this has since been demonstrated to not be the case.⁶

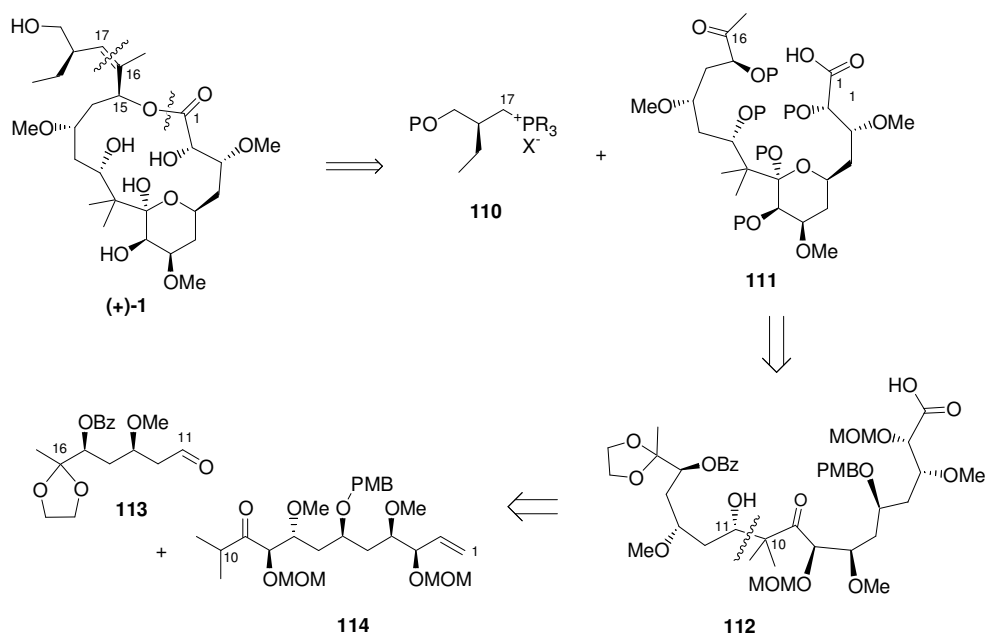
A unique, chiral pool approach to the C-1 to C-11 segment of (-)-**1** (unnatural peloruside A) has been published by Gurjar *et al.*⁶⁸ The overall retrosynthetic analysis is presented in scheme 1.29, with the key C-11 to C-12 disconnect being the same as that proposed in this thesis. However, Gurjar *et al.*

envisage a Mukaiyama aldol reaction between **103** and **104** as the key transformation to form this bond. They used D-glucose as a starting material for the reported synthesis of the C-1 to C-11 segment **105**, with the stereogenic centres at C-5, C-3 and C-2 of peloruside A to be derived from the glucose. Dihydroxylation of the key intermediate lactone **107** (itself derived from a ring-closing metathesis of **108**) provides the correct stereochemistry at C-7 and C-8.



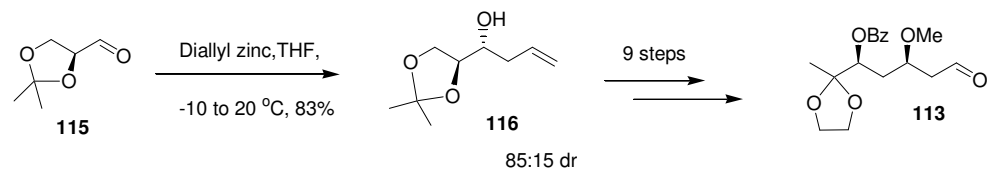
Scheme 1.29. Gurjar *et al.*'s retrosynthetic analysis of peloruside A .

Thereupon followed a paper by Liu and Zhou⁶⁹ reporting a stereoselective synthesis of 'the backbone of the core' of natural peloruside A. A convergent retrosynthetic plan was presented (scheme 1.30 overleaf), with disconnects between C-10 and C-11, and a previously unproposed disconnect between C-16 and C-17. In their paper, the synthesis of fragments **113** and **114** were presented. Their successful coupling to give **112**, representing the carbon skeleton of the macrocycle of peloruside A, was also reported.



Scheme 1.30. Liu and Zhou's retrosynthesis.

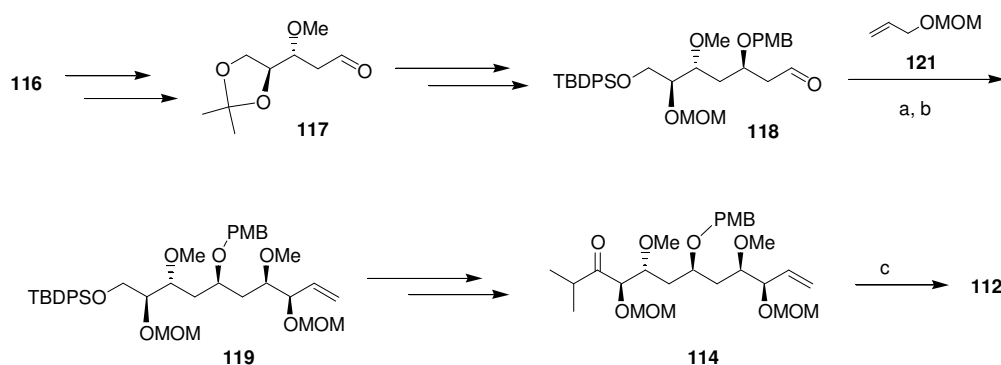
Both **113** and **114** were derived from L-glyceraldehyde acetonide **115**. The synthesis of fragment **113** (scheme 1.31) began with a substrate-controlled stereoselective allylation with diallyl zinc to give **116**, followed by Mitsunobu inversion of the free hydroxyl group. A further nine-step sequence, including a second stereoselective allylation reaction using Brown's *B*-allyldiisopinocampheyl borane reagent, gave the aldehydic fragment **113**.



Scheme 1.31. Synthesis of fragment **113**.

The synthesis of fragment **114** started with the common intermediate **116** (scheme 1.32). In this case, the stereochemistry of the alcohol was retained. Methylation and Johnson-Lemieux oxidation (with cat. OsO₄ and NaIO₄ in THF-H₂O) gave the aldehyde **117**, ready for allylation, again with Brown's *B*-allyldiisopinocampheyl borane reagent. A series of protecting group manipulations and another Johnson-Lemieux oxidation gave aldehyde **118**. To this was added *Z*-alkoxyallylborane generated in-situ from **121**, and the resultant

alcohol methylated to give **119**. Finally, after removal of the TBDPS group and oxidation to give the aldehyde, the isopropyl group was introduced. Use of isopropyl Grignard reagents was not successful, but it was found that treatment of the aldehyde with freshly prepared isopropyllithium, followed by oxidation with Dess-Martin periodonane gave the desired product **114** in satisfactory yield of 70%.

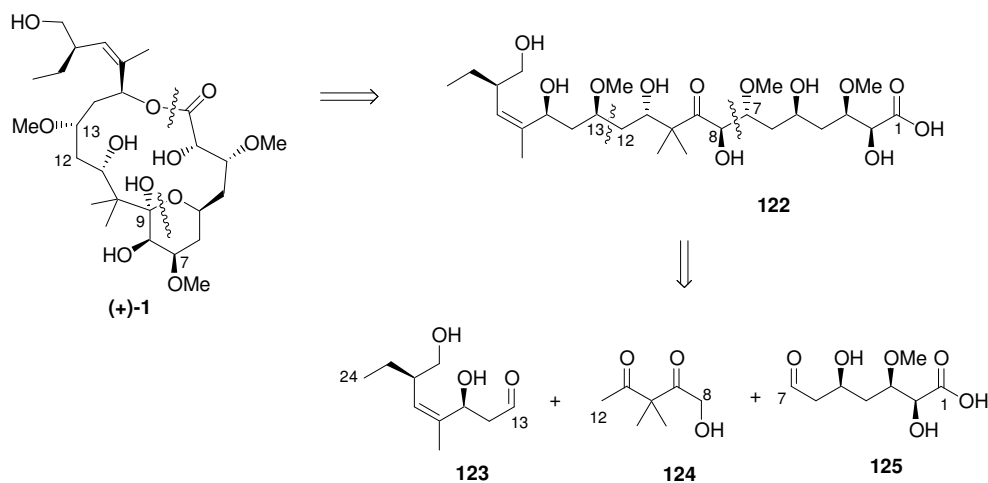


Scheme 1.32. Synthesis of fragment **114** and LDA coupling to **113**. Reagents and conditions: a) **121**, *s*BuLi, THF, -78 °C, 40 min then (-)-Ipc₂BOMe, -78 °C, 1.5 h, then aldehyde **118**, -78 °C, 3.5 h, 75%; b) MeI, NaH, THF, RT, 85%; c) LDA, THF, -78 °C, then aldehyde **113**, THF, -78 °C to -40 °C, 74:26 dr, 60%.

The final coupling of **113** and **114** proved to be troublesome. No satisfactory reaction was obtained under BF₃.Et₂O or TiCl₄ – promoted Mukaiyama aldol conditions (although the TMS enol ether of **114** was readily prepared). Aldol reaction with TiCl₄/*i*PrNEt₂, and a range of boron-mediated aldol reactions were also unsuccessful, as was reaction with LiHMDS. The sterically hindered nature of the ketone, next to the isopropyl group, was suggested as the cause of these problems. Fortunately, LDA-induced aldol reaction provided the desired product **112** in 74:26 dr in 60% yield.

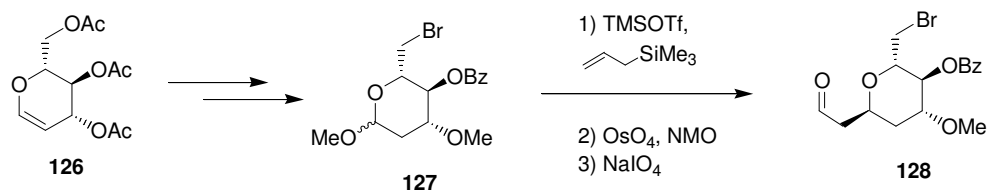
Finally, Pagenkopf *et al.* have reported recently an elegant synthesis of the C-1 to C-12 portion of natural peloruside A.⁷⁰ Their retrosynthetic analysis of the molecule is shown in scheme 1.33. As can be seen, the disconnections are similar to those proposed in this thesis. Three key fragments are identified, with two aldol reactions required for the final assembly of the carbon skeleton; a methyl ketone aldol reaction to form the C-12 to C-13 bond (not discussed in the

publication) and an α -hydroxy ketone aldol reaction to form the C-7 to C-8 bond, which is reported.



Scheme 1.33. Pagenkopf *et al.*'s retrosynthesis of peloruside A.

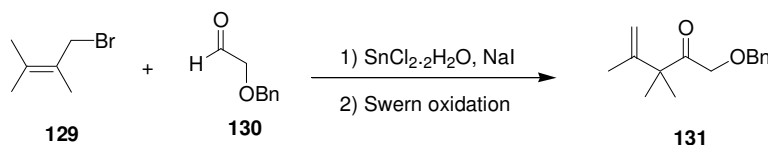
The synthesis of **128**, a suitably protected analogue of the C-1 to C-7 subunit **125**, notably began with commercially available triacetyl D-glucal **126** (scheme 1.34). The glucal was converted to the known pyranoside **127** via a five-step sequence involving reaction with methanol and catalytic $\text{Ph}_3\text{P.HBr}$ (to give the 2-deoxypyranoside), acetate cleavage, benzylidene acetal formation, methylation, and selective primary benzylidene ether cleavage under Hanessian-Hullar radical bromination conditions. Allylation of **127** afforded one diastereomer exclusively, then dihydroxylation and oxidative cleavage with NaIO_4 gave the aldehyde **128**. This preparation has been carried out on 50 g of triacetal D-glucal to yield 31 g of **128**, in a very respectable overall yield of 46%.



Scheme 1.34. Synthesis of the C-1 to C-7 fragment, **128**.

To allow study of the C-7 to C-8 bond forming aldol reactions, an analogue of **124** was prepared. Hence, **131** was synthesised in 69% overall yield

by addition of an allylic stannane generated in-situ from Barbier-type reaction of **129** with $\text{SnCl}_2 \cdot 2\text{H}_2\text{O}$ and benzyloxy acetaldehyde **130** (scheme 1.35).

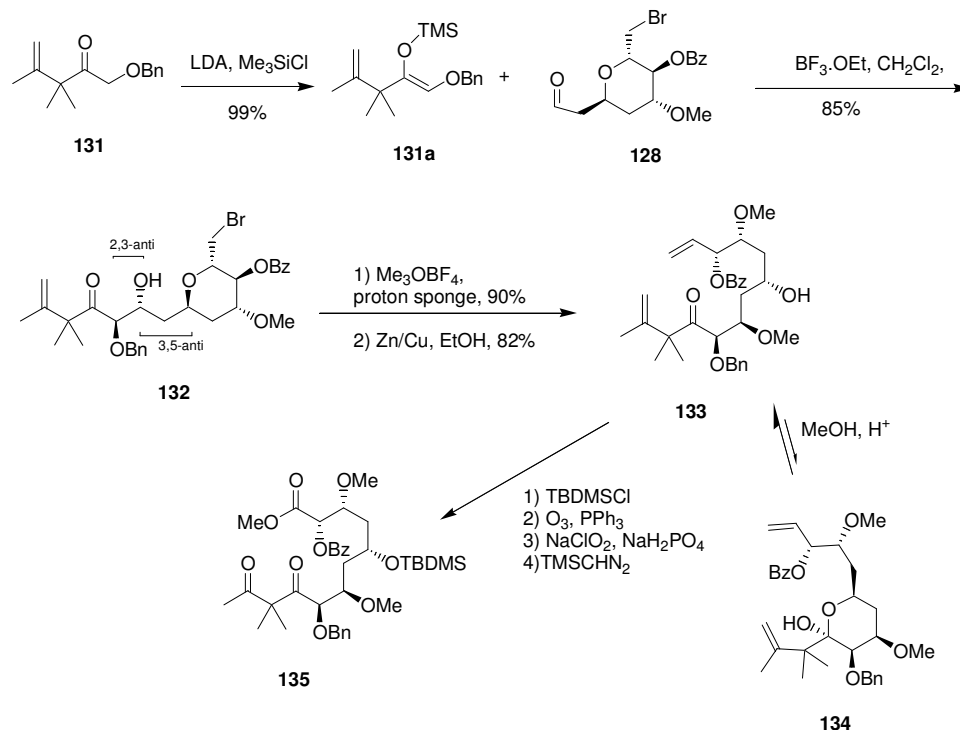


Scheme 1.35. Synthesis of an analogue of the C-8 to C-12 fragment.

With the two fragments in hand, extensive screening of aldol reaction conditions to discover means for accessing all four possible diastereomeric products were carried out. It was reported that the best method for obtaining the desired 2,3-*anti*-3,5-*anti* product **132** was a Mukaiyama aldol reaction promoted by $\text{BF}_3 \cdot \text{OEt}_2$ (scheme 1.36). Optimised conditions were found to be adding 1.1 equivalents of $\text{BF}_3 \cdot \text{OEt}_2$ to a -20°C solution of **131a** and **128** in CH_2Cl_2 , warming the reaction to 0°C and maintaining that temperature for 2 h. Under these conditions, an 85% yield of the 2,3-*anti*-3,5-*anti* and the 2,3-*anti*-3,5-*syn* aldol products^v in a 3.5 to 1 ratio; this modest ratio was considered satisfactory in view of the complex and challenging nature of the problem.

The synthesis continued with methylation and then reduction of the alkyl bromide by zinc-copper couple. Spontaneous β -elimination of the alkyl zinc generated in-situ (Vasella ring cleavage) provided the acyclic **133**. It was hoped that cyclisation to form the hemiketal **134** (or the corresponding methyl ketal) could be induced at this point (scheme 1.36), however obtaining **134** proved elusive. Hence, the open chain molecule with the ketone intact was advanced further; TBDMS protection, cleavage of both alkenes by ozonolysis, and then immediate oxidation of the aldehyde (at C-1) to the carboxylic acid, followed by esterification, gave the methyl ester **135**.

^v The stereochemistry was assigned based on NOE analysis of cyclic di-*tert*-butylsilylene ether derivatives prepared at a later stage in the synthesis, and on comparison of coupling constants and literature precedence with *tert*-butyl ethyl ketones.



Scheme 1.36. Aldol reaction to form C-7 to C-8 bond and further elaboration.

1.7 The eight retrosynthetic strategies – summary and final comment

It is clear from the above survey that the total synthesis of peloruside A is far from a simple matter. Despite the fact that eight groups have published fragment syntheses since the structure of peloruside A was revealed in 1999, only the de Brabander group has achieved a total synthesis to date.^{vi} Figure 1.8 overleaf shows a brief summary of the disconnections proposed by seven of the eight groups (although Taylor and Jin published a synthesis of the C-8 to C-19 region of peloruside A, they did not present an overall retrosynthetic analysis). The macrolactonisation between C-1 and C-15 is common to all groups, although de Brabander used an interesting Mitsunobu-type macrolactonisation while other groups propose the more traditional Yamaguchi macrolactonisation strategy. De Brabander's strategy is among the more linear. The retrosynthesis of Gurjar *et al.*, although apparently also quite linear, represents an elegant approach starting with a substrate from the chiral pool, D-glucose. Unfortunately, this strategy will

^{vi} NB: A total synthesis of natural peloruside A has since appeared - see footnote iii, page 28.

yield the (-) peloruside A, and L-glucose, which would yield the natural product, is considerably more expensive. Pagenkopf *et al.* also use D-glucose as a starting material, while Liu and Zhou use L-glyceraldehyde. Paterson *et al.*, Pagenkopf *et al.* and Hoberg *et al.* propose more convergent syntheses.

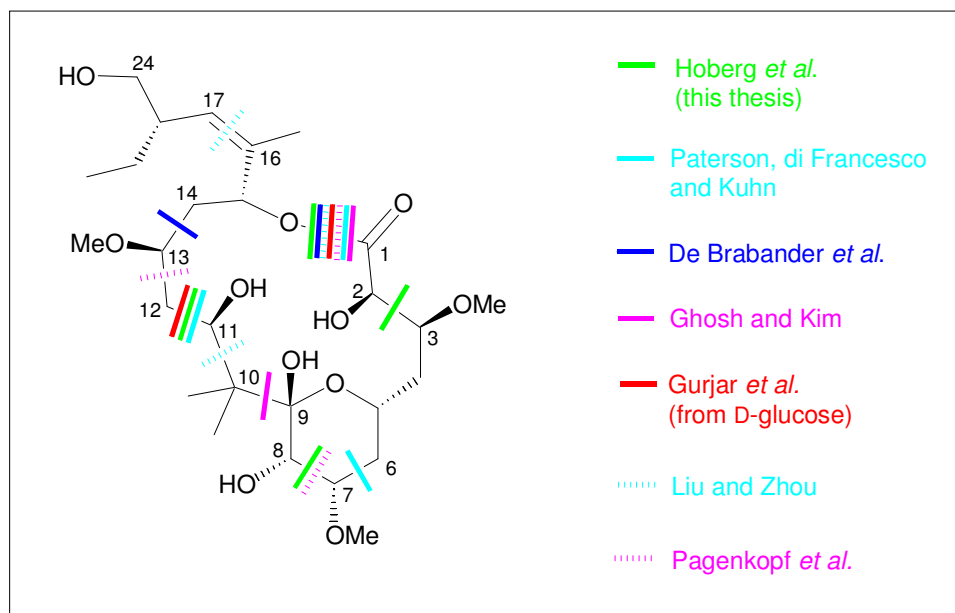


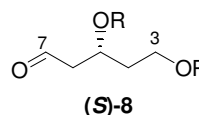
Figure 1.8. Summary of the retrosynthetic strategies adopted by various groups.

The assembly of the pyranose ring with the correct stereochemistry in the sterically crowded C-7 to C-11 region appears to be one of the greatest challenges of this structure. The greatest variation in approach also occurs in this region, although the C-11 to C-12 disconnection was also common to three groups, including that of Hoberg *et al.* (the strategy presented in this thesis). No other published strategy has all of the same disconnections as that presented in this thesis, although there are some similarities as noted throughout this chapter, particularly with Paterson *et al.*'s strategy in the C-12 to C-24 region and with Pagenkopf *et al.*'s in the pyranose ring region. Overall, however, the different approaches to peloruside A can be said to be both creative and diverse.

Chapter Two

Synthesis of the C-3 to C-7 Fragment of Peloruside A

The retrosynthetic analysis of peloruside A presented in chapter one required the preparation of a protected variant of the C-3 to C-7 fragment **8**.ⁱ Brown's boron-mediated allylation procedure was used to prepare significant quantities of both enantiomers of the C-3 to C-7 fragment, but several other routes were also investigated, and these are discussed in this chapter. Significantly, the Grignard reaction route presented in section 2.1.2 was investigated as it gave the option of entry to a nitrogen-containing analogue of peloruside A.



2.1 Racemic synthesis of the C-3 to C-7 fragment

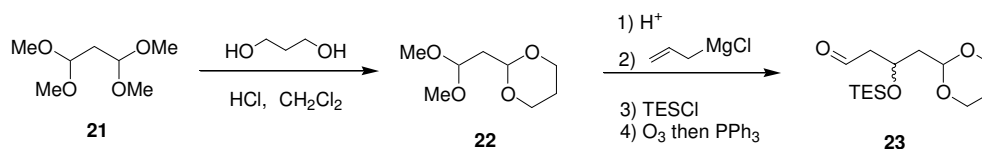
2.1.1 Strategy One

Racemic syntheses were considered initially, to provide quantities of suitably protected **8** to begin the aldol reaction studies presented in chapter three. Initially, a route commencing with malonaldehyde bis(dimethyl acetal) **21** was proposed (scheme 2.1). Acid-catalysed conversion of **21** to malonaldehyde mixed bisacetal **22** with 1,3-propane diol has been reported.⁴⁵ Subsequent selective acetal cleavage, allylation, protection and ozonolysis would yield **23** (which constitutes a suitably protected variant of **8**). If this route had been successful, a suitable chiral allylation procedure would have been investigated.

However, it rapidly became clear that the formation of the mixed acetal **22** was not as straightforward as had been indicated in the literature. A complex

ⁱ As in chapter one and three, the numbering of fragments throughout this chapter relates to the numbering of peloruside A itself (rather than the IUPAC numbering of individual fragments).

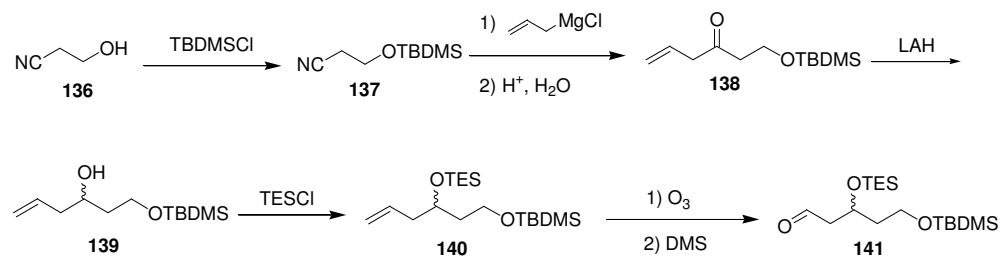
mixture of products was obtained, which was extremely difficult to purify. This strategy was not pursued further.



Scheme 2.1. Route to the C-3 to C-7 fragment from **21**.

2.1.2 Strategy Two

The plan for the second strategy for preparing a variant of **8** is shown in scheme 2.2 (scheme 2.5 shows the modified procedure adopted after optimisation of the reactions, with yields included). Initial protection of 3-hydroxypropionitrile (**136**) with *tert*-butyldimethylsilyl (TBDMS) chloride to form the silyl ether **137** was planned, followed by a Grignard reaction of the nitrile⁴⁶ with commercially available allyl magnesium chloride,ⁱⁱ and acid hydrolysis to give ketone **138**. Subsequent reduction, protection and ozonolysis would give the target precursor **141**.

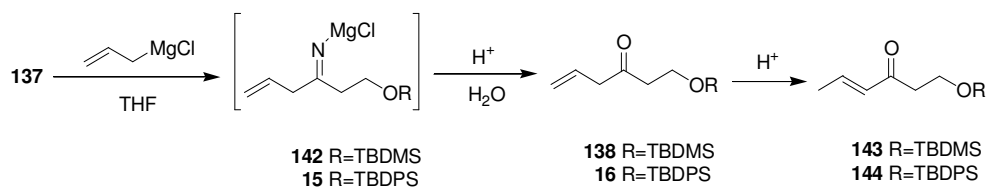


Scheme 2.2. Planned Grignard reaction synthesis of C-3 to C-11 fragment.

The initial protection proceeded well with TBDMSCl and imidazole in DMF, to give **137** in 97% yield. The subsequent Grignard reaction, however, proved to be extremely troublesome. When the reaction was run in diethyl ether overnight at ambient temperature and the resulting iminium magnesium salt (scheme 2.3) hydrolysed with dilute sulphuric acid, TLC analysis of the crude

ⁱⁱ Allylmagnesium chloride, 2 M in Et₂O, purchased from Aldrich Chemical Company.

product revealed a myriad of products along with the desired **138**. A significant by-product was the conjugated isomer **143** (scheme 2.3), which was isolated. Aside from a large amount (often > 50%) of unreacted starting material, the other side products were not identified. Attempts to drive the reaction to completion by heating to reflux or extending the reaction times to several days did not significantly increase the amount of product, while seeming to cause more by-product formation. Other modifications such as changing the order of addition, using a slow addition rate, and changing the ratio of allylmagnesium chloride to nitrile, gave little improvement in yield or quality of the product. Changing the reaction solvent from diethyl ether to THF did give moderate improvement in yield and reproducibility of the reaction but the typical yield for the Grignard reaction of **137** was still less than 35%. Careful flash column chromatography did, however, provide sufficient **138** to further the synthesis.



Scheme 2.3. Hydrolysis and isomerization of the Grignard product.

The isomerization to the more stable α,β -unsaturated compounds (**143** or **144**) shown in scheme 2.3 represents one of the key problems with this route. Unfortunately, the aqueous acid workup (that is required to hydrolyse the intermediate product to the ketone), also promotes this isomerization. Workup of **142** with dilute aqueous sulphuric acid at ambient temperature for three hours, gave the isomer **143** as the major product. The internal double bond of **143/144** was clearly differentiable from the terminal double bond in **138/16** in the ^1H NMR spectrum. For compound **144**, the two olefinic protons appear as doublets of quartets at 6.82 and 6.14 ppm (coupling to each other with a coupling constant $J = 15.9$, and both also coupling to the methyl group). Fortunately, it was found that by using a milder workup procedure, using cold (0 °C) dilute acetic acid, conversion of **138** to **143** could be minimised. Prompt purification of the crude product **138** was required after workup, to preclude the isomerization occurring

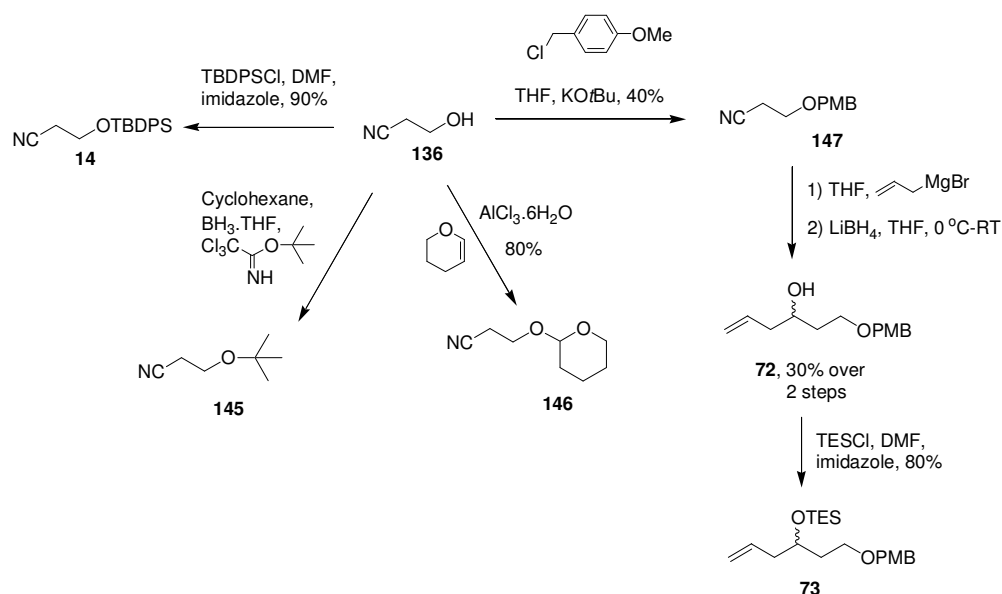
in the crude product, presumably catalysed by residual traces of acid. Fortunately, the subsequent reduction of the ketone (scheme 2.2) was found to be very robust. Semi-crude **138** can (and should) be rapidly carried through the reduction step to the stable alcohol **139**.

There have been reports in the literature that Cu(I) salts can facilitate the addition of Grignard reagents to nitriles. For example, the addition of *tert*-butylmagnesium chloride to 4-methoxybenzonitrile, which proceeded in only 7% yield after 24 hours, was improved dramatically by the addition of 2 mol% of CuCl.⁷¹ The yield after only 1.5 hours was increased to 85%, and reported to be 100% after 14 hours. The procedure was applied to the Grignard system described here, however in this case the yield and quality of the product were not improved. In fact, it appeared that the cleavage of the silyl ether present in **137** (and in **14**) was more marked under the Cu(I)-catalysed conditions.

The most significant improvement to the Grignard procedure was obtained by changing the protecting group used to protect the hydroxyl moiety of **136**. The original TBDMS protecting group was somewhat labile under the forcing Grignard reaction conditions (particularly at elevated temperatures), and was also partially cleaved during the acidic workup. Replacing the TBDMS group with the significantly more stable TBDPS group alleviated these problems. The TBDPS group was successfully introduced⁷² using TBDPSCl and imidazole in DMF (scheme 2.4).ⁱⁱⁱ A welcome consequence of this change was that the incorporation of UV-active functionality into the molecule made visualisation of the compounds on TLC much easier. The TBDPS-protected nitrile **14** could be heated to reflux in THF without significant cleavage of the silyl ether, during the Grignard reaction - with a consequent improvement in yield to 40% – 50% (scheme 2.5). The optimum reaction time was found to be approximately three hours; any longer and even the TBDPS group was cleaved. The best yield of 53% was obtained upon a moderate scaleup of the reaction to 1.5 g scale.

ⁱⁱⁱ An alternative procedure⁷³ using pyridine and DMAP was also attempted but found to be less satisfactory, requiring longer reaction times.

Other analogues of **137** were also prepared, in the hope that these would further improve the yield of the Grignard reaction (scheme 2.4). The *tert*-butyl ether **145**, was introduced by treatment of **136** with *tert*-butyl-2,2,2-trichloroacetimidate.^{iv} Although the desired product **145** was formed, it was in low yield (< 50%) and purification was not satisfactory. Also, the stability of the *tert*-butyl ether means that reasonably strongly acidic conditions are required for its removal,^{75(a)} and hence it was not considered ideal for the orthogonal protection strategy.

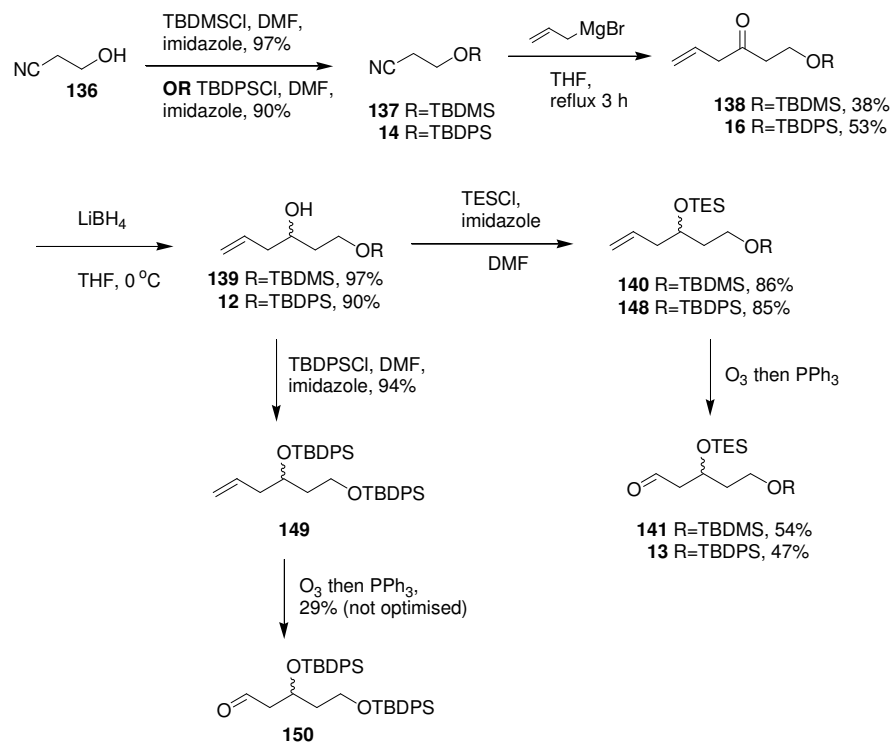


Scheme 2.4. Alternative protection reactions of 3-hydroxypropionitrile.

The tetrahydropyranyl (THP) ether **146** was prepared in good yield of 80%, by treatment of **136** with 3,4-dihydro-2-*H*-pyran and AlCl₃·6H₂O.⁷⁶ Although **146** was shown to be stable to the Grignard reaction workup conditions for a prolonged period, the Grignard reaction of **146** did not give better results than with the silyl ether **137**. The Cu(I)-catalysed Grignard reaction was also attempted, in the hope that the THP ether would be more stable to the conditions than the silyl ethers, but again, unsatisfactory results were obtained (low yield and quality of product). This was perhaps fortuitous, since the NMR spectra of the subsequent products would have been complicated due to the presence of the diastereotopic THP group.

^{iv} This reagent was prepared according to literature procedure⁷⁴ by treatment of *tert*-butyl alcohol with KO^tBu and trichloroacetonitrile.

Finally, the *para*-methoxybenzyl (PMB) ether **147** was prepared.^{76(b)} Initially, this was attempted with excess NaH as base, resulting in a polymeric brown mass. This was attributed to deprotonation of both the alcohol and the acidic proton α - to the nitrile, resulting in polymerisation *via* attack of the carbanion on the nitrile group of a second molecule. Alternatively, attack of the alkoxide ion on the nitrile could also lead to polymerisation. With 0.95 equivalents of KO^{*t*}Bu as the base, better results were obtained. Although the yield of **147** was still low at approximately 40% (this was partly attributed to poor quality reagent), the material was carried through to the Grignard reaction, run in THF at ambient temperature overnight. The product was not rigorously purified but carried through the reduction to **72**, with a 30% yield over the two steps. This was comparable to the yields obtained with the TBDPS protected analogue, **14**. Alcohol **72** was protected with TESCl and the resultant silyl ether **73** used in the deprotection trial (discussed below). However, since PMB did not confer any great advantage over TBDPS and the initial protection step had been difficult, this approach was not pursued further.



Scheme 2.5. Racemic synthesis, final version.

The next step in the synthesis, reduction of the ketone to provide the alcohol **139** (or **12**), was straightforward. Sodium borohydride and LAH could be used, with yields of 70% – 80%, but the best results were obtained with lithium borohydride at 0 °C for 30-40 minutes (scheme 2.5). This reagent was available in the laboratory as a solution in THF, which made it very easy to use, and clean product was obtained in high yield (97% for **139**). As already mentioned, the reduction could be carried out on relatively impure starting material, and purification of the alcohol was fortunately much easier than purification of the ketone. The alcohols **139** and **12** were protected with triethyl silyl (TES) chloride, also in high yield, to provide **140** and **148** respectively (scheme 2.5), and then subjected to ozonolysis.

Adventures with ozonolysis

The final step of the synthesis was ozonolysis of the alkene **140** (or **148**) and subsequent reductive workup with DMS. The first ozonolysis reaction, done on **140**, used the ozoniser available at Industrial Research Limited (IRL). The yield from this reaction was only 54%, but there were high hopes that this could be easily improved, and an ozoniser was purchased by the research group at VUW – an Envirozone V.T-2A (produced and marketed by Ozone Technologies, Napier, N.Z.). Anticipating that **141** would soon be readily in hand for aldol studies, ozonolysis of **140** was embarked upon. Unexpectedly, the initial attempts using the new machine were extremely disappointing. Significant amount of both **140** and **13** were destroyed in attempts to optimise the reaction conditions.

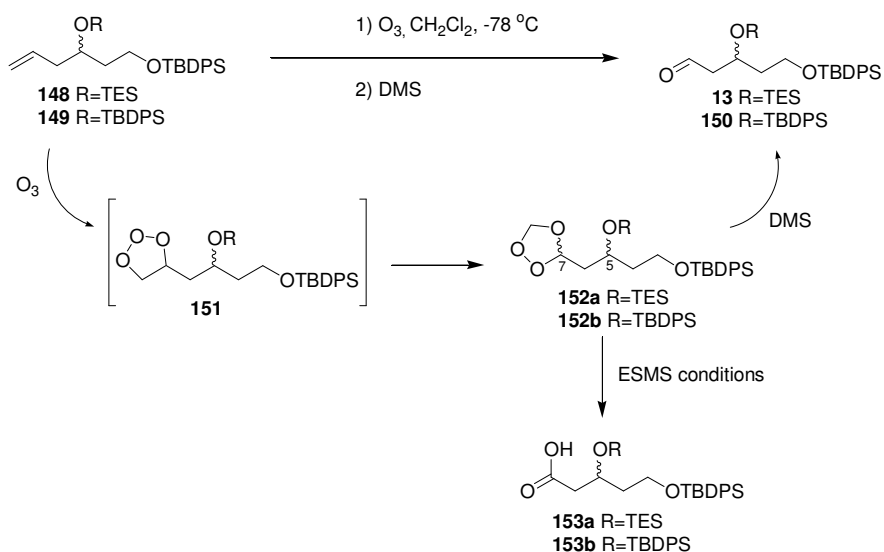
The problems encountered were threefold. Firstly, the new ozoniser appeared to be tearing apart the molecules – the TES group was certainly lost, and unexpectedly the TBDMS and TBDPS groups were also cleaved to some degree. Other degradation may also have been taking place. Starting material **148** was found to be somewhat more robust to the conditions, but yields were still very poor (< 30%). After numerous experiments, it was realised that a very short burst of ozone from the new machine was sufficient to effect complete reaction

of the alkene, and that prolonged reaction times led to the degradation. This was surprising, because ozonolyses are usually continued until either a blue solution is observed (indicating excess ozone in CH₂Cl₂ solution) or until a red indicator dye, Sudan III, decolourises (also indicating excess ozone present). In our case, if the ozone was allowed to flow until those observations were made, essentially complete degradation of the molecule was observed. In addition to reducing the time that the ozone was bubbled into the reaction, consultation with a technician from Ozone Technologies revealed that the ozoniser incorporated a preset function that turned off the ozone generation when the oxygen flow into the machine dropped below a certain level. This was reset so that a minimum flow rate could be used. The resultant reduction in the 'aggressiveness' of the ozone stream significantly improved the yield that could be obtained in the ozonolysis reaction. Careful experimentation with the lower flow rate led to the ability to predict the number of seconds of ozone flow required to convert a given amount of starting material **148** (up to ca. 400 mg).

Secondly, the formation of a persistent side product was encountered. This product was first isolated from an ozonolysis of **149**, prepared during the attempts to optimise the ozonolysis because it lacked the labile TES group. For example, when 185 mg of **149** was subjected to bubbling ozone for 70 seconds, 50 mg of product **150** was obtained together with 117 mg of the by-product. ¹H, ¹³C and COSY NMR analysis of the by-product revealed it was similar in structure to the starting material, retaining both the TBDPS protecting groups and with the C-3 to C-6 portion of the molecule intact. After this, the analogous by-product was also noted in reactions of **140** (the TES/TBDPS protected variant), and it was even identified in the ¹H NMR of the crude product of the first reaction, which had been conducted using a different ozoniser. Varying the reaction time or workup time did not appear to affect whether the by-product was formed. However, it was found that the byproduct was not observed when PPh₃ was used in place of DMS. Hence, the use of DMS was abandoned and PPh₃ was adopted for all ozonolysis workups. Together with the modified flows discussed above, this change allowed ozonolysis of up to ca. 250 mg of alkene with good results and yields routinely > 80%. However by the time that this level of control

was obtained, the enantioselective synthesis was being used (see the next section), so yields for ozonolysis of the racemic fragment are relatively low.

The by-product was tentatively identified as being the intermediate ozonide, **152** (scheme 2.6). In the ozonolysis reaction, the intermediate molozonide (**151**) is produced by addition of ozone to the double bond. The molozonide then rearranges to form the ozonide (**152**), which is treated with DMS in a reductive workup to give the ketone. Ozonides are typically not very stable, but can be isolated. The fact that the by-product was only observed when DMS was used in the workup adds weight to the argument for the by-product being **152**; DMS is volatile and may have been lost from the reaction mixture before all of the ozonide had reacted. Molecule **152** contains two stereogenic centres, and four diastereomers are therefore possible (as two enantiomeric pairs; 1,3-*syn* or 1,3-*anti* between C-5 and C-7). In the ^{13}C NMR spectrum of the by-product, the signals are paired, suggesting two diastereomers are present. The ESMS spectrum of the by-products did not show a signal corresponding to **152a** or **152b**, but did show signals at m/z 509.2 and 633.3, respectively. These correspond to the carboxylic acids **153a** and **153b** ($+\text{Na}^+$), which are likely degradation products of **152a** and **152b**.



Scheme 2.6. Ozonolysis of **149**, showing the formation of by-product **152**.

The third major problem was encountered when attempting to scale up the procedure. In every case, when an ozonolysis of greater than approximately 300 mg of **148** was attempted, decreased yields and increased levels of by-products were observed, or, if a shorter burst of ozone was used, incomplete conversion. Modifications such as adjusting the flow, increasing the dilution, or adjusting the time of the reaction did not alleviate the problems. An answer to this problem was not exhaustively pursued, partly because the 'large' scale destruction of the starting material was hindering progress in the subsequent aldol reaction studies, and partly because, at this stage, there was no need to form large amounts of **13**. In any case, although it was found that the aldehyde could be stored for short periods (up to a week) under argon in the freezer, best results were always obtained in the aldol reactions when the aldehyde was freshly prepared, ideally on the same day as the aldol reaction. Hence, the preparation of large amounts of aldehyde at one time was not desirable.

Deprotection trial

At this point a short study was conducted to ensure that the TES group could be reliably removed without loss of the primary hydroxyl protecting group. This would be necessary at a later stage in the synthesis, and it was considered prudent to do this trial using the alkenes **140**, **148** and **73** rather than the corresponding aldehydes, which were less readily available. The results of this trial are shown in table 2.1 (in which A is starting material, B is the desired product, and C is the unwanted diol **154**). As expected, removal of TES group without cleavage of the TBDPS group⁷⁷ (entries 4-7) or the PMB group^{76(c)} (entries 8-10) was easy. Both were achieved in either THF-H₂O or MeOH-H₂O, with catalytic pTsOH. Removal of the TES group in preference to TBDMS was more difficult, with mixtures of products being obtained (entries 1-3). Although this trial was by no means exhaustive,^v this did add weight to the decision to

^v A review has been published⁷⁷ covering the selective deprotection of silyl ethers, in which the TBDPS group is described as one of the most stable silyl protecting groups available. For example, the half-life of hydrolysis of 1° TBDPS in 1% HCl/MeOH at 25 °C was reported to be 225 min, while the half-life of the TBDMS ether under the same conditions was ≤ 1 min.

switch to using TBDPS rather than TBDMS as the group used to protect the primary hydroxyl moiety.

Table 2.1. Selective deprotection of the TES group of **140**, **148** and **73**.

<div style="display: flex; justify-content: space-around; align-items: flex-start;"> <div style="text-align: center;"> 140 R=TBDMS 148 R=TBDPS 73 R=PMB A </div> <div style="text-align: center;"> 139 R=TBDMS 12 R=TBDPS 72 R=PMB B </div> <div style="text-align: center;"> 154 C </div> </div>			
Entry	Substrate	Conditions	Ratio of products A:B:C
1	140	THF-H ₂ O 9:1, RT, 10 min, 5 mol % pTsOH	0 : 1 : 1
2	140	MeOH-H ₂ O 9:1, RT, 10 min, 5 mol % pTsOH	0 : 0 : 1
3	140	MeCN-H ₂ O 9:1, RT, 5 min, 5 mol % DDQ	0 : 1 : 1
4	148	THF-H ₂ O 9:1, 0 °C, 5 min, 5 mol % pTsOH	1 : 4 : 0
5	148	THF-H ₂ O 9:1, RT, 40 min, 5 mol % pTsOH	0 : 1 : 0
6	148	MeOH-H ₂ O 9:1, 0 °C, 5 min, 5 mol % pTsOH	1 : 20 : 0
7	148	MeOH-H ₂ O 9:1, RT, 40 min, 5 mol % pTsOH	1 : 50 : 0
8	73	THF-H ₂ O 9:1, RT, 5 min, 5 mol % pTsOH	1 : 10 : 0
9	73	MeOH-H ₂ O 9:1, RT, 5 min, 5 mol % pTsOH	1 : 20 : 0
10	73	MeOH-H ₂ O 9:1, RT, 1.5 hr, 5 mol % pTsOH	1 : 50 : 0

Summary

The racemic synthesis of the C-3 to C-7 aldehyde (scheme 2.5) gave **141** in a yield of 17% and **13** in 17% over five steps. Aside from the relatively low-yielding Grignard reaction with a difficult purification, this route is straightforward and can provide useful quantities of the aldehyde from readily available, inexpensive starting materials. Work towards the key aldol reaction forming the C-7 to C-8 bond (described in chapter three) could now be initiated, while work on an enantioselective synthesis of the C-3 to C-7 aldehyde also began.

2.2 Enantioselective synthesis

2.2.1 Strategy One

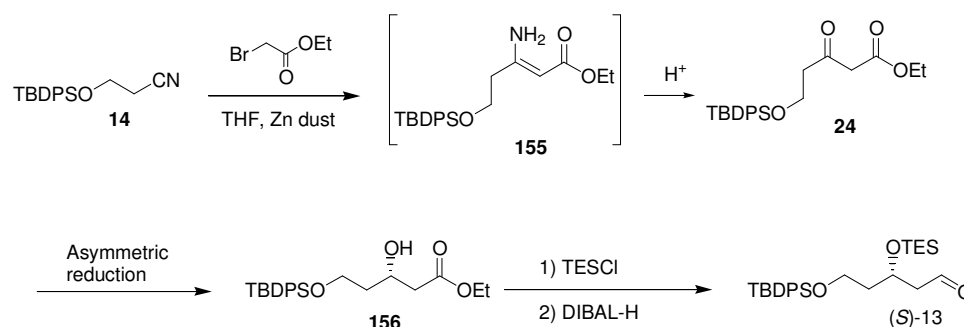
The first strategy that was investigated for an enantiomerically selective synthesis of the C-3 to C-7 fragment was the inclusion of an asymmetric reduction of the ketone in the racemic synthesis described in section 2.1.2. A number of literature methods were investigated for this reduction, such as a reduction with ruthenium-BINAP complex and H₂, as reported in the literature.⁴³ The use of L-*N,N'*-di(benzoyl)cystine as a ligand with sodium borohydride as the reducing agent was also considered. The ligand was prepared⁴¹ and the reduction of **16** conducted⁴² according to literature procedures, to give **12** in moderate yield (ca. 40%). The enantiomeric excess of the product was not measured, chiral GC was unavailable at that time at VUW, and in any case, the low yield prompted investigation of other potential enantioselective routes instead.

2.2.2 Strategy two

Although the potentially versatile nitrile-based route was not completely abandoned, the need to obtain quantities of the C-3 to C-7 aldehyde prompted a search for an enantioselective literature method to reliably prepare the aldehyde for use in aldol reaction studies.

The addition of a zinc ester enolate (formed from ethyl bromoacetate and zinc metal), to the nitrile was considered. Such additions, to form β -keto esters, were first reported by Blaise in 1901.⁴⁷ This would yield the β -keto ester **24**, which could then be subjected to asymmetric reduction to give **156**, followed by protection of the hydroxyl moiety, and finally reduction of the ester to the aldehyde **13** as shown in scheme 2.7. An advantage of using a Blaise reaction in this synthesis is that it is possible to isolate either the β -keto ester **24** or the initially formed β -amino- α,β -unsaturated ester **155**. Therefore, as with the Grignard route, this approach would still allow access to the nitrogen-containing

analogues of peloruside A (as discussed in chapter one). This potentially useful reaction has not been widely applied in the literature, with problems of low yield, narrow scope and competing side reactions. A Blaise reaction has been employed to prepare the TBDMS (rather than TBDPS) protected analogue of **24**.⁷⁸ No yield was reported, but the route was described as ‘unsatisfactory’ by a group attempting to repeat the synthesis,⁷⁹ who ultimately used an alternative route.



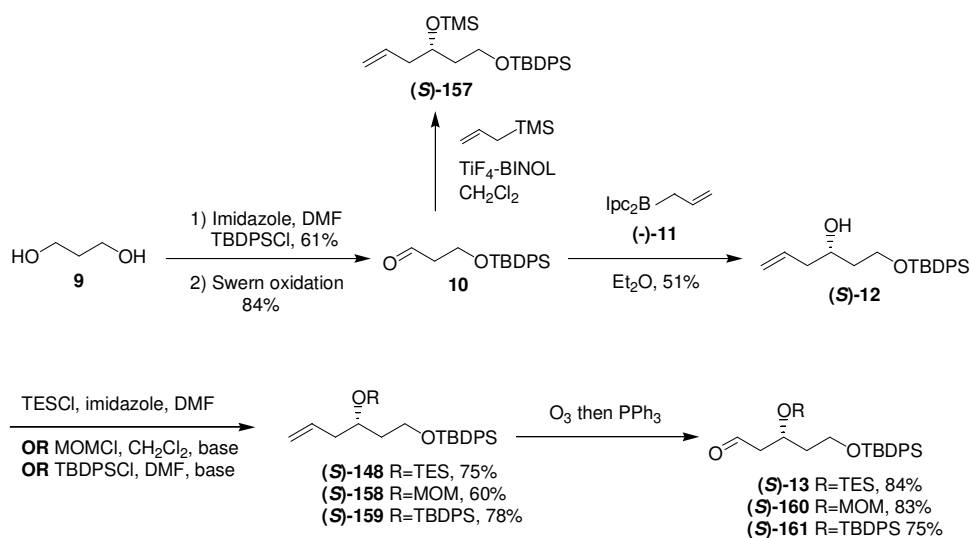
Scheme 2.7. Proposed route to key fragment **13** employing a Blaise reaction.

A modified method for carrying out a Blaise reaction, published by Hannick and Kishi,⁸⁰ reported substantially improved yields of α -monosubstituted β -keto esters compared to previous literature results. The method differs from the usual Blaise reaction in that it employs THF as solvent, uses *activated* zinc dust, and the α -bromoester is added over 30-60 minutes rather than in one portion. A sonochemical Blaise reaction has been reported⁸¹ to successfully prepare both α -monosubstituted and α -disubstituted β -keto esters. Another variation, in which TMS-Cl was used as a catalyst, was reported by Johnson *et al.*⁸² The methods of Hannick and Kishi and of Johnson were both used in attempts to prepare **24** in the course of this work, but the reported improvements could not be reproduced. Unfortunately, low yields and product mixtures that were very difficult to purify were obtained, and hence the Blaise reaction route was subsequently abandoned.

2.2.3 Strategy three

There are a number of published methods for the asymmetric allylation of aldehydes such as **10**. Since a large supply of the nitrile **14** was available, the

preparation of **10** was attempted *via* reduction of the nitrile using DIBAL-H. Although good results have been reported in the literature, this reaction could not be driven to completion, and efficient separation of **14** and **10** was difficult. An alternative preparation of **10** from 1,3-propane diol **9** by monoprotection with TBDPSCl and then a Swern oxidation (scheme 2.8) was found to be more facile. The low yield of 61% in the protection step was due to formation of significant amounts of the di-protected analogue. Allylation of **10** with TiF₄-BINOL and TMS-allyl⁸³ to give **157** (scheme 2.8) was briefly considered; however Brown's boron mediated allylation procedure using *B*-allyldiisopinocampheylborane (**11**) was settled upon as the most suitable method in this case.

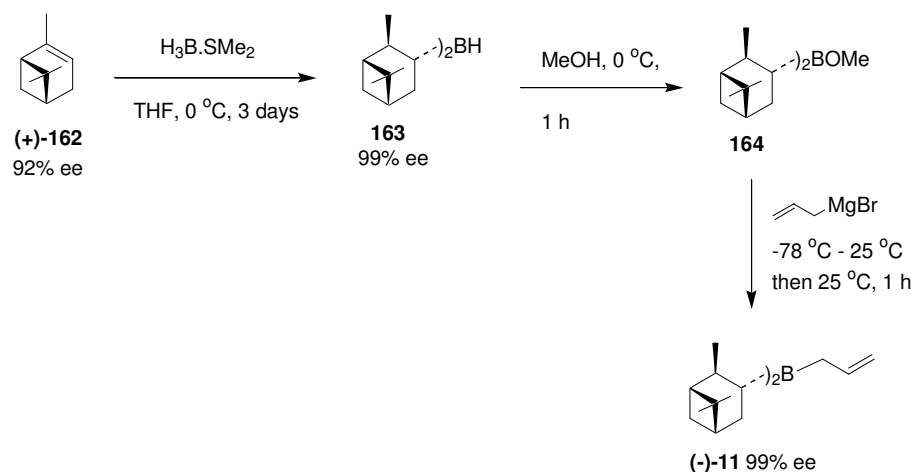


Scheme 2.8. Enantioselective synthesis of the C-3 to C-7 fragment.

Preparation of the *B*-allyldiisopinocampheylborane reagent (**11**),^{38,39} although a somewhat lengthy preparation that required rigorously dry conditions, was successfully carried out several times on 50 mmol scale during this work (scheme 2.9).^{vi} The reagent was prepared from the commercially available and relatively stable borane-methyl sulfide complex and either (+)- or (-)- α -pinene (**162**) of 92% enantiomeric purity. Following hydroboration of the α -pinene, the diisopinocampheylborane (**163**) is equilibrated in THF with 15% excess α -pinene

^{vi} The experimental procedure for the preparation of *B*-allyldiisopinocampheylborane is described in chapter eight, being a slightly modified version of that published in the literature.^{38,39}

at 0 °C for three days, during which time the major isomer is selectively incorporated into the reagent, to give an enantiomeric purity (percentage of one enantiomer incorporated in the reagent) in excess of 99%. This is followed by methanolysis of **163** to give **164**, and subsequent reaction with allylmagnesium bromide at ambient temperature for one hour to yield the desired *B*-allyldiisopinocampheylborane, **11**. Salts were filtered out and solvents removed under argon, the reagent was then dissolved in dry diethyl ether and kept under argon in a Schlenk flask. It could be stored in this way for several weeks before use.



Scheme 2.9. Preparation of (-)-*B*-allyldiisopinocampheylborane ((-)-**11**) from (+)- α -pinene ((+)-**162**).

Both (+) and (-)- α -pinene were used to make the reagent during the course of this work, allowing selective access to either of the two enantiomers of the alcohol **12**.^{vii} Use of (+)-*B*-allyldiisopinocampheylborane (prepared from (-)- α -pinene) yields the alcohol with the *R*- configuration, and use of the reagent prepared from (+)- α -pinene yields the alcohol with the *S*- configuration (scheme 2.8).⁴⁰ The allylation reaction itself is straightforward, with the only real drawback being that the by-product from the reaction co-elutes with the product in flash column chromatography. Fortunately, alcohol **12** is very stable, and a crude purification of the product (by passing through a short plug of silica) was

^{vii} Both were prepared because when the total synthesis of peloruside A was published, and the stereochemistry of the natural isolate thereby revealed, it was demonstrated that the original synthetic plan would prepare the unnatural enantiomer.

sufficient to prevent degradation upon storage. Smaller amounts of **12** were purified by more careful flash column chromatography as they were required.

The free hydroxyl group of **12** was initially protected with the triethyl silyl (TES) protecting group to give **148**, as part of the orthogonal protection strategy described in the introductory chapter. The protection step proceeded readily in good yield, and the subsequent ozonolysis, once the problems described in the previous section had been ironed out, was also reasonably straightforward, proceeding with yields upwards of 85%. Hence, the chiral C-3 to C-7 aldehyde **13** was prepared in a total of five steps in an overall yield of 17% from propanediol (equivalent yields were obtained for the preparation of (*R*)-**13** and (*S*)-**13**) as shown in scheme 2.8.

As is discussed in the next chapter, aldehyde **141** was susceptible to elimination in the subsequent aldol reaction with ketone **7**. This observation led to the preparation of the potentially more stable MOM and TBDPS containing analogues, aldehydes **160** and **161** (in 13% and 15% overall yields respectively, scheme 2.8). Both the MOM and the TBDPS protection reactions were successful, and the subsequent ozonolyses of **158** and **159** proceeded in similar yields to the ozonolysis of the original TES-protected **148** (see scheme 2.8).

The ^1H NMR spectrum of **13** is shown in figure 2.1 (overleaf), with the 1.5 – 2.2 ppm region of the spectra of **160** and **161** shown in the insets. The signals attributed to the methylene protons on C-4 (β to the protected primary hydroxyl group) appear in this region. Interestingly, as the size of the protecting group of the secondary hydroxyl at C-5 increases, the degree that the enantiotopic protons of the methylene moiety are split increases. This reflects the bulk of the TBDPS at O-3, which is so large that the molecule cannot freely rotate about the bonds between C-3 and C-5. This is further observed in the spectrum of **160**, where the signal due to the methylene protons of the MOM group is also split, into two doublets at 4.67 and 4.61 ppm, coupling to each other with $J = 7.1$ Hz. Even this relatively small protecting group's conformation is

Figure 2.1. ^1H NMR spectrum of aldehyde **13**, with (insets) portion of the ^1H NMR spectra of **160** and **161**.

affected by the proximity of the large TBDPS protecting group. In the ^{13}C NMR spectrum of **13**, the two phenyl groups of the TBDPS group give two sets of signals, indicating that they are not equivalent. This is presumably because the TBDPS group cannot freely rotate. In the spectrum of **160**, the two phenyl groups give rise to only one set of signals. The smaller MOM group present in **160** allows the TBDPS to rotate more freely.

2.3 Summary

Racemic variants of the C-3 to C-7 fragment **141**, **150** and **13**, containing different protecting groups, were successfully prepared from hydroxypropionitrile over five steps (protection, Grignard reaction, reduction, protection and ozonolysis) in an optimal overall yield of 31% for **13**. All steps of this synthesis proceeded in excellent yield except the Grignard reaction step. There is still potential for elaborating this synthetic route by incorporating an asymmetric reduction, and hence providing a new and versatile route to enantiopure variants of the C-3 to C-7 fragment **8**.

Both enantiomers of the C-3 to C-7 fragment have also been prepared via literature methods from 1,3-propanediol, with an asymmetric allylation using (+)- or (-)-*B*-allyldiisopinocampheylborane as the key reaction setting the crucial stereochemistry at C-5. An overall yield of 17% for either enantiomer of the TES-protected fragment **13**, and 15% for the analogous MOM-protected fragment **149** were obtained.

Both the racemic and the chiral aldehydes described in this chapter were used in the aldol reaction studies discussed in chapter three.

Towards the C-3 to C-11 Pyranose Ring Fragment

This chapter is an account of the work done towards the synthesis of the C-3 to C-11 fragment of peloruside A (figure 3.1). As described in chapter one, the synthetic plan was based on an aldol reactionⁱ between the key fragments **7** and **8**. Hence the work described herein is largely concerned with aldol reactions of fragment **7**, and of a variant thereof with MOM protecting groups, **188**. The elaboration of the aldol products and the progress made towards the formation of the pyranose ring is described and finally a consideration of the future work required to complete the synthesis of peloruside A is presented.

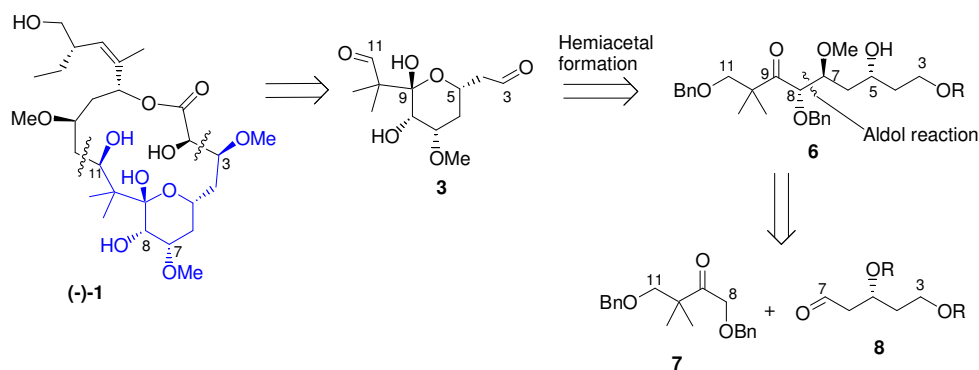


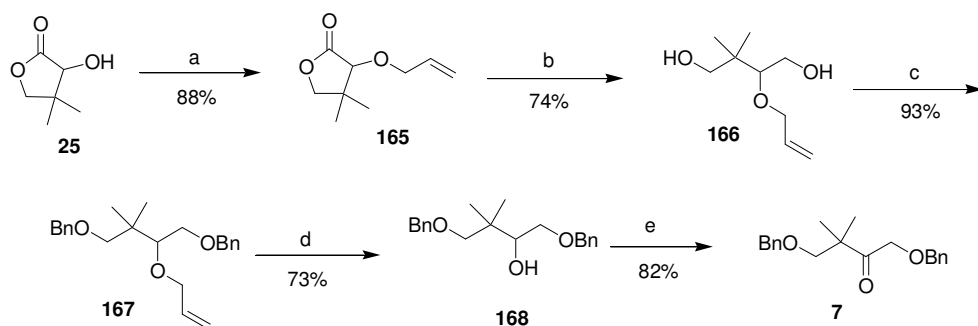
Figure 3.1. Peloruside A, with the retrosynthesis of the C-3 to C-11 fragment.

3.1 Preparation of the C-8 to C-11 ketone, **7**, on large scale

A synthesis of the *gem*-dimethyl ketone fragment **7**, developed by Dr. Bridget Stocker (scheme 3.1), is described in her PhD thesis.⁴⁸ As significant quantities of **7** were required for the work described in this chapter, a scale-up of the synthesis shown in scheme 3.1 was undertaken. The experimental for this scaled up synthesis is presented in chapter eight, and a brief overview follows.

ⁱ As in chapters one and two, the numbering of fragments throughout this chapter relates to the numbering of peloruside A itself (rather than the IUPAC numbering of individual fragments).

The allylation of racemic pantolactone **25** was undertaken on a 10 g scale, and a yield of 88% (equivalent to those obtained on smaller scale) was obtained. The subsequent reductive ring opening of **165** to give **166** incorporates what is undoubtedly the most troublesome part of this synthesis – a slow, difficult filtration of the reaction mixture through a celite/silica plug during the workup. This step proceeded in a yield of 74%, slightly lower than expected based on smaller scale experiments. This was attributed to poor product recovery (in the filtration) rather than incomplete conversion or formation of side products. The benzylation step initially did not go to completion. Inadequate washing of the NaH (done to remove the mineral oil that is 40% of the weight in the jar) and consequently not having enough NaH present was part of the reason for this, but did not entirely explain this result. Fortunately, resubmission of the mono-benzylated material to the reaction conditions resulted in a total yield of 93% of **167**. The subsequent deprotection of the allyl protecting group was plagued by the fact that the catalyst, Pd(PPh₃)₄, had a limited shelf life once opened – often, more catalyst was required than the original experimental procedure called for, longer reaction times were required, and lower than expected yields were obtained. Finally, the oxidation proceeded smoothly to give **7** in a very good yield of 82%. The overall yield of **7** over the five steps, from 10 g of pantolactone, was 38%.



Scheme 3.1. Synthesis of *gem*-dimethyl ketone fragment **7**. Reagents and conditions: a) KO^tBu (1 eq), DMF-THF, 0 °C, 30 min; then allyl bromide, RT, 14 h; b) LAH (1.5 eq), THF, reflux, 3 h; c) NaH (5 eq) DMF, 0°C, 30 min; then BnBr (2 eq), RT, 14 h; d) Pd(Ph₃)₄, *para*-toluenesulfonic acid, THF, RT, 6 h; e) PDC, AcOH, 3 Å molecular sieves, CH₂Cl₂, 3 h.

3.2 Model aldol reactions of the *gem*-dimethyl ketone fragment, **7**

Early on in the work done towards an asymmetric aldol reaction with **7**, and particularly because of the difficulties experienced making variants of aldehyde **8**, it was decided to perform some model aldol reactions. Benzaldehyde was chosen as a substrate to gain some understanding of the reactivity of the enolate of **7**. Reactions were carried out with lithium enolates of **7**; boron enolates of **7**; and Mukaiyama aldol reactions of the trimethylsilyl enol ether of **7**, **169** (the preparation of which is discussed in section 3.2.3). The results are summarised in table 3.1.

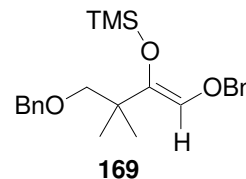


Table 3.1. Results of aldol reactions of **7** and **169** with benzaldehyde.

Entry	Substrate	Conditions	Yield	<i>Syn</i> :- <i>anti</i> -
1	7	LDA	65%	14:1
2	7	LiTMP	55%	13:1
3	7	LDA then Ti(OiPr) ₄	59%	4:1
4	7	BF ₃ .OEt ₂	**	-
5	169	BF ₃ .OEt ₂	**	-
6	7	Cy ₂ BCl	42%	1:4
7	7	ClB(Ipc) ₂	No reaction [†]	-
8	7	Cy ₂ BOTf	60%	>20:1
9	169	TiCl ₄	33%	1:3
10	169	Ti(OiPr) ₄	No reaction [†]	-

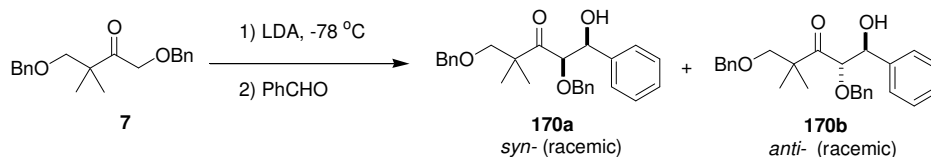
** A myriad of spots were observed in TLC analysis; degradation of starting materials was assumed and neither a meaningful yield nor a product ratio could be determined.

[†] Even after overnight reaction at room temperature, only starting materials were recovered.

3.2.1 Lithium enolates - LDA and LiTMP

An aldol reaction between **7** and benzaldehyde can give two possible diastereomeric products, each present as a racemic pair of enantiomers (scheme 3.2). At this stage, attention was focussed on achieving an *anti* aldol product in line with the retrosynthetic analysis presented in chapter one, so formation of an

excess of one *diastereomer* (rather than one enantiomer) was the initial focus of this work.



Scheme 3.2. Aldol reaction of **7** with benzaldehyde to give **170**.

The lithium enolate of **7** (formed using LDA) probably forms by way of a six-centred, lithium-chelated transition state as shown in scheme 1.8 (pg 18, chapter one).⁸⁴ Due to the large steric bulk of the *gem*-dimethyl groups α - to the carbonyl group, formation of the *Z* enolate is favoured^{53,54} (as discussed in chapter one) and its subsequent reaction, also *via* a six-membered transition state, gives the *syn*-aldol product as the major diastereomer. In the reaction of **7** with LDA and benzaldehyde, a yield of 65% was obtained, with a *syn:anti* product ratio of 14:1 (see table 3.1 above).ⁱⁱ

The assignment of the aldol products **170** as *syn*- or *anti*- was supported by analysis of the coupling constants between H^b and H^a (see figure 3.2 on the following page). There is considerable literature precedence demonstrating that β -hydroxy carbonyl compounds such as **170** exist in an intra-molecularly hydrogen-bonded chair conformation, and that the coupling constant between H^a and H^b (α - and β - to the carbonyl group, see figure 3.2) can hence be used to differentiate between the *syn*- and *anti*- diastereomers.^{85,86} The chair conformer that minimises axial interactions will dominate, and hence it is expected that $J_{ab}(\text{anti-}) > J_{ab}(\text{syn-})$.⁸⁵ In this case, **170a** (the *syn*- diastereomer) has J_{ab} of 4.2 Hz, consistent with the expected coupling for vicinal axial-equatorial protons in six-membered rings, while **170b** (the *anti*- diastereomer) has J_{ab} of 7.3 Hz, a considerably larger coupling constant consistent with the expected coupling for vicinal axial-axial protons. An interesting observation was made in the ^1H NMR spectra of **170a** and **170b**. In some cases, the signal for proton H^b appeared as a doublet (coupling to H^a) while sometimes H^b was also coupled to H^c (the alcoholic proton) with a coupling constant $J = 5.4$ Hz, so that the signal due to H^c

ⁱⁱ The *syn:anti* diastereomeric ratios were determined by inspection of the ^1H NMR spectra.

at 3.22 ppm appeared as a doublet and the H^b signal as a doublet of doublets, appearing as a pseudo-triplet (see figure 3.3). This was attributed to the hydrogen bonding between H^c and the carbonyl oxygen (figure 3.2) locking the molecule into a conformation containing a six-membered ring and slowing down exchange of the hydroxyl proton H^c .

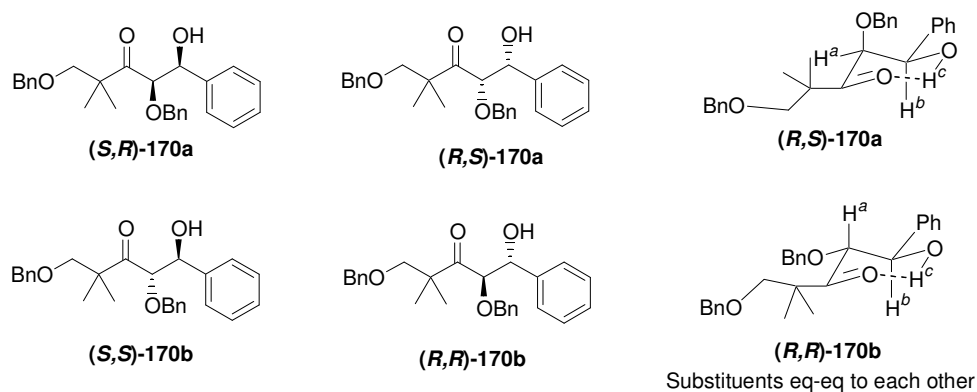


Figure 3.2. The four possible isomeric products, and chair conformations resulting from hydrogen-bonding.

When lithium 2,2,6,6-tetramethylpiperidide (LiTMP) was used in place of LDA, an essentially equivalent *syn:anti* ratio of 13:1 was obtained, in a slightly lower total yield of 55% (table 3.1, entry 2). This indicates that the 1,3-diaxial interactions between the dimethyl groups of the base and the OBn group of **7** were not large enough to force the OBn group to an equatorial position in the cyclic six-membered transition state during enolate formation as had been hoped (see scheme 1.8, page 18). The *gem*-dimethyl groups of **7**, therefore, have a dominant effect on the arrangement of the transition state, their bulkiness precluding an equatorial orientation for the OBn group in the transition state and hence precluding the formation of an *E* enolate. In fact, it has been reported that in some cases the use of LiTMP in place of LDA can enhance the selectivity of aldol reactions to give higher *syn:anti* ratios of aldol products.⁸⁷

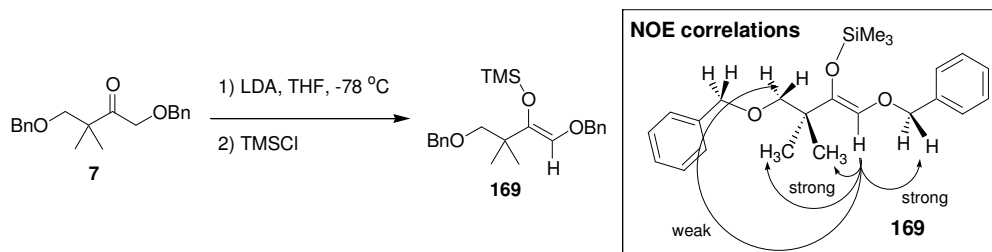
Titanium enolates may be formed by addition of titanium complexes to pre-formed lithium enolates.^{88(a)} The addition of 1 mol equivalent of $Ti(OiPr)_4$ to Li enolates (formed with LDA) and subsequent successful addition of the enolates to a variety of systems has been reported. When the titanium enolate of

Figure 3.3. ^1H NMR spectrum of **170b** with (inset) portions of the spectrum of **170a** with and without coupling to the hydroxyl proton.

7 was prepared according to the described procedure,⁸⁹ and then reacted with benzaldehyde, a reasonably good 59% yield was obtained, with a *syn:anti* ratio of 4:1. Although the reaction was tried using aldehyde (*S*)-**160** (described below) these conditions were not pursued.

3.2.2 Mukaiyama aldol reactions

Given the attention that has been focussed on the development of asymmetric catalysts for aldol reactions using silyl enol ethers of ketones (the Mukaiyama aldol reaction),^{90,88(b)} the trimethyl silyl enol ether **169** was prepared for aldol studies. The enolate of **7** was formed using LDA, and then trapped with TMSCl to give **169** (scheme 3.3), which was surprisingly stable and able to be purified by column chromatography. The reaction proceeded in excellent yield and with good *Z/E* selectivity (only one product could be detected by ¹H NMR). The ¹H NMR spectrum of this material showed a distinctive series of singlets – the alkene proton at 5.67, and the three methylene groups at 4.70, 4.51, and 3.26 ppm. The stereochemistry of **169** was determined to be *Z* by NOE experiments. Positive NOE correlations were observed between the vinyl proton and the *gem*-dimethyl groups (at 1.02 ppm), and between the vinyl proton and the methylene group at 4.70 ppm (scheme 3.3). This is consistent with the *Z* alkene geometry. A very weak interaction was also seen between the alkene and the methylene group α - to the *gem*-dimethyl group, the signal for which appears significantly upfield of the benzyl methylene groups, at 3.26 ppm. No interaction was observed between the vinyl proton and the methyl groups of the trimethyl silyl moiety.



Scheme 3.3. Preparation and NOE analysis of trimethylsilyl enol ether **169**.

The Mukaiyama aldol reaction of **169** catalysed with titanium tetrachloride was initially attempted in THF. In this solvent, the mixture of

benzaldehyde and Lewis acid resulted in a thick gelatinous precipitate. Changing the solvent to CH_2Cl_2 resulted in some improvement, with a mobile slurry being formed rather than a gelatinous precipitate. Under these modified conditions, a 33% yield of aldol product was obtained and as had been hoped, the *anti*- aldol product was formed as the major product, in a ratio of 4:1 *anti* to *syn*.

These observations are consistent with those of Heathcock *et al.*⁵³ who obtained 'preparatively useful' ratios of the *anti*- diastereomers from the aldol reactions of the *Z* enol silane formed from ethyl *tert*-butyl ketone. In the reaction with benzaldehyde, using boron trifluoride etherate as catalyst, they obtained *anti* and *syn* aldol products in a 5:1 ratio. With titanium tetrachloride, the products were obtained in a ratio of 9:1. Their rationalisation of these observations was based on an analysis of the unfavourable dipole-dipole and steric interactions present in the staggered transition states of the Lewis acid mediated reaction.

In the case of the titanium tetrachloride catalysed aldol reaction of **169** with benzaldehyde, the staggered transition states shown in figure 3.4 are available. Of these, A3 and B3 are clearly disfavoured by two dipole-dipole interactions: between the oxygen atoms of the approaching aldehyde, and those of the silyl ether and of the benzyl ether of **169**. Conformations A2 and B2 both involve an unfavourable electronic interaction between the oxygen of the

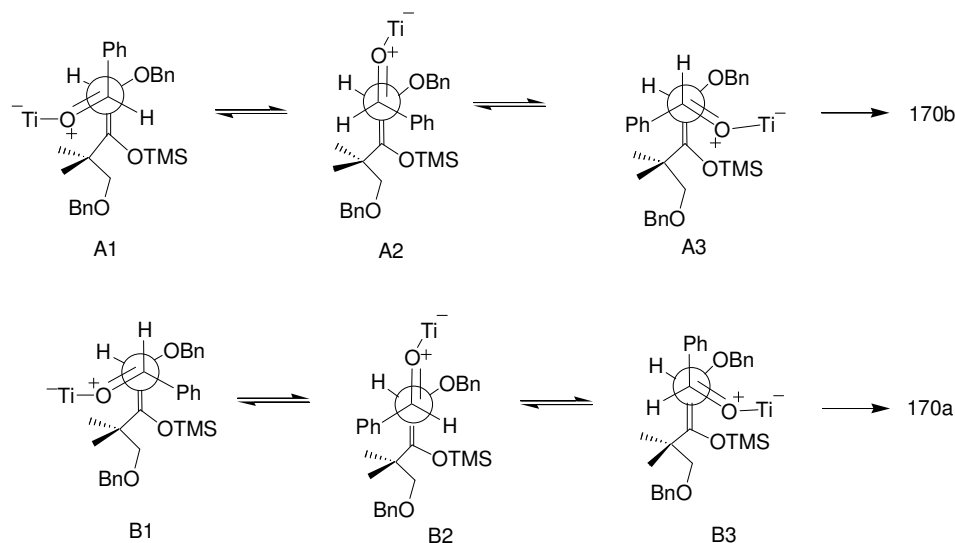


Figure 3.4. Model for the selectivity of the TiCl_4 catalysed aldol reaction of **169**.

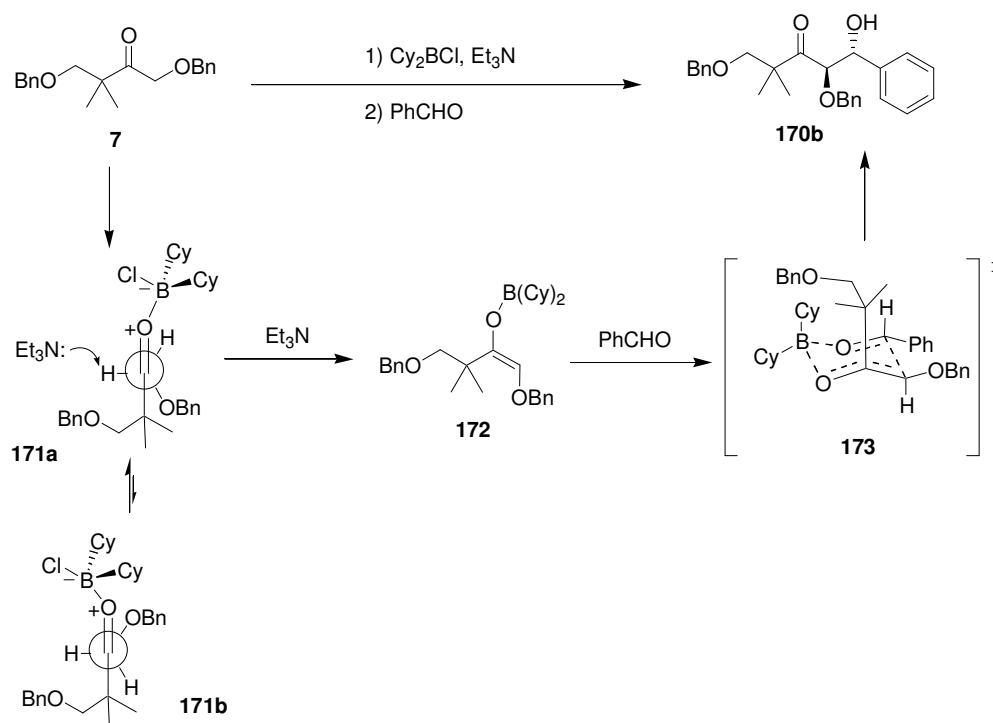
aldehyde, and the oxygen of the benzyl ether, although B2 contains only two significant steric interactions (phenyl group - *gem*-dimethyls and aldehydic oxygen – OBn). Conformation B1 has three destabilising steric interactions. The most favourable of the available conformations appears to be A1, since although it incorporates two major steric interactions (Ph – OBn and aldehydic oxygen – *gem*-dimethyl groups), unfavourable electronic interactions are minimised. Thus, the reaction proceeds to give the *anti*- aldol product **170b**.

The reaction of **169** using other Lewis acids was also attempted. Use of titanium tetraisopropoxide (Ti(O*i*Pr)₄) in place of TiCl₄ (entry 10, table 3.1) gave no reaction, even after prolonged reaction times. In this system, the sterically hindered nature of the ketone seems to be a barrier to reaction, hence the lack of reaction with Ti(O*i*Pr)₄ could be due to the bulky nature of the ⁻O*i*Pr ligands. The Mukaiyama aldol reaction with boron trifluoride etherate was also attempted (entry 5, table 3.1).⁹¹ After addition of the catalyst TLC analysis of the reaction mixture quickly showed several different spots. After workup, the crude product was found to contain significant amounts of ketone **7** (i.e. decomposed starting material), benzaldehyde, and also suspected to contain BnOH (presumably from further decomposition of **7**), and other unidentified spots. Use of this catalyst was not pursued further.

3.2.3 Boron-mediated aldol reactions

The use of enolborinates derived from reaction of ketones with organoborane derivatives (R₂BX, X=leaving group, R=alkyl group) in the presence of a suitable tertiary amine and their use in aldol reactions was introduced by Mukaiyama, who introduced the dialkylboron triflates (R₂BOTf) for this purpose.^{92,93} Dialkylboron chlorides, which are reported to be easier to prepare and handle,^{94(a),94(b)} were developed by Brown, and have been found to be particularly useful for the generation of *E* enolates, although a range of factors influence enolate geometry.^{94,95} The R₂BX reagents used during this work were prepared according to literature procedures for the synthesis of Cy₂BCl,^{94(b)} (Ipc)₂BCl,^{94(b)} and Cy₂BOTf.^{94(d)}

Treatment of a variety of ketones with Cy_2BCl and Et_3N selectively gives *E*-enolates.⁹⁴ In the case of a boron-mediated aldol reaction between ketone **7** and benzaldehyde, conducted using these reagents, the *anti*-aldol product **170b** was isolated as the major product of the reaction. This may be attributed to activation of those α -protons which are *cis*- to the Cl during the formation of the enolate.⁹⁵ Conformation **171a** would be favoured over **171b** (scheme 3.4) because unfavourable dipole-dipole interactions are minimised. The small, unhindered base Et_3N would deprotonate α - to the ketone from **171a**, hence forming the *E*-boron enolate **172**. Upon reaction of enolate **172** with benzaldehyde through six-membered transition state **173** (with the phenyl group of benzaldehyde adopting an equatorial position as shown), the *anti*-aldol product **170b** results.



Scheme 3.4. Formation of *anti*-aldol product (racemic) **170b** with Cy_2BCl .

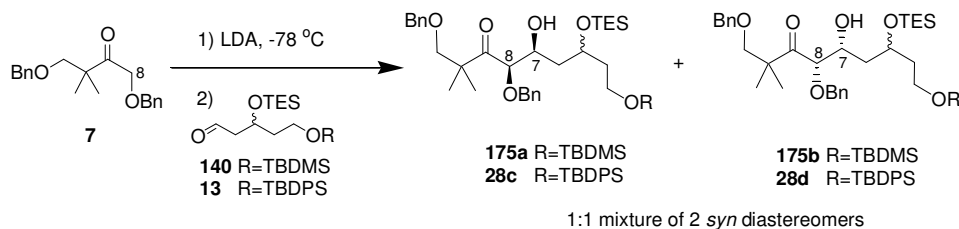
Interestingly, when the aldol reaction between **7** and benzaldehyde was attempted with $(\text{Ipc})_2\text{BCl}$ reagent, no reaction was observed. This is likely to be due to steric factors, in that the Ipc ligands are much bulkier than the Cy ligands and it may be the case that the initial coordination of boron to the ketone (analogous to structure **171**, scheme 3.4) may be sterically disfavoured.

Alternatively, the initial coordination may occur but the subsequent deprotonation be unfavourable due to steric hindrance.

The boron dialkyl triflate reagents on the other hand, generally show a preference for forming *Z*-, rather than *E*-, enolates.⁹⁵ Accordingly, when **7** was treated with Cy₂BOTf and Et₃N in dichloromethane the *Z*- boron enolate was formed, as evidenced by the subsequent treatment with benzaldehyde and isolation of the *syn*- aldol product **170a** as the major product of that aldol reaction.

3.3 Aldol reactions between ketone **7** and the C-3 to C-7 fragment

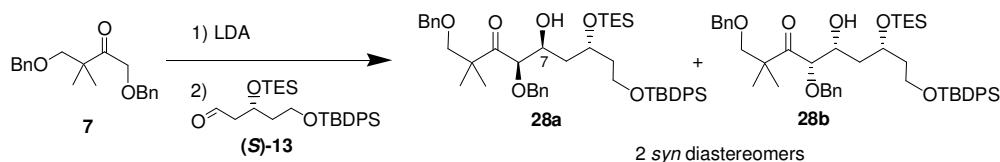
The first attempts to perform an aldol reaction were between **7** and the racemic C-3 to C-11 fragments **140** and **13**. The product of this reaction was presumed to be the 7,8-*syn* diastereomers shown in scheme 3.5; four diastereomers (two pairs of enantiomers) are possible because the stereochemistry at C-5 was not fixed. Although product was observed, and in one case, isolation of a small amount of a *single* (unidentified) diastereomer of the aldol product **28** was achieved,ⁱⁱⁱ in general the results of these reactions were not good, with low yields and poor product recovery, particularly when aldehyde **140** was used. Although in retrospect this was attributed to the inexperience of the author at the time, and particularly to lack of attention to rigorous purification of starting materials, it was noted that the TBDMS-containing **140** was significantly more susceptible to degradation than the TBDPS-containing **13**.



Scheme 3.5. Initial aldol reactions between ketone **7** and racemic **140**.

ⁱⁱⁱ It was later assumed that the other diastereomers had been inadvertently discarded after column chromatography due to inexperience of the author at the time.

With the knowledge gained, when chiral aldehydes (*R*)-**13** and (*S*)-**13** were used in LDA aldol reactions with **7**, better results were obtained. The enolate of **7** was prepared by adding **7** to freshly prepared LDA at $-78\text{ }^{\circ}\text{C}$, stirring for 50 min at that temperature, and then adding the aldehyde and stirring for approximately 1 hour before quenching. Using these conditions, yields of up to 40% of the aldol product were obtained, although significant quantities of ketone **7** were also recovered in all cases. It was planned to confirm the stereochemistry of the aldol products by NMR analysis at a later stage when a locked ring system was present in the molecule, but based on the work described in the previous section, it was assumed that at this stage the product was a mixture of the two 7,8-*syn* diastereomers shown in scheme 3.6. With the stereochemistry at C-5 fixed, only two *syn*- diastereomers are available (present in a 1:1 ratio). However, it was found that aldol product **28** had an R_f very close to that of the *gem*-dimethyl ketone fragment **7**, and separation of the diastereomers **28a** and **28b** proved to be very difficult. Further reactions were carried out with the mixed diastereomers, contaminated with small amounts of **7**.

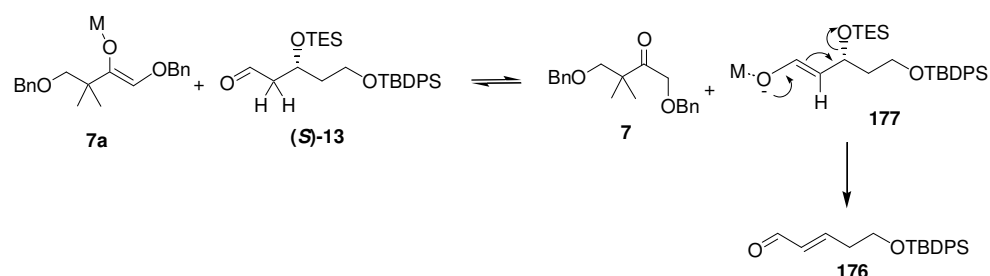


Scheme 3.6. Aldol reaction with fragment (*S*)-**13**.

The reasons for the low yields observed in these aldol reactions were not entirely clear. After extending the reaction time at $-78\text{ }^{\circ}\text{C}$ to several hours, significant quantities of the starting material **7** were still observed by TLC analysis of the reaction mixture. Warming the reaction (to $-40\text{ }^{\circ}\text{C}$, $0\text{ }^{\circ}\text{C}$ or RT) also did not significantly increase the amount of aldol product that was formed.

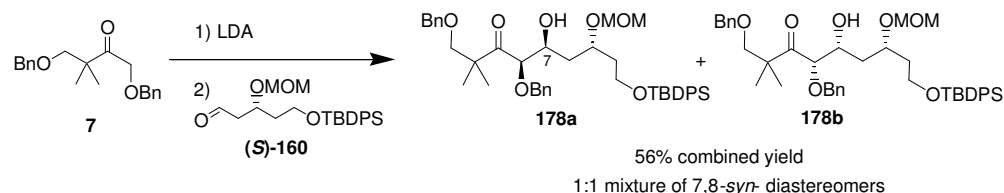
One of the reasons that was identified for the relatively low yields was elimination of aldehydes **140** and **13** under the aldol reaction conditions to give the conjugated by-product, **176** (scheme 3.7). This by-product was isolated from the reaction in 5 – 70% yields, depending on the reaction conditions used. Its

formation was particularly noted when reaction time was extended, or when the aldol reaction was warmed as described above. The formation of the by-product might be promoted by the chelation of the aldehyde (transition state **27**, scheme 1.10, page 19), withdrawing electron density from the OTES oxygen and thus promoting the elimination. Alternatively, an E1_{CB} elimination could occur by abstraction of the α-H of the aldehyde by the enolate, to give **177**, followed by elimination of the OTES group to give conjugated molecule **176** (as shown in scheme 3.7) and reformation of ketone **7**. The elimination also occurred if any aldehyde was left in the crude product after workup of the aldol reaction, unless purification was done immediately.



Scheme 3.7. Elimination of aldehyde **13** to give the conjugated by-product, **176**.

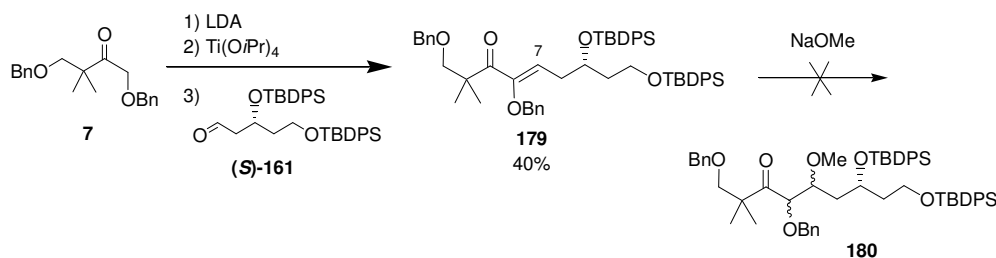
The problem of elimination from the starting material was somewhat alleviated by substituting the TES group by MOM, hence conducting the aldol reaction with aldehyde **(S)-160** (scheme 3.8). The diastereomeric aldol products **178a** and **178b** were prepared in 56% (combined) yield, when an excess of the enolate of **7** was used. With the MOM group, the aldehyde fragment was much more stable to the reaction conditions, and **160** could be recovered if the reaction was quenched at $-78\text{ }^{\circ}\text{C}$. However, even with this improvement higher yields could not be obtained by extended reaction time or by warming the reaction to $-40\text{ }^{\circ}\text{C}$ or $0\text{ }^{\circ}\text{C}$ (the elimination product was observed in this case only when the reaction was warmed).



Scheme 3.8. Aldol reaction with **(S)-160**.

Having achieved satisfactory yields with the LDA aldol reaction conditions, the next challenge was to perform an aldol reaction that would give the *anti*- aldol product. The conditions described in section 3.2 that had been successfully employed to give *anti*- aldol products with the model substrate, were therefore attempted. Unfortunately, isolable amounts of aldol product were obtained from neither the Cy₂BCl mediated aldol reaction, nor from an attempted Mukaiyama aldol reaction with TiCl₄. In some cases small traces of what were presumed to be aldol products were detectable in the ¹H NMR spectra of the crude product. However, despite trying a variety of conditions (longer reaction times or allowing the reactions to warm to -40 °C, 0 °C or RT), the major products of the reactions were always the ketone **7**, and either the aldehyde (**160** or **13**) or degradation products thereof.

Finally, the aldol reaction using LDA and Ti(OiPr)₄ as described in section 3.2 was attempted using **161** as the aldehyde. In the analysis of the crude product from the reaction, along with the usual unreacted starting materials and byproduct **176**, was found the eliminated aldol product **179** (scheme 3.9). Again, this elimination was attributed to an E1_{CB} mechanism similar to that shown in scheme 3.7, with abstraction of the α-H of the ketone of the newly formed aldol product, and subsequent elimination of the hydroxyl group (possibly assisted by co-ordination of titanium) to give **179**.

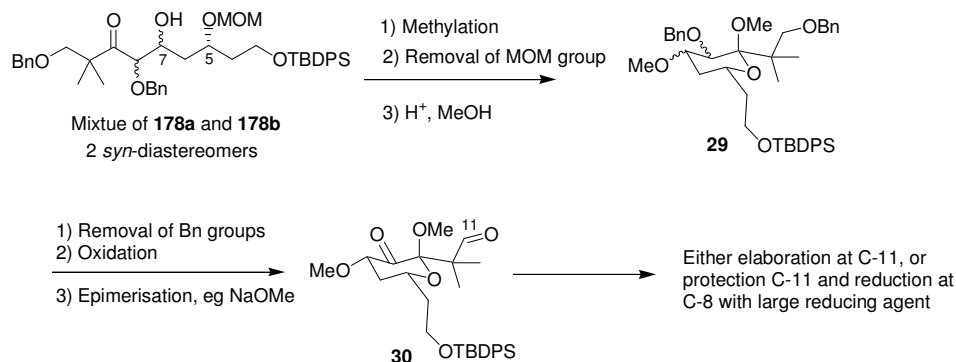


Scheme 3.9. Formation of eliminated aldol product **179** with Ti(OiPr)₄.

It was proposed that, if **179** could be reliably prepared, then nucleophilic 1,4- Michael-type addition at C-7 of **179** with methoxide anion could be used to give product **180**, essentially methylated aldol product. Unfortunately the methoxide addition was not achieved, and this route was not pursued.

3.4 Elaboration of the LDA aldol products

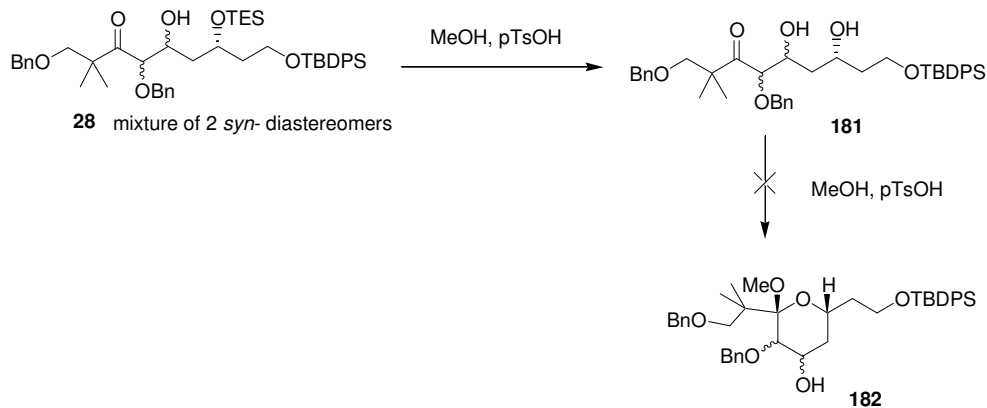
The subsequent steps in the planned synthesis of the pyranose ring were protection of the newly formed hydroxyl moiety of the *anti*- aldol product as the methyl ether, then deprotection at C-5 and subsequent cyclisation of the pyranose ring, which would be converted into an acetal such as **29** (scheme 1.10, page 19). In view of the difficulties experienced obtaining the *anti*- aldol product, it was decided to proceed with the largely *syn*- aldol product obtained from LDA reaction. Hence, a slightly modified synthetic plan (shown in scheme 3.10) was adopted, in which the methylation, deprotection-cyclisation and acetal formation steps are followed by cleavage of the benzyl ethers, oxidation and subsequent epimerisation of the methoxy substituent at C-7 to the thermodynamically favoured equatorial position. This would eventually be followed by reduction of the resultant C-8 ketone³⁴ to the axial hydroxyl, giving the required stereochemistry around the pyranose ring. This strategy takes advantage of the locked pyranose ring system to ‘correct’ the stereochemistry around the ring. Although introducing extra steps, this strategy has the advantage that all the diastereomers formed in the aldol reaction can be carried through the synthesis, maximising the overall yield.



Scheme 3.10. Modified strategy for pyranose ring formation.

3.4.1 Initial cyclisation attempt and subsequent strategy modification

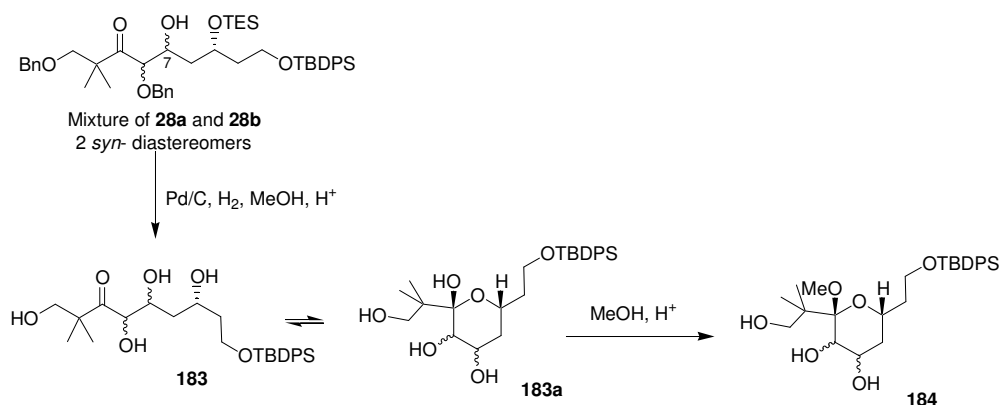
Initially, to investigate the viability of the proposed cyclisation, the TES group of **28** was removed without first protecting at C-7. Hence, the aldol product **28** was stirred at 0 °C in MeOH with a catalytic amount of *p*TsOH, and the deprotected product **181** was isolated in 82% yield (scheme 3.11). However, it was clear from the ^{13}C NMR spectrum that **181** was present as the open chain form, not, as had been hoped, as the pyranose ring (scheme 3.11). In the ^{13}C NMR spectrum, the ketone carbon signal was clearly present at 213.4 ppm, and no signals were seen around 100-110 ppm where they would be expected for a cyclic acetal. The major HRMS (ESI) signal was found at 691.3453, which correlates to the mass calculated for **181** + Na^+ (the cyclic acetal would have mass for **182** + Na^+ of 705.3587). It was postulated that the benzyl groups present at O-8 and O-11 might be a steric hindrance to ring closing. This hypothesis has since been supported by literature reports indicating that the closed ring structure is elusive until the molecule is largely deprotected.^{34,70}



Scheme 3.11. Product of deprotection of **28**.

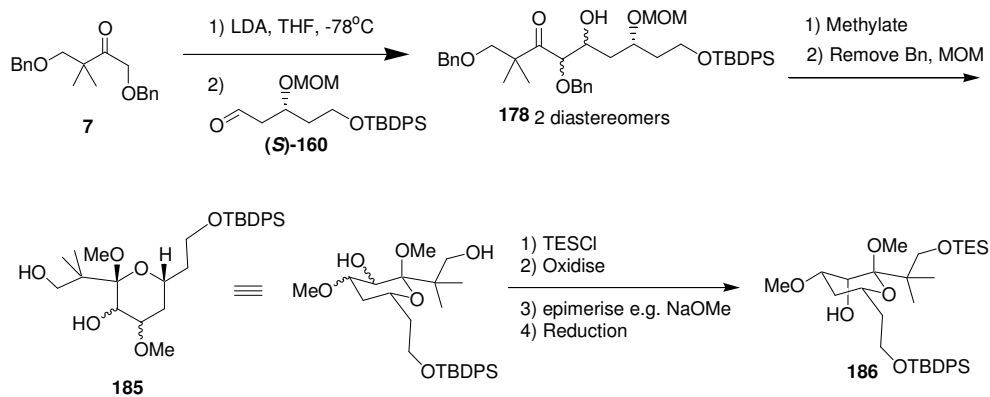
Removal of both the benzyl groups and the TES group appeared to be necessary to effect cyclisation. This could be done with the unprotected aldol product **28** as shown in scheme 3.12, using a published method for the simultaneous deprotection of TES groups and benzyl groups in methanol with Pd on charcoal⁹⁶ to liberate the hydroxyl groups present in the molecule, providing

183 which would be in an equilibrium with the pyranose ring form (**183a**). The acetal **184** could then be formed with acidic methanol.



Scheme 3.12. Pd/C deprotection of TES and Bn groups of aldol product **28**.

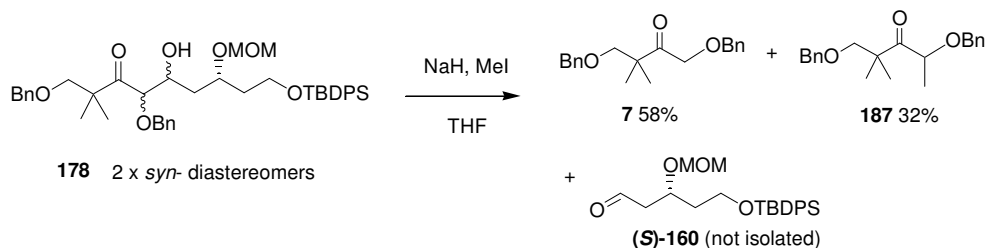
However, the polyol **183** would be very polar and consequently difficult to handle, and it was considered prudent to return to the original strategy and methylate the free hydroxyl at C-7 before attempting the debenzyl/silyl ether cleavage step. Hence, the modified strategy, shown in scheme 3.13, consisted of methylation, then deprotection at O-5, O-8 and O-11, in the presence of MeOH and acid, to form the cyclic acetal **185**, with undefined stereochemistry at C-7 and C-8. Subsequent oxidation at C-8, epimerisation at C-7 to give the desired equatorial position, and then reduction of the ketone with a large reducing agent such as L-selectride to give **186**, with an axial hydroxyl as required at C-8, would set the required stereochemistry around the pyranose ring.



Scheme 3.13. Modified new strategy.

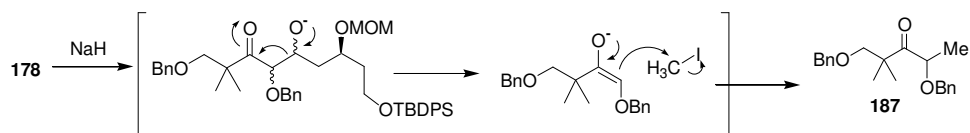
3.4.2 Methylations

Attempts to methylate the aldol product **178** were initiated by trying the standard Williamson ether synthesis (scheme 3.14). Monitoring the reaction by TLC revealed a product being formed with a higher R_f than the starting material, but unfortunately, upon workup and column chromatography, the methylated aldol product was not isolated. It appeared that, upon deprotonation, **178** had undergone a retro-aldol reaction. Ketone **7** was isolated from the crude reaction mixture in 58% yield, along with 32% of compound **187** as a by-product (scheme 3.14).



Scheme 3.14. Attempted methylation of **178**.

The formation of the by-product **187** was attributed to nucleophilic attack of the enolate product of the retro-aldol reaction, on methyl iodide (as in scheme 3.15). The retro-aldol reaction was observed even when only one equivalent of NaH was used. It was hoped that milder bases might reduce the tendency for the retro-aldol reaction to occur. However, the same products **7** and **187** were obtained from attempts to methylate **178** with KOH or KO^{*t*}Bu and methyl iodide in THF.



Scheme 3.15. Origin of byproduct **187**.

Alternative, mild methylation conditions were sought, but unfortunately no reaction was observed, and unmethylated aldol product was recovered after treatment of **178** with any of the following methylation conditions: K₂CO₃ and methyl iodide in THF; AgOTf, pyridine, and methyl iodide in dichloromethane;⁹⁷

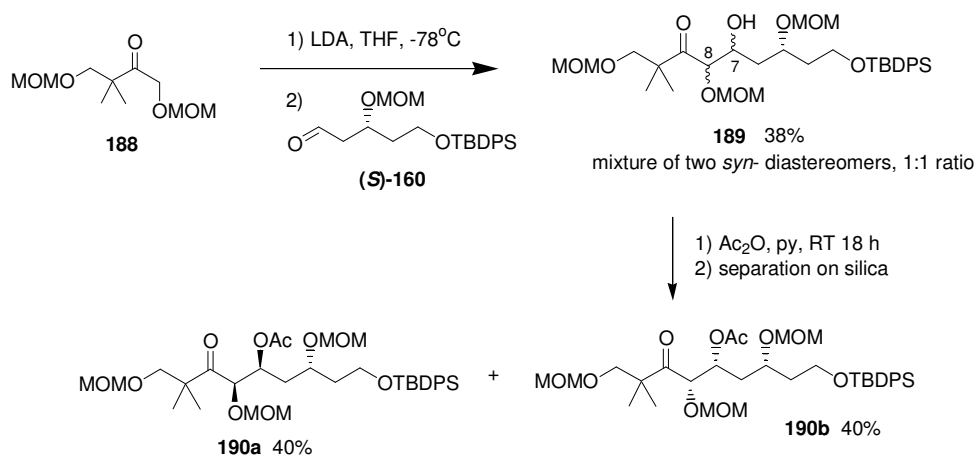
HC(OMe)₂.BF₄ in dichloromethane;⁹⁸ or methyl trifluoromethanesulfonate in trimethyl phosphate (a mild procedure reported for the methylation of carbohydrates).⁹⁹ It was concluded that methylation of the aldol product was not a viable strategy, and a different approach was required. One such alternative approach is described in the next section, 3.5.

3.5 Fragment 188, a variant of *gem*-dimethyl ketone 7

The use of a variant of the *gem*-dimethyl ketone fragment protected with two MOM groups (**188**, scheme 3.16) was briefly investigated. Use of **188** as the ketone would give rise to **189** after an aldol reaction with **160** (scheme 3.16). Subsequent global deprotection of the three MOM groups would give **191** and **192** (scheme 3.17), which should be free to cyclise to give the pyranose ring fragment with *syn*- stereochemistry between C-7 and C-8. The oxidation-epimerisation-reduction sequence described above would then be used to set the desired stereochemistry at those centres.

3.5.1 Aldol reaction of 188 and subsequent protection of the hydroxyl group

The *gem*-dimethyl ketone fragment **188** was prepared by Dr John Hoberg, following a procedure analogous to that used for the synthesis of **7**. The aldol reaction between **188** and **160** proceeded in 38% yield, giving two diastereomers in 1:1 ratio. This yield is somewhat lower than the best yields obtained with fragment **7**, however this reaction was only carried out once on a small scale. Due to the difficulties encountered previously with the methylation of **178**, it was considered prudent not to attempt a methylation of the small supply of **189** in hand. Instead, **189** was acetylated in a 1:1 mixture of acetic anhydride:pyridine overnight at room temperature, to yield **190** in 80% yield. Fortuitously, the two resulting 7,8-*syn*- diastereomers were found to be separable on silica gel, and were independently characterised, although it was not possible to determine which of the isolated diastereomers was **190a** and which was **190b**.



Scheme 3.16. Aldol reaction of **188** and subsequent acetylation.

3.5.2 Selective cleavage of the MOM ether

In order to identify the best conditions for the cleavage of the MOM ethers of the aldol product, **189**, alkene **158** was used as a model substrate. The objective was to cleave the MOM ether while retaining the silyl ether, hence to give alcohol **B** as the major product of the reaction (see table 3.2 overleaf). Surprisingly, removal of the MOM ether in preference to the TBDPS ether was not as straightforward as had been hoped. A wide range of both Brönsted and Lewis acidic conditions have been used for the cleavage of the MOM ether,^{76(d)} and a number of these were tested, as summarised in table 3.2.

The usual conditions for MOM ether removal, trace concentrated HCl in methanol, were found in this case to cause cleavage of the silyl ether even at room temperature. Although MOM ether cleavage with aqueous HCl has been reported at ice-cold temperatures,¹⁰⁰ heating to 50 or 60 °C is often required for MOM ether cleavage under methanolic conditions. Hence it is not surprising that only traces of diol **D** (having lost both the TBDPS and MOM groups) were observed in the reaction mixtures at the point where all of the starting material was consumed (entries 1 and 2, table 3.2). Catalytic HCl in warmed *i*PrOH¹⁰¹ has been reported to cleave a MOM group in the presence of a secondary TIPS group. However in this case, although diol **D** was observed, the MOM ether was cleaved after the TBDPS had already been lost (entry 3). Using boron tribromide

Table 3.2. Attempts at selective cleavage of the MOM ether group of **158**.

Entry	Conditions	Ratio of products A:B:C:D*
1	0.05% HCl in MeOH, RT, 2 hr	0 : 0 : 1 : trace
2	0.5% HCl in MeOH, RT, 0.5 hr	0 : 0 : 1 : trace
3	0.05% HCl in <i>i</i> PrOH, 55 °C, 4 hr	0 : 0 : 1 : 1
4	BBr ₃ , CH ₂ Cl ₂ , -45 °C, 0.5 hr	1 : 0 : 1 : ? + other spots
5	AcOH, cat. H ₂ SO ₄ , 10 °C, 0.5 hr	0 : 1 : 0 : 0
6	AcOH, cat. H ₂ SO ₄ , 10 °C, 4 hr	0 : 1 : 0 : 10

* Approximate ratios as determined by TLC analysis of the reaction mixtures.^{iv}

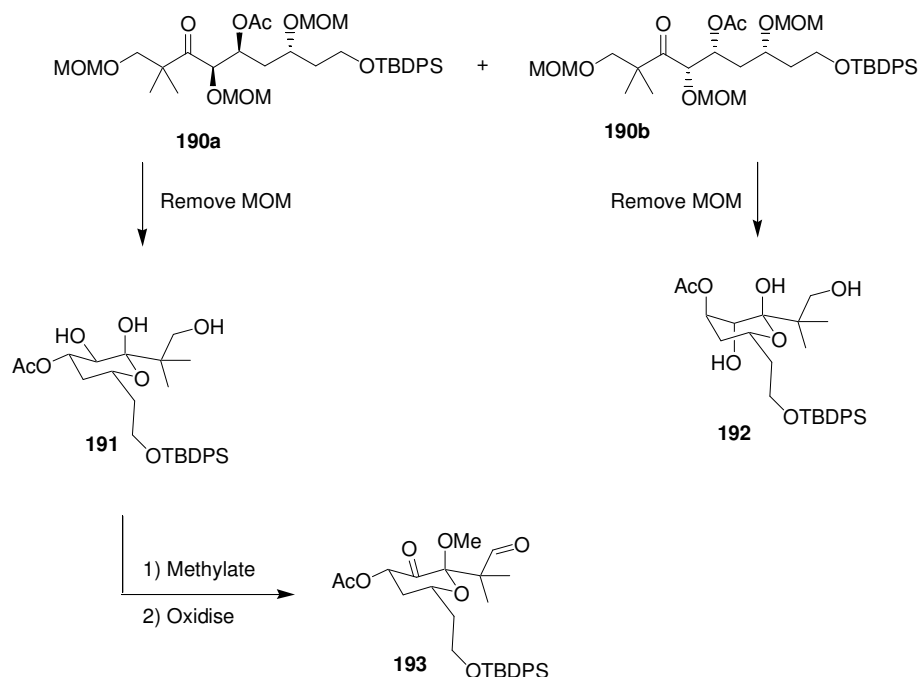
in CH₂Cl₂, conditions that are used for methyl ether cleavage (entry 4),^{76(e)} the TBDPS ether was again cleaved, and significant other degradation also seemed to be taking place as evidenced by a number of unidentified spots appearing on the TLC. Again, the desired alcohol **12** was not observed. Finally, acetic acid with catalytic H₂SO₄¹⁰² was used to successfully cleave the MOM ether while retaining the TBDPS group (entry 5). Although extended reaction times did lead to the formation of the diol (entry 6), it was considered that TBDPS cleavage could be minimised by keeping the reaction cold, careful monitoring, and quenching after between 0.5 and 1 hours reaction time.

3.5.3 Deprotection and Cyclisation of the tris-MOM-ether **190**

Having established suitable conditions for the deprotection of the MOM ether, the cleavage of all three MOM groups of the acetylated aldol products **190a** and **190b** was embarked upon. The planned synthesis involved deprotection of each diastereomer separately (scheme 3.17), followed by spontaneous cyclisation to give the pyranose ring systems **191** and **192**. In the cyclic form, the

^{iv} Thanks go to Shivali Gulab for providing an authentic sample of alcohol **C** for TLC analysis.

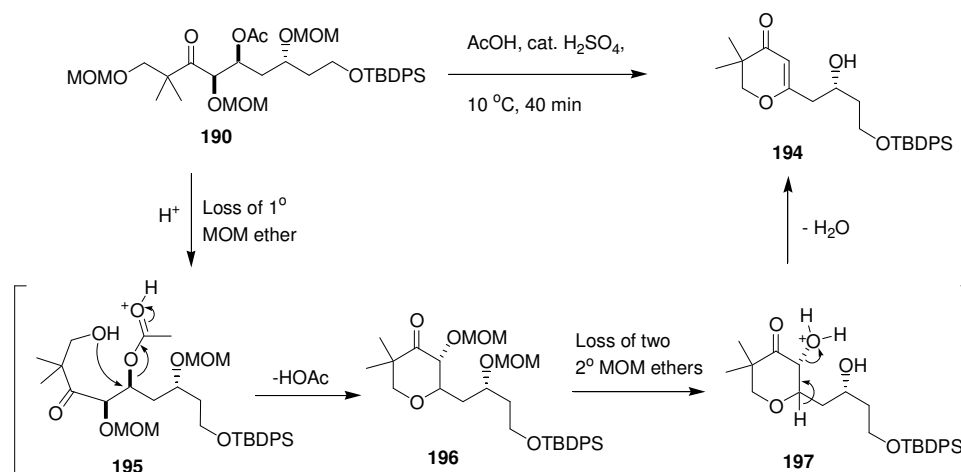
configuration at C-7 and C-8 would be identifiable by NMR analysis, and hence **191** could be identified and further elaborated as shown in scheme 3.17 to give **193**, which represents an analogue of the pyranose ring fragment **3** in the retrosynthesis presented in chapter one (page 14). Reduction of the ketone at C-8 to the equatorial hydroxyl group would occur at a later stage in the synthesis.



Scheme 3.17. Deprotection of MOM ethers of **190**, and further elaboration.

However, when the compounds **190a** and **190b** were subjected to the conditions described above for the MOM ether cleavage, a *higher* R_f product was observed rather than the expected *lower* R_f product. The same product was observed in the reaction of both diastereomers, although in one case the spot was lost after workup (these reactions were only done on 12 and 14 mg scale). Hence, milder workup conditions were used after reaction of the second diastereomer, and in this case the product was isolated, albeit on small scale. Spectral analysis indicated that the three MOM ethers had certainly been cleaved, the acetyl group had been lost, and two molecules of water had been eliminated but the molecule had not cyclised in the desired manner. The likely identity of the high R_f product was **194** (scheme 3.18). As shown, one possible mechanism of formation of **194** begins with loss of the primary MOM ether to give **195**, subsequent nucleophilic attack at C-7 with acid-catalysed displacement of the OAc group to yield cyclic

molecule **196**. Then, the remaining MOM ethers could also be cleaved to yield the diol **197**, and finally one molecule of water eliminated as shown.



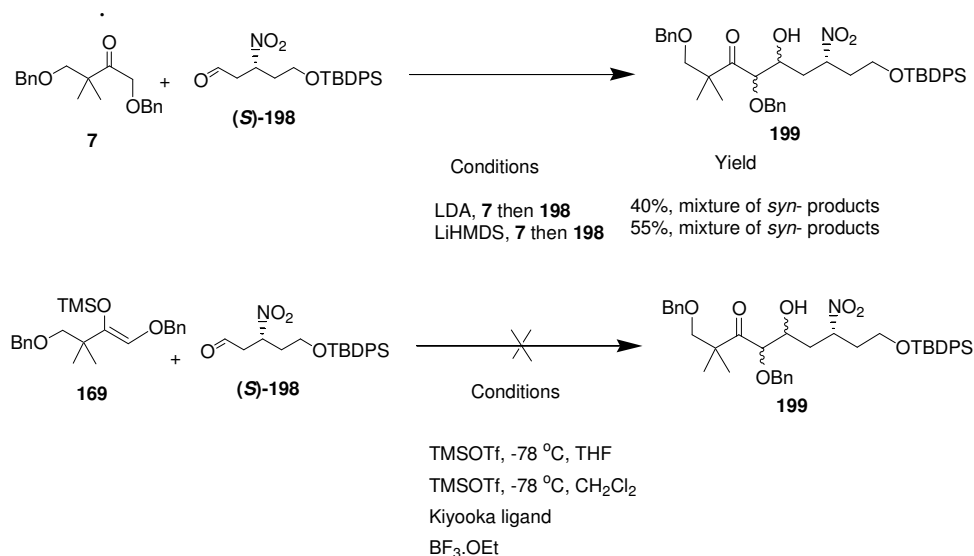
Scheme 3.18. Unexpected product **194**, and a possible mechanism of formation.

3.6 Discussion, conclusions and future work

Although successful aldol reactions between ketone **8** and variants of aldehyde **7** have been achieved using LDA, as described in the previous sections, the resultant aldol product would lead to the undesired *syn*- relationship between C-7 and C-8 of peloruside A. Unfortunately, the aldol reaction conditions that were found to give *anti*- aldol products from reactions between ketone **8** and benzaldehyde did not give isolable aldol products when conducted with variants of aldehyde **7**.

The results obtained during this work have been echoed in the work of a post-doctoral fellow working in the same group on synthesis of analogues of peloruside A. A variety of aldol reactions were attempted between ketone **7** and an aldehyde similar to fragment **8**. Again, only very limited success was obtained, and although the aldol reaction, to form **199**, was successfully performed using LDA- and LiTMP- mediated aldol reaction conditions (scheme 3.19), no other aldol reaction conditions were found to give satisfactory results.¹⁰³ The aldol reaction conditions reported to give an *anti* aldol product

using similar substrates in Pagenkopf's partial synthesis of peloruside A⁷⁰ were found not to work here.



Scheme 3.19. Aldol reactions between **7**, **169** and aldehyde **(S)-198**.

Why it should be that the aldol reaction with benzaldehyde and **7** proceeds under a variety of conditions, while the aldol reaction between fragment **8** and ketone **7** should be much less facile, may be explained by a combination of steric hindrance and π -stacking. The generalised *Z* enolate of **7**, **7a**, is reasonably sterically crowded because of the *gem*-dimethyl groups and the benzyl group. Hence, approach of an aldehyde might be hindered. However, in the case of

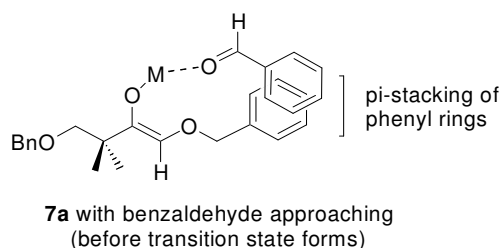


Figure 3.5. Enolate **7a** with π -stacking of two aromatic groups.

benzaldehyde, the incoming phenyl group could exhibit π -stacking with the phenyl group of the benzyl moiety (figure 3.5), hence bringing the aldehyde into closer proximity. As the aldehyde also coordinates with the metal of the enolate, the aldol reaction can then take place.

Even in the case of benzaldehyde, the sterically hindered nature of the system was suggested by the observation that the aldol reaction did not take place when the larger Ipc ligands (rather than Cy), were present. The O-B bond

distances are largely covalent in character, and shorter than the O-Li bond distance, leading to a more compact transition state for boron, which magnifies any steric interactions that may inhibit or control reactivity.^{88(c)} Titanium enolates are intermediate in structural character between the largely ionic lithium enolates and the largely covalent boron enolates.^{88(d)} This may be why the LDA aldol reaction of **7** with variants of fragment **8** was viable while the boron and titanium-mediated aldol reactions were not.

It is worth noting at this point that Pagenkopf's group had a great deal of difficulty finding suitable aldol reaction conditions for their formation of the C-7 to C-8 bond (refer chapter one, page 40). They were happy to accept a modest diastereomeric ratio of 3.5:1 for the aldol reaction with their C-8 to C-12 ketone **131** (scheme 1.36, chapter one). Comparing fragment **131** to fragment **7**, the major difference is that **131** lacks the benzyloxy group β - to the ketone as found in **7**. The lack of reactivity of enolates of **7** observed in this work may partially result from coordination of metal of the enolate (**7a**) to the benzyloxy oxygen, to form a conformationally stable six-membered ring (figure 3.6). The *gem*-dimethyl groups may be blocking the attack of the aldehyde onto the enolate, and the stability of the six-membered ring formation may to some degree reduce the tendency of the enolate to react with nucleophiles. Coordination of the metal to give the five membered ring shown in figure 3.6 is also possible, in which case the reactivity of the enolate would also be reduced by the increased electron density at C-8, due to the inductive effect. However this conformation is also available to **131** and hence does not specifically explain the lack of reactivity of the enolate of ketone **7**.

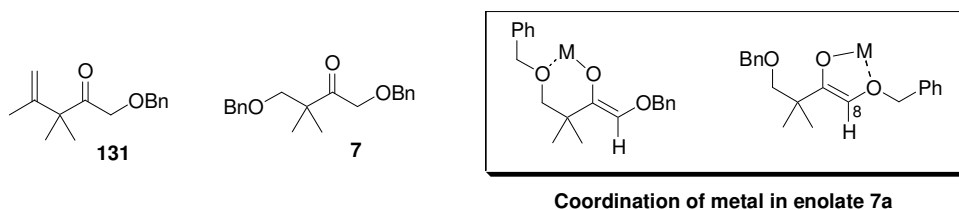


Figure 3.6. Pagenkopf's C-12 to C-8 fragment, **131**, fragment **7**, enolate **7a**.

The overall conclusion of the work done towards the aldol reaction between **7** and **8**, therefore, is that it is difficult to perform an aldol reaction with

ketone **7**, and particularly that the likelihood of effecting a preparatively useful *anti*- aldol reaction using fragments **7** and **8** is slim. Although the alternative strategy for progressing the LDA aldol products may still yield a possible solution to the overall goal of forming the pyranose ring fragment, **3**, and ultimately to completing the total synthesis of peloruside A, considerable difficulties have been experienced working with products from the LDA aldol reaction such as **28** and **178**. Hence, a new strategy is now being pursued in the group for the preparation of the C-1 to C-11 portion of peloruside A, with the approach of using chiral auxiliaries such as Evan's oxazolidinone (as proposed in chapter one for the introduction of the C-1 to C-2 fragment) to set the crucial stereochemistry in the C-5 to C-9 region.¹⁰⁴

Chapter Four

The Inositols; Isomers, Biology and Functionalisation

This chapter is a prelude to the work described in the following chapters towards the functionalisation of inositols, as precursors to natural products and potentially bioactive compounds. Following an introduction to inositols, a brief overview of their biological significance and ubiquity will be given. This will establish the importance of synthetically useful and varied inositol precursors. The work presented in this thesis covers two broad areas of inositol chemistry: a) the use of quebrachitol as a synthetic precursor (chapter five); and b) the resolution of *myo*-inositol derivatives (chapters six and seven). A discussion of relevant literature in each of these areas will conclude this chapter.

4.1 The Inositols

When Scherer isolated an optically inactive cyclohexanehexol from muscle tissue extract in 1850,¹⁰⁵ he gave it the name ‘inosit’. With the addition of the suffix *-ol*, this has become the generic term for the nine isomeric inositols, shown in figure 4.1. The naming and numbering of the inositols is a complex problem that has caused confusion in the past, although this has been ameliorated since the publication of the ‘IUPAC/IUB Tentative Rules for Cyclitols’ in 1967, and further by the ‘IUPAC Nomenclature of Cyclitols’ published in 1976.¹⁰⁶ Though classed as members of the carbohydrate family,ⁱ the inositols are significantly different from the more widely known sugars such as glucose, mannose, and galactose. This difference lies primarily in their six-membered all-carbon ring structure, which necessarily precludes the presence of a carbonyl group, of an open-chain form, and therefore of anomeric reactions. All of the hydroxyl groups on the inositol ring are secondary.

ⁱ Inositols are classed as carbohydrates because they conform to the general formula $C_n(H_2O)_n$.

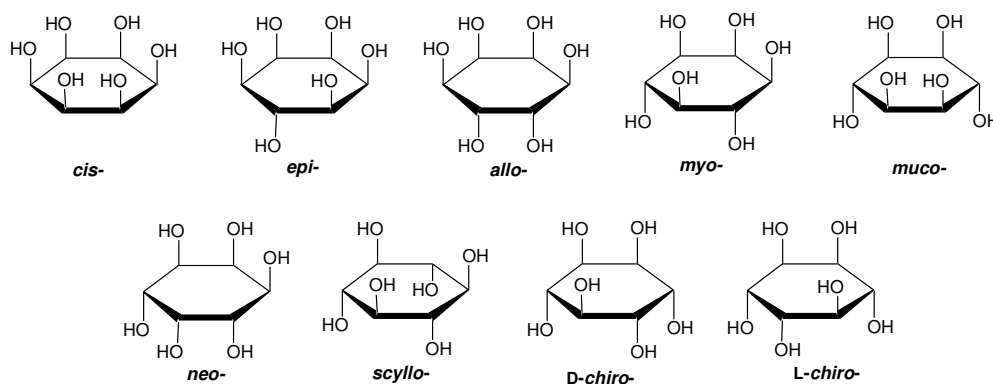


Figure 4.1. The nine isomeric inositols.

Six of the nine inositol isomers are present in nature: *myo*-, *scyllo*-, *L-chiro*-, *D-chiro*-, *neo*- and *muco*- (the latter two only in trace amounts). *Myo*-inositol is found in the cells of almost all living organisms and hence is the most widely occurring of the nine inositols, and is also the cheapest at less than 50 cents per gram.ⁱⁱ It is required by all animals for the synthesis of phospholipids, which play vital roles in intracellular signalling.¹⁰⁷ It is also found in plants, for example as the methyl ethers sequoyitol (5-*O*-methyl-*myo*-inositol) and ononitol (1-*D*-4-*O*-methyl-*myo*-inositol, which is a biological precursor to *D*-pinitol). Phytic acid (*myo*-inositol hexaphosphate), is widely found in cereals and legumes and is associated with dietary fibre. *Myo*-inositol for sale and use is generally derived from the hexaphosphate, isolated from corn starch liquor or sugar cane liquor. Phytic acid and *myo*-inositol containing phospholipids from both plant and animal sources constitute the major sources of dietary *myo*-inositol, and are so ubiquitous that *myo*-inositol intake in the average diet is approximately one gram daily. Humans are also able to synthesise *myo*-inositol endogenously, from glucose.¹⁰⁸ *Myo*-inositol is sometimes referred to as a vitamin, and although this is not the case, the levels of dietary *myo*-inositol can influence the levels of circulating and bound *myo*-inositol in the body. One of the deoxygenated

ⁱⁱ At the time of this work, *myo*-inositol was available for \$105 per 250 g from Scientific supplies in New Zealand. It was also available from Aldrich for AU\$59.50 per 100 g (evidently not the cheapest source). For comparison, Aldrich prices for some other inositols and inositol derivatives follow: quebrachitol, AU\$200.80 per 1 g; pinitol, AU\$63.30 per 500 mg; *D*- or *L-chiro*-inositol, AU\$276.20 per 1 g; *allo*-inositol, AU\$227.70 per 100 mg; *muco*-inositol, AU\$185.90 per 100 mg; *neo*-inositol, AU\$255.60 per 100 mg.

derivatives of *myo*-inositol, 1-D-3-deoxy-*myo*-inositol (D-viburnitol, figure 4.2) is also found in a number of plant species.

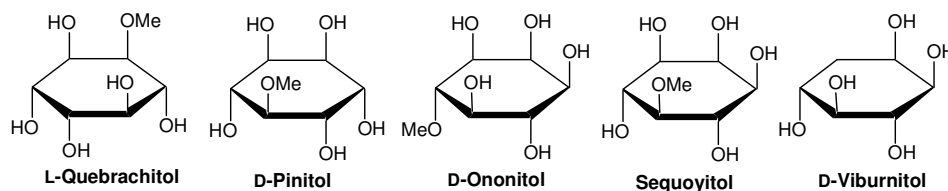


Figure 4.2. Some naturally occurring inositol derivatives.

Scyllo-inositol has been isolated from mammals, plants, sharks and several species of insect. It occurs in mammalian urine, where it is thought to be a metabolite of *myo*-inositol. *L-chiro*- and *D-chiro*-inositols are found in plants both as the free inositols and as derivatives thereof, significantly as the methyl ethers *L-quebrachitol* and *D-pinitol* respectively (figure 4.2). Both are readily demethylated to give the parent inositols.¹⁰⁹ Quebrachitol (2-*O*-methyl-*L-chiro*-inositol) is extracted from rubber serum as a by-product of the rubber processing industry, and is available for sale from the Rubber Research Institute of Malaysia. Pinitol (3-*O*-methyl-*D-chiro*-inositol) is isolated in New Zealand from pine trees and may be purchased from New Zealand Pharmaceuticals. *Epi*-, *allo*-, and *cis*-inositols, not found in nature, have been synthetically prepared.¹¹⁰

4.2 Biological Significance of the Inositols

As is evident from the brief survey of the inositols given above, these molecules are ubiquitous in nature and important to all living organisms. *Myo*-inositol, in particular, is a key component of many organisms. It is vital in cell signalling molecules (inositol phospholipids) in all eukaryotic cells, and is an important component of cell surface molecules essential to the function of many microorganisms. These biological functions will be introduced in the following sections. Recognition of the important role of the inositols has been the catalyst for synthetic chemists' attention to the preparation of inositol derivatives.

4.2.1 Inositol phospholipids and cell signalling processes

In order to place the importance of the inositol phospholipids in context, a brief overview of cell signalling processes will be presented here. Cells in multicellular organisms convey signals to each other by way of substances such as hormones and neurotransmitters. For signal transmission to occur, the 'message' must cross the cell surface membrane, and this is done in a number of ways (see figure 4.3).¹¹¹ Some of the signalling substances are able to pass through the lipid bilayer into the cell and bind directly to their target receptors. Many, however are too hydrophilic to cross the membrane. In this case, some form of signal transduction across the cell membrane is required. The chemical messengers are received by receptors located on the surface of the cell and their message passed into the cell by way of one of the following mechanisms:

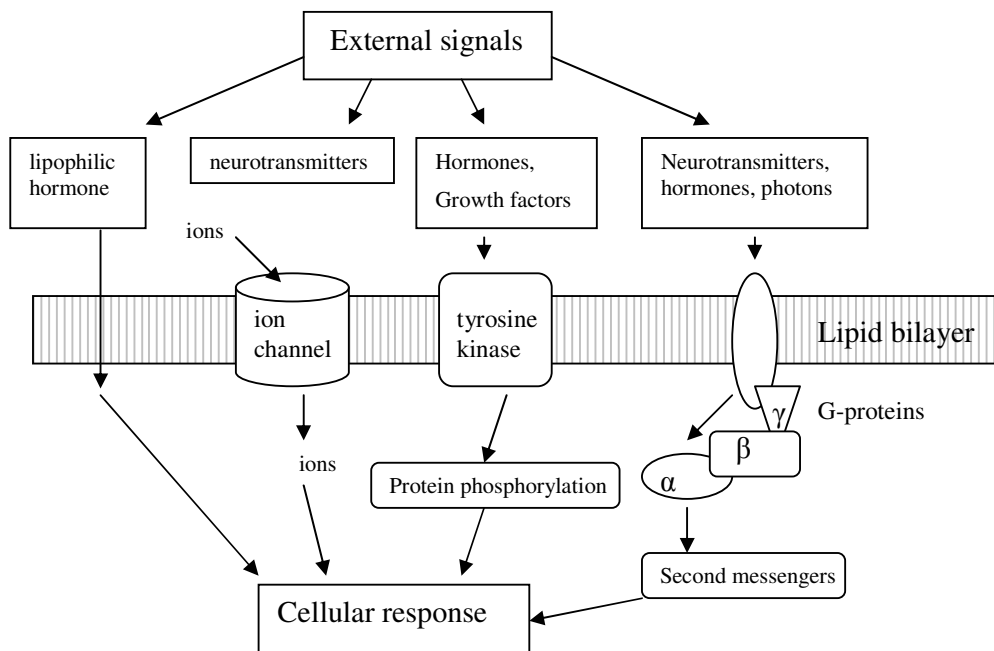


Figure 4.3. Signal transduction mechanisms.¹¹¹

A. Receptors that are linked to an ion channel which spans the membrane. These receptors are specific for a particular ion. Stimulation of the receptor can trigger the influx or efflux of ions from the cell, and the resultant change of ion concentration in the cytosol activates enzymes within the cell.

B. Membrane-spanning enzymes called tyrosine kinases, which have receptor sites on the outside of the cell and an active site on the inner surface of the membrane. When the binding of a chemical messenger stimulates the receptor site, the enzyme phosphorylates tyrosine residues on target proteins within the cell. This mechanism is used by many growth factors and by hormones such as insulin.

C. A receptor (which has no intrinsic membrane spanning function) is 'coupled' to a membrane-bound GTP-binding protein ('G-protein'). The family of G-proteins includes several members that regulate different intracellular pathways. Upon activation of the receptor, the G-protein releases guanosine diphosphate (GDP) from its α subunit and binds guanosine triphosphate (GTP) in its place. The $\beta\gamma$ subunit is then released, which stimulates or inhibits the activity of the ion channel or enzyme that is the next 'link' in the chain. In the case of an enzyme, so-called 'second messenger' species are generated or released within the cell. The subsequent change in intracellular levels of second messengers produces an observed overall cellular response. Finally, the α subunit hydrolyses the GTP to GDP (it has intrinsic GTPase activity), the $\beta\gamma$ subunit recombines with the α subunit, and the G-protein returns to its basal state. The classic example of this type of receptor system produces the second messenger cyclic adenosine monophosphate (cAMP) from adenosine triphosphate (ATP) via the G-protein regulated enzyme adenylate cyclase.

It had long been known that inositol-containing phospholipids were present in mammalian tissues, and it was suggested that they played a role in stimulus-response coupling. In the late 1950's emergent analytical techniques allowed the separation and elucidation of the structures of phosphatidylinositol (PtdIns), phosphatidylinositol-4-phosphate [PtdIns(4)*P*], and phosphatidylinositol-4,5-bisphosphate [PtdIns(4,5)*P*₂].¹¹² However their physiological significance remained something of a mystery until in 1975 Michell suggested that the receptor-controlled hydrolysis of inositol phospholipids could be directly linked to the levels of Ca^{2+} (which had been identified as being linked to a variety

of cellular processes) within cells.¹¹³ In 1983, Berridge and co-workers identified the chemical link between these two events as the second messenger, *myo*-inositol-1,4,5-triphosphate [$\text{Ins}(1,4,5)P_3$].¹¹⁴ It is now known that the receptor-stimulated hydrolysis of $\text{PtdIns}(4,5)P_2$ occurs via a G-protein controlled enzyme, phospholipase C (PLC). Two second messengers are released, diacylglycerol (DAG) and $\text{Ins}(1,4,5)P_3$. The former binds to and activates protein kinase C, and also acts as a precursor to the metabolites of the arachidonic acid cascade. The latter binds to receptors of Ca^{2+} channels on the endoplasmic reticulum resulting in the release of Ca^{2+} from an intracellular store.¹¹¹

Complex metabolic pathways exist for the conversion of $\text{Ins}(1,4,5)P_3$ back to free *myo*-inositol, which is used for the resynthesis of $\text{PtdIns}(4,5)P_2$. Higher phosphates [$\text{Ins}(1,3,4,5)P_4$,¹¹⁵ $\text{Ins}P_6$ and even the pyrophosphate-containing $\text{Ins}P_7$ and $\text{Ins}P_8$] and lower phosphates [$\text{Ins}(1,4)P_2$, $\text{Ins}(1,3)P_2$, $\text{Ins}(3,4)P_2$, $\text{Ins}(4)P$, and other inositol monophosphates] have been identified as part of these pathways. Other phospholipids have also been identified, for example $\text{PtdIns}(3)P$, $\text{PtdIns}(3,4)P_2$, $\text{PtdIns}(3,4,5)P_3$ and $\text{Ins}(1,3,4,5)P_4$, which may be second messengers in their own right.^{107,111}

The complexity of the inositol-phosphate cycle, and the significance of these molecules to cellular processes, has generated intense interest in this area of biology in the last two decades. Hand in hand with this has been the synthesis of the inositol derivatives, and many laboratories have provided synthetic methodology to this end. Pharmacological intervention in the phosphoinositide signalling system seems a logical extension of this work, with potential targets for logical drug design being found in the receptors that bind the second messengers, in the complex metabolic pathways, and in the biosynthetic pathways that generate the functionalised inositol moieties. Hence, synthesis of modified inositol phosphates with new biological properties is also underway.

4.2.2 Glycosylphosphatidylinositol

There are many proteins, with a myriad of functions, attached to biological membranes. Some are embedded directly into the lipid bilayer (via a hydrophobic portion of their structure), while many are attached to intermediary structures, which anchor them to the membrane. It has been shown that many of these proteins (and also glycoproteins) are covalently bonded (through the C-terminal amino acid of the protein) to phosphatidylinositol anchors via an intervening glycan structure. These anchor structures are known as glycosylphosphatidylinositols (GPI's). Ferguson *et al.* reported the first structure of a GPI in 1988,¹¹⁶ that of the GPI anchor of the variant surface glycoprotein of the parasitic protozoan that causes sleeping sickness, *Trypanosoma brucei* (figure 4.4).

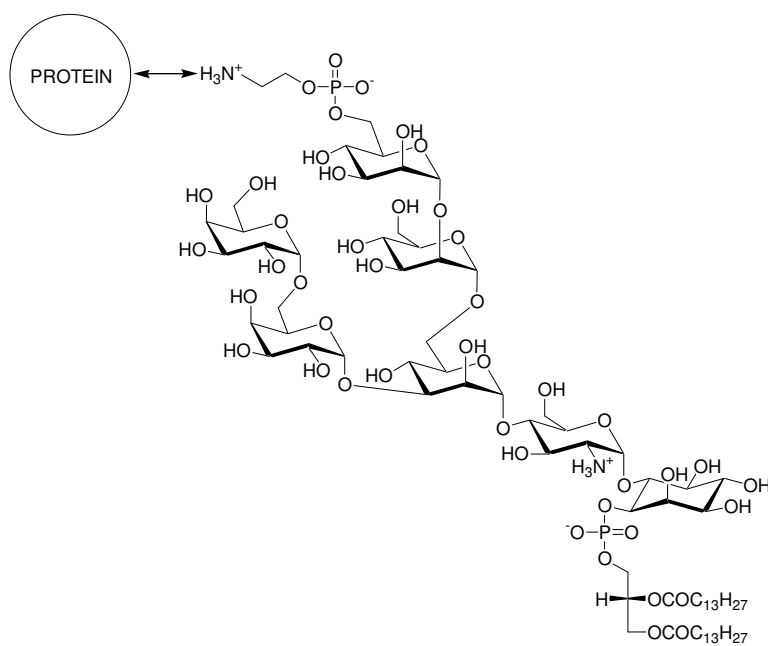


Figure 4.4. Structure of the GPI anchor of *Trypanosoma brucei*.¹¹⁶

Shortly thereafter, the structures for the GPI anchors of rat-brain Thy-1 glycoprotein¹¹⁷ and human erythrocyte acetylcholinesterase¹¹⁸ were reported. Based on these, and upon the many subsequent reports of GPI anchors from various eukaryotes, a general GPI structure has been elucidated, shown in figure 4.5. The general structure appears to have been conserved in the evolutionary process, although there may be species-specific additional carbohydrate side

chains (at R¹ and/or R²), and there are variations in the membrane-anchoring lipid structures depending on species and on cell type.

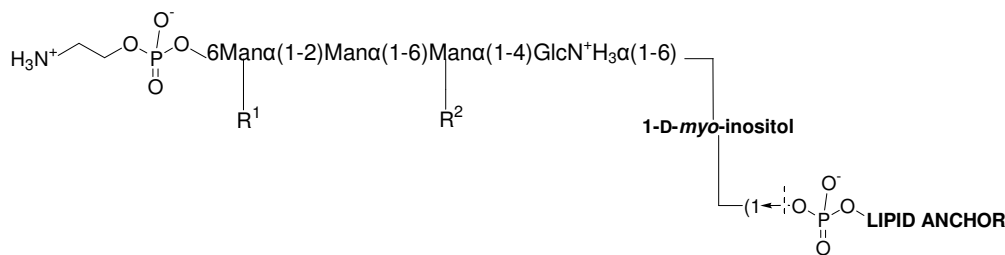


Figure 4.5. General structure of a GPI.

The GPI anchors of membrane proteins are found in all eukaryotes, although in higher eukaryotes only a minority of surface proteins are anchored in this manner. There is evidence however that GPI-anchored proteins are involved in specific tasks related to multicellular existence; they have been studied in their roles as enzymes, in interactions with bioactive factors, and in cell-cell recognition processes. More recently, there have been reports that metabolites derived from GPI anchors themselves, or from structurally related compounds, are mediators of regulatory processes. For instance, GPI fragments are thought to be involved in the signal transduction process triggered by insulin.¹¹⁹

In the protozoa, GPI anchors are much more prevalent, and are the most common form of surface protein anchorage. The protozoan parasites that are responsible for certain devastating diseases exhibit unusually high levels of GPI-anchored variant surface glycoproteins (VSG)'s on their surface. As well as *Trypanosoma brucei* (sleeping sickness) these include *Plasmodium* (malaria), *Trypanosoma cruzi* (Chagas disease) and *Leishmania* species (leishmaniasis). The VSG's are arranged in tightly packed monolayers and form a barrier, protecting the parasite from lytic factors in the host serum. Thus, the integrity of their cell-surface coat is essential to the parasite for survival. By expressing different VSG's at different times, the parasite is able to evade the host's immune response, by making it difficult for the host to supply the matching antibodies at the right time. A consequence of this behaviour is that drugs targetted against specific VSG's are rendered ineffectual. However, drugs that target the

biosynthesis of the GPI anchor, or drugs that target species-specific features of the GPI anchor (for example, in the case of the VSG GPI isolated from *Trypanosoma brucei*, the α -galactose side chain seems to be parasite-specific) could prove successful.

The treatments currently available for the diseases caused by the parasites mentioned above are far from satisfactory. Over the last decade work has been undertaken to elucidate the biosynthesis of the GPI anchors, and a biosynthetic pathway starting from phosphatidylinositol^{120,121} has been generally accepted. Much work is currently being undertaken focussing on the biosynthetic intermediates and enzymes involved, in particular focussing on any species dependent specificity that might reveal a possible drug target.

Synthetic efforts towards the generalised GPI and related structures have been underway since the biological significance of these molecules was first discovered. The first total synthesis of the *Trypanosoma brucei* VSG GPI was reported in 1992¹²² by Murakata and Ogawa. Other total syntheses of this GPI,¹²³ and syntheses of other GPIs have appeared since, as well as syntheses of labelled GPI structures and of intermediates in the biosynthetic pathway.

4.2.3 Lipoglycan cell surface structures related to GPIs

A number of protein-free GPI structures, that are not involved in protein anchoring are also prevalent on the surface of protozoan parasites.¹²⁰ These include the lipophosphoglycans (LPGs), and the glycoinositolphospholipids (GIPLs) isolated from *Leishmania* species. Interestingly, there is marked difference in the size of the LPGs and GIPLs, and in the nature of the side chains that are present, in the different developmental stages of the parasite. Certain LPG-deficient strains of *Leishmania* are unable to survive in the sandfly vector, or to infect the mammalian host, indicating that the LPG is essential to the virulence of the parasite.¹²⁰

Another related class of lipoglycans are the lipoarabinomannan (LAM) structures. These are restricted to the mycobacteria, and are cell surface molecules that modulate the function of the immune system of the host.¹²⁴ The LAM structure has a carbohydrate backbone, which consists of a D-mannan core and a D-arabinan domain. The mannan core is terminated at one end by a GPI anchor, and the arabinan domain is capped by mannosyl (the Man-LAMs) or phosphoinositide (the PI-LAMs) residues.¹²⁴ The Man-LAM has been shown to bind to immature dendritic cells, which normally play a crucial role in the immune response against pathogens. The LAM allows the mycobacteria to interfere with the normal function of the dendritic cells and hence evade the immune response of the host, and it is therefore important to the bacteria's survival. In the purification of lipoarabinomannans, three clear size classes of lipoglycan are seen, being the LAM, lipomannan (LM) and phosphatidylinositol manno-oligosaccharides (PIMs). The LAM and LM appear to be based on the PIM 'core' motif, and hence the PIM structures are important in gaining an understanding of the biosynthesis of LAMs.

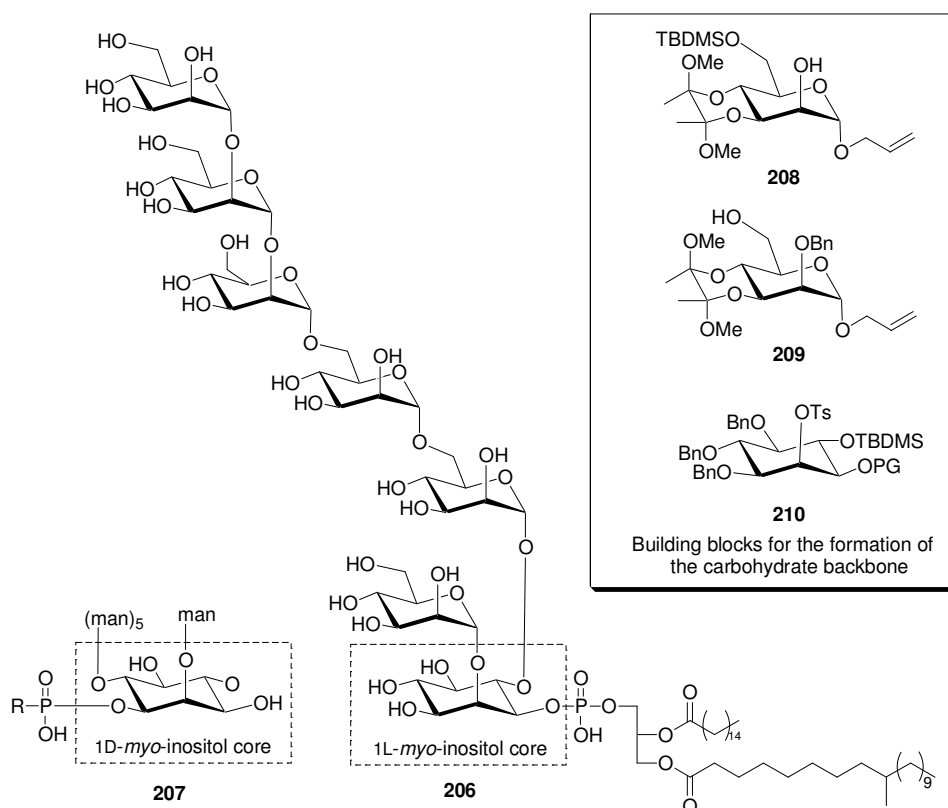


Figure 4.6. PIM-6 isolated from *Mycobacterium bovis* and *M. smegmatis*.¹²⁷

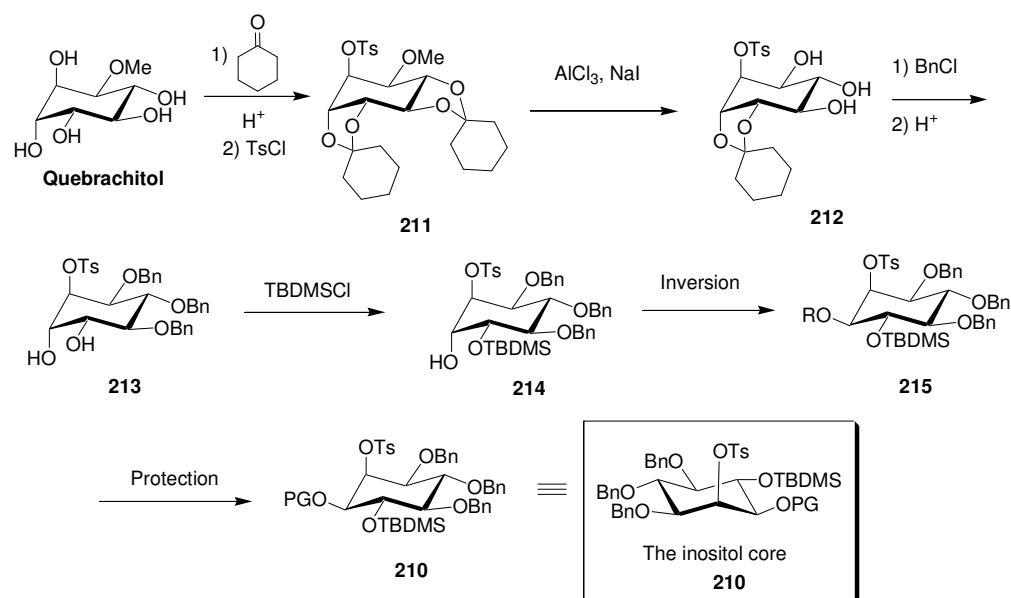
A series of glycerol phosphatidylinositol di-, tri- tetra- and penta-manno-oligosaccharides (PIM-2, PIM-3, PIM-4 and PIM-5 respectively) were the first PIM structures isolated, from *Mycobacterium bovis* strain BCG,¹²⁵ *M. tuberculosis*, and *M. phlei*.¹²⁶ An NMR-based method for the identification of the structure of PIM-6 (figure 4.6) was described by Severn *et al.*,¹²⁷ who also reported a method for *O*-deacylation and isolation of the size classes (utilising size-exclusion chromatography) within PIM. Hence, the deacylated version of the PIM-6 molecule in figure 4.6, and also PIM-2, were isolated from *M. bovis* AN5 and Wag201, and from *M. smegmatis* mc² 155.¹²⁷ In that report, it was not specified whether the *myo*-inositol core had the L- (as shown in structure **206**, figure 4.6) or the D- (as shown in **207**) configuration, although it was suggested that the L-configuration might be correct.¹²⁸ However, it is notable that the inositol core of the related GPI structures such as that shown in figure 4.4 has a substitution pattern equivalent to a D- configured *myo*-inositol core in PIM. It is reasonable to presume that this would be conserved. More recent reports have established that the 1D-*myo*-inositol core is a basic structural feature of both LAM and PIM,¹²⁹ with a biosynthetic pathway existing in which LAM is formed from PIM, which in turn is formed from PI (phosphatidyl-*myo*-inositol).^{129(b)}

4.3 Synthetic Plan for the 1L-*myo*-Inositol Core of the PIM-6 Molecule

The original driver for the work done towards the functionalisation of quebrachitol presented in this thesis, was a planned total synthesis of the PIM-6 molecule shown in figure 4.6. It was decided to synthesise the PIM-6 molecule with the 1L-*myo*-inositol core as shown in figure 4.6, as even though at the time of planning it was not clear whether L- or D- was the natural configuration, having access to both structures would be useful in the evaluation of the biological roles of these molecules.

The synthesis of the carbohydrate backbone was envisaged from just three building blocks, shown in the box in figure 4.6 – the C-2 acceptor **208**, the C-6 acceptor **209**, and the inositol core **210**. The retrosynthetic plan incorporated

the unusual approach of using quebrachitol (rather than *myo*-inositol) as a starting point for the core inositol moiety. Unfortunately, this total synthesis project had to be discontinued approximately twelve months into the PhD program. Fortunately, the quebrachitol functionalisation work itself had given some interesting results, and several mono- and di- substituted *L-chiro*-inositol derivatives were prepared from quebrachitol, and tested against *myo*-inositol (the optimal substrate) in uptake assays of two micro-organisms, *Candida albicans* and *Leishmania donovani*. All of this work is described in chapter five, while the original synthetic plan for the preparation of suitably protected inositol core in the synthesis of PIM-6 is presented here.



Scheme 4.1. Planned synthesis of suitably protected inositol core for PIM-6.

The triol **212** (scheme 4.1 above) was a key intermediate in the synthetic plan. According to literature reports, this molecule is available in three steps from quebrachitol; first, formation of the quebrachitol dicyclohexylidene acetal,^{130,131} subsequent protection of the free axial hydroxyl group to give **211**,¹³² and then a selective AlCl_3 -mediated dual cleavage of the *trans*-acetal and the methyl ether to yield the triol, in a reported yield of 75%.^{133,134} The three hydroxyl groups, which would become the three free hydroxyl groups of the inositol core of PIM-6, would then be protected with a suitable protecting group such as the benzyl ether. Then, the rest of the inositol core would be prepared.

Acid-catalysed cleavage of the *cis*-acetal reveals a differentiable pair of hydroxyl groups. Selective protection of the equatorial hydroxyl group should be possible because the axial position is sterically disfavoured by 1,3-diaxial interactions with the axial ring protons (if this is not successful, Sn-acetal mediated protection of one of the hydroxyl groups is another option). Inversion of the stereochemistry at the free hydroxyl of **214** is then required, which could be achieved via a Mitsunobu reaction (e.g. with EtOCON=NCOOEt, PPh₃, and RCOOH) to give **215**. Alternatively, conversion of the hydroxyl group in **214** to a good leaving group (triflate or mesylate) and subsequent S_N2 displacement with a nucleophile,¹³⁵ or an oxidation-reduction sequence, forming the more thermodynamically favourable equatorial hydroxyl¹³⁵ could be used. Suitable protection of the resulting hydroxyl would give the target **210**, orthogonally protected at O-2, O-3 and O-4, ready for deprotection at those positions and introduction of the single mannose residue (at O-2), the phospholipid (at O-3) and the mannose chain (at O-4).

The preparation of the mannose building blocks was envisaged from formation of allyl mannoside, then a combination of selective protection of the primary (O-6) hydroxyl group with TBDMSCl, and protection at O-3 and O-4 with the butane-bis acetal (BBA) protecting group to give the O-2 donor **208**. Subsequent protection, for example benzyl ether formation, and removal of the TBDMS group would yield the C-6 donor **209**. Imidate coupling methodology was planned both for coupling of the mannose residues, and their linkage to the inositol core. Due to the abandonment of this total synthesis project however, this work is not discussed further in this thesis.

4.4 Quebrachitol as a Synthetic Precursor from the Chiral Pool

4.4.1 Quebrachitol

L-Quebrachitol (figure 4.2), a natural L-*chiro*-inositol derivative, occurs in eleven different families of dicotyledons. It was first reported in 1889 by

Tanret, who isolated it from the bark of *Aspidosperma quebracho*.¹³⁶ Although it is found in many plant species, including in mistletoe (unusually, together with its isomer D-pinitol), it occurs in notably high concentrations in the rubber tree *Hevea brasiliensis* and therefore is isolated as a by-product from the rubber industry. Quebrachitol's ready availability and unique carbon framework make it a useful addition to the chiral pool of starting materials for organic chemists to use, particularly in the synthesis of polyhydroxylated natural products. A laboratory method for the isolation of L-quebrachitol was published in 1951,¹³⁷ although patents for its isolation were held before that date. However L-quebrachitol did not find widespread synthetic use until several decades later.

4.4.2 Quebrachitol as a synthetic precursor

Many groups have contributed synthetic work using L-quebrachitol. The groups of Ogawa, Ozaki and Angyal have been particularly active in this area. The first reported synthesis of a natural product from L-quebrachitol was a short, practical route to L-mannitol, then unknown in nature, in 1963.¹³⁸ Since then L-quebrachitol has been used as a starting point for the synthesis of other inositols and inositol derivatives (see below for examples), other carbohydrates, a number of inositol phosphates and related structures (see examples below), and numerous other natural and potentially bioactive products including (-)-conduiritol F,^{139,140} (+)-conduiritol B,¹⁴⁰ cyclophellitol,¹⁴⁰ and (-)-ovalicin.¹⁴¹ The following examples are intended to give an idea of the range of related structures that have been prepared from L-quebrachitol, rather than a comprehensive overview. A review has been published covering the use of quebrachitol as a precursor to naturally occurring bioactive materials (other than other inositols and analogues thereof).¹⁴²

Inositols and inositol derivatives

Some examples of inositols and inositol derivatives prepared from L-quebrachitol (figure 4.7 overleaf) include *muco*-inositol,¹⁴³ 1D-2-deoxy-2-fluoro-

chiro-inositol **216**,¹⁴⁴ the azido and amino derivatives **217** and **218**,¹⁴⁵ and 1L-1,2-anhydro-*myo*-inositol **219**.¹⁴⁶

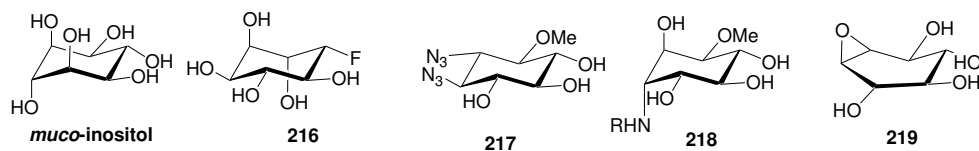


Figure 4.7. Some inositols and inositol derivatives prepared from L-quebrachitol

Myo-inositol phosphates and related structures

A number of examples of *myo*-inositol phosphates and analogues derived from L-quebrachitol are shown in figure 4.8. Akiyama's group published one of the early syntheses of a *myo*-inositol phosphate, D-*myo*-inositol-1-phosphate (**220**).^{135,147} The L-*chiro*-inositol derivative **221**, L-*chiro*-inositol-2,3,5-trisphosphate, was synthesised by Potter's group and shown to be an inhibitor of the enzymes of Ins(1,4,5) P_3 metabolism. Similarly, the compound 3-deoxy-3-fluoro-D-*myo*-inositol-1,4-bisphosphate-5-phosphorothioate (**222**), along with two isomers (synthesised by another group) were also shown to be inhibitors.¹⁴⁹ The trisphosphorothioate **223** has also been prepared.¹⁵⁰ Deoxy-inositol analogues have also been prepared from L-quebrachitol; for example D-3-deoxy-3-phosphonomethyl-*myo*-inositol **224**,¹⁵¹ which was shown to inhibit the growth of NIH 3T3 cancer cells at millimolar concentration, and what was claimed to be the first novel PI analogue, 1D-3,4-dideoxy-phosphatidylinositol ether lipid (**225**)¹⁵² which was found to block a cellular signalling pathway that has the ability to repress apoptosis in cancer cells.

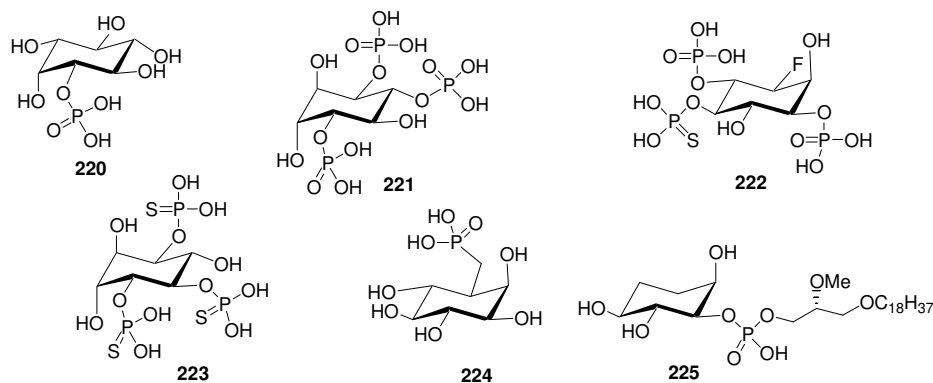


Figure 4.8. Examples of *myo*-inositol phosphates and analogues.

4.5 The Formation of Chiral *Myo*-inositol Derivatives

4.5.1 *Myo*-inositol

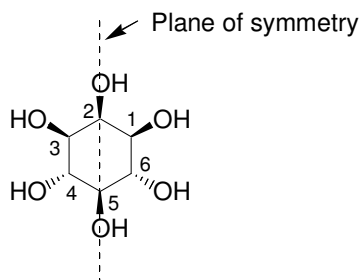


Figure 4.9. *Myo*-inositol.

Being the most abundant inositol found in nature, *myo*-inositol is also the cheapest of the commercially available inositols, priced at less than 50 cents per gram. Hence it is also the logical starting point for syntheses of the various inositol phospholipids, GPI's, and related structures.

Myo-inositol has a single axial hydroxyl at O-2 and a plane of symmetry between O-2 and O-5 (figure 4.9). Hence, *myo*-inositol itself is an optically inactive, meso- compound. Substitution at O-2 and/or O-5 leads to derivatives in which the plane of symmetry is retained. Substitution at O-1 (enantiotopic to O-3) and/or O-4 (enantiotopic to O-6) breaks the plane of symmetry and hence gives rise to a pair of enantiomers. Every example of naturally occurring *myo*-inositol derivatives (inositol phospholipids, GPI's, and related structures), is optically active, and hence their preparation requires methods for the obtention of single enantiomer chiral derivatives of *myo*-inositol.

4.5.2 The Preparation of Chiral *Myo*-inositol Derivatives

The preparation of chiral *myo*-inositol derivatives, including the *myo*-inositol phosphates and any number of other structures, is imperative for the study of the biological processes described above. It also represents a synthetic challenge in itself for the organic chemist. Chiral *myo*-inositol derivatives have been obtained by a variety of different methods, which are summarised in figure 4.10 below. Illustrative examples of each of these routes are presented in the following sections.

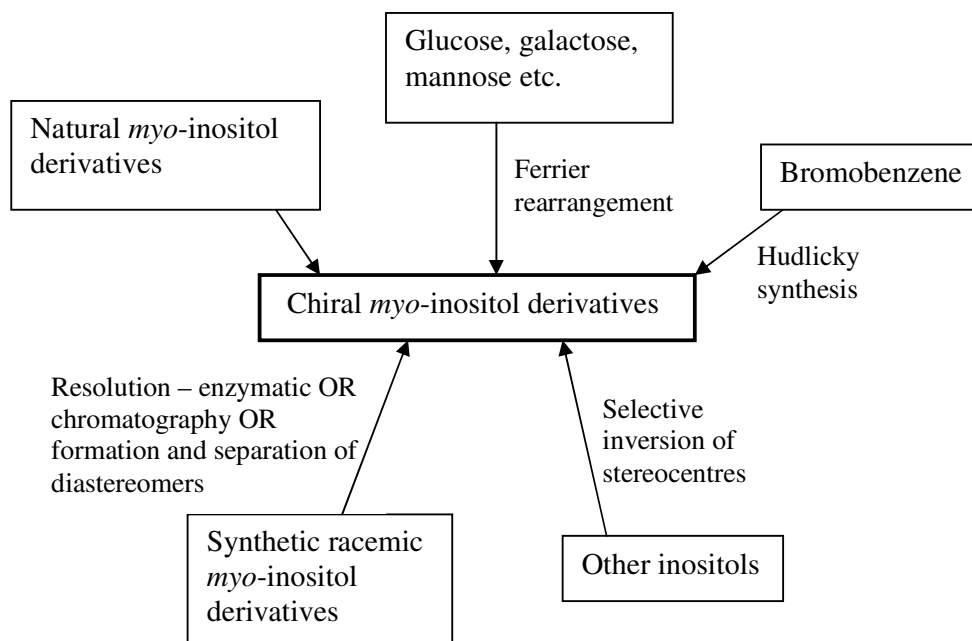
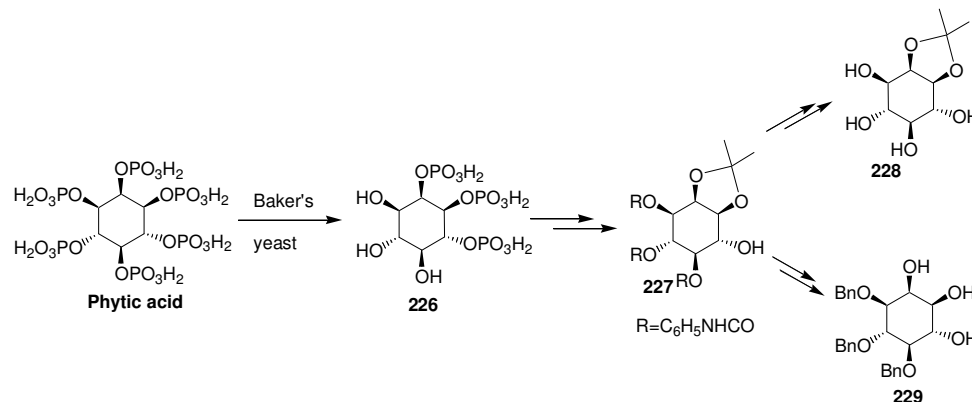


Figure 4.10. Sources of chiral *myo*-inositol derivatives.

Synthesis from natural *myo*-inositol derivatives

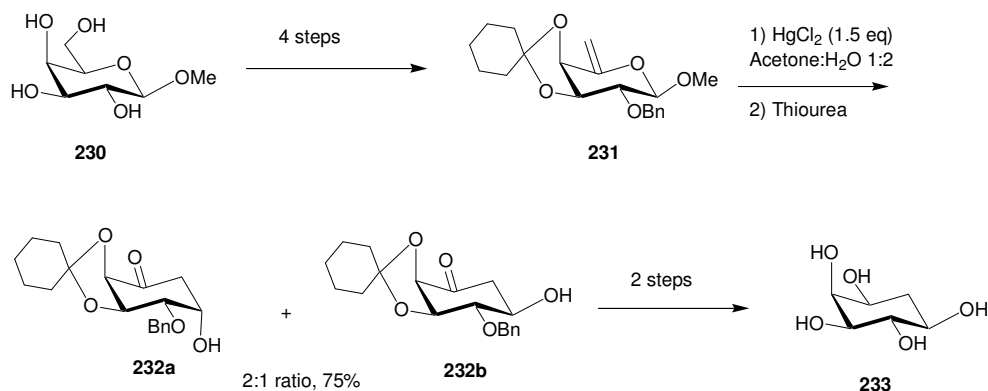
Phytic acid has been used as a starting material for the preparation of (+)-D-1,2-*O*-isopropylidene-*myo*-inositol (**228**) and (-)-D-3,4,5-tri-*O*-benzyl-*myo*-inositol (**229**), two key intermediates in the synthesis of optically active *myo*-inositol derivatives. Phytic acid was treated with Baker's yeast (scheme 4.2) which contains phosphatases that selectively hydrolyse phosphates at O-3, O-4, and O-5 to give **226**.¹⁵³ Further elaboration gave the common intermediate **227**, which was subsequently converted to either **228** or **229**.^{153(b)}



Scheme 4.2. Synthesis of **228** and **229** from naturally occurring phytic acid.

Synthesis from other carbohydrates using the Ferrier Rearrangement

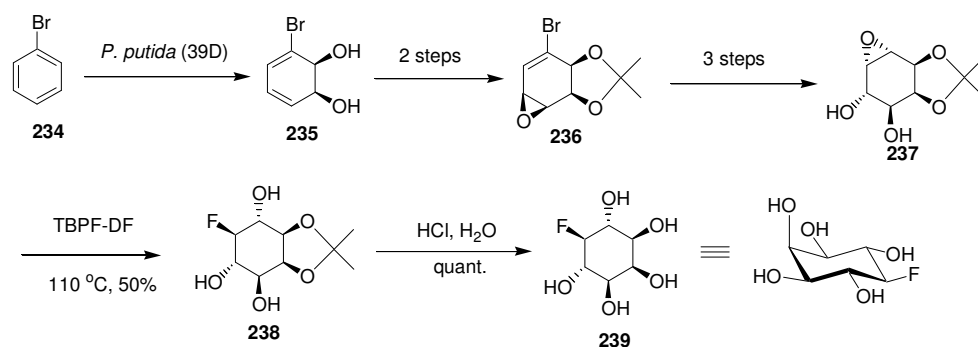
A number of groups have utilised Ferrier rearrangements as the basis for synthesis of all of the inositol isomers, including *myo*-inositol. This has been achieved from glucose, galactose and mannose substrates using a Pd(II)-mediated Ferrier reaction,^{154(a),(b)} or with an HgCl₂ or Hg(OAc)₂ mediated Ferrier reaction.^{154(c),(d)} For example, the rearrangement of **231** (synthesised in four steps from methyl-β-D-galactopyranoside (**230**)), gave **232b** (along with **232a**) which was further elaborated to give 1D-6-deoxy-*myo*-inositol, **233** (scheme 4.3).^{154(c)}



Scheme 4.3. Synthesis of 1D-6-deoxy-*myo*-inositol via Ferrier rearrangement.

Synthesis from Bromobenzene (the Hudlicky route)

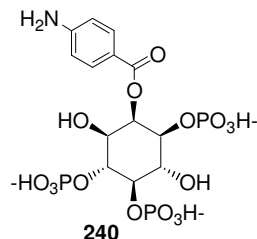
Hudlicky *et al.* have prepared a range of inositols and inositol derivatives from bromocyclohexadiene *cis*-diol (**235**, scheme 4.4, overleaf), obtained by microbial oxidation of bromobenzene (**234**). These include syntheses of *neo*-inositol,^{155(b)} *L-chiro*- and *muco*-inositols,^{155(c)} and *allo*-inositol.^{110(b)} The synthesis of the *myo*-inositol derivative 5-deoxy-5-fluoro-*myo*-inositol, **239** (along with a deoxyfluoro-*L-chiro*-inositol) has also been reported using this approach.^{155(a)} As shown in scheme 4.4, the oxidation of bromobenzene was accomplished in this case using *P. putida* (39D) strain. The synthesis is fairly lengthy, but although the final product **239** is a meso-compound (like *myo*-inositol itself), the precursor **238** is a chiral *myo*-inositol derivative and could be further elaborated before deprotection of the acetonide.



Scheme 4.4. Synthesis of a *myo*-inositol derivative from bromobenzene.

Chiral Chromatography

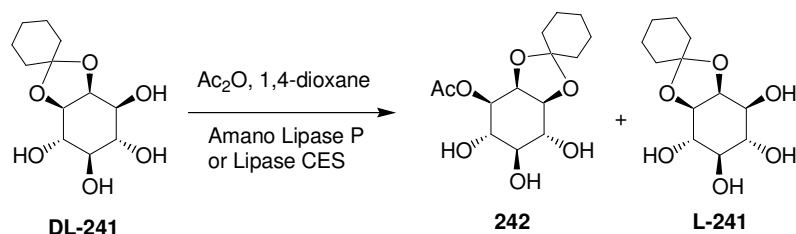
In many cases, chiral chromatographic methods are used for separation of enantiomers of *myo*-inositol derivatives, often at the end of the synthesis. The chromatographic methods employed include chiral HPLC,¹⁵⁶ chiral GC, and affinity chromatography. For example, Ozaki *et al.*¹⁵⁷ reported the successful separation of the enantiomers of **240** (right) by affinity chromatography in 1992, as part of their studies of the synthesis and biological properties of 2-substituted *myo*-inositol-1,4,5-trisphosphate analogues.



Although it may sometimes be useful to prepare both enantiomers, usually only one is required and therefore 50% of the material is essentially wasted. Also, the practical difficulties (and the cost) of large-scale chiral chromatography make this an unfavourable method for the preparation of chiral *myo*-inositol derivatives on larger scale.

Enzymatic Resolution

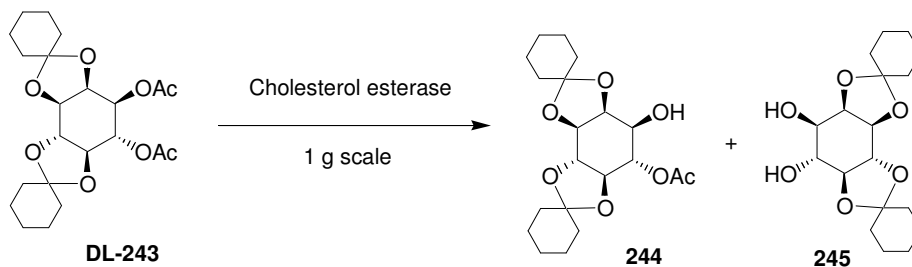
Enzyme-mediated esterification and hydrolysis have both been used to resolve racemic mixtures of *myo*-inositol derivatives. Ling and Ozaki effected a kinetic resolution of 2,3-*O*-cyclohexylidene-*myo*-inositol (**DL-241**) by enzymatic esterification using the *Pseudomonas* lipases in organic solvent (scheme 4.5).¹³²



Scheme 4.5. Example of enzyme-mediated esterification.

The 1-acetylated product **242** and the optically pure **L-241** were obtained in 49% yield each after separation by column chromatography. The enzyme could be reused after reactivation by hydration.

Similarly, enzymatic hydrolysis is also used effectively to resolve *myo*-inositol derivatives, as for example by Liu and Chen¹⁵⁸ in their synthesis of optically active *D-myo*-inositol 1,4,5-triphosphate (scheme 4.6). They used cholesterol esterase to obtain **244** and **245**, which were separated by flash chromatography.

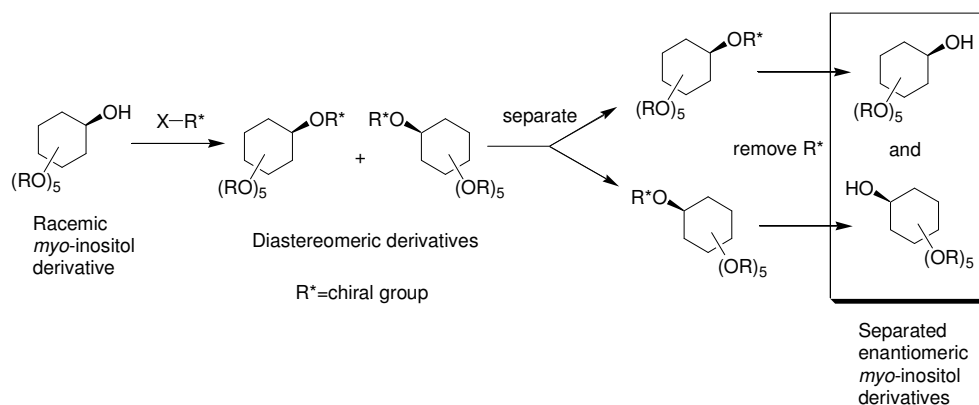


Scheme 4.6. Example of enzymatic hydrolysis.

Formation and Separation of Diastereomers of *Myo*-inositol derivatives

A widely used method for the preparation of chiral *myo*-inositol derivatives is the formation and separation of diastereomers of racemic *myo*-inositol derivatives with a chirally pure reagent (scheme 4.7). Usually a diastereomeric pair is formed in a 1:1 ratio. The two diastereomers are then separated by crystallisation or chromatography. In order to maximise the efficiency of the synthesis, this resolution step should take place as close to the beginning of the synthesis as possible *i.e.* a minimum number of synthetic steps from *myo*-inositol. In a few cases, which are discussed below, the derivatisation

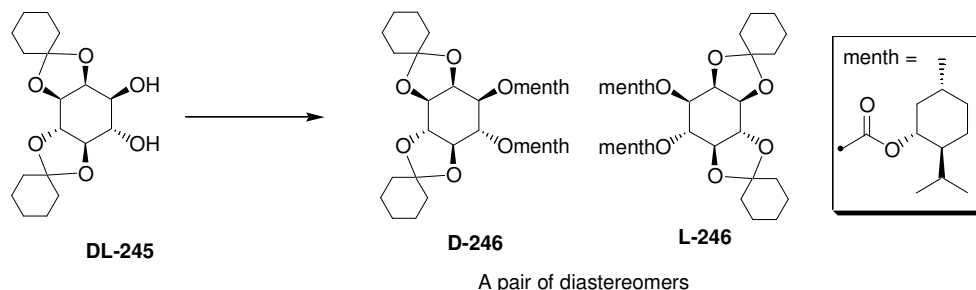
favours the formation of one diastereomer over the other. The ideal case, in which only *one* diastereomer is formed in 100% yield from *myo*-inositol, has not yet been realised in practise.



Scheme 4.7. Resolution by formation and separation of diastereomers.

Many different chiral groups (R^* in scheme 4.7) have been used for the derivatisation, including menthyl, menthoxyacetyl, camphanate and mandelate esters, the bis-dihydropyran reagents, and camphanylde acetals. Examples of the use of different chiral (R^*) groups will be given below.

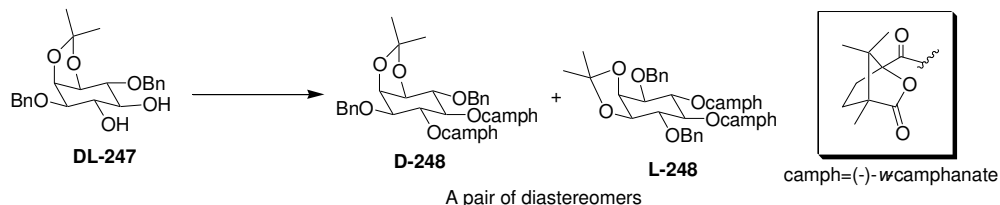
Schmidt *et al.* used a single diastereomer of a menthyl ester derivative of *myo*-inositol as a starting material in their 1992 synthesis¹⁵⁹ of a GPI anchor of yeast. In another example, Liu and Chen¹⁵⁸ successfully separated the two diastereomers of the di-L-menthyl carbonate **246** (scheme 4.8) by flash column chromatography. They obtained excellent yields of both diastereomers.



Scheme 4.8. Use of a menthyl carbonate derivative.

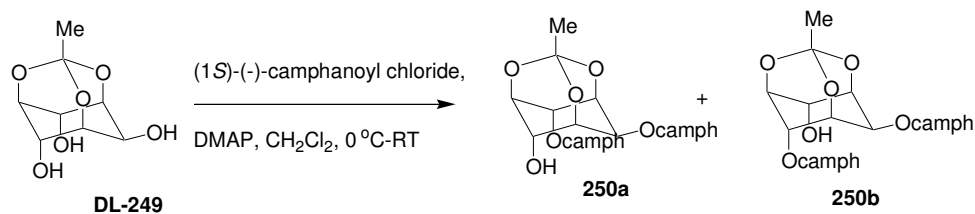
Camphanate esters have been often used to form separable diastereomers. For example, Desai *et al.*¹⁶⁰ reported a resolution of **247** (scheme 4.9) by forming

the camphanate ester **248** and isolating one diastereomer by crystallisation. They were unable to isolate significant amounts of the other diastereomer from the mother liquors, and instead recovered their starting material by cleaving the ester and then repeating the process using the oppositely configured camphanate.



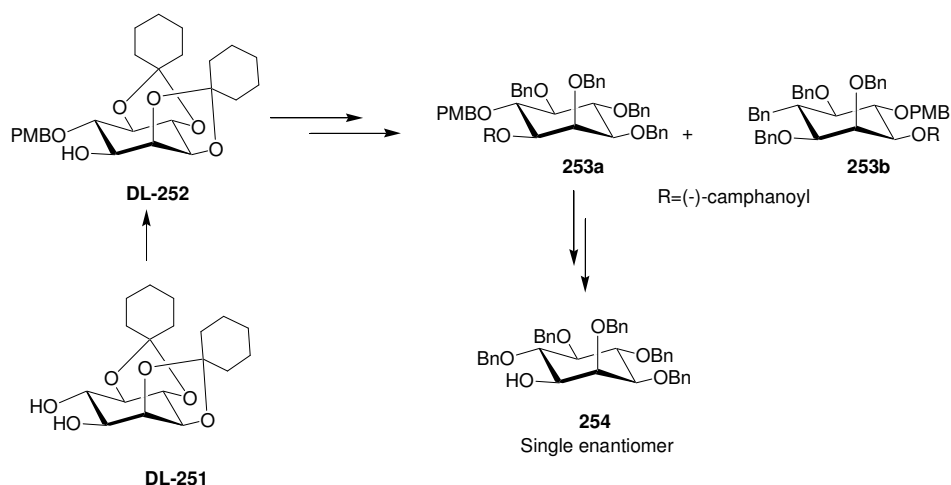
Scheme 4.9. Camphanate ester example.

Another interesting example of camphanate ester use begins with racemic *myo*-inositol orthoacetate **249** (obtained in one step from *myo*-inositol in 65% yield).¹⁶¹ This is treated with (1*S*)-(-)-camphanoyl chloride and DMAP to give a mixture of diastereomers **250a** and **250b** (scheme 4.10), with **250b** present in excess (although the actual ratio was not reported). Crystallisation gave the pure 1*D*-2,6-diester **250b** in 37% yield. Under different reaction conditions, with no DMAP present in the reaction mixture, the ratio of products changed to give an excess of the 2,4-diester **250a**, which was then crystallised in 40% yield.



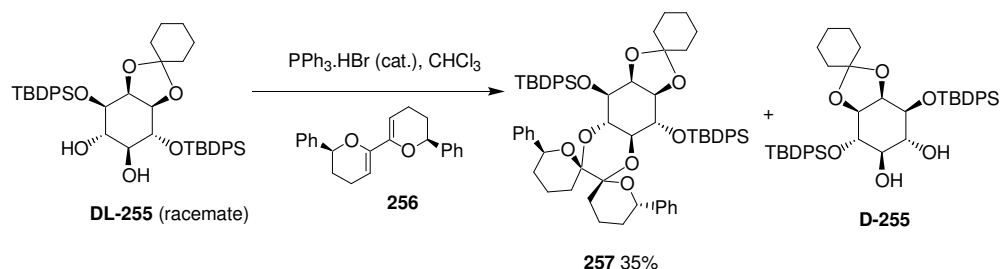
Scheme 4.10. Derivatisation of *myo*-inositol orthoacetate as camphanate ester.

Murakata and Ogawa, in their total synthesis of the *Trypanosoma brucei* VSG GPI,^{122(b)} prepared the inositol core from racemic 1,2:5,6-di-*O*-cyclohexylidene-*myo*-inositol (**251**, scheme 4.11 overleaf). Selective protection with *para*-methoxy-benzylchloride was followed by formation of separable diastereomers with (-)-camphanoyl chloride to give the mixture of diastereomers **253a** and **253b**. Further protecting group manipulation of **253a** gave their target molecule, **254**.



Scheme 4.11. From the first total synthesis of the *T. brucei* VSG GPI.

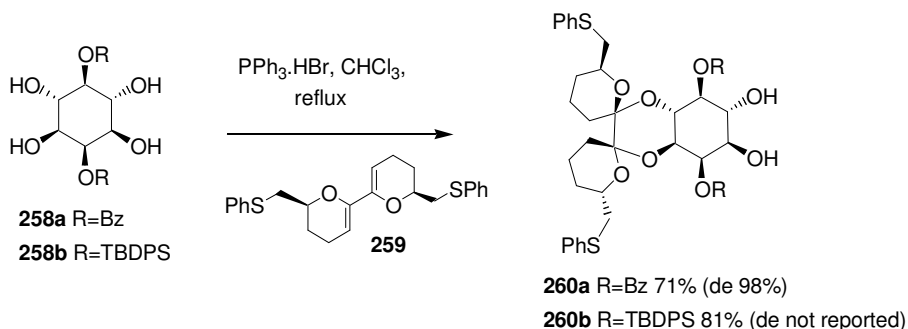
Ley and co-workers¹⁶² achieved a clever resolution by use of a chiral bis(dihydropyran) reagent (scheme 4.12). Racemic *myo*-inositol derivative **255** (obtained in three steps from *myo*-inositol) was treated with the bis-dihydropyran reagent **256**. Only one enantiomer (**L-255**) was able to react to give a single diastereomer **257**, and unreacted **D-255** was recovered. This was due to the congested nature of the system, where only the diastereomer that allows all the 6-membered rings to adopt a chair conformation could be formed.



Scheme 4.12. Resolution using bis-dihydropyran reagent.

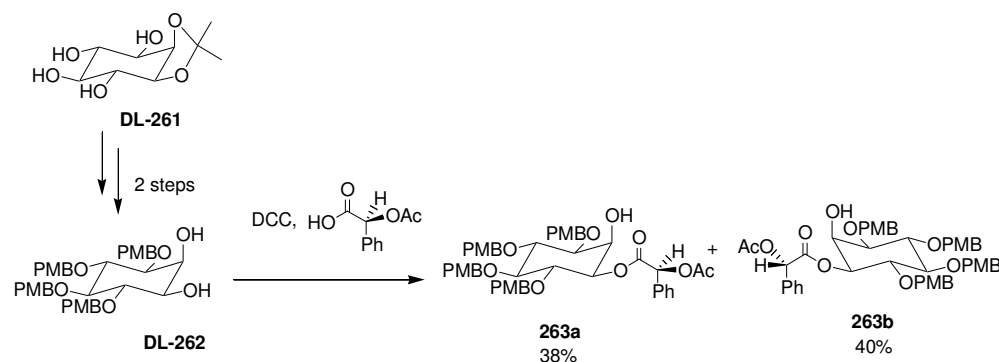
The single diastereomer **257** was crystallised in 35% yield (based on the racemic starting material), and the other (unreacted) enantiomer was recovered from the residues and purified by column chromatography. Unfortunately, further reaction of **257** was hindered by the bulky TBDPS groups, which were replaced with benzyl groups before further reaction. Unfortunately, the ketalisation did not proceed when the benzyl groups were present from the start as the analogous material was not sufficiently soluble.

In a later publication of their total synthesis of the *Trypanosoma brucei* VSG GPI,¹²³ the same group reported an improvement in their procedure, using the modified bis(dihhydropyran) reagent **259** in the desymmetrisation of the meso-compounds **258a** or **258b** (scheme 4.13) both of which were obtained in three steps from *myo*-inositol, using butane-2,3-dione to selectively protect the pairs of *trans*-diequatorial diols. Although yields of 71% (for **260a**) and 81% (for **260b**) were obtained on small scale, the yield upon scale-up (277 mmol) was only 28%.



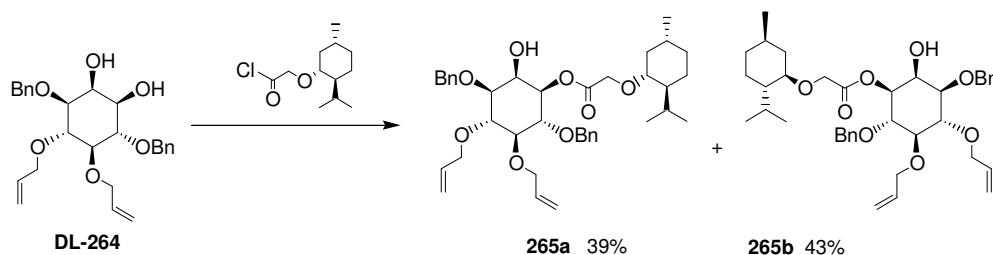
Scheme 4.13. Resolution using an improved bis(dihhydropyran) reagent.

Another chiral reagent that has been used for *myo*-inositol diastereomer formation is acetyl mandelic acid. For example, Horne and Potter, in their synthesis of the enantiomers of 6-deoxy-*myo*-inositol-1,3,4,5-tetrakisphosphate,¹⁶³ obtained **261** in one step from *myo*-inositol¹⁶⁴ and then further elaborated to give **262** (scheme 4.14). Subsequent treatment with acetyl mandelic acid and DCC gave **263a** and **263b**, which were separated by column chromatography.



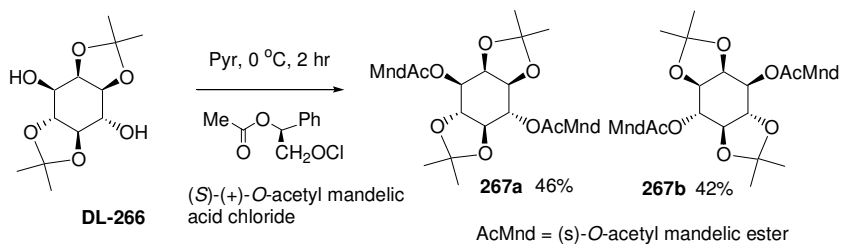
Scheme 4.14. Formation of diastereomers with acetyl mandelic acid.

Menthoxycetylchloride has also been used for diastereomer formation. In a 1986 publication,¹⁶⁴ the racemic compound **264** (formed in five steps from *myo*-inositol) was treated with 1-menthoxycetylchloride to give the diastereomers **265a** and **265b**. The former was isolated by crystallisation from hexanes (in 39% total yield) and the other, which was oily, was isolated by flash chromatography of the filtrate in 43% yield (scheme 4.15).



Scheme 4.15. Use of menthoxycetylchloride in diastereomer formation.

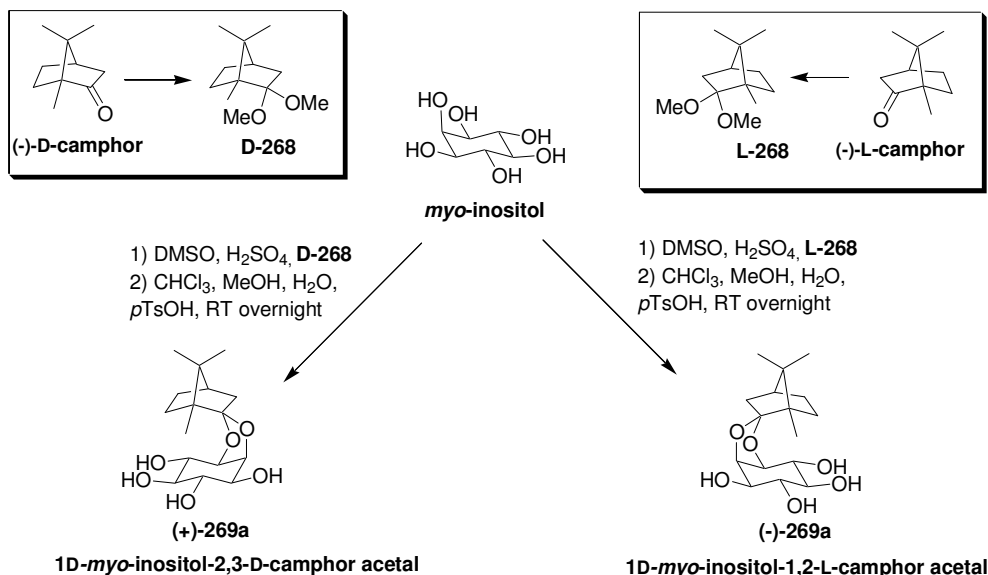
A recent publication, claiming the first example where both diastereomers of a *myo*-inositol derivative could be obtained by sequential crystallisation, used acetylmandelic acid chloride to form diastereomers of the diketal **266** (scheme 4.16).¹⁶⁵ These were then separated by crystallisation, first from hexane-ethyl acetate to give **267a** in 46% yield and then a second crystallisation from chloroform-hexane to yield **267b** in 42% yield. The very good yields in this step are somewhat offset by the fact that **266** is obtained in three steps from *myo*-inositol,¹⁶⁶ in an overall yield of 22% (although all three steps involve purification by crystallisation). Hence, the yields of **267a** and **267b** from *myo*-inositol are only 10 and 9% respectively.



Scheme 4.16. Use of acetyl mandelic acid chloride in diastereomer formation.

In 1989, Bruzik and Salamończyk reported the use of D- or L-camphor for the formation of diastereomers directly from *myo*-inositol (scheme 4.17).¹⁶⁷

Notably, the formation of ONE diastereomer as the major product (rather than a 1:1 ratio of diastereomeric products) is observed in this reaction, and hence *myo*-inositol can be directly and regioselectively protected and resolved in one step. The theoretical yield of the reaction is 100%, a vast improvement over the 50% maximum yield of many of the previous examples.



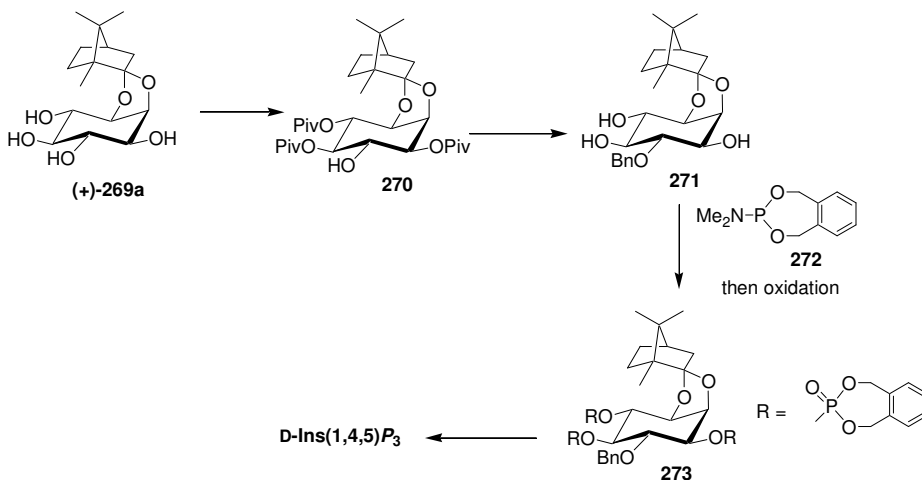
Scheme 4.17. Formation of *myo*-inositol camphanylidene acetals.

Use of L-camphor gives 1D-*myo*-inositol-1,2-camphanylidene acetal **(-)-269a** while use of D-camphor gives the opposite enantiomer, **(+)-269a**. There have been numerous slight variations on the original procedure,^{168,169,170,171} but essentially all involve the treatment of *myo*-inositol with > 2 equivalents of camphor dimethyl acetal (**268**).ⁱⁱⁱ The crude product (a complex mixture of mono- and di-acetals) is then ‘equilibrated’ by stirring in an acidified solution of chloroform, methanol and water at room temperature overnight. The product **(-)-269a** (or **(+)-269a**) is isolated by filtration in between 65-75% yields, contaminated with small amounts of the other three possible diastereomers (see

ⁱⁱⁱ A further significant publication has appeared since submission of this thesis, which details a) a method for reworking the mother liquors which allows preparation of both enantiomers of *tetra-O*-benzyl-*myo*-inositol via the *myo*-inositol camphanylidene acetal mixture prepared from cheaper D-camphor; b) a method for preparation of *myo*-inositol camphanylidene acetal that gives a low selectivity, so that a *ca.* 1:1 ratio of the two enantiomers of *tetra-O*-benzyl-*myo*-inositol may be obtained; c) an HPLC method for separation of the four diastereomers of *myo*-inositol camphanylidene acetal. The latter development appears to be the most useful element of this work. Wewers, W.; Gillandt, H.; Traub, H. S. *Tetrahedron Asym.*, **2005**, *16*, 1723-1728.

figure 6.1, page 143 and accompanying discussion in chapter six). The major diastereomer is then isolated by recrystallisation from methanol or methanol-water, in reported yields of 25-55% from *myo*-inositol.

Demonstrating the utility of the new procedure, Salamończyk and Pietrusiewicz used the acetal **(+)-269a** as a starting point for a short, elegant synthesis¹⁷² of D-Ins(1,4,5)*P*₃ (scheme 4.18). **(+)-269a** was treated with five equivalents of pivaloyl chloride to give **270**, which was then benzylated. Cleavage of the pivaloyl esters and phosphorylation of the resulting triol with reagent **272**, and subsequent oxidation gave **273**, which was finally deprotected to give the target molecule D-Ins(1,4,5)*P*₃.



Scheme 4.18. Synthesis of D-Ins(1,4,5)*P*₃ from **(+)-269a**.

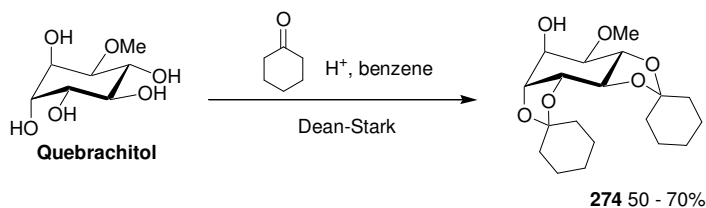
4.6 Chapters Six and Seven of this Thesis

The objective of the work described in chapters six and seven was to develop and perform a large-scale resolution of *myo*-inositol. The *myo*-inositol camphanylidene acetal procedure described above was chosen as an ideal basis for this objective. The reasons for this choice are elaborated in chapter six, which describes the process development work and investigation into analogues of the camphanylidene acetal, and in chapter seven, which describes the ensuing scale-up campaign. As part of this work, previously unpublished X-ray crystal structures were obtained for the major product of the reaction, **(-)-269a**, and for two of the diastereomeric impurities.

Functionalisation of Quebrachitol

5.1 Preparation of quebrachitol dicyclohexylidene acetal

Quebrachitol dicyclohexylidene ketal **274** was a key precursor to all of the work described in this chapter, and hence the efficient and facile preparation of **274** was paramount. In the literature, **274** is prepared by treatment of quebrachitol with cyclohexanone in refluxing benzene under Dean-Stark conditions (scheme 5.1), followed by extraction with chloroform.^{130,131}



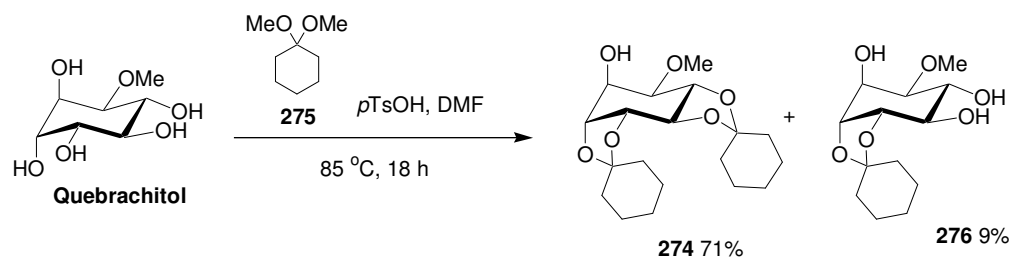
Scheme 5.1. Preparation of **274** from quebrachitol under Dean-Stark conditions.

The yields reported for this procedure are typically 50 – 70% (using recrystallised quebrachitol). In the course of this work yields below this range were obtained. In addition, a by-product, which was believed to be the product of an acid-catalysed aldol condensation of cyclohexanone, was formed in large amounts. Angyal and co-workers, who pioneered the use of the cyclohexylidene protecting groups with inositols, noted that ‘in larger concentration, *p*TsOH promotes the self-condensation of cyclohexanone, producing water which actually represses formation of the desired ketal’.¹³¹ The reaction was also attempted in neat refluxing cyclohexanone with catalytic *p*TsOH, however in this case **274** was isolated from the reaction in only 37% yield.

Thus, a new, improved procedure, eliminating the toxic benzene and chloroform was designed that involved treatment of quebrachitol with 1,1-dimethoxycyclohexane (**275**) under acidic conditions (scheme 5.2 overleaf). The reagent was easily prepared by heating cyclohexanone with 2.5 volumes of trimethylorthoformate and two volumes of methanol in the presence of catalytic

*p*TsOH. The workup is straightforward, involving quenching with triethylamine, removal of solvents and then an aqueous-diethyl ether partition. On small (2 mL of cyclohexanone) scale, the reaction proceeded to give essentially quantitative yield. When the reaction was scaled up to 400 mL of cyclohexanone, the crude product was of similar quality and yield to the product obtained on smaller scale. Unfortunately, accidental mechanical losses during distillation resulted in a yield of 77%, and the reaction was only performed once on this scale.

The protection of quebrachitol using this reagent was based on a literature preparation^{173,174} for the protection of *L-chiro*-inositol in which the triacetone derivative is prepared using acetone and 2,2-dimethoxypropane with catalytic acid. The diacetone derivative of quebrachitol, analogous to the dicyclohexylidene derivative **274** was also prepared during the course of this work, in very satisfactory 85% yield. That reaction proceeded smoothly at RT, however for the preparation of **274** itself with 1,1-dimethoxycyclohexane it was necessary to heat the reaction mixture in order to drive the reaction forward. The conditions were also modified to reduce the total reaction volume; cyclohexanone was omitted as it was found that the reaction proceeded well with 1,1-dimethoxycyclohexane only. The volume of DMF was also reduced to eight volumes of DMF to quebrachitol. Hence, 50 g of quebrachitol was heated overnight (to ca. 85 °C) in 400 mL DMF with reagent **275** (scheme 5.2) and *p*TsOH, and the reaction was quenched and worked up in the usual manner. From the residues of the first organic extracts, 64.8 g (71%) of crystalline product **274** was obtained. Additionally, when the aqueous fractions were concentrated and then re-extracted with ethyl acetate, 6.6 g (9%) of the mono-cyclohexylidene derivative **276** was isolated as a by-product.

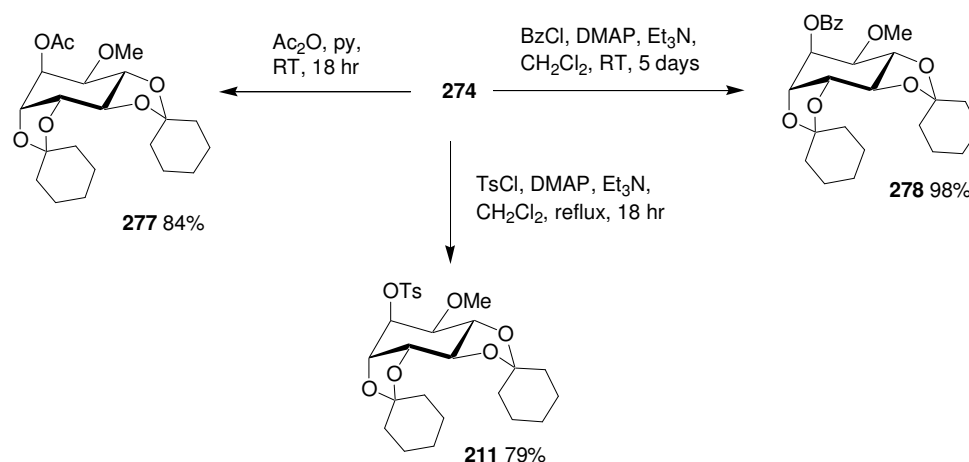


Scheme 5.2. Synthesis of 1L-1,2,3,4-di-*O*-cyclohexylidene-5-*O*-methyl-*chiro*-inositol (**274**) and 1L-1,2-*O*-cyclohexylidene-5-*O*-methyl-*chiro*-inositol (**276**).

The ^1H NMR spectra of **274** and **276** were quite different. In the spectrum of **274**, the signals for the inositol ring protons appeared as overlapping multiplets at 4.6 (3 H) and 3.6 (3 H) ppm. In the spectrum of **276** however, all of the ring proton signals were well-resolved and their coupling constants readily apparent. The signal attributed to the axial proton on the methoxy-bearing carbon (C-5) was furthest upfield at 3.38 ppm, and coupled to the neighbouring axial proton with $J = 8.8$ Hz and the neighbouring equatorial proton with $J = 3.2$ Hz.

5.2 Further protection of quebrachitol dicyclohexylidene acetal

As described in chapter four, the synthetic plan for the inositol core involved protection at the free hydroxyl (at O-6) of **274**, and subsequent deprotection at C-2, C-3 and C-4 to give a triol. Protection of the hydroxyl group to give the derivatives **277**, **278** and **211** (scheme 5.3) was based on literature procedures. Benzoylation was achieved in excellent yields of up to 98% using the DMAP-catalysed procedure of Ozaki *et al.*¹³⁵ The best yields were achieved with extended reaction times, rather than by increasing the amount of benzoyl chloride, which made purification of **278** more difficult.



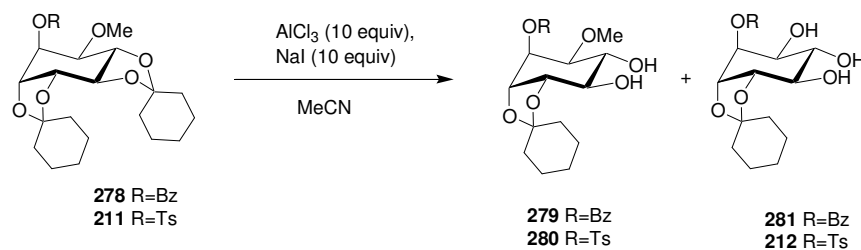
Scheme 5.3. Preparation of derivatives **277**, **278** and **211** from **274**.

Tosylation proved more troublesome; however, by heating to reflux in dichloromethane overnight, a 79% yield of **211** was achieved. Previously, vigorous tosylation conditions have been reported to be necessary for the

preparation of this derivative.¹³⁰ Acetylation under standard conditions, using acetic anhydride in pyridine proceeded readily in yields > 80%.

5.3 Demethylation of **278** and of **211**

In line with the planned strategy for the synthesis of the L-GPI core (scheme 4.1, page 98), the concurrent cleavage of the methyl ether and the *trans*-cyclohexylidene groups of **278** or **211** was next attempted (scheme 5.4). Ozaki and co-workers report using AlCl₃ and NaI in acetonitrile at RT to effect this cleavage.¹³³ Triol **281** was obtained in 83% yield after overnight stirring.^{135,147,175} Ozaki *et al.* also report that after three hours at RT, only 52% of **281** was isolated, along with 22% of **279**, in which only the *trans*-cyclohexylidene group had been cleaved. When the reaction was performed at 0 °C for one hour, with half the amounts of AlCl₃ and NaI, an 89% yield of **279** was reported. These results indicate that the cyclohexylidene moiety is lost first, with subsequent cleavage of the methyl ether assisted by the vicinal hydroxyl group. Synthesis of triol **212** under similar conditions has also been reported, in 75% yield.^{133,147}



Scheme 5.4. Cleavage of *trans*-cyclohexylidene moiety and demethylation.

Unfortunately the results of Ozaki *et al.* could not be repeated in the course of this work. The demethylation of both **278** and **211** was attempted, and although the *trans*-cyclohexylidene group was cleaved, the methyl ether was not, even under more forcing conditions (increased temperature or time). Some cleavage of the *cis*-cyclohexylidene group was also suspected. The results of relevant experiments are summarised in table 5.1 overleaf.

Table 5.1. Conditions and results of attempted demethylations.*

Entry	Start	AlCl ₃ (equiv)	Iodide source (equiv)	Time h	Temp	Isolated yield (%)		
	mat.					278/ 211	279/ 280	281/ 212
1	278	10	NaI (10)	18	RT	0	30	0
2	278	10	NaI (10)	2	RT	11	75	0
3	278	10	<i>n</i> -Bu ₄ NI (10)	18	RT	0	24	0
4	211	10	<i>n</i> -Bu ₄ NI (10)	18	RT	0	35	0
5	211	10	NaI (10)	16	RT	0	12	0
6 [§]	211	5	NaI (5)	1	0 °C	10	57	0

* 30 vols MeCN in all cases. Isolated yields.

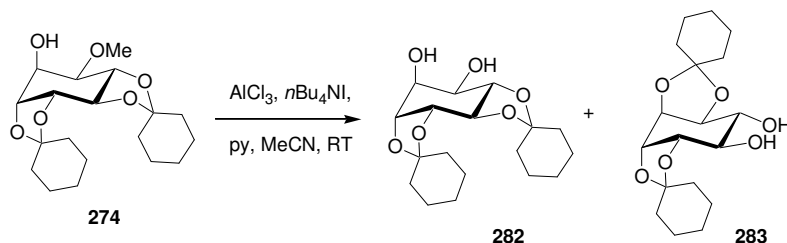
[§] Formation of **280** was the intent of this reaction.

It is evident from a number of the reactions summarised in table 5.1 that material was being lost and this was attributed to the cleavage of both Cy groups and loss of the resultant tetra-ols in the aqueous washings. Concentration and subsequent analysis (¹H NMR) of the aqueous washings confirmed these suspicions. The residues from the aqueous washings contained inositol with the methyl ether still present, clearly visible as a singlet at approximately 3.4 ppm.

Material that had lost only the *trans*-cyclohexylidene group (**280**) was isolated (entry 6) and then subjected to demethylation with NaI (10 equiv) and *n*Bu₄NI (10 equiv), with 10 equivalents of pyridine added to suppress the cleavage of the cyclohexylidene group.^{139,140} The reaction was heated to 70 °C overnight, in line with demethylation conditions used successfully for the cleavage of the methyl ether of molecule **274** (which is vicinal to a *cis*-hydroxyl group, accelerating the cleavage¹³⁵ - see discussion below). However, only starting material was recovered from this attempt. This suggests that under the conditions with pyridine present, the cleavage of a methyl ether vicinal to a *trans*-hydroxyl group will not proceed.

Given the lack of success in the preparation of the triols **281** or **212**, it was decided to attempt instead the formation of the diol **282**, directly from **274** (scheme 5.5). Ozaki and co-workers have reported^{133,139} that the methyl ether

with the vicinal *cis*-hydroxyl is cleaved chemoselectively, in preference to the normally very labile *trans*-cyclohexylidene moiety, by $\text{AlCl}_3\text{-NaI}$ or $\text{AlCl}_3\text{-}n\text{Bu}_4\text{NI}$ in acetonitrile (the cleavage of methyl ethers with a vicinal *trans*-hydroxyl group was reported to be much slower). The latter system, with $n\text{Bu}_4\text{NI}$ as the iodide source, was found to be preferable^{139,140} because of a lesser tendency for the *trans*-cyclohexylidene moiety to be cleaved. Addition of pyridine to the reaction mixture also helps to suppress cleavage of the *trans*-cyclohexylidene ketal.^{139,140} A number of reported attempts to optimise the reaction conditions have been made, with variations in the number of equivalents of AlCl_3 and iodide reagent used (typically 10 equivalents of each are added), the nature of the base added to suppress cleavage of the *trans*-cyclohexylidene moiety, and reaction times. Optimal conditions for the preparation of **282** seem to be the use of 10 equivalents each of AlCl_3 , $n\text{Bu}_4\text{NI}$, and pyridine, in acetonitrile, at RT for 5 to 26 hours, but reported results do vary. It has also been observed^{133,140} that under acidic conditions, after demethylation, the *trans*-cyclohexylidene can migrate to give **283**, in which both cyclohexylidene groups protect a pair of vicinal *cis* hydroxyl groups. It was found that when the NaI-AlCl_3 system was used with no added pyridine, **283** was the sole isolated product in 40 – 60% yield.



Scheme 5.5. Formation of the diol **282** by demethylation of **274**.

Hence, the dicyclohexylidene derivative **274** prepared as described above, was subjected to the demethylation conditions. Unfortunately, reproduction of the reported results was again not achieved. Stirring overnight at room temperature with either $\text{AlCl}_3\text{-NaI}$ or $\text{AlCl}_3\text{-}n\text{Bu}_4\text{NI}$ and pyridine in acetonitrile, gave largely unreacted starting material. Acetonitrile and pyridine were freshly distilled, and hence it was suspected that the AlCl_3 being used was of poor quality, but only a small improvement was observed upon using fresh reagent. These results were therefore extremely puzzling. Fortunately, it was

found that heating the reaction mixture for a period of hours induced the desired methyl ether cleavage. A range of conditions was used with varying degrees of success, and the summary is presented in table 5.2.

Table 5.2. Conditions and results of demethylations of **274**.*

Entry	Equiv. AlCl ₃	Equiv. <i>n</i> Bu ₄ NI	Time h	Temp	Isolated yield (%)		
					274	282	283
1	10	10	18	RT	78	0	0
2	10	10	96	RT	38	0 [#]	0
3	10	10	26	RT	71	15	0
4	10	10	72	RT	60	24	0
5	10	10	48	40 °C	52	39	5
6	10	10	18	60 °C	50	43	0
7	10	10	18	reflux	5	23	55
8	10	10	48	reflux	2	10	74
9	10	7	18	62 °C	30	55	10
10 [§]	8	5	18	62 °C	24	51	0

* All reactions run in 30 volumes of MeCN and with 10 equiv of pyridine added.

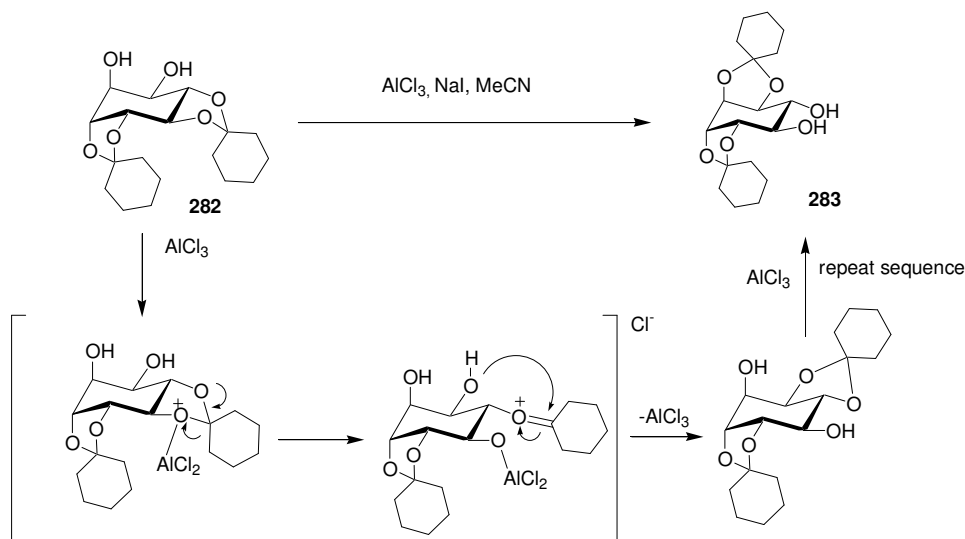
[#] TLC suggested ca. 50% conversion, but **282** was not isolated after workup.

[§] Scaled up reaction, material was lost crystallising on the column.

Although heating to 40 °C or over did induce the methyl ether cleavage, these more forcing reaction conditions also induced the rearrangement of **282**, to give the isomeric product **283**, via the Lewis-acid catalysed mechanism shown in scheme 5.6 overleaf. The identity of **283** was confirmed by comparison with literature NMR data for the same compound. This product possesses a rotational axis of symmetry and hence displays simple NMR spectra compared to **282**. Three discrete signals appear for the inositol ring proton region of the ¹H NMR spectrum (each equivalent to two protons), and nine signals appear in the ¹³C NMR spectrum (three for the symmetrical inositol ring and six for the equivalent cyclohexylidene moieties).

The isomerization to give **283** even in the presence of pyridine, was found to be aggravated both by prolonged reaction time (entries 5 and 8) and excessive heating (entries 7 and 8). Heating the reaction mixture to just over 60 °C overnight was found to give the best yield of **282**, so that although the

results were somewhat variable (entries 9 and 10), **282** could be isolated in useful quantities.



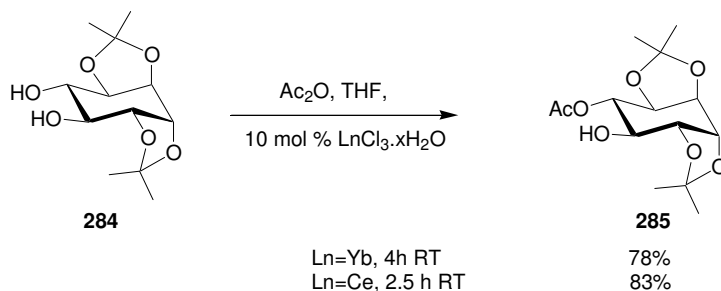
Scheme 5.6. Likely mechanism of migration of cyclohexylidene groups.

The efficacy of the pyridine in suppressing the *cleavage* (rather than the migration) of the *trans*-cyclohexylidene moiety was demonstrated when the pyridine was accidentally added 10 minutes after all the other reagents had been stirring at RT. When this reaction was worked up after stirring overnight at RT, the crude product was found to contain **274** and **276** in an approximately 1:1 ratio. Again, no demethylation was observed. It was assumed that the cyclohexylidene cleavage to give **276** had occurred in the first 10 minutes, before the addition of pyridine.

Several attempts were made to cleave the methyl ether of either **278** or **211** using either the $\text{AlCl}_3\text{-NaI}$ or the $\text{AlCl}_3\text{-}n\text{Bu}_4\text{NI}$ system in the presence of pyridine, in the hope that the methyl ether might be cleaved without loss of the *trans*-cyclohexylidene moiety (this had not been reported in the literature). At room temperature, in all cases no cleavage was observed. At 60 °C, **211** (Ts version) began to lose the *trans*-cyclohexylidene group, but retained the methyl ether. These results again demonstrate the need for a vicinal *cis*-hydroxyl group for a successful demethylation using this procedure.

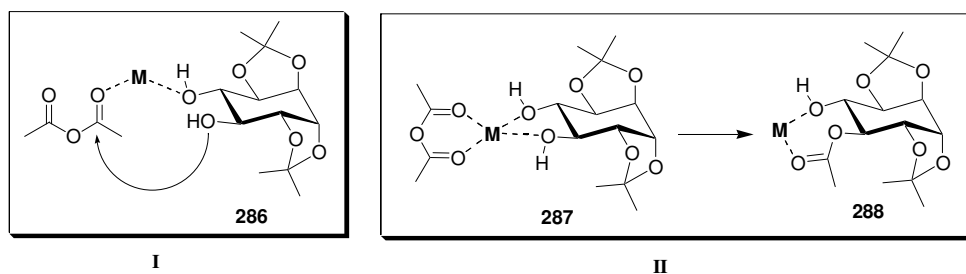
5.4 Mono-acetylation of diol **282**

As part of a project being undertaken by G. S. Cousins in the same laboratory, the mono-esterification of certain symmetrical inositol derivatives containing vicinal di-equatorial diols was achieved^{174,176} using the method of Clarke and co-workers (scheme 5.7).¹⁷⁷ Clarke's group reported that mono-acetylation of a C-2 symmetric diol was readily achieved in good yield in a simple one-step procedure using acetic anhydride and a Lanthanide salt catalyst. Best results were obtained with CeCl_3 and YbCl_3 in either THF or dichloromethane, with reported yields in excess of 90%. When these conditions were applied to the inositol derivative **284**, similarly good yields of the monoesters such as **285** (scheme 5.7) were achieved with no trace of any diester products being formed. It was found that for the inositol substrate, the catalyst loading could be reduced to 5 mol% without loss of yield. A variety of other anhydrides were also successfully used; chloroacetic, propionic, crotonic, benzoic and pivalic monoesters were prepared. Monoesters of the dicyclohexylidene analogue of **284** were also successfully prepared.



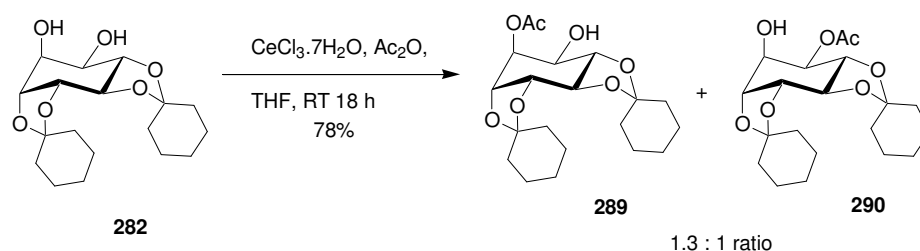
Scheme 5.7. Monoacetylation of inositol derivative **284**.

Two different mechanisms have been proposed to explain the selectivity.^{176,177} The first (**I**, scheme 5.8) proposes that the metal coordinates to one of the diol hydroxyl groups and one carbonyl from the anhydride, leaving the uncoordinated hydroxyl group free to attack the activated anhydride carbonyl. Alternatively (**II**, scheme 5.8), both the diol and the anhydride could chelate to the metal centre to give **287**. Acyl transfer from the anhydride to the diol then occurs, resulting in the seven-membered chelate **288**, which, being less energetically stable than the five-membered chelated diol (**287**), is released and a new diol chelated to continue the reaction.



Scheme 5.8. Proposed transition states for the monoacetylation reaction.

This method had not been applied to non-symmetrical inositol derivatives. It was thought that this reaction might show some selectivity in a vicinal axial-equatorial diol such as 1L-1,2:3,4-di-*O*-cyclohexylidene-*chiro*-inositol (**282**), because in **I** above, it could be favourable to coordinate the metal in an equatorial or axial position, and in **II**, steric effects or ring strain effects could favour acetylation at only one of the available positions.ⁱ Hence, 75 mg (0.22 mmol) of diol **282** were treated with CeCl₃·7H₂O (0.02 mmol) and Ac₂O (1.10 mmol) and stirred in THF at RT overnight (scheme 5.9). After this time, ¹H NMR and TLC analysis indicated that no starting material remained, and one major product spot was evident. After workup, ¹H NMR analysis demonstrated that these reaction conditions had indeed given a mono-acetylated product in good yield of 78%. Analysis by HRMS (ESI) found a signal at *m/z* 383.2051; the calculated *m/z* for the protonated mono-acetylated product (C₂₀H₃₁O₇ [M + H⁺]) being 383.2064. No signal was observed that could be attributed to a di-acetylated product.

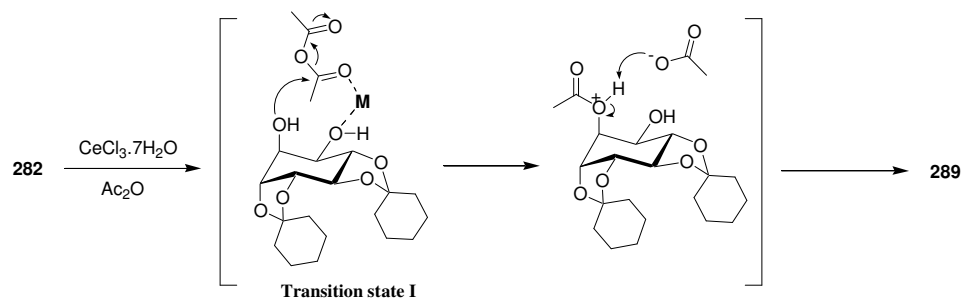


Scheme 5.9. Monoacetylation reaction applied to non-symmetrical diol **282**.

ⁱ Literature reports suggest that acylation of sugars is often selective for equatorial hydroxyl groups, whereas alkylation tends to be selective for axial hydroxyl groups; this has been rationalised on the basis of transition state bulk: Bert Fraser-Reid *et al. Aust. J. Chem.* **2002**, 55, 123-130, and references therein.

However, examination of the ^1H NMR spectrum revealed that acetylation had occurred at both the O-5 and O-6 position of **282** to give **289** and **290** in an approximately 1.3:1 ratio. The ^1H NMR of the mixture of products showed a doublet of doublets at 5.55 ppm ($J_{\text{eq-eq}} = 3.2$, $J_{\text{ax-eq}} = 2.6$ Hz), which was attributed to the equatorial proton vicinal to the acetyloxy group in **289**, and a doublet of doublets at 5.05 ppm ($J_{\text{ax-ax}} = 8.1$, $J_{\text{ax-eq}} = 2.5$ Hz) attributed to the axial proton vicinal to the acetyloxy group in **290**. To further confirm the presence of two products, gCOSY analysis was done and showed no correlation between the two protons at 5.55 and 5.05 ppm. The relative integration for these two protons was used to determine the product ratio, and the relative integration of the other inositol ring protons (signals between 3.5 – 4.4 ppm) were correct for a monoacetylated product. The methyl signals for the acetyl groups of the two products appeared as singlets at 2.16 and 2.13 ppm.

The reaction mechanism evidently does not significantly favour the esterification of either the axial or the equatorial hydroxyl of this vicinal axial-equatorial diol, under these conditions. However, the slight excess of axial product **289** may be explained by invoking transition state **I** as discussed above. Co-ordination of the equatorial hydroxyl group to the metal centre would form transition state **I** as shown in scheme 5.10.



Scheme 5.10. Formation of the axial acetyl product **289** via transition state **I**.

This would be the thermodynamically favoured transition state, and lead to the formation of the axial acetyl product **289**. It is conceivable that modified reaction conditions might be able to enhance the selectivity of this reaction. Preferentially forming the equatorial acetyl product **290** might be possible by

using conditions that might favour the kinetically favoured transition state, such as running the reaction at lower temperatures.

5.5 Butane diacetal derivatives

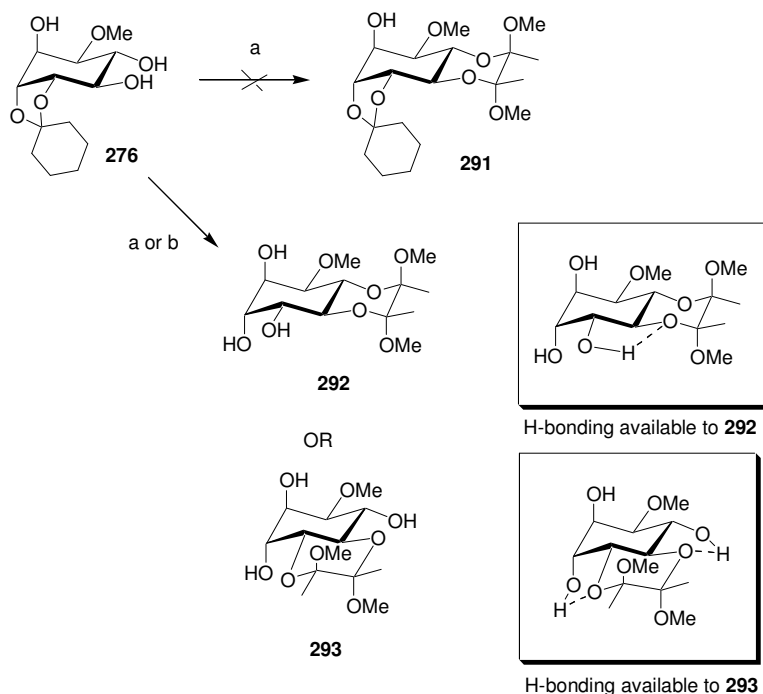
The butane diacetal (BDA) protecting group is a useful and widely used protecting group that is specific for *trans*-diequatorial diols. It is reasonably inexpensive and simple to introduce, the products are often crystalline, and the NMR spectra simple, displaying four diagnostic singlets per BDA group.

Its introduction, using the reagent 2,2,3,3-tetramethoxybutane (TMB) was first reported¹⁷⁸ in 1996.ⁱⁱ The TMB reagent was prepared by refluxing a methanol solution of trimethyl orthoformate and 2,3-butanedione with catalytic sulphuric acid, followed by distillation to purify the crude product. Reaction of TMB with the diol was again done in refluxing methanolic solution and in the presence of trimethyl orthoformate, but catalysed by camphor sulphonic acid. A variety of carbohydrates were successfully derivatised using this procedure. Soon after this, a paper appeared evaluating a range of cyclic and open chain 1,2-diketones as potential protecting groups, in-situ generation of the TMB reagent, and use of BF₃.OEt₂ as an (not necessarily better) alternative to CSA.¹⁷⁹ In the one-step procedure, butanedione, trimethyl orthoformate, and CSA are all added to a methanolic solution of the diol and after refluxing for a period of hours the resultant BDA derivative is often able to be isolated by crystallisation.

In the course of this work, the BDA group was used for the protection of O-3 and O-4 of mannose, as part of the strategy for the synthesis of the GPI presented in chapter four. Upon isolation of the mono-cyclohexylidene protected quebrachitol derivative **276**, it was decided to attempt the protection of the free vicinal diequatorial diols of **276** using BDA (scheme 5.11). Thus, **276** was treated with butanedione, trimethyl orthoformate and CSA in refluxing methanol overnight.¹⁸⁰ Upon workup, product was isolated as a fine white solid that crystallised from the crude reaction product by addition of a small amount of

ⁱⁱ In this first report, the term 'butane bis-acetal' (BBA) was used to denote these derivatives, however the term butane diacetal has now been widely adopted.

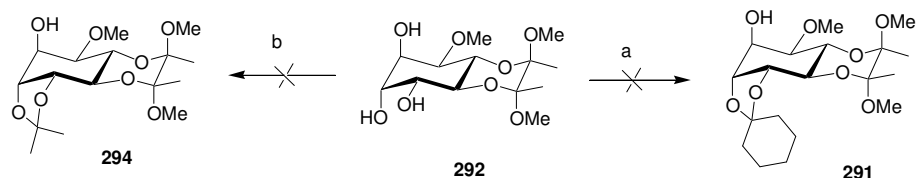
acetone. This product was initially presumed to be **292**, in which the free hydroxyl pair had been protected with the BDA moiety, and the *cis*-cyclohexylidene group had then been lost. However, **293** could also be a possible structure for the product. It could be formed if the cyclohexylidene group was lost first, and the BDA protection occurred next. It was found that essentially identical results were obtained if the reaction was only refluxed for three hours.



Scheme 5.11. Attempted protection of the vicinal diequatorial diol of **276** with BDA. Reagents and conditions, a) Butanedione, MeOH, HC(OMe)₃, CSA, reflux, 18 h; b) butanedione, MeOH, HC(OMe)₃, CSA, reflux, 3 h.

It was not clear whether any of the expected product **291**, retaining the *cis*-cyclohexylidene group, had been formed in the reaction. Careful TLC monitoring was inconclusive and column chromatography of the evaporated filtrate from the product filtration failed to isolate any **291**. Assuming then that the product was **292**, it was postulated that the loss of the *cis*-cyclohexylidene group was accelerated by the formation of the fused inositol-dioxane ring system of the BDA group. The rigidity imposed by the BDA group invokes some conformational restriction and possibly also strain in the five-membered ring of the cyclohexylidene acetal, thus destabilising it. Although it is much more stable than the *trans*-cyclohexylidene group, the *cis*-cyclohexylidene could also be lost.

Presuming that the product was **292**, protection of the pair of *cis*-hydroxyl groups as a cyclic acetal was also attempted (scheme 5.12). When **292** was treated with 1,1-dimethoxy-cyclohexane and pTsOH in DMF at 85 °C (the procedure which had been used very successfully for the protection of quebrachitol), there was no sign of **291** being formed in the reaction. Even after heating for several days, no likely-looking spots were seen in TLC analysis and ^1H NMR analysis showed that starting material was the only significant inositol component present in the reaction mixture. It was postulated that the isopropylidene derivative **294** might form more readily, since it is acyclic and hence has less inherent conformational restrictions. However, similarly no sign of product was seen when literature methods¹⁷³ were applied.

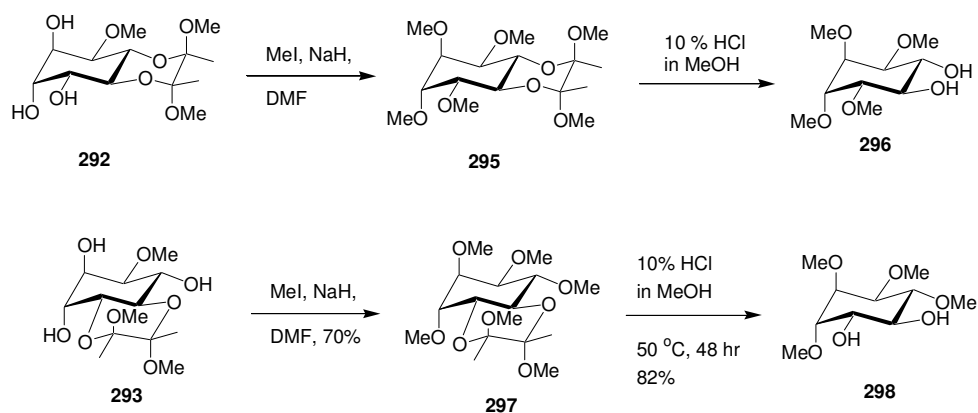


Scheme 5.12. Attempts to protect O-3 and O-4 of (presumed) **292** as a cyclic acetal. Reagents and conditions: a) Dimethoxycyclohexane, *p*TsOH, DMF, 85 °C, 3 days; b) Acetone, 2,2-dimethoxypropane, *p*TsOH, RT, several days.

Having still not conclusively identified the structure of the BDA product as either **292** or **293**, the white solid was subjected to per-methylation and the BDA moiety then removed with methanolic HCl. The two possible structures of the tetra-methylated product are shown in scheme 5.13. The deprotection was achieved by warming to 50 °C for two days, and did not proceed at RT. The tetra-methoxy derivative was readily synthesised, with the methylation proceeding in 70% yield and the deprotection in 82% yield.

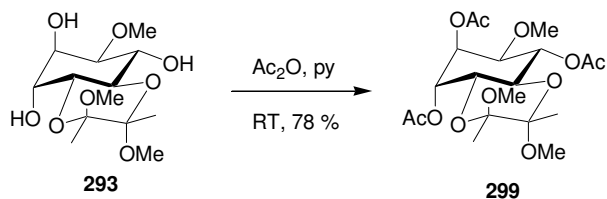
The NMR spectra of the tetra-methoxy derivative were revealing. Had the product been the symmetrical molecule **296**, the ^{13}C NMR spectrum would have been a simple spectrum showing only five signals.ⁱⁱⁱ However, there were

ⁱⁱⁱ Authentic NMR spectra of the enantiomer of **296** (the *D-chiro* tetra-methoxy derivative) were kindly supplied for comparison by Dr. Andy Falshaw, Industrial Research Limited.



Scheme 5.13. Per-methylation and deprotection of the BDA product, **292** or **293**.

ten signals in the spectrum, six in the region where signals for inositol ring carbons are usually found (70 – 85 ppm), and four discrete methoxy carbon signals (around 60 ppm). This indicated that the product that had been formed was **298**, and hence that the original product from the BDA reaction of quebrachitol cyclohexylidene acetal was **293**. This was further confirmed by acetylation of the product, now presumed to be **293** (scheme 5.14). NMR analysis of the acetylated product (including gCOSY analysis) confirmed the structure to be **299**. The inositol ring protons next to the three acetyl groups were shifted downfield to 5.43, 5.26 and 5.20 ppm, and hence the proton couplings around the ring could be identified.



Scheme 5.14. Acetylation of the BDA derivative **293**.

The ^1H NMR spectrum of the product **293** is shown in figure 5.1 on the following page. The distinctive pattern of four singlets of the BDA group is clearly discernible - the two singlets attributed to the methyl groups at 1.32 and 1.33 ppm and the two attributed to the methoxyl groups at 3.28 and 3.25 ppm.

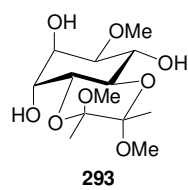
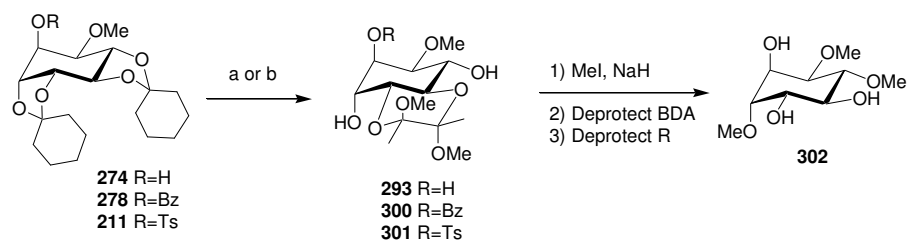


Figure 5.1. ^1H NMR spectrum of **293**.

The reason for the preferential formation of **293** over **292** may be attributed to increased stability of **293** due to extra hydrogen-bonding available within the structure. The five-membered rings formed by hydrogen bonds between the ring oxygens of the BDA moiety and the vicinal inositol ring hydroxyl protons are shown in scheme 5.11 (page 126). In **292**, only one hydrogen bond is possible, either as shown or between the equatorial alcohol and the neighbouring axial alcohol, whereas in **293**, two such five-membered rings are available.

It was postulated that **274** could also serve as a substrate for the formation of **293**, via in-situ generation of **276** by cleavage of the more labile *trans*-cyclohexylidene group under the acidic reaction conditions. Indeed, upon subjecting **274** to analogous reaction conditions, the same product was isolated in comparable yield (scheme 5.15). Reaction of **278** and **211** under the same conditions was also performed. In both cases, product was again crystallised out of the crude reaction mixture, after removal of solvents, by the addition of a small amount of acetone. These products were identified as **300** and **301** by analogy with the triol product **293**. The acetate derivative **277** was also subjected to the reaction conditions, but the analogous product was not isolated. A very small amount (approx. 5%) of **293**, having lost the acetyl group, was obtained, but since this reaction was only done on a small scale it was not clear whether any of the desired product had been formed.

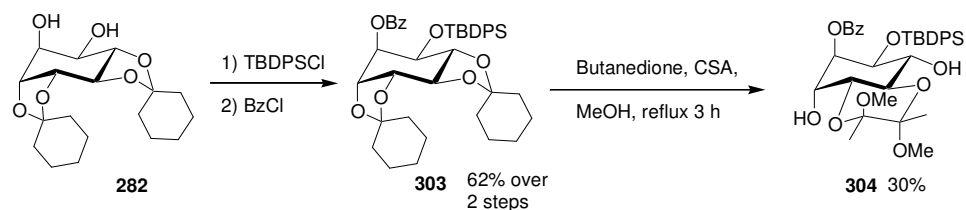


Scheme 5.15. Preparation of a trimethoxy derivative. Reagents and conditions, a) Butanedione, MeOH, HC(OMe)₃, CSA, reflux, overnight; b) butanedione, MeOH, HC(OMe)₃, CSA, reflux, 3 hours.

The trimethoxy derivative **302**, would also be readily available using a similar methodology to that used for the preparation of the tetra-methoxy

derivative, but starting with the benzoyl or tosyl-containing molecules **278** or **211** (scheme 5.15).

Due to the harsh conditions normally required for the cleavage of a methyl ether, the BDA derivatives formed from quebrachitol without demethylation may have only limited usefulness in many cases (unless a methyl ether is present in the target molecule at the equivalent position). Hence, it would be useful to demethylate the dicyclohexylidene derivative **274** (for example, as above) and then proceed to protect both hydroxyls of the resulting diol **282**, with either the same or different protecting groups before effecting the simultaneous introduction of BDA moiety and cleavage of both cyclohexylidene groups. This has been achieved using TBDPS to protect the equatorial hydroxyl of **282** (scheme 5.16). This reaction was selective for the equatorial hydroxyl, giving an approximately 5:1 ratio of equatorial:axial OTBDPS products that could be separated by flash column chromatography (the selectivity of this reaction is discussed further later in this chapter). Material contaminated with a small amount of the regioisomer was carried through the subsequent benzoylation to give **303** and then subjected to the conditions for the introduction of the BDA moiety. The major product **304** was isolated by flash column chromatography (rather than by the crystallisation method used for the other BDA derivatives).



Scheme 5.16. BDA derivative from demethylated compound.

The ^1H NMR spectrum of **304** is shown in figure 5.2 overleaf, and the ^{13}C NMR spectrum on page 133. Note the distinctive pattern of the BDA group in the ^1H spectrum, of two methyl and two methoxy groups which appear at 1.32 and 1.27 ppm, and at 3.22 and 3.15 ppm respectively. The ring proton next to the benzoyl protecting group appears at 5.28 as a doublet of doublets (see the expansion box in figure 5.2), with coupling constants $J_{\text{eq-eq}} = 3.5$ Hz and $J_{\text{ax-eq}} =$

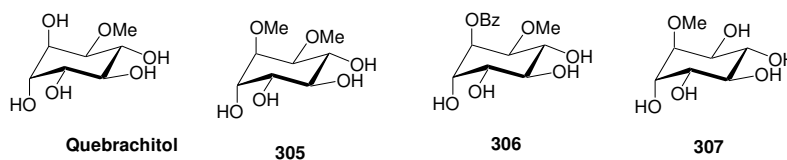
Figure 5.2. ^1H NMR spectrum of **304**.

Figure 5.3. ^{13}C NMR spectrum of **304**.

3.4 Hz. The observed couplings of this proton allowed the two regioisomers to be differentiated and quantified in compound **303**, as is discussed further in the next section. In the ^{13}C NMR spectrum the two phenyl groups of the TBDPS group are differentiable. This indicates that the two are not equivalent, due to the rigid structure and steric interactions precluding free rotation of the large TBDPS group. The distinctive pattern of the BDA moiety is again visible, with the two methoxy carbon signals appearing at 47.9 and 48.0 ppm, and the two methyl signals at 17.5 and 17.2 ppm.

5.6 Synthesis of quebrachitol derivatives for uptake inhibition assays

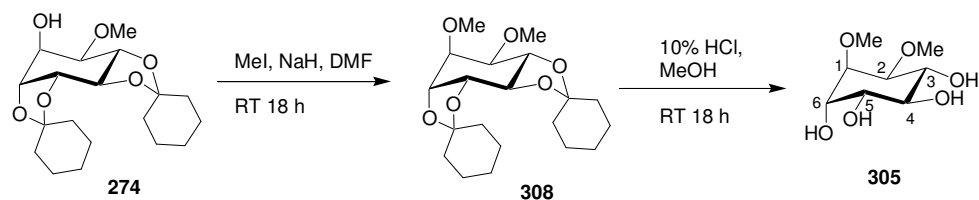
The work described here was done in order to extend the usefulness of quebrachitol and its derivatives as potential inhibitors of the biosynthesis of inositol-containing cell surface molecules. These are important to the function of certain bacterial species (eg *Mycobacterium tuberculosis*), as discussed in chapter four. The four derivatives shown in scheme 5.17 were prepared and tested, with biological activity results discussed at the end of this section.



Scheme 5.17. The derivatives prepared for the enzyme inhibition study.

Preparation of the dimethyl derivative 1L-1,2-di-*O*-methyl-*chiro*-inositol (**305**) was achieved readily in two steps from the dicyclohexylidene derivative **274** (scheme 5.18). Methylation of the free hydroxyl group with sodium hydride and methyl iodide in DMF proceeded to give **308** in 94% yield (this reaction has also been reported¹⁸¹ using silver oxide and methyl iodide in DMF). Subsequent cleavage of the two cyclohexylidene groups was accomplished upon stirring in 10% HCl in methanol at room temperature overnight. This deprotection was also attempted using 80% acetic acid in water, but after stirring for 18 hours, TLC

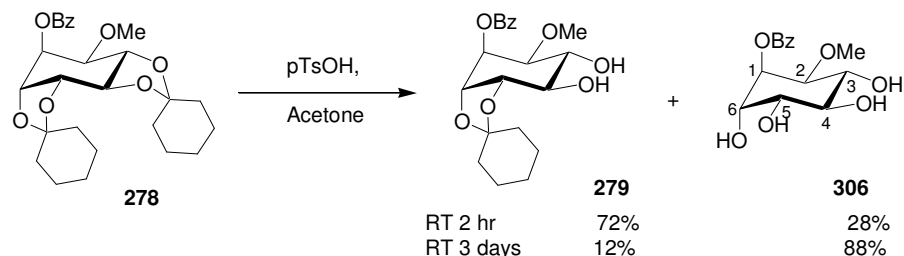
analysis of the reaction mixture revealed that a significant amount of mono-cyclohexylidene protected material was still present.



Scheme 5.18. Synthesis of 1L-1,2-di-*O*-methyl-*chiro*-inositol, **305**.

The dimethyl derivative **305**, was not soluble in CDCl_3 or deuterated acetone, and thus its NMR spectra were run in deuterated DMSO. In this solvent, the hydroxyl protons are essentially non-exchangeable and the four hydroxyl signals were clearly visible as doublets at 4.86, 4.60, 4.55, and 4.45 ppm. The signal attributed to the one equatorial proton on a hydroxyl-bearing carbon, at C-6, was significantly downfield of the other ring protons, appearing at 3.80 ppm. The other three ring protons (identified by HSQC, and by coupling to three of the hydroxyl protons in the gCOSY spectrum) on hydroxyl-bearing carbons C-3 to C-5 gave signals that were indistinguishable from each other as overlapping multiplets at 3.26 ppm.

The preparation of 1L-1-*O*-benzoyl-2-*O*-methyl-*chiro*-inositol (**306**) was also effected in two steps from **274** (scheme 5.19). Benzoylation as discussed earlier in this chapter and subsequent cleavage of the cyclohexylidene groups gave the tetra-ol **306**. As shown in scheme 5.19, a catalytic amount of *para*-toluene sulfonic acid in acetone was used to remove both groups in acceptable yield after three days. The same conditions, but stirring for a much shorter time were also used to cleave only the *trans*- acetal, allowing the isolation of diol **279**.



Scheme 5.19. Synthesis of 1L-1-*O*-benzoyl-2-*O*-methyl-*chiro*-inositol.

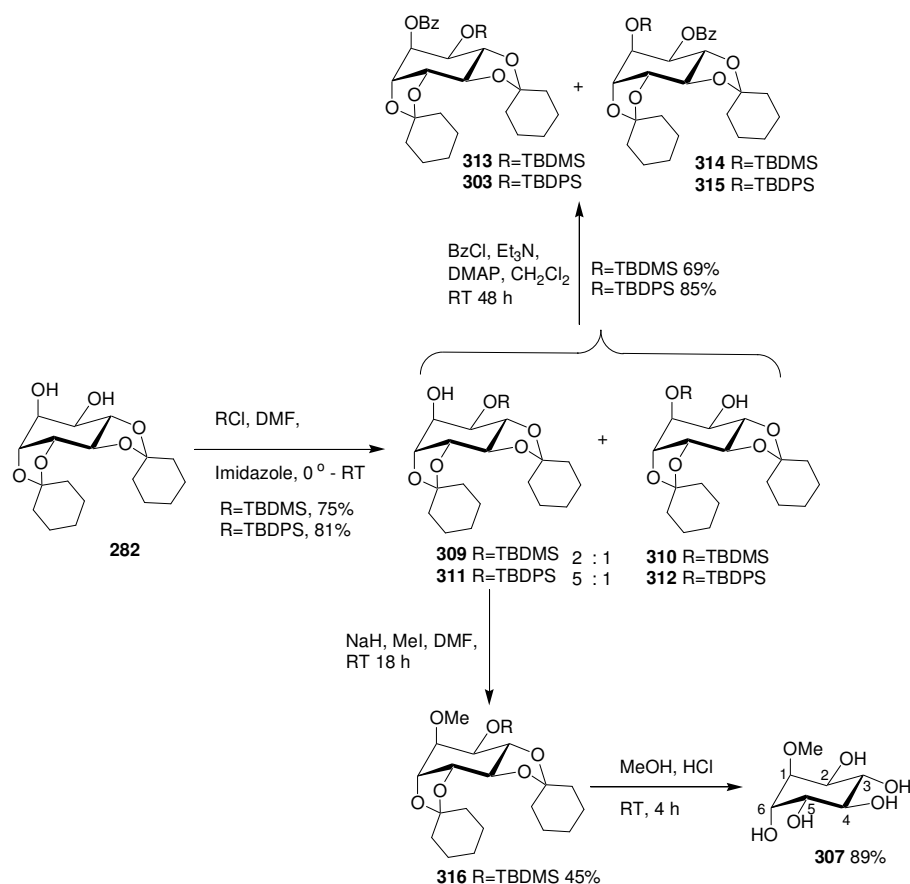
The NMR spectra of the tetra-ol **306** were run in deuterated acetone (although **306** was sparingly soluble in CDCl₃). In the ¹H NMR spectrum, although signals for all of the hydroxyl protons could be seen, only the signal attributed to the proton of the axial hydroxyl on C-6 was coupled to the nearest inositol ring proton, appearing as a doublet at 4.65 ppm. It was also significantly downfield of the other three hydroxyl proton signals, which appeared as broad singlets at 4.32, 4.24, and 4.15 ppm. Similarly, the equatorial ring proton on C-6 appeared at 4.06 ppm, downfield of the three axial protons on hydroxyl-bearing carbons (C-3 to C-5), which were indistinguishable from each other as overlapping multiplets at 3.66 ppm.

By contrast, in the ¹H NMR spectrum of the diol **279**, run in CDCl₃, all of the inositol ring proton signals were well resolved. The signal for the proton on the methoxy-bearing carbon (C-2) appeared furthest upfield at 3.53 ppm, as a distinct doublet of doublets, with coupling constants $J_{ax-ax} = 9.3$ Hz and $J_{ax-eq} = 2.9$ Hz. The C-1 ring proton signal appeared at 6.00 ppm, the furthest downfield of the ring proton signals in the ¹H NMR spectrum. In the ¹³C NMR spectrum of **306** (shown overleaf in figure 5.4), the C-1 signal appeared at 70.6 ppm, well upfield amongst the six inositol ring carbons. These observations are consistent with the benzoyl substituent on C-1, and gCOSY and HSQC analyses supported the assignment of these signals. There is one previous report of compound **306**,¹⁸² which reports an optical rotation of $[\alpha]_D = +50.1^\circ$ (*c* 1.01, MeOH). However, repeated measurements of the optical rotation of compound **306** prepared during this work gave $[\alpha]_D = -48^\circ$ (*c* 0.06, MeOH or acetone). This data suggests that the sign of the optical rotation may have been incorrectly reported in the literature.¹⁸²

The third derivative was prepared from diol **282**, which was prepared as described in section 5.3 of this chapter. Selective protection of the equatorial hydroxyl group of **282** is possible because the protection at the axial hydroxyl is disfavoured by 1,3-diaxial interactions with the axial ring protons. The diol was initially protected as the *tert*-butyldimethylsilyl ether by treatment with *tert*-

Figure 5.4. ^{13}C NMR spectrum of **306**.

butyldimethylsilyl chloride and imidazole in DMF (scheme 5.20). Mono-protected product was isolated in 75% yield, but silylation had occurred at both O-5 and O-6 of **282** to give a mixture of **309** and **310**, with **309** as the major product. The two methyl groups of the TBDMS moiety were found to give unique signals in both the ^1H and ^{13}C NMR spectra, indicating that the bulky *tert*-butyl group also attached to the silicon restricted rotation about the Si-C bond. Benzoylation of a portion of the product to give a mixture of **313** and **314** simplified the determination of the regioisomeric ratio due to the downfield shift of the signal attributed to the proton vicinal to the OBz group. The ^1H NMR of the crude product, a doublet of doublets at 5.58 ppm ($J_{\text{eq-eq}} = 4.9$, $J_{\text{ax-eq}} = 3.5$ Hz) which was attributed to the equatorial proton vicinal to the OBz group in the major product **313**, and a doublet of doublets at 5.41 ppm ($J_{\text{ax-ax}} = 9.6$, $J_{\text{ax-eq}} = 4.4$ Hz) attributed to the axial proton vicinal to the OBz group in the regioisomeric product **314**. The ratio of **313:314** (and hence of **309:310**) was obtained from the ratio of the integrals of those two signals, and was approximately 2:1.



Scheme 5.20. Preparation of 1L-1-O-methyl-*chiro*-inositol.

Despite this poor regioselectivity, compound **309** was progressed to the methyl ether **316**, via a Williamson ether synthesis. The yield of this reaction was moderate, but upon purification by column chromatography, it was found that essentially pure **316** could be obtained in 45% yield. Subsequent simultaneous acid hydrolysis of the silyl ether and both of the cyclohexylidene groups, followed by workup and purification by flash column chromatography in CH₂Cl₂:methanol, gave the target penta-ol **307** in 89% yield, with an optical rotation $[\alpha]_D = -57^\circ$ (*c* 0.05, D₂O), equivalent but opposite in sign to that reported for the enantiomer, 1D-1-*O*-methyl-*chiro*-inositol; $[\alpha]_D = +59^\circ$ (*c* 1.3, D₂O).¹⁸³

Since the selectivity of the above silylation is based on steric bulk of the silyl group, the *tert*-butyl diphenyl silyl ether **311** was also prepared, in the hope that the larger group would enhance the regioselectivity. When the monosilylated product was benzoylated (as discussed previously), the ¹H NMR spectrum of the product showed a doublet of doublets at 5.45 ppm ($J_{eq-eq} = 3.9$, $J_{ax-eq} = 3.8$ Hz) which was attributed to the equatorial proton vicinal to the OBz group in the major product **303**, and a doublet of doublets at 5.36 ppm ($J_{ax-ax} = 10.2$, $J_{ax-eq} = 3.9$ Hz) attributed to the axial proton vicinal to the OBz group in **315**. The ratio of products **303** and **315** (and hence of **311** and **312**) was found to be approximately 5:1; significantly better than the analogous TBDMS analogue. It was found that **311** could be separated from the regioisomer by careful flash column chromatography. However, as the desired *L-chiro*-inositol derivative **307** had already been prepared, the TBDPS protected compound was not progressed further. A potential disadvantage of using TBDPS over TBDMS is that harsher reaction conditions would be required for its removal.

5.7 Biological testing of the derivatives

The testing of these derivatives was carried out in the Department of Biochemistry and Molecular Biology, Medical College of Georgia. All four compounds were tested in uptake assays of two microorganisms, *Candida albicans*¹⁸⁴ and *Leishmania donovani*.¹⁸⁵ The former is an opportunistic fungus that is a normal part of the human endogenous microflora. However it is one of

the most common human pathogens, and can cause a variety of infections from unpleasant mucosal infections in generally healthy people, to potentially life-threatening systemic infections in already compromised individuals such as cancer patients. The second microorganism, *Leishmania donovani* is a parasitic protozoan flagellate that is responsible for the most severe form of leishmaniasis, known as visceral leishmaniasis or kala-azar. An estimated twelve million people worldwide are infected with this chronic disease, which is fatal if left untreated.

Myo-inositol is an important component of these parasitic organisms. In *C. albicans* (yeast cells) it is an essential precursor for phospholipomannan, a GPI-anchored glycolipid that is involved in the cell's pathogenic nature, binding to and stimulating human macrophages.¹⁸⁴ In *L. donovani*, *myo*-inositol is essential for the formation of the GPI-anchors that form most of the surface molecules.¹⁸⁵ As in all eukaryotic cells, *myo*-inositol is also important for the cell-cycle regulating phosphatidylinositol signal transduction pathways in both microorganisms. Hence, inhibition of GPI-anchor biosynthesis or of *myo*-inositol transport in these organisms are attractive drug targets.^{184,185}

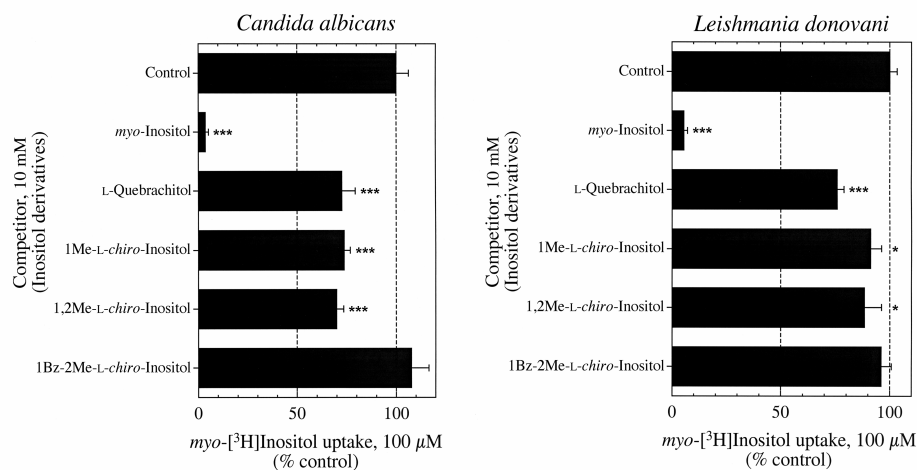
In the uptake assays, the uptake of radiolabelled *myo*-inositol by the microorganisms was measured in the presence of the four L-*chiro*-inositol derivatives, and the inhibition of uptake of labelled *myo*-inositol was compared against the inhibition observed with unlabelled *myo*-inositol, as the optimal competitor. The concentration of radiolabelled *myo*-inositol was 100 μ M and of the unlabelled compounds was 10 mM. For both microorganisms, the mono- and

Table 5.3. Results of the uptake assays in *C. albicans* and *L. donovani*.*

	<i>C. albicans</i>	<i>L. donovani</i>
Control	100 \pm 6.3%	100 \pm 3.4%
<i>Myo</i> -Inositol	5.4 \pm 1.7% (P < 0.001)	5.4 \pm 1.7% (P < 0.001)
Quebrachitol	72.5 \pm 6.8% (P < 0.001)	75.9 \pm 3.1% (P < 0.001)
307	73.7 \pm 3.1% (P < 0.001)	91.2 \pm 5.1% (P < 0.02)
305	69.9 \pm 3.5% (P < 0.0001)	88.4 \pm 7.8% (P < 0.05)
306	107.7 \pm 8.8% (P < 0.20, n.s.)	96.1 \pm 4.6% (P < 0.20, n.s.)

* Results presented as percentage of (radiolabelled) *myo*-inositol uptake compared to control, as mean \pm S.D. of 4-5 uptake assays, each. Statistical analysis performed by paired sample t-test.

Figure 5.5. Graphical presentation of the results of the uptake assays in *C. albicans* and *L. donovani* (the data shown in table 5.3), as mean \pm S.D. of 4-5 uptake assays, each. Statistical analysis performed by paired sample t-test (***) $P < 0.001$, * $P < 0.05$, all others $P < 0.20$ /not significant).



di-*O*-methylated *L-chiro*-inositol derivatives **307** and **305**, as well as quebrachitol, gave significant inhibition results, with P values from $P < 0.001$ to $P < 0.05$ for paired-sample t-test analyses, i.e. 99.9% to 95% confidence for significant inhibition, respectively.¹⁸⁶ The benzoylated derivative **306** did not induce any inhibition of *myo*-inositol uptake, indicating that the substrates showed no recognition for **306**.¹⁸⁶ This could be due either to the bulkiness of the benzoyl group, or perhaps that the benzoyl group, with its π -electron system, has higher affinity for other amino acid side groups outside the binding site involved in the uptake assay, and hence does not compete with the *myo*-inositol uptake. The results are presented in table 5.3, and also graphically in figure 5.5.

Although none of the compounds showed inhibition as high as for *myo*-inositol (i.e. the substrate specificity was highest for *myo*-inositol) these results show that the *L-chiro* inositol derivatives are recognised by the microorganisms. Hence, this work could form the starting point for further work on the effects of these compounds on the growth rate of the microorganisms, or for the synthesis and testing of other derivatives.

Variations and Improvements on the Preparation of *myo*-Inositol Camphanylidenes Acetal

The resolution of *myo*-inositol via the formation of a camphanylidenes acetal, (-)-**269a** (with L-camphor, or (+)-**269a** with D-camphor, see scheme 4.17) was considered one of the most promising methods for large-scale preparation of enantiomerically pure *myo*-inositol derivatives.

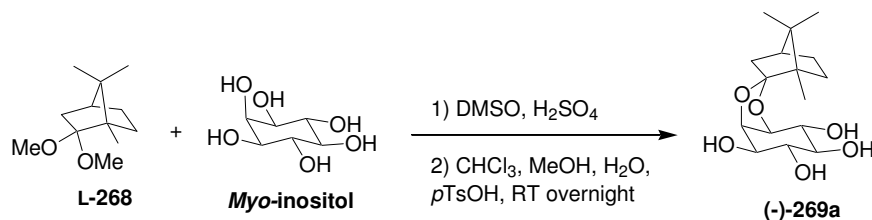
The work described in this chapter had the dual aims of a) gaining a better understanding of, and hence possibly improving the diastereoselectivity of, the procedure by using analogues of camphor in the acetal formation (section 6.1), and b) process development to improve the procedure with a view to scaleup (section 6.2). A campaign to prepare 1.2 kg of (-)-**269a** was subsequently conducted, and is presented in chapter seven.

6.1 *Myo*-inositol camphanylidenes acetal and variations thereof

6.1.1 Introduction

The procedure for the preparation of *myo*-inositol camphanylidenes acetal, which is discussed in detail in section 6.2, involves reaction of *myo*-inositol with camphor dimethyl acetal and catalytic sulphuric acid in DMSO at 70 °C. The product of this reaction, a complex mixture of acetals, is then ‘equilibrated’ in a mixture of chloroform, methanol and water acidified with *p*TsOH. It is unclear whether this equilibration step serves only to cleave the *trans*-acetals that also form in the initial reaction, or whether there is also interconversion between the four possible diastereomeric *cis*-acetals. Bruzik *et al.*^{168,171} report an increase in the level of desired diastereomer present from 47% to 65% during the equilibration. During the equilibration step, a slurry forms, and filtration of the slurry gives the crude product ((-)-**269a** or (+)-**269a**) in typically 75% yield. As discussed in chapter four, the major product is the 1,2- acetal (-)-**269a** shown in

scheme 6.1, when L-camphor is used, and the enantiomer (+)-**269a** when D-camphor is used.



Scheme 6.1. Formation of (-)-**269a**.

The product is contaminated with the other three possible diastereomers, **269b**, **269c**, and **269d** (when L-camphor is used as the starting material) shown in figure 6.1, and is purified further by recrystallisation. Although the reaction works well, recovered yields of purified product vary from 25% - 65% in the literature. There appears to be a lack of understanding of why the selectivity for (-)-**269a** is so marked, or how the selectivity may be increased. The major yield loss seems to be in the recrystallisation, and if cleaner crude product could be obtained, this could potentially be improved.

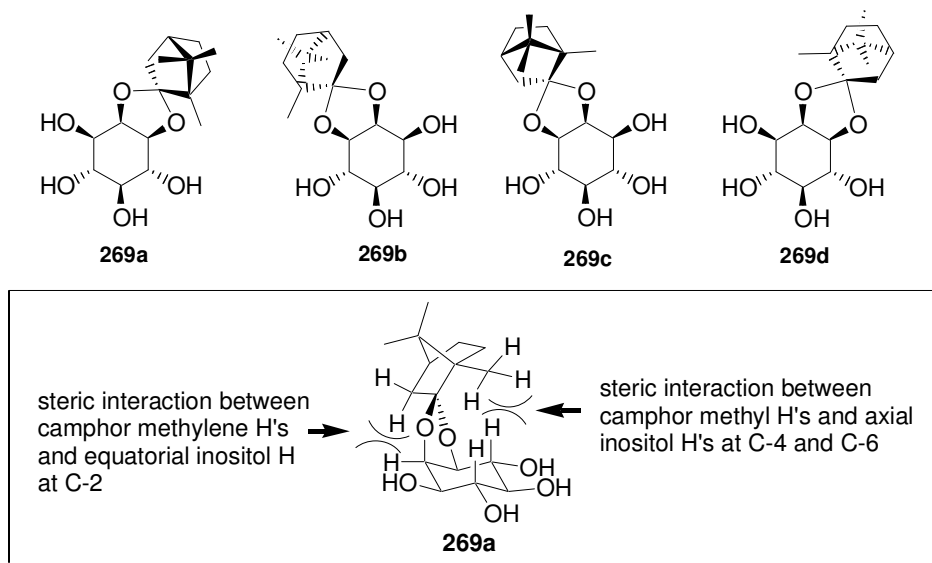


Figure 6.1. The four possible diastereomers of *myo*-inositol L-camphanylidene acetal, and the major steric interactions found in (-)-**269a**.

Analysis of the structures of (-)-**269a**, **269b**, **269c** and **269d** (using molecular models) shows that both the methyl group and the methylene H's α to the acetal centre are responsible for the steric interactions within the molecule

(figure 6.1 shows those for (-)-**269a**). The interactions in each of the four diastereomers appear to be similar, with no interaction evident (from the molecular models) in the structure of **269b**, **269c**, or **269d** that is significantly larger than those in (-)-**269a**. It was postulated that changing the steric bulk of the camphanylidene moiety at either the methylene or the methyl positions might enhance or decrease one of the interactions and thus increase the selectivity of the reaction. Several analogues of camphor (figure 6.2) were identified as candidates for acetal formation. Fenchone and norcamphor are commercially available, while the synthesis of C-10 substituted camphor derivatives is reported in the literature.¹⁸⁷

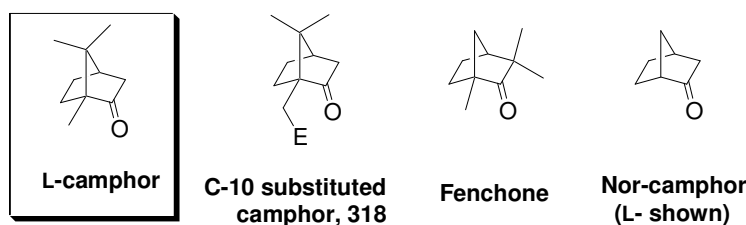
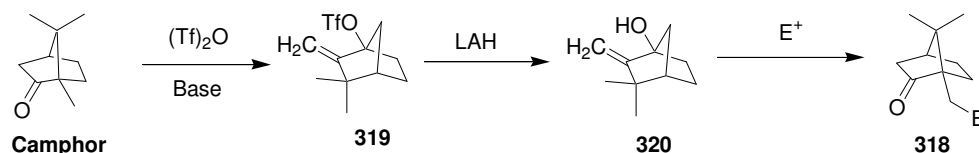


Figure 6.2. Analogues of camphor for preparation of *myo*-inositol camphanylidene acetal analogues.

6.1.2 Synthesis of a C-10 substituted camphor analogue

The planned synthesis of a camphor analogue substituted at the C-10 (methyl group α - to the carbonyl) is shown in scheme 6.2 overleaf. Treatment of camphor with trifluoromethane sulfonic anhydride gives the triflate **319** by means of a Wagner-Meerwein rearrangement.^{187,188} Subsequent treatment with LAH or KOH gives the alcohol **320**, then nucleophilic attack of the carbon-carbon-double bond on an electrophile (E^+) to give a tertiary carbocation, followed by a second Wagner-Meerwein rearrangement gives the C-10 C-substituted camphor analogues, **318**. A variety of electrophiles have been used to give 10-dimethyl-aminomethylcamphor,^{187(b)} 10-hydroxycamphor,^{187(c)} and 10-bromo-camphor,^{187(d)} among other examples. The possibility of introducing a hydrogen bond was appealing, as this could introduce different interactions, which again might favour one diastereomer.

Treatment of camphor with trifluoromethane sulfonic anhydride was found to give product that appeared to contain two products by NMR analysis. Camphor was completely consumed during the reaction, but the two products could not be separated by TLC or column chromatography and further progress with this synthesis was limited. Unfortunately reaction of the mixed product could not be effected with LAH, or with KOH in diethyl ether.




Scheme 6.2. Planned synthesis of a camphor analogue.

6.1.3 Fenchone

The preparation of the di-methyl acetal **321** of fenchone proved to be difficult, with low yields obtained using a variety of conditions (table 6.1). Using the analogous procedure to that used for the preparation of the dimethyl acetal of camphor (trimethyl orthoformate, methanol and *p*TsOH at RT for two days), only 5 - 10% conversion was obtained (by ^1H NMR). Heating the reaction mixture gave somewhat improved conversion, but the reaction mixture began to discolour over time. Extending the reaction time to six days gave approximately 30% conversion.

Table 6.1. Formation of dimethyl acetal **321** from fenchone.

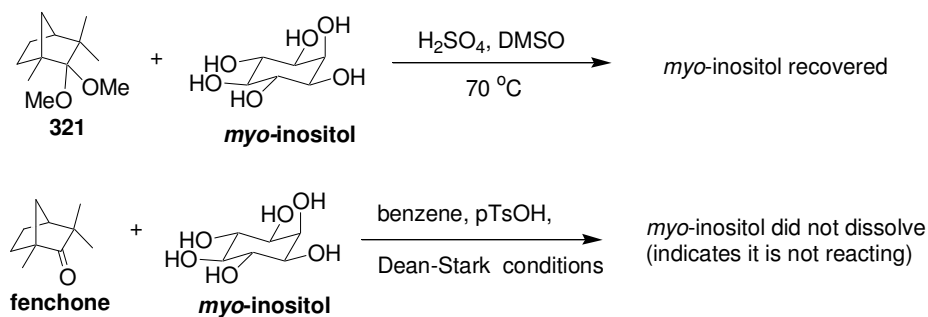
				
Fenchone		321		
entry	conditions	temp	time	conversion*
1	HC(OMe) ₃ , MeOH, H ₂ SO ₄	RT	2 days	5 – 10%
2	HC(OMe) ₃ , MeOH, H ₂ SO ₄	60 °C	2 days	10%
3	HC(OMe) ₃ , MeOH, H ₂ SO ₄	RT	6 days	30%
4	MeOH, TMSCl	RT	3 days	< 5%

*Starting material to product ratio was determined by inspection of the crude ^1H NMR spectrum.

Literature reports echo this difficulty. The preparation of **321**, as one of a range of acetals, was reported by treatment of fenchone with an excess of TMSCl in methanol, at RT for one hour.¹⁸⁹ This was on a small scale for GC analysis of the products, and yields for individual reactions were not reported. Preparation of **321** in this manner was attempted (table 6.1, entry 4), but after three days stirring at RT only traces of the product were detected in the reaction mixture. The acetalisation of fenchone at high pressure (15 mbar) with ethylene glycol in benzene with triethyl orthoformate and *p*TsOH has also been reported.¹⁹⁰ At 20 °C and 15 mbar for 48 h, the yield of the acetal was still only 22%, while at 40 °C at that pressure a yield of 90% was reported.^{190(b)} The authors mention^{190(a)} that this acetalisation ‘failed to undergo reaction effectively with heating at atmospheric pressure’.

It was decided to use the procedure in entry 3, table 6.1 to prepare **321**, and purify the product by column chromatography (in petroleum ether) to free it from the unreacted fenchone. Approximately 5 g of **321** were thus obtained. The acetal was found to be a white solid that was volatile under hi-vacuum.

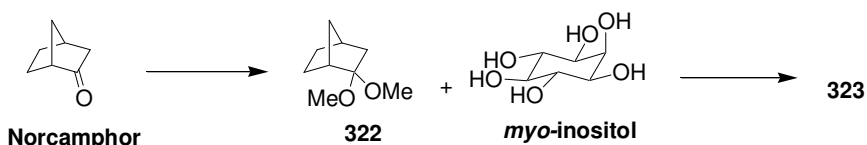
With the reagent prepared, attempts to prepare the fenchone acetal of *myo*-inositol were conducted. Attempts to use the crude (30%) dimethyl acetal were unsuccessful - the *myo*-inositol never dissolved (indicating it was not reacting) and quantitative amounts of *myo*-inositol were recovered, even after several days of heating at 70 °C. However, when the purified reagent was used, a clear solution was obtained, suggesting that the *myo*-inositol was reacting. Unfortunately, the acetal products could not be isolated from the mixture. When the ‘equilibration’ was attempted on the crude material, *myo*-inositol was again recovered, indicating that the fenchone acetal (had it been present) had been cleaved. Direct reaction of fenchone with *myo*-inositol was also attempted (scheme 6.3), but again the *myo*-inositol did not dissolve and was recovered quantitatively. These results suggest that the increase in steric bulk obtained by replacing the protons of the methylene group α to the acetal centre (in the camphanylidene case) with a gem-dimethyl group, as in fenchone, precludes the formation of the analogous *myo*-inositol acetal.



Scheme 6.3. Attempts to prepare a fenchone acetal of *myo*-inositol.

6.1.4 Norcamphor

The second commercially available camphor analogue that was investigated was (racemic) norcamphor. Using the original acetalisation procedure that worked well with camphor, conversion of norcamphor to the dimethyl acetal **322** was achieved (scheme 6.5). However, some hydrolysis back to the ketone was observed upon workup. It was found to be preferable to use *p*TsOH as the acid catalyst, and quench the reaction with solid sodium carbonate before workup to give crude **322** in essentially quantitative yield. If water was added to quench the reaction, rapid hydrolysis of product to the ketone was observed. The crude acetal was purified by short-path distillation to give a clear, colourless liquid.



Scheme 6.5. Formation of *myo*-inositol norcamphanylidene acetal.

Subsequent reaction of the norcamphor dimethyl acetal with *myo*-inositol was much more successful than the analogous fenchone reaction had been. Reaction in DMSO with catalytic H₂SO₄ led to rapid disappearance of the solid *myo*-inositol to give a clear, very pale yellow solution. After neutralisation and concentration as in the camphanylidene acetal procedure described in the next section (section 6.2), two different workup procedures were employed. Firstly, the normal ‘equilibration step’ was conducted, stirring overnight in an acidic

mixture of CHCl_3 , MeOH, and water. This treatment gave a thick precipitate which, when filtered, gave an 80% yield of crude *myo*-inositol norcamphor acetals. In the second case, after neutralisation, more volatile components of the reaction mixture were removed in-vacuo, and then DMSO, any unreacted *myo*-inositol and salts were removed by dissolving in toluene and washing with water and brine. The toluene was then concentrated and the residues subjected to the equilibration step as normal. It was thought that this might be a less harsh method to remove DMSO, avoiding the need to heat the product to 80 °C for what would become extended periods on scale. However, only a 30% yield of the norcamphor acetals was obtained from the equilibration step using this method, suggesting a significant amount of the product had been lost to the aqueous washes despite the fact that at that point each *myo*-inositol should, in theory, have had two norcamphor acetal moieties.

The composition of the products from the two workups described above was very similar. Although the product of the toluene workup was cleaner, containing less *myo*-inositol and other (unidentified) impurities, both contained two major products. These were two diastereomers of *myo*-inositol norcamphanylidene acetal (the four possible diastereomers are shown in figure 6.3). Since the norcamphor that was used was racemic, each would be present as an enantiomeric pair. The two diastereomers could not be separated, and hence were not identified, but it may be proposed that either **323a** and **323b** OR **323c** and **323d** were present. This is based on the fact that the methyl group, which, in the camphanylidene acetal, provides one of the two major steric interactions with *myo*-inositol, had been removed. Hence, steric interaction with the protons of the methylene group α to the acetal centre provides the major steric interaction in the nor-camphanylidene acetal. In **323a** and **323b**, interaction with the axial protons on the 'top' face of the inositol ring is minimised. In **323c** and **323d**, interaction with the equatorial inositol proton at C-2 is minimised.

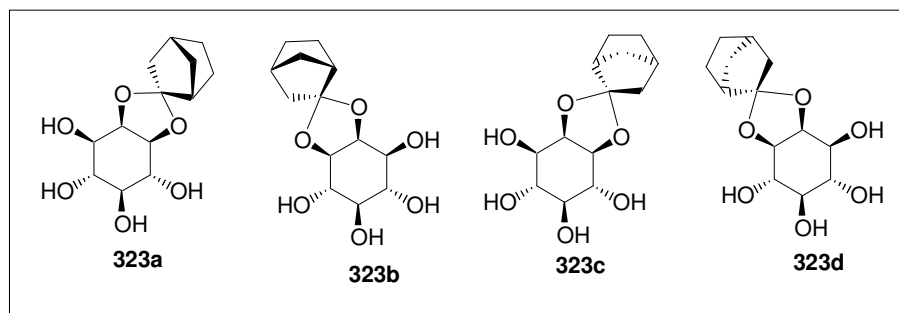


Figure 6.3. The four diastereomeric *myo*-inositol norcamphanylidene acetals that are possible from one of the enantiomers of norcamphor.

Recrystallisation of the crude *myo*-inositol norcamphanylidene acetals did result in enrichment in one of the products, but isolation of a sample of a single isomer proved elusive. Per-acetylation of the crude product was also carried out, in the hope that the products could be chromatographically separated, but the products still appeared as one spot on TLC.

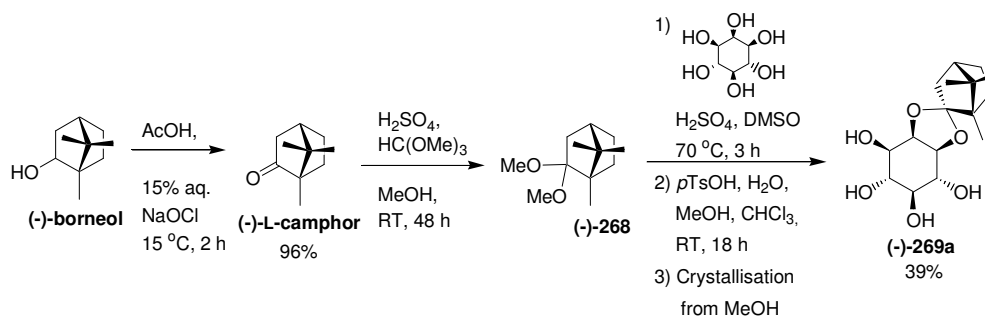
6.2 Process development for *myo*-inositol camphanylidene acetal

The formation of *myo*-inositol camphanylidene acetal was chosen for further development with a view to scale up. To summarise the advantages of the procedure that led to this decision:

- Resolution occurs early in the synthesis (minimum number of steps).
- Use of L-camphor gives 1D-1,2-*myo*-inositol-camphanylidene acetal, while use of D-camphor gives 1D-2,3-*myo*-inositol-camphanylidene acetal. Hence access to both enantiomers is easy.
- Both D- and L-camphor are commercially available.
- The starting materials are readily available and not expensive (although L-camphor is significantly more costly than D-camphor, L-camphor may be prepared from the more reasonably priced (-)-borneol).
- The reaction is performed at reasonable temperature of 70 °C (easy to achieve in the scale up equipment).
- The product is isolable by crystallisation (this is far preferable to chromatography when considering scale up).

- When overall yield is considered, the method is superior to most of the other methods in the literature, with theoretical yield of 100%.
- 1,2-protected D-*myo*-inositol was required by chemists in the carbohydrate team at IRL as part of their research program and for the synthesis of a target molecule requested by a client. The procedure had already been carried out in-house to give high quality product but in low yields (on several gram scale).

The procedure published by Lindberg *et al.*¹⁶⁹ was the basis of the work presented in this chapter, along with a published oxidation of (-)-borneol¹⁹¹ to give L-camphor. The complete synthesis that was intended to be scaled up is shown in scheme 6.6. In Lindberg's procedure, the camphor dimethyl acetal reagent is prepared in-situ, avoiding the need for a purification step. This was a reason for choosing this procedure as a basis. Subsequent reaction of the crude camphor dimethyl acetal with *myo*-inositol and sulphuric acid in DMSO gives a complex mixture of acetals, which after removal of the DMSO (likely to be a difficulty on larger scale) is 'equilibrated' overnight in the solvent mixture shown (scheme 6.6) with *p*TsOH. The crude product precipitates from this mixture, and is collected by filtration in reported yields of typically 60 – 70%. Recrystallisation of the crude material from unspecified volumes of methanol or methanol: water to give pure (-)-**269a** in 39% is reported in the literature. These crystallisations were found to be unsatisfactory for potential scale up, primarily due to the large volumes required (discussed in section 6.3.4).



Scheme 6.6. The synthesis of 1D-1,2-*myo*-inositol-L-camphanylidene acetal, proposed for process development and scale up.

One of the important considerations upon scale-up of a procedure is the total volume of the reaction or workup being considered. In the large-scale

laboratory, the size of the reactor and receiver vessels is fixed. Hence, the procedure must be scaled so that the largest volume step of the synthesis will fit in the available equipment. Generally, the lower the volume the better (assuming product quality and yield are not compromised), both for reasons of cost and efficiency, and simply because smaller volumes are easier to handle and take less time to process (eg a filtration that needs to be done with the 24 cm Buchner filters and 10 L Buchner flasks that are available will take twice the time if there are 20 L of filtrate versus 10 L of filtrate). Significant changes were made to the crystallisation procedure (discussed in section 6.2.4). In the following sections (6.2.1, 6.2.2 and 6.2.3), each step of the synthesis is considered and the process development that was done to address the likely scale-up issues is described.

6.2.1 Oxidation of (-)-borneol to give L-camphor

Naturally occurring (1*R*)-(+)-camphor, (D-camphor), is available at a cost of \$209.70 for 500g.ⁱ The unnatural enantiomer, (1*S*)-(-)-camphor (L-camphor), is available commercially but for the much higher price of \$109.90 for 10 g (95% purity) or \$104.00 for 5 g (99% purity). Unfortunately, the latter was the isomer required for the derivatisation of *myo*-inositol described in chapter seven. Approximately 5.7 kg of (-)-camphor were required for the planned synthesis, which at the price quoted would cost \$62,643.00, which far exceeded the available budget! Fortunately, (-)-borneol is available at a much more reasonable cost and a synthesis of camphor *via* the oxidation of borneol that was reported to be suitable for large-scale work has been reported.¹⁹¹ The synthesis involves treating camphor with aqueous sodium hypochlorite in glacial acetic acid, followed by a quench with sodium bisulfite, precipitation of the product in ice/brine, and then a petroleum ether:water partition. This procedure should be able to be completed in three days in the scale-up laboratory. A conservative estimated total cost of preparing the L-camphor in-house using this method is presented in table 6.2. Searching different suppliers would almost certainly identify cheaper sources of the reagents, and bulk order rates usually apply on

ⁱ Prices quoted in this section are all from the Aldrich Chemical Company 2003-04 catalogue. Prices quoted are in Australian dollars. In chapter seven, different prices may be quoted because different suppliers were used for some items, and bulk order rates applied.

this scale. Two scientists are required at all times in the scale up laboratory for safety reasons, and the figure shown in the table is for two IRL scientists. However in this case, this cost, usually one of the biggest costs of scale-up synthesis, was mitigated because one of the two scientists would be the student.

This analysis demonstrated that it would be far preferable to prepare the camphor in-house. However, in order to demonstrate that the highly exothermic oxidation could be carried out safely with the available equipment, a calorimetric analysis of the exotherm was required.

Table 6.2. Estimated cost of in-house synthesis of ca. 5.6 kg of L-camphor.

Item	Unit cost	# required	Total cost
(-)-Borneol	\$312.30/500 g	12	\$3,747.60
Glacial acetic acid	\$393.40/19 kg	1	\$393.40
15% aq. NaOCl	\$12/5 L	4	\$48
Sodium bisulfite	\$58.20/500 g	1	\$58.20
NaCl (for 60 L brine)	\$256.70/12 kg	1	\$256.70
Petroleum ether	\$345.70/20L	1	\$345.70
LT9 facility charge	\$250/day	3	\$750
2 Scientist's time	\$120/hour	2 x (3 x 7.5 h days)	\$5,400
TOTAL			\$10,999.60

Calorimetric analysis of the oxidation

Two pieces of information were required to confirm the safety of the oxidation procedure; the magnitude of reaction exotherm, and the heat transfer capacity of the reactor, together with the power available from the heater/cooler unit. These two pieces of data were necessary in order to determine whether there was enough cooling power available to control the exotherm of the oxidation, even in a worst-case scenario (i.e. all reagent added at once and cooling failure).

Dr Graham Caygill (IRL) calibrated the then new 50 L reactor (which was commissioned during the scaleup synthesis of 1,2-D-myo-inositol-L-

camphanylidene acetal, see chapter seven) in order to obtain the second piece of information listed above. A known volume of methanol was heated to 40 °C in the reactor and the temperature change of both the jacket and the reactor contents were logged for 50 minutes after the jacket setpoint was changed from 40 °C to 5 °C. Although it took only 8 minutes for the jacket temperature to reach the new setpoint, the reactor contents temperature lagged far behind. After 50 minutes the contents temperature was 9.5 °C. From this data, the rate of heat transfer between the jacket and the contents could be calculated. This value changes somewhat with the volume and composition of the reactor contents, but it is reasonably low (as evident from the slow rate of methanol cooling) because the thick glass walls do not transfer heat very well. The result of this calibration was deemed a good approximation for the borneol oxidation. Having this figure, and knowing the theoretical output of the heating/cooling unit and the physical dimensions of the system, the cooling power that would be available for the oxidation reaction on the planned scale of 38 L was calculated to be approximately 2 kW.

To determine the magnitude of the reaction exotherm, the calorimetry equipment available at Industrial Research Limited was used, with the help of Dr Graham Caygill (IRL). The reaction was run in a 1 L glass vessel on the scale of 65 g (0.42 mol) of borneol, 200 mL of glacial acetic acid and 215 mL of 15% aqueous NaOCl. During the course of the experiment, a range of parameters were logged, including oil temperature going into and coming out of the heating/cooling jacket, heater power, and reactor contents temperature. Four key reaction steps were undertaken:

1. After stabilisation of the reactor contents (borneol and acetic acid) at 15 °C with the heater set at a 'baseline' low level (5%), an initial calibration step was done. Thus, the heater power was increased to a fixed power of 30%, and a new steady state established. On reaching the new jacket temperature required to maintain the contents at 15 °C, and after a steady state had been maintained for 20 minutes, the heater power was reduced back to the original 5%. The data collected allowed calculation of the UA (heat transfer rate) of the system.
2. The original baseline steady state was re-established.

3. The NaOCl solution was added at a constant feed rate over a period of two hours. This was the planned rate of addition in the 50 L reactor. The heater was kept at a fixed power of 5% to provide a ‘background’, and the reactor contents were held isothermally at 15 °C. A slight increase in reactor contents temperature to 17 °C was observed before the jacket temperature dropped to allow for the reaction exotherm, and a slight drop was observed when the reaction was essentially complete and when the NaOCl feed was complete. After the end of the addition, the reaction was allowed to stir until a steady state had been maintained for 30 minutes.
4. A second calibration step was done in the same way as in step 2.

The specific reaction power calculated for the AcOH/NaOCl oxidation of 65 g of borneol from the data collected above was 20 W. Since the volume of this reaction was 415 mL, the reaction power was calculated to be $20/0.415 = 48 \text{ WL}^{-1}$. The planned scale of the reaction on scale-up was 5.9 kg of borneol, with a total reaction volume of 37 L. Hence, the reaction power on that scale was calculated to be $48 \times 37 = 1776 \text{ W}$ (1.78 kW). Given that the cooling power of the equipment at the planned reaction temperature (15 °C) was ca. 2 kW based on the calibration discussed above, this indicates that the cooling power should be sufficient to control the exotherm.

Also calculated as part of this analysis was the maximum temperature that would be reached (maximum temperature of the synthesis reaction, MTSR) if the NaOCl solution were to be dumped into the reactor (in this case the calorimeter) in one portion, and cooling should fail. The MTSR is the adiabatic temperature rise (ATR) plus the reaction temperature (T_{reaction} , 15 °C), and:

$$\text{ATR} = -\Delta H / \sum m c_p$$

where $\Delta H = -128 \text{ kJ}$ (the total energy output of this reaction)

m = mass of each component of the reaction mixture

c_p = specific heat capacity at constant P of each component

The mass of borneol in the reactor is small relative to the amounts of AcOH and aqueous NaOCl, hence the borneol component was ignored (this was allowable

since it would give a more conservative estimate of the ATR). The 15% NaOCl solution, for the purposes of this calculation was assumed to have the properties of water. Hence:

$$mc_p \text{ for HOAc} = 0.20 \text{ L} * 1.05 \text{ kgL}^{-1} * 2.04 \text{ kJkg}^{-1}\text{K}^{-1}$$

$$mc_p \text{ for NaOCl} = 0.215 \text{ kg} * 1.00 \text{ kgL}^{-1} * 4.18 \text{ kJkg}^{-1}\text{K}^{-1}$$

$$mc_p \text{ for borneol} = \text{negligible (may be ignored)}$$

$$\text{therefore, } ATR = 128 \text{ kJ} / (0.428 \text{ kJ}^{-1} + 0.899 \text{ kJ}^{-1}) = + 96 \text{ K}$$

$$\text{and } MTSR = ATR + T_{\text{reaction}} = 96 + 15 = 111 \text{ }^{\circ}\text{C}$$

The MTSR is above the boiling point of the lowest boiling component of the mixture, water (b.p. 100 °C), and hence this indicates that in the worst case, the reaction mixture could be caused to boil, or even to suddenly volatilise and explode out of the reaction vessel. However, it was decided that the reaction would be safe to run in the available equipment, given that the calculation was a conservative one, and that in this case it would be easy to avoid addition of the entire amount of NaOCl solution at once. In fact, adding all the solution at once would be impossible, since it was to be added slowly from the header vessel, which holds only 5 L, while 19.6 L would be required.

Unfortunately, when the oxidation was carried out in the calorimeter, the HCl evolved from the aqueous NaOCl solution corroded the stainless steel probe, discolouring the reaction to a brown colour. This did not appear to affect product quality or yield, which were comparable to other laboratory scale runs. However, corrosion of stainless steel is a major issue in scaleup, as stainless steel is commonly present in plant-scale equipment. The available 50 L reactor that was planned to be used was made of glass, with no stainless steel fittings that normally come into contact with the reaction mixture, but the framing and some fittings that support the reactor were made of stainless steel. Therefore, it was decided to use a positive flow of air through the reactor and away from the stainless steel fittings at the top of the condenser when it was run on scale, as well as running the fume hood on ‘boost’ and washing everything down with

water as soon as possible after the reaction was complete, to avoid corrosion by chlorine gas as much as possible.

The workup of this oxidation involves quenching the reaction with saturated aqueous sodium bisulfite solution (approximately 25 mL was required for the 65 g of borneol scale run in the calorimeter), and then pouring the entire contents of the reactor into ice/brine to precipitate the product. In the literature procedure, 20 volumes (relative to the mass of the borneol used) of ice/brine were used. The planned scale of 5.9 kg of borneol would equate to 120 L, which added to the reaction volume would have been in excess of 150 L. This was too large a volume to reasonably manage. Fortunately, it was found that using only 8-10 volumes of ice/brine had no apparent negative effects on yield or quality of product. The reaction mixture from the calorimetry experiment discussed above was quenched with sodium bisulfite as in the literature and then poured onto 650 mL (10 volumes) of ice/brine. The solid product was collected by filtration and then dissolved in petroleum ether. The solution was then washed with water, dried with brine, and subsequently evaporated to give 60.2 g (94%) of L-camphor. This yield was comparable to those achieved on laboratory scale during this work and also to the literature yield of 95.8%. ^1H and ^{13}C NMR spectra were analogous to those obtained on smaller scale, and to those from an authentic sample of camphor.

6.2.2 Preparation of (-)-L-camphor dimethyl acetal ((-)-268)

This step, as reported by Lindberg *et al.*,¹⁶⁹ involves treatment of camphor with trimethyl orthoformate, methanol and sulphuric acid, and stirring at RT for 48 hours. The mixture is then neutralised with solid sodium methoxide, and the solvent and excess trimethyl orthoformate removed under vacuum. The residues are dissolved in toluene, and Na_2SO_4 salts precipitated out. These are removed by filtration, and the toluene removed under vacuum to give crude camphor dimethyl acetal, suitable for use in the next step.

Since every operation (e.g. separation, filtration etc.) takes an extended time on scale, the 'in-situ' preparation of the camphor dimethyl acetal reagent

was very desirable. The drawback of the reported procedure was that the reaction was run for 48 hours. This equates to inefficient use of time on large scale, since the equipment cannot be used for any other process while the 48 h stir takes place, and the facility charges (and scientist's time) must still to be paid for. Fortunately, monitoring of the reaction (by workup of a small aliquot of the reaction mixture and subsequent ^1H NMR analysis) showed that after 20 h the reaction was essentially complete. Stirring for the full 48 h did not detectably change the composition of the reaction mixture.

Also, a significant reduction in the amount of trimethyl orthoformate used in this step was effected. Although the total volume of this reaction, at seven volumes, was not excessive, the cost of the trimethyl orthoformate reagent (A\$217.90 for 2 Lⁱⁱ) made any reduction of the amount required worthwhile. Lindberg's procedure used seven equivalents (five volumes) of trimethyl orthoformate. It was found that this could be reduced to five equivalents (3.5 volumes) without detectable (^1H NMR) loss of product quality or yield. Reducing the amount of trimethyl orthoformate further to two equivalents did result in a lower conversion of camphor to product (ca. 10% camphor was still present after 20 hr). Since there is no purification step at this stage, the product quality needs to be high, and it was decided to use no less than five equivalents.

The precipitation of salts with toluene and subsequent filtration was not expected to cause any particular issues on scale up. The use of a toluene azeotrope is an effective method for drying materials on large scale because it is efficient and requires a minimum amount of manual handling.

6.2.3 *Myo*-inositol camphanylidene acetal formation

The formation of *myo*-inositol camphanylidene acetal is a two-step procedure. In the first step, the crude camphor dimethyl acetal is dissolved in DMSO and then *myo*-inositol and catalytic sulphuric acid are added. Then, the mixture is heated to 70 °C for three hours, during which time the suspension

ⁱⁱ Aldrich Chemical Company 2003-2004 catalogue price.

changes to a clear solution as the *myo*-inositol reacts (*myo*-inositol itself is not readily soluble in DMSO). Workup of the reaction involves neutralisation with triethylamine and then concentration of the mixture to give a viscous crude product, which is a complex mixture of acetals. It is likely that each molecule of *myo*-inositol has two camphanylidene acetal substituents at this point; one *cis*-acetal (i.e. the desired product, at the 1,2- position, or one of the three other isomeric possibilities), and one less stable *trans*-acetal. The equilibration step then involves dissolving the crude product in a 50:5:1 mixture of chloroform:methanol:water, adding catalytic *p*TsOH and stirring at ambient temperature overnight. In this process, cleavage of the *trans*-acetals occurs, and there may also be some interconversion between the four possible diastereomeric *cis*-acetal products. This would be an equilibrium-type process favouring the major product for a combination of solubility and steric reasons. The desired diastereomer precipitates out as the major product during the equilibration and the crude product is collected by filtration, in yields 65 – 75% (typically containing 10-20% of the other three diastereomers). The crude product is then recrystallised (discussed in section 6.3 below).

A number of issues were identified that would be likely to cause difficulty with the scale-up of this procedure:

- The boiling point of DMSO is 182-3 °C. In the lab, removal of DMSO was done at 1-2 mm Hg with a hi-vacuum pump attached to a rotovap with the water bath at 80-90 °C; on large scale these conditions will be difficult to reproduce. The available 50 L rotovap is connected to house vacuum and a typically the best vacuum obtainable is 12 mm;
- Chloroform is a toxic and undesirable solvent;
- Large volumes (22 volumes) of solvent are required for the equilibration.

Reaction solvent

Ideally, replacement of DMSO with another solvent was envisaged, thereby completely eliminating the problem of DMSO removal. DMF and dioxane were both tried as alternatives, however neither was satisfactory. With

dioxane as the solvent, after heating to 95 °C overnight (c.f. the three hours at 70°C in DMSO) nearly quantitative amounts of *myo*-inositol were recovered. In DMF, after stirring for two days at 85 °C there was still solid *myo*-inositol present. Even after further heating to 110 °C for ten hours, 80% of the *myo*-inositol was recovered after quenching and filtering.

As replacing the DMSO was clearly not viable, the focus turned to reducing the total volume of DMSO in order to minimise the difficulties of removing it in the workup. Lindberg *et al.* had noted that a small amount of DMSO present in the equilibration increased the yield and quality of product. Hence, it was thought that if the reaction could be performed in a minimal volume, the removal of the DMSO might be avoided altogether. It was found that with one volume of DMSO a biphasic mixture formed and incomplete reaction of *myo*-inositol was observed. With two volumes, the reaction did proceed, and was carried through the equilibration step as usual to give crude product in 70% yield. However, the quality of the product was not satisfactory, with increased amounts (compared to the crude product made following the literature procedure) of the undesired diastereomers present in the product. Using three volumes of DMSO, a similar crude yield was obtained but the quality of the crude product was now comparable (by ¹H and ¹³C NMR) to the crude product mixtures obtained using the original literature procedure. Three volumes of DMSO were preferable to the original ten, as the time required to remove the solvent would be much shorter.ⁱⁱⁱ In the worst case scenario, the reaction mixture from a large scale run with three volumes of DMSO could be portioned up and concentrated in the laboratory.

Equilibration step

The solvent system for the equilibration step, 20 volumes (relative to the amount of *myo*-inositol used) of 50:5:1 chloroform:methanol:water, was reported in the original procedure (Bruzik *et al.*)^{167,168} and is repeated in the subsequent literature with little change. Evidently this solvent system was arrived at with a significant amount of experimentation, since efforts during this work to modify

ⁱⁱⁱ In fact, as reported in chapter seven, the removal of four litres (of the 7.5 that were used) of DMSO from the reaction mixture on large scale took 7 h at 15-20 mbar and 95±5 °C.

the system had limited success. Replacement of toxic chloroform with dichloromethane led to somewhat lower yields of crude product (50-55%). Although (-)-**269a** was still the major product, significantly more of the diastereomeric impurities were also present. Whether this was because the solvent system was less preferential for precipitation of the major product, or because the different system was affecting the equilibration/interconversion between the diastereomers was not clear. The subsequent crystallisation step was attempted, but purifying the crude product proved to be very difficult. After two crystallisations (with the new acetone:water procedure described in the next section), with a loss of approximately 20% of the mass each time, the product still contained significant amounts of the undesired diastereomers.

Reducing the volume of the equilibration step also proved tricky. With 20 volumes of the specified solvent mixture, after the precipitation a reasonably mobile slurry is formed that filters readily. When ten volumes^{iv} of the solvent mixture were used, the result was an essentially immobile slurry which required a large amount of solvent (at least another ten volumes on the laboratory scale) to a) mobilise the slurry so it could be poured from the flask and b) rinse the flask effectively to get all of the product out. Use of 15 volumes of solvent gave slightly better results, but extra solvent was still required to get all the material onto the filter. On large scale, very thick mixtures are undesirable for two reasons. Firstly, if a mixture is not stirred consistently, loss of control of the process may occur, and secondly, the thicker the mixture, the more likely it is that lines or valves will block as the mixture is being transferred from vessel to vessel. It was decided to avoid these risks and therefore to use the full 20 volumes of solvent upon scale-up of this process.

6.2.4 Improved Crystallisation Procedure

The crude *myo*-inositol camphanylidene acetal obtained from the equilibration step described above requires recrystallisation to remove the other three diastereomers, which are invariably also precipitated. In the literature,

^{iv} Upon scale-up of a reaction, 10 volumes is generally considered an acceptable volume, any more than 10 volumes becomes too inefficient and is less than ideal.

recrystallisation from unspecified volumes of methanol or methanol-water are reported. However, these solvents were found to be far from ideal, with extremely large solvent volumes (up to 300 volumes) required to effect complete dissolution of the crude *myo*-inositol camphanylidene acetal. Often, the solution would not clarify, and hot filtration was done. The solids thus removed were shown to be fairly clean product. Both the quality and the recovered yield of the product was variable, with yields typically well below 40%. In the literature, the initial report¹⁶⁸ quotes a 65% crude yield of ‘sufficiently high purity for direct synthetic use’, but does mention that spectrally (NMR) detectable amounts of diastereomers are present, and also that difficulty was experienced in preparing completely transparent solutions of **(-)-269a** and **(+)-269a**. Other reports describe two, three or more crystallisations to obtain material ‘essentially free of other isomers’ in typically 25 - 30% yield,¹⁷¹ or use unspecified ‘modified procedures’ and report yields in the low 30%’s.¹⁷⁰

Crystallisation is always the preferred method for purification on scale (far preferable to column chromatography for example). However it was clear that the literature method for recrystallising **(-)-269a** was far from satisfactory. Therefore, a series of alternative crystallisations were tried on a small scale, with selected results presented in table 6.3. In each case, the crude camphanylidene acetal was dissolved hot in the indicated solvent and then allowed to cool slowly (by standing on a warm hotplate that had just been turned off), to better approximate the slower rate of cooling that occurs in a larger volume of solution.

The crude *myo*-inositol camphanylidene acetal was essentially insoluble in any solvent other than acetone:water or methanol/ethanol:water mixtures. Attempts to use co-solvents (such as diethyl ether or ethyl acetate) to precipitate out the product invariably caused all of the diastereomers to crash out of solution. In the acetone:water case, approximately 1:1 mixtures allowed dissolution of the material in the lowest volume of solvent (30-50 volumes depending on the quality of the starting material; less clean material required less solvent); using 1:4 or 4:1 mixtures of acetone:water both required larger volumes (ca. 100 volumes) for complete dissolution. Additionally, the camphanylidene acetal was very difficult to dissolve in either acetone or water alone.

Table 6.3. Alternative crystallisation procedure – small scale trials.

Amount of crude material	Crystallisation solvent	Volume	Yield (% recovery)	Comments*
300 mg	MeOH	100 mL	90 mg (30%)	Hot filtration required to clarify the solution
350 mg	MeOH:H ₂ O:Acetone 1:1:1	40 mL	117 mg (33%)	Good quality
300 mg	Acetone:water 1:2	25 mL	113 mg (39%)	Good quality
300 mg	EtOH:water 1:1	30 mL	117 mg (39%)	Good quality but somewhat slow to filter
200 mg	EtOAc	-	-	Wouldn't dissolve even upon MeOH and/or acetone addition
300 mg	Acetone:H₂O 3:2	17 mL	120 mg (40%)	Excellent quality
360 mg	Acetone:H₂O 1:1	23 mL	142 mg (39%)	Excellent quality
360 mg	Acetone:H ₂ O 4:1	42 mL	124 mg (34%)	Excellent quality
360 mg	Acetone:H ₂ O 1:4	37 mL	155 mg (43%)	Fine crystals – lower quality – slow to filter

* Quality of the crystals assessed by a combination of ¹H and ¹³C NMR analysis, physical appearance and ease of filtration of the crystals, and optical rotation.

Based on these results, the acetone:water procedure was chosen for further investigation. This was due in large part to the nature of the crystals obtained - fine platelet-like crystals that filtered rapidly. Such crystalline material had never been obtained from methanol, which gave white amorphous material. Hence, the acetone:water procedures were scaled up to the several gram scale (selected results, table 6.4). On this slightly larger scale the solutions were stirred as they cooled, which is the usual crystallisation procedure in a kilo-scale laboratory due to better control with a stirred solution. Heat transfer upon cooling is better (a homogeneous mixture is more easily maintained), especially important if a ramp cooling of a jacketed vessel is used.

In this case, the stirred 1:1 acetone:water solution gave a relatively impure (though still much cleaner than the crude material) white powdery instead of the crystals previously observed; this was probably due to the stirring of the solution causing a change in the way nucleation occurred. Generally, larger crystals seemed to form when solutions were not stirred as they cooled. Also, the best recovered yield obtained for the 3:2 acetone:water procedure was obtained for a crystallisation that was not stirred. Attempts to prepare a second crop of

Table 6.4. Alternative crystallisation procedure – larger scale trials.

Amount of crude material	Crystallisation solvent	Volume	Yield (% recovery)	Comments*
2.8 g	Acetone:H ₂ O 1:1 stirred	170 mL	1.2 g (43%)	Fine white powder – slow to filter, containing some diastereomeric impurities
2.8 g	Acetone:H ₂ O 3:2 stirred	140 mL	1.1 g (38%)	Good quality
2 g	Acetone:H ₂ O 3:2 not stirred	80 mL	0.9 g (47%)	Excellent quality
12 g	Acetone:H ₂ O 3:2 stirred	450 mL	5.1 g (43%)	Excellent quality

* Quality of the crystals assessed by a combination of ¹H and ¹³C NMR analysis, physical appearance and ease of filtration of the crystals, and optical rotation.

crystals from the filtrate of these larger scale trials were of limited use. Solid product could be obtained from the filtrate in reasonable yield (40 - 50%), but this was invariably contaminated with significant amounts of diastereomeric acetals.

The modified crystallisation procedure using 3:2 acetone:water at a rate of 30-50 volumes (mL g⁻¹) was soon adopted as the preferred purification method in the preparation of the *myo*-inositol camphanylidene acetal. This method consistently gave 35-40% recovery of product from the crude material, which equates to more than 25% yield (from *myo*-inositol) of good quality crystalline product. This is comparable to reported literature yields, while the method is less problematic than the published crystallisation procedure. Very good quality crystals could now be obtained, and a single crystal X-ray structure (figure 6.4) was obtained. This crystal structure had not been previously published.

The crystal structure confirmed the orientation of the camphor moiety in the major camphanylidene acetal (-)-**269a**. The *gem*-dimethyl group does not interact with the inositol ring but is well away. The methyl group (labelled as C 13 in figure 6.4) is oriented over the plane of the inositol ring. The potential for steric interaction between the C-13 protons and the axial inositol ring protons is evident in the structure, as well as that between the equatorial C-2 inositol ring

proton and the methylene protons of C-12 (in figure 6.4) of the camphor moiety. The balance between these two interactions, and with the analogous interactions in the other three isomers, along with solubility effects during the equilibration, must form the basis of the selectivity seen in this reaction.

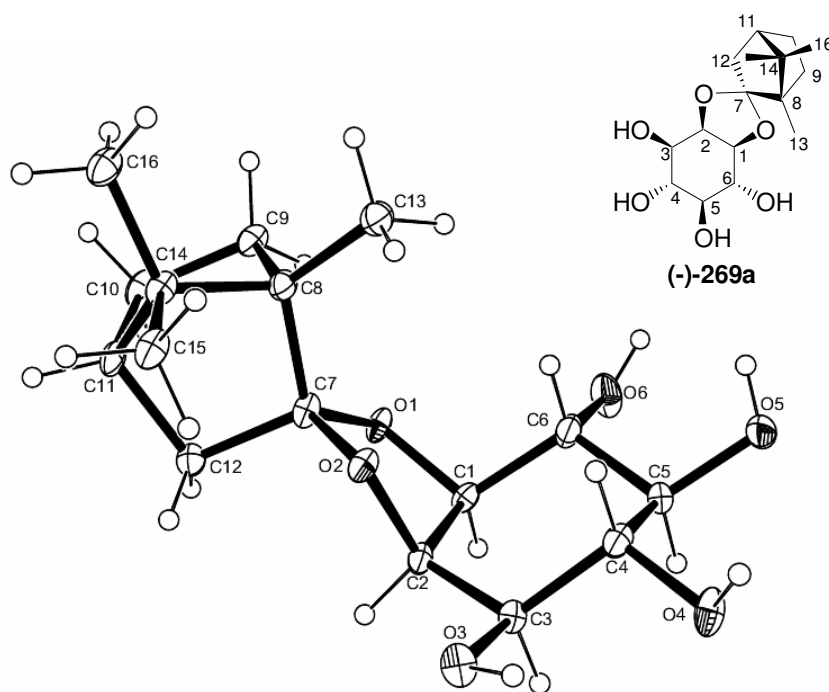


Figure 6.4. X-ray crystal structure of 1D-(6'-*S*)-1,2-*O*-(L-1',7',7'-trimethyl[2',2',1'] bicyclohept-6'-ylidene)-*myo*-inositol, (-)-**269a**.^v

6.2.5 Summary and Conclusions

The process development work described in the previous sections is partially summarised in table 6.5. The significant volumes of reagents used in Lindberg's procedure are shown, alongside the volumes that were arrived at after the process development described in the previous sections. The reaction volume required for the formation of (-)-L-camphor dimethyl acetal ((-)-**268**) has been reduced, which is beneficial because the trimethyl orthoformate used in that step is relatively expensive. Also, the volume of DMSO used in the reaction with *myo*-inositol was significantly reduced. This was important because removal of DMSO was forecast to be one of the major problems with the procedure on

^v Numbering of the atoms in the X-ray structure is not equivalent to the IUPAC numbering.

scaleup (DMSO could not be replaced with another solvent, see section 6.2.3). Reducing the volume of the equilibration step was not possible, and unfortunately this is the ‘limiting’ volume step in this synthesis.

Table 6.5. Volumes (mL/g) used in the *myo*-inositol camphanylidene acetal preparation before[§] and after process development.**

Reagent		Before	After
Borneol oxidation	(-)-L-camphor	1	1
	Trimethyl orthoformate	5	3.5
	Methanol	1	1
TOTAL REACTION VOLUME		7	5.5
Toluene		4.8	4.8
WORKUP VOLUME		5.8	5.8
Reaction of <i>myo</i>-inositol	<i>Myo</i> -inositol	1	1
	(-)-L-camphor dimethyl acetal (from step 1)	2.6	2.6
	DMSO	10	3
	TOTAL REACTION VOLUME	13.6	7.6
Equilibration	Chloroform	17	17
	Methanol	1	1
	Water	0.4	0.4
EQUILIBRATION VOLUME*		22	22

[§] i.e. volumes used in the procedure published by Lindberg.¹⁶⁹

* Includes volumes of *myo*-inositol and (-)-L-camphor dimethyl acetal from step 2.

** Relatively small-volume reagents such as catalytic sulphuric acid are omitted for clarity.

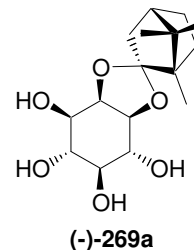
The crystallisation step is not included in the table because the volumes required were not reported in the literature. However the crystallisation step was significantly improved, as changing to an acetone:water mixed solvent allowed a smaller crystallisation volume to be used and excellent quality final product to be obtained.

Chapter Seven

Myo-Inositol Camphanylidene Acetal Scaleup Campaign

In December 2003, the opportunity arose to perform a larger scale synthesis of 1,2-D-*myo*-inositol-L-camphanylidene acetal, **(-)-269a**. The scale up laboratory (Light Technology Laboratory Number 9 (LT9)) at Industrial Research Ltd, Gracefield, Lower Hutt, became available for this project, and the objectives of the work were as follows:

- 1) To perform a commissioning run on the (then) new 50 L reactor ideally demonstrating that all of the following operations could be performed successfully: heat a solvent to reflux, add reagents (solids and liquids), cool, distil, distil under vacuum, perform vacuum transfers, clean in place.
- 2) To provide quantities of **(-)-269a** to chemists in the carbohydrate team, as starting material for the synthesis of a target requested by a commercial client, and for research use.



7.1 Work and Procedure in the scaleup laboratory

Equipment available in LT9

The equipment available in LT9 and used in this campaign included:

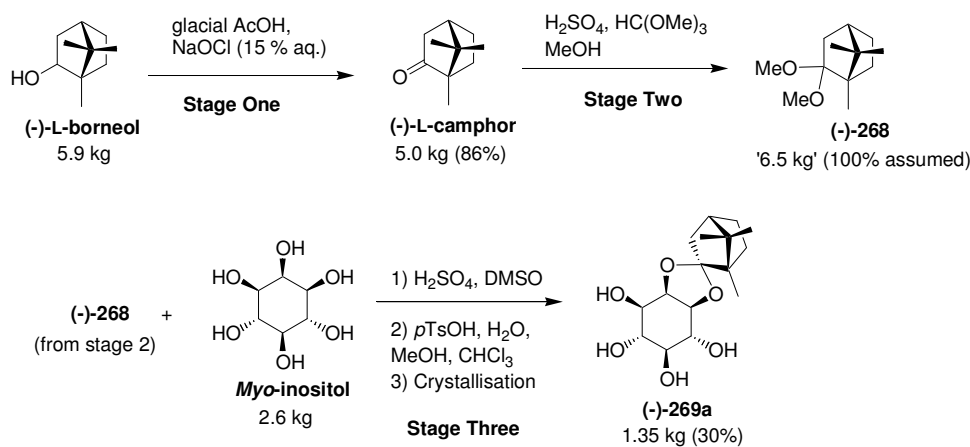
- the new **50 L, glass, jacketed reactor** (see figure 7.4), fitted with a heating/cooling unit. The reactor is capable of reflux and distillation, is able to be placed under vacuum, and is fitted with a header vessel for the addition of liquids to the reactor.
- a large scale **Buchi rotary evaporator** with 50 L and 20 L flasks.
- two 20 L sealed glass vessels (known as the 20 L transfer skids, see figure 7.2) mounted on a trolley that could be placed under

vacuum or pumped into/out of, used for transferring solutions or liquids without operator.

- a benchtop suction filter (for typically > 5 kg of solid) called a **Table top Buchner** (pictured in figure 7.1). Mother liquors are sucked through the filter into 20 L transfer skids.
- several 24 cm Buchner funnels and 10 L Buchner flasks for filtration of 1-5 kg of solids.
- a range of associated glassware and equipment (including a large number of extremely useful 20 L yellow buckets!).

The *myo*-inositol camphor acetal campaign

The synthetic scheme that was used to prepare **(-)-269a** (as discussed in chapter six) is shown in scheme 7.1, with the planned amounts and expected yields of each product. **(-)-L-camphor** was to be prepared from the oxidation of 5.9 kg of **(-)-borneol**, followed by conversion to the dimethyl acetal **(-)-268**. Then, reaction of **(-)-268** with *myo*-inositol, after the equilibration and crystallisation steps also discussed in chapter six, would give 1.35 kg of **(-)-269a**.



Scheme 7.1. Planned scale up campaign, showing the expected yields.

As part of the preparation for the scaleup synthesis, a large amount of paperwork was required. Most importantly, the required amounts of each solvent, reagent, etc were calculated and ordered. For this campaign, a balance was struck

between using the maximum capacity of the reactor, and preparing a quantity of material that would be manageable in the work-up stages. For example, the borneol oxidation step involves pouring the reaction mixture onto almost three times the reaction volume of ice-water before isolating the resultant precipitate by filtration. The oxidation was done on smaller scale than the maximum reactor volume, to make this filtration manageable.

The limiting step volume-wise for this campaign, based on the maximum volume of the reactor and on obtaining yields equal to those obtained in the laboratory, is the equilibration step of stage three. As detailed in chapter six, it was not possible to reduce the volume of this step significantly. The amounts of each material that were required based on these considerations and on the process development described in chapter six, are presented in table 7.1.

A ‘batch process record’ and a ‘reaction scaleup assessment’ were also required for each step of the campaign before work could begin in LT9. The batch process record is a step-by-step description of what will be done. This includes all additions of reagents (amounts and addition times), reaction times, temperatures, and all the details of the workup and cleaning procedures. The planned/required values are entered before the process begins, and the actual values entered during the process. Every step is signed off as complete by the chemist carrying out the work, and verified by another (two chemists are always present for safety reasons). This procedure ensures an accurate record of what actually happened, and is particularly useful for tracking errors, or for improving a procedure if it is to be repeated at a later date.

The ‘reaction scaleup assessment’ is a questionnaire that allows an overall assessment of whether the reaction (as written) is safe and suitable for scale-up using the equipment and facilities that are available in LT9. It focuses on potential hazards and requires the chemist to plan mitigations for potential problems (e.g how will a runaway reaction be brought under control; how will spills of toxic or hazardous chemicals be contained; are the reagents/solvents compatible with the reactor vessel and other equipment they will come in contact with). The head process chemist must sign off the document before work begins.

Table 7.1. Materials required and ordered for the scaleup preparation of (-)-269a.

	Material	Amount required	Cost/unit	Amount ordered	Cost
Stage 1	1(<i>S</i>)- <i>endo</i> -borneol	5.9 kg	\$213/500 g	6 kg	\$2,556
	NaOCl 15%	19.65 L	\$12/5 L	20 L	\$48
	Acetic acid glacial	17.7 L	\$62/5L	20 L	\$248
	Aq.sat. sodium bisulphite	2.35 L			
	Ice/brine	60 L			
	Reaction volume	45.6 L			
	Workup volume	105.6 L			
Stage 2	L-Camphor (ex step 1)	5 kg	-	-	-
	Trimethyl orthoformate	17.5 L	\$264.50/2.5 L	20 L	\$2,116
	Methanol	5 L			
	Sulphuric acid conc.	47 mL			
	NaOMe	105 g			
	Toluene	24 L			
	Reaction volume	27.5 L			
	Workup volume	51.5 L			
Stage 3	di-Me acetal (ex step 2)	5 kg	-	-	-
	<i>Myo</i> -inositol	2.58 kg	\$105/250 g	3 kg	\$1,260
	DMSO	7.5 L	\$89/2.5 L	7.5 L	\$267
	Sulphuric acid conc.	145 ml			
	Triethylamine	970 ml			
	Chloroform (AR)	42.5 L	\$402.50/20 L	40 L	\$805
	Methanol	4.25 L			
	Water	850 ml			
	pTsOH.H ₂ O	9.75 g			
	Triethylamine	323 ml			
	Chloroform (wash)	30 L	\$390/20 L	40 L	\$780
	Reaction volume	16.2 L			
	Equilibration volume	63.0 L			
	Expected yield	1350 g			
TOTAL* materials cost					\$8,080



Materials used from stock

* Materials used from stock not included in this total.

7.2 Stage 1 – Oxidation of (-)-Borneol

The oxidation of (-)-borneolⁱ to L-camphor was conducted according to the literature procedure¹⁹¹ that was deemed suitable for scale up based on the work described in chapter six. This step proceeded smoothly on scale, with little deviation from the procedure laid out in the batch record. Five kgⁱⁱ of (-)-borneol were dissolved in 15 L of glacial acetic acid (breathing masks were worn during the charging of the reactor) and subsequently 16.7 L of 15% aqueous sodium hypochlorite was added over 2.5 hours. The addition time was longer than the planned two hours, due to the temperature increase observed, resulting from the



Figure 7.1. The author with the L-camphor filter cake, in the tabletop Buchner filter.

reaction exotherm. The desired reaction temperature of 15 °C could not be maintained with the available cooling; in fact, the reaction was run at about 25 °C for most of the addition. This was with the jacket of the 50 L reactor set to -20 °C (for most of the duration of the addition). Although cooling the jacket further would have resulted in a lower reaction temperature, it may also have caused a layer of glacial acetic acid to freeze to the internal glass wall of the reactor. Should

this have happened, heat transfer would have become even less efficient, and this risk was considered to be too great to warrant cooling the jacket further.

ⁱ (-)-Borneol = *endo*-(1*S*)-1,7,7-trimethylbicyclo[2.2.1]heptan-2-ol.

ⁱⁱ Although it was planned to run the reaction on a slightly larger scale starting with 5.9 kg of (-)-borneol, as indicated in table 7.1, a decision was later made to start with only 5 kg of (-)-borneol.

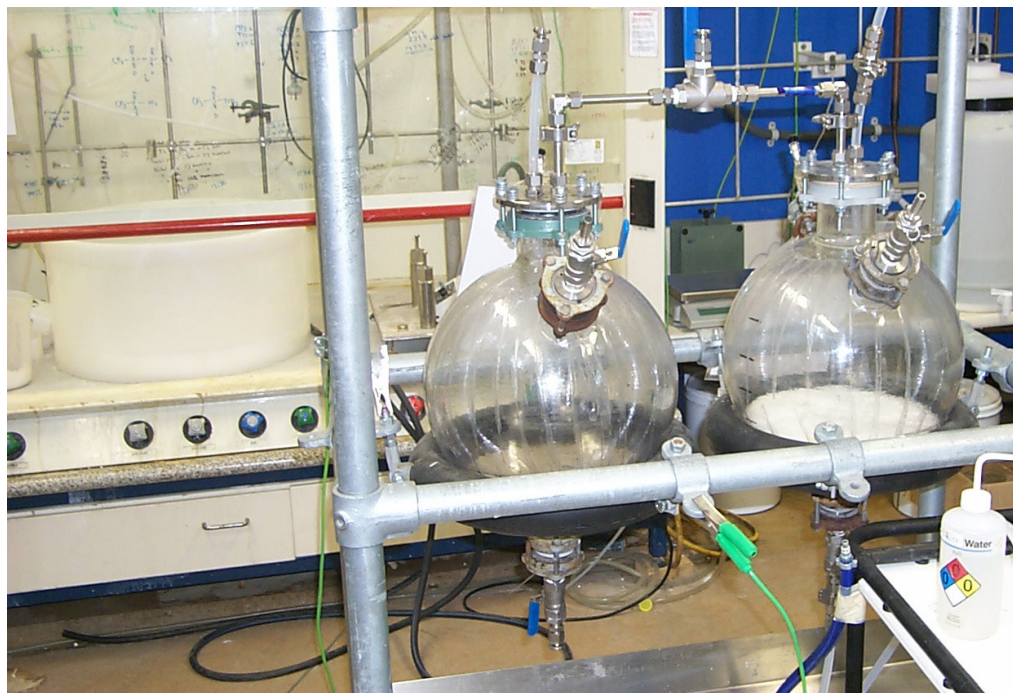


Figure 7.2. The table-top Buchner filter (in fume hood) and 20 L transfer skids

The workup of the reaction involved pouring the entire contents of the reactor (ca. 38 L) into a further 40 L of ice/brine to precipitate a white solid. This was the most challenging part of the reaction in a practical sense. A series of 20 L buckets were used for this step, with the resulting white solid being collected by filtration using the ‘table-top buchner’ unit (pictured in figure 7.1, previous page, and figure 7.2, above), and washed with aqueous sodium bicarbonate (to neutralise the residual acetic acid) and water. A large volume of solvent waste was produced in this step, and careful management thereof was required. For example, the aqueous sodium bicarbonate was collected into a 20 L transfer skid that was empty of any acidic filtrate. This precaution avoided any effervescence and foaming that could lead to material being sucked into the house vacuum system. Acidic wastes were collected into 20 L plastic drums for disposal, while the neutral aqueous wastes were collected into normal (stainless steel) waste drums for the same. The wet filter cake was then returned to the 50 L reactor, dissolved in 20 L of petroleum ether, and the resulting solution washed with water and brine. Solvents were then removed in the 50 L rotary evaporator (figure 7.3).



Figure 7.3. The (-)-L-camphor in the 50 L flask of the Buchi rotary evaporator.

The crude product was dried by use of a toluene azeotrope. The solid residue was dissolved in toluene, which was subsequently removed under reduced pressure. This was somewhat troublesome, as the camphor began to sublime before all of the toluene was removed. Fortunately, the slightly toluene-wet camphor was successfully carried through the next step. The experimental procedure for the 50 L reactor run of this step is contained in the experimental section. The total yield for stage 2 was approximately 4.55 kg (92%) – including 300 g of material that was recovered from the base plate of the table-top buchner filtration unit. The yield allows for the retained toluene, which was quantified by ^1H NMR and by the mass loss after removal of the toluene from a portion of the bulk material in the laboratory.

7.3 Stage 2 - Camphor di-methyl acetal

Formation of (-)-L-camphor dimethyl acetal, (-)-**268**, from the stage 1 product was the most straightforward of the three stages in the scaleup campaign.

The (-)-L-camphor from stage 1 was carried through to stage 2 while still slightly toluene-wet. This was done to minimise loss of camphor, as it had begun to sublime in the 50 L rotary evaporator. A lab-scale run of the dimethyl acetal formation using the toluene-wet material proceeded without apparent loss of yield or quality. The reaction was therefore run in the 50 L reactor on the full 4.55 kg of crude (-)-L-camphor. The modified literature procedure discussed in chapter six was followed (experimental details of the scaleup may be found in chapter eight).

The acidified mixture of (-)-L-camphor, trimethyl orthoformate and methanol was stirred at 20 °C for a full 24 hours, after which time ¹H NMR analysis showed essentially complete conversion to the dimethyl acetal. After neutralisation with solid sodium methoxide,ⁱⁱⁱ the entire 26 L reaction mixture was vacuum transferred to the 50 L Buchi. Subsequent removal of the solvents took approximately four hours, and salts began to precipitate out during the concentration. In order to further precipitate the salts formed during the reaction, the residues in the 50 L Buchi were dissolved in a further 12 L^{iv} of toluene (in two 20 L vessels). The mixture was allowed to stand overnight to allow maximum precipitation and the solids were removed by filtration the next day. There appeared to be efficient removal of salts, as a clear solution was obtained. After evaporation of most of the toluene, 6.40 kg of crude (-)-L-camphor dimethyl acetal was obtained as a clear, pale yellow liquid. The theoretical yield of this reaction was 5.92 kg, so there was clearly residual toluene present, but it was decided to proceed to the third the third stage with the toluene present for the following reasons:

- a) Evaporation of the product (as well as toluene) was occurring – as evidenced when the flask was removed from the Buchi for weighing, and the characteristic greasiness and smell of the product was noted around the neck of the 50 L Buchi flask;
- b) material containing residual toluene had been used successfully in stage three in laboratory scale experiments; and

ⁱⁱⁱ The pH of the reaction mixture was determined by removing a small sample from the reactor, diluting it with distilled water, and testing using pH paper to confirm that pH 7 had been reached.

^{iv} This was less than the 20 L of toluene that would have represented a proportional scaleup of the laboratory procedure, but physical constraints in LT9 precluded the use of 20 L in this case.

c) time constraints due to another campaign being scheduled in LT9. Effecting complete toluene removal would have added a day to the processing time since stage three needed to begin early in the day (in order to reach a point at which it was safe to leave the product overnight). The mass of 6.40 kg had been achieved at the end of a day.

7.4 Stage 3 - 1,2-D-Myo-inositol-L-camphanlylidene acetal, (-)-269a

The amounts of *myo*-inositol and other reagents used in this stage were based on a 100% yield in stage 2 (i.e, 5.92 kg of (-)-**268** going into the reaction). Hence, 2.40 kg of *myo*-inositol were charged to the 50 L reactor and to this was added all of the L-camphor dimethyl acetal from stage 2, dissolved in 7.5 L of DMSO. The mixture was acidified with concentrated sulphuric acid, and then heated to 70 °C.

At this point, the reaction began to behave differently from the laboratory scale reactions. Whereas in the laboratory, the *myo*-inositol reacted and dissolved (generally within 30 minutes of reaching 70 °C) to give a clear, essentially colourless solution, the mixture in the 50 L reactor began to go orange within one hour, and after the prescribed three hours of heating, the colour was red-brown. In addition, there were still significant amounts of solid material not dissolved. It was noted at this point that fine air bubbles were being entrained into the viscous solution by the powerful stirring mechanism in the 50 L reactor. This had not been apparent at the beginning of the reaction time, because the bubbles resembled particulate matter when being vigorously stirred, and their presence was masked by the large amount of solid *myo*-inositol initially present. Inert atmosphere was not available in the 50 L reactor at the time this work was carried out, so the reaction was carried out under air, which had previously been successfully carried out in the laboratory.

Although in the laboratory, the reaction would normally be heated until all the solids had dissolved (indicating complete reaction of the *myo*-inositol,

which is not significantly soluble in DMSO), it was decided in view of the unpleasant and unusual colour change to quench the reaction at this point. The mixture was cooled and triethylamine added, which resulted in a disturbing darkening of the colour to dark red-brown.

Undissolved solids were removed from the reaction mixture by filtration (using the 10 L Buchi flasks / 24 cm filters) to give 30 g of white material, which was insoluble in chloroform or DMSO. The red-brown filtrates were then transferred to the 50 L Buchi for removal of solvents. Residual toluene, and the petroleum ether and methanol that had been used to rinse reactor and lines, were removed rapidly. Not unexpectedly, removal of the 7.5 L of DMSO was significantly more troublesome. Seven hours of distilling at 15-20 mbar, with the bath temperature maintained at 95 ± 5 °C, resulted in the recovery of only 4 L of DMSO. At that point the evaporation was stopped, because the flask contents had dropped below the ‘critical weight’ of 4.9 times the mass of *myo*-inositol used.^v Although the flask was too heavy to be removed physically from the rotary evaporator and weighed, contents of the 50 L flask after 4 L of DMSO had been removed were calculated to be:

	7.5 – 4 = 3.5 L DMSO (d=1.102)	3.86 kg
<i>plus</i>	the mass of salts [(Et ₃ NH) ₂ SO ₄] from 132 mL H ₂ SO ₄	0.75 kg
<i>plus</i>	13.32 mol <i>myo</i> -inositol bis-camphor acetal (MW 448.6)	<u>5.98 kg</u>
	EQUALS A TOTAL OF	10.59 kg
<i>minus</i>	the solids filtered out	<u>0.30 kg</u>
	A FINAL TOTAL OF	10.29 kg

This total is less than the 11.76 kg that represent the ‘critical mass’. Concern about the stability of the product over extended periods of time at temperatures over 90 °C also prompted the end of the distillation. Hence, the mixture was cooled, dissolved in 20 L of CHCl₃, and transferred back to the 50 L reactor. Gratifyingly, the material was largely soluble in the CHCl₃, indicating

^v Lindberg *et al.*¹⁶⁹ removed the solvents from their crude product and then added DMSO *back* to the flask to 4.9 times the weight of the *myo*-inositol used. They found this amount of DMSO to be important for the success of the subsequent equilibration step; this was not the case in our hands but the extra DMSO was not found to be detrimental.

that the major component was camphanylidene acetals of *myo*-inositol (rather than unreacted *myo*-inositol!). To the reactor was then added the CHCl_3 , methanol, water, and catalytic pTsoH required for the equilibration step, and the mixture (still red-brown, and much less inclined to form a thick precipitate than had previous laboratory scale reactions) was left to stir for three days.

The slurry that had formed after this time (figure 7.4) was drained from the reactor into buckets and filtered using two 10 L Buchi/24 cm filters. After washing with CHCl_3 , each cake was blended with 4 L of CHCl_3 to give a slurry (which had the consistency of paint) and filtered again. This process was repeated once more to yield a pale tan coloured solid, which upon air-drying for three days gave 2.26 kg of product. Had this solid been clean (-)-**269a**, this would represent a yield of 54%. However, ^1H NMR analysis quickly revealed that this solid had a significantly different composition than had been expected. The desired product (-)-**269a** had been formed, but in conjunction with the other three possible diastereomers, **269b**, **269c** and **269d** (see figure 7.5).



Figure 7.4. The 50 L reactor containing the *myo*-inositol camphanylidene acetal in CHCl_3 , MeOH and H_2O at the end of the equilibration step.

Although signal overlap in the ^1H NMR spectrum suggested the presence of only three diastereomers, ^{13}C NMR and single crystal XRD analysis

demonstrated that all four had been formed. Substantial amounts of *myo*-inositol were also present in the crude product (approximately 19% by ^1H NMR analysis). It was not clear whether the *myo*-inositol present was due to incomplete conversion during the reaction, or to the hydrolysis of the product during the workup or equilibration.

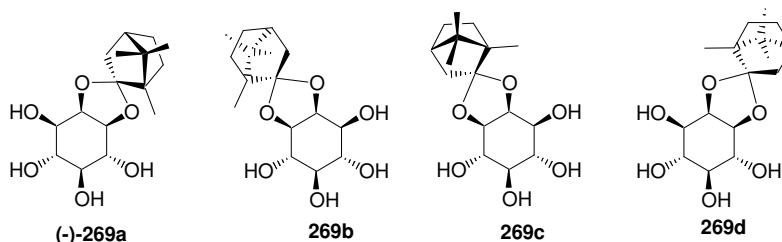


Figure 7.5. The four diastereomers of camphanylidene acetal **269**.

In the analysis of this unexpected result, it was clear that the major problem lay in the reaction, rather than the workup or the equilibration. The observations made during the reaction were dramatically different to those made during laboratory-scale runs. The deep red-brown colour and the failure of all of the solids to dissolve were key indicators that the problem had occurred during the reaction. The possible reasons for the unusual behaviour, and consequent reduced diastereoselectivity of the reaction include:

- The quality of the DMSO;
- The lack of inert atmosphere in the 50 L reactor. Although the reaction had been carried out in the laboratory under air (using anhydrous solvents), in the 50 L reactor the stirring action was very powerful and air bubbles were entrained very effectively into the viscous reaction mixture. A much higher degree of aeration of the reaction was obtained on scale;
- Contamination of the (-)-L-camphor dimethyl acetal with inorganic salts due, potentially, to the salts removal in stage 2 being less efficient on scale - not a likely scenario (as discussed in section 7.3);
- Overheating. In the laboratory, reactions were normally run with the flask immersed in an oil bath at 70 °C (so contents of the flask were probably several degrees cooler), whereas in the reactor, the temperature was set to hold the reactor contents at 70 °C. However, the reaction has previously

been carried out at 90 °C, in this work and in the literature,¹⁷¹ so this is unlikely to be the cause of the problem;

- That, having reduced the volume of DMSO used in the process development, we were already pushing the limits of the reaction's selectivity, and that combined with one or more of the above factors this reduced the selectivity of the reaction much more dramatically.

Although the major problem evidently lay in the reaction, the workup may well have exacerbated the troubles. In particular, the lengthy (compared to laboratory scale) period of heating for the DMSO removal could have aggravated the low yield by causing further hydrolysis, perhaps of the desired product in favour of one of the other diastereomers. Interconversion between the diastereomers is also possible, if traces of acid remained in the mixture (and even if the sulphuric acid had been neutralised, the resulting triethyl ammonium salt can act as a weak acid). Unfortunately, no analysis was done on the crude reaction mixture before DMSO removal. The complex mixture of products at this stage and the presence of DMSO solvent makes TLC analysis extremely difficult. The NMR spectrum is similarly difficult to interpret. Ideally, an HPLC method could be developed to monitor the mixture at this stage (and during the equilibration). This should be a definite focus of any future work.

7.5 Crystallisation of *myo*-inositol camphanylidenes acetals

The ¹³C NMR spectrum of the expected major product from this reaction, (-)-**269a**, is shown in figure 7.6 overleaf, and that of the crude product from stage three in figure 7.7 on page 180. It is clear from inspection of these that although the (-)-**269a** was present, this was in conjunction with three other products **269b**, **269c** and **269d**, which were identified by single crystal XRD as described later in this section. This is particularly clear upon inspection of the 115-118 ppm portion of the spectra; the signal attributed to the acetal carbon of (-)-**269a** appears at 116.3 ppm, and in the crude product, three other acetal peaks are present. *Myo*-inositol was also present in the crude product, and was able to be

Figure 7.6. ^{13}C NMR spectrum of the desired camphanylidene acetal, (-)-**269a**.

Figure 7.7. ^{13}C NMR spectrum of the crude product, containing (-)-**269a**, **269b-d**, and *myo*-inositol.

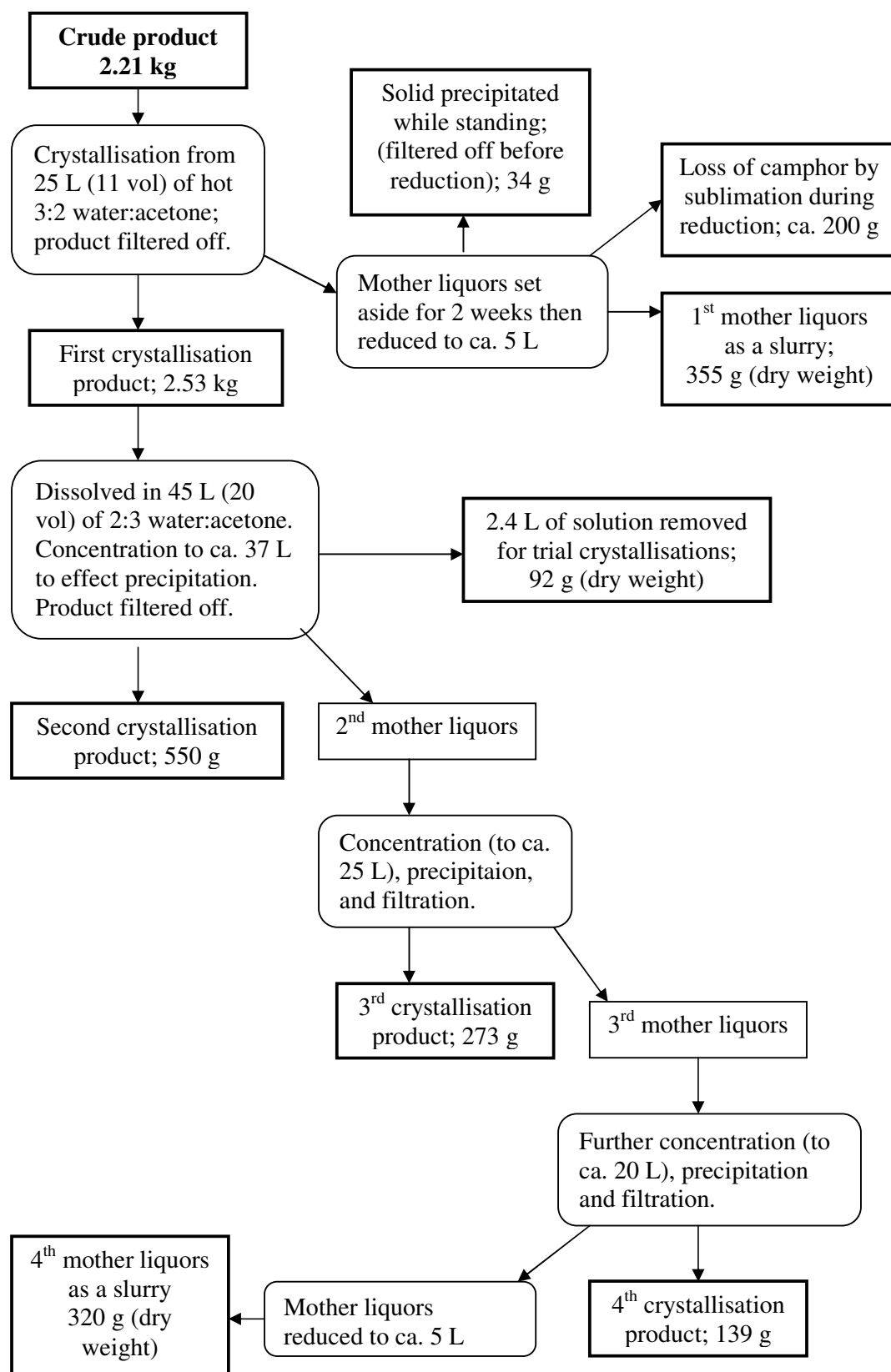


Figure 7.8. Crystallisation flow chart.

quantified because the *myo*-inositol hydroxyl protons are well-resolved and upfield of the *myo*-inositol camphanylidene hydroxyl protons (see figure 7.11).

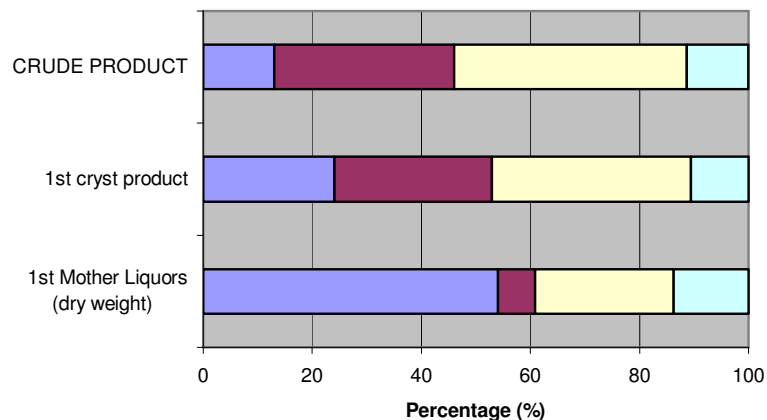
It was decided to attempt purification of the crude material via a series of crystallisations. Laboratory-scale (5-10 g) trial crystallisations of the crude material from stage 3 were encouraging; an initial crystallisation from approximately 10 volumes of 3:2 acetone:water efficiently removed the *myo*-inositol. This was a much smaller volume of solvent than would dissolve the crude product from laboratory reactions (which contained (-)-**269a** as the major diastereomer), indicating that **269b** is more soluble than (-)-**269a** in the 3:2 acetone:water system. A subsequent series of crystallisations from 30-40 volumes of the same solvent were shown by NMR analysis to give material that was progressively richer in the desired (-)-**269a**. Unfortunately, the most successful crystallisations were slow – several days – and with commercial projects due to begin in LT9, there was limited time available for large-scale recrystallisations. It was decided to attempt a partial purification of the crude material on large scale. Further crystallisations of smaller portions could be more easily carried out in the laboratory.

The series of crystallisations that were done in LT9 are summarised in the flow chart shown in figure 7.8. The first step was to dissolve all 2.21 kg of the crude material in acetone:water (3:2), in the 50 L reactor. The jacket temperature was set to 75 °C until the acetone was refluxing, and then reduced to 65 °C for two hours, during which time the solids all dissolved. The temperature was then ramped down to 16 °C over 2.5 h during which time a cloudiness developed; stirring overnight at that temperature resulted in a thick white precipitate. This was filtered and washed with acetone:water to yield 2.53 kg (wet weight) of a white solid. Unfortunately, ¹H NMR analysis of the solid^{vi} showed that this first recrystallisation had not changed the composition of the material significantly; it

^{vi} The ratio of *myo*-inositol to the four diastereomers was calculated from the integrals of the hydroxyl protons in the ¹H NMR spectrum. This analysis is fairly crude but is adequate for this analysis. It was facilitated by the fact that the *myo*-inositol hydroxyl signals do not overlap at all with the camphor acetal hydroxyl signals, which appear further downfield. See figure 7.11. The camphanylidene acetals would not dissolve satisfactorily in any common NMR solvent other than DMSO.

appeared that everything had simply precipitated out again. If anything, there was more *myo*-inositol present (*ca.* 32% rather than the original 19%) in the first crystallisation product, as is clear in figure 7.9.

Figure 7.9. Comparison of the percentage composition of the crude product, the first crystallisation product, and the first mother liquors.



This suggested that hydrolysis of one or more of the diastereomers of *myo*-inositol camphanylidene acetal had occurred; this was confirmed when the mother liquors from this initial crystallisation were reduced *in-vacuo*, and significant quantities of camphor were seen to sublime. In addition, the *overall* mass balance (see table 7.2) reveals a loss of *ca.* 185 g, approximately equivalent to the amount of camphor that would need be lost to cause the observed increase in the mass of *myo*-inositol.

The significant hydrolysis observed during the first crystallisation was not seen in subsequent crystallisations. This suggests that an acidic impurity, which catalysed the hydrolysis, was present in the crude material and was largely removed during the first crystallisation. If the hydrolysis of *myo*-inositol camphanylidene acetal had been due to prolonged heating in the acetone:water solvent system, the usefulness of this crystallisation method would have been called into question. Gratifyingly, this was not the case, since in subsequent crystallisations the solution was heated for much longer in the same solvent system, and further significant hydrolysis was not observed.

The second crystallisation was performed at a much higher volume:solid ratio than the first in the hope that the camphanylidene acetal products would precipitate and leave the *myo*-inositol in solution. The entire first crystallisation product was submitted to the second crystallisation, and readily dissolved in 20 volumes (45 L) of solvent, but in this case, when the solution was cooled, no precipitate formed. Some of the solution was removed from the 50 L reactor and allowed to stand without stirring (as laboratory trials had suggested that this gave a more crystalline product), while the remaining solution was stirred slowly in the 50 L reactor. All parts of the solution were seeded with crystals of the desired (-)-**269a**, but after leaving for 18 hours none of the solutions had developed any precipitate. With limited time in hand the solution in the reactor was heated and approximately 8 L of solvent was distilled out under vacuum at *ca.* 40 °C. When the concentrated solution was cooled, a white solid precipitated out, and was isolated by filtration. Although the second crystallisation product (yield 550 g) now contained only about 5% *myo*-inositol, it was also enriched in **269b** rather than the desired (-)-**269a**. Only approximately 20% of the desired diastereomer (-)-**269a** was present, while approximately 75% of the mass was attributed to **269b** and **269c** (based on integrals in the ¹H NMR spectrum).

Analysis of the Products of the Crystallisation Sequence

In the ¹H NMR spectrum, peaks attributed to single inositol ring protons of (-)-**269a** and of **269d** are well resolved in the region 3.8-4.2 ppm (see figure 7.10 overleaf and 7.11 on the following page). However, the equivalent peaks for **269b** and **269c** overlap, and hence it is impossible to determine the relative proportions of these two diastereomers from the ¹H NMR spectrum. They have been analysed together in the mass balance, which follows. It is a fair assumption, based on the ¹³C NMR and other observations, that the actual amount of **269c** is similar to that of **269d** (i.e. (-)-**269a** and **269b** are the major and **269c** and **269d** the minor diastereomers).

It has also been observed that **269b** and **269c** co-crystallise. Very good-looking, plate-like crystals were obtained when attempts were made to obtain a

Figure 7.10. ^1H NMR spectra of (-)-**269a**, and of the co-crystals of **269b** and **269c**, in d_6 -DMSO.

Figure 7.11. ^1H NMR spectra of *myo*-inositol, and of a sample that contains all four diastereomers including **269d**, and *myo*-inositol, in d_6 -DMSO.

pure, crystalline sample of the major impurity **269b**. These crystals were sent for single crystal XRD analysis, and it was found that a mixture of **269b** and **269c** was present. XRD was able to resolve the crystal structures of the two diastereomers (figures 7.12 and 7.13 respectively), which had formed a crystal structure in a 2:1 ratio together with three water molecules. Indeed, ^{13}C NMR analysis of the crystals revealed two diastereomers present in an approximately 2:1 ratio, allowing assignment of the spectral peaks. The major component of the crystals sent for XRD was also the major impurity seen in the ^{13}C NMR spectrum of the crude product (see figure 7.7), and hence it was possible to assign the major and one of the minor diastereomeric impurities as **269b** and **269c**. Having therefore identified three of the diastereomers by their X-ray structures, the fourth could also be assigned by the process of elimination (spectral data are presented in chapter eight).

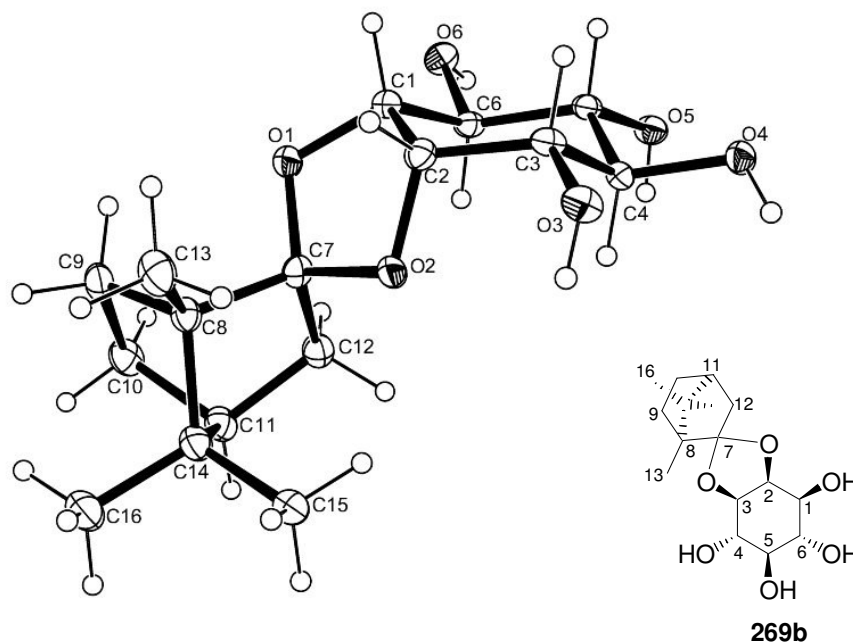


Figure 7.12. X-ray crystal structure of 1D-(6'-*S*)-2,3-*O*-(L-1',7',7'-trimethyl[2',2',1']bicyclohept-6'-ylidene)-*myo*-inositol, **269b**.^{vii}

The crystal structure of **269b**, the major impurity, revealed it to be the 2,3-*D*-*myo*-inositol-*L*-camphanylidene acetal, with the camphanylidene moiety

^{vii} Numbering of the atoms in the X-ray structure is not equivalent to the IUPAC numbering.

oriented so that the methyl group is away from the inositol ring. This is interesting in that (-)-**269a**, the favoured diastereomer, has the configuration with the methyl group over the inositol ring. The structure of **269c**, the minor impurity that co-crystallised with **269b**, had the methyl group over the ring as in (-)-**269a**. The selectivity that is normally observed with this reaction is attributed to steric factors favouring (-)-**269a**, but evidently the selectivity observed cannot be attributed to steric interaction with just one part of the camphanylidene moiety. These results suggest that the steric difference between the conformations, particularly between (-)-**269a** and **269b**, is not large.

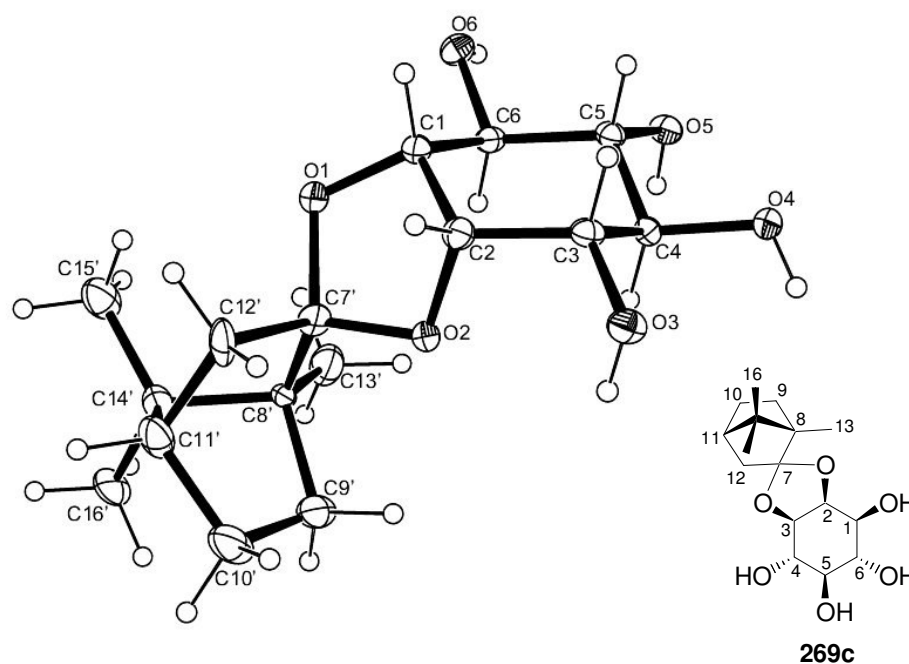


Figure 7.13. X-ray crystal structure of 1D-(6'-R)-2,3-O-(L-1',7',7'-trimethyl[2',2',1']bicyclohept-6'-ylidene)-*myo*-inositol, **269c**.^{viii}

Back to the crystallisation story

Preferential crystallisation of **269b**,^{ix} as was observed in the second crystallisation of the crude *myo*-inositol camphor acetal on large scale, had never

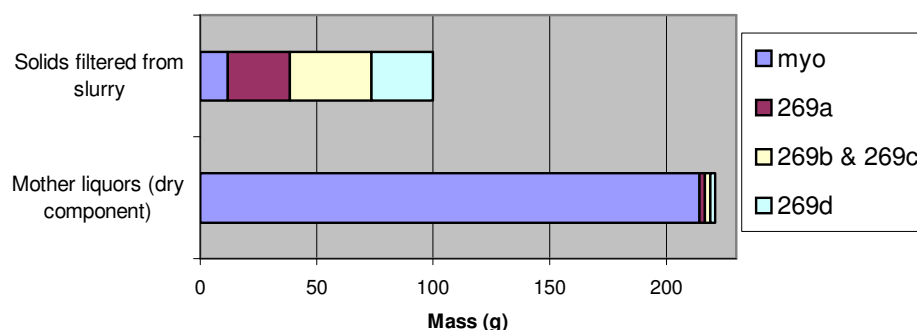
^{viii} Numbering of the atoms in the X-ray structure is not equivalent to the IUPAC numbering.

^{ix} It was assumed that when **269b** crystallised, **269c** always co-crystallised, because of the observed XRD spectrum and also because the ¹H NMR spectrum always gave 'messy' signals in the 3.8-4.2 ppm region for the **269b/269c** inositol ring protons. As opposed to the 'tidy' signals seen in that region for (-)-**269a** and **269d** (figure 7.10 and 7.11).

been observed in the laboratory. However, it was hoped that if levels of **269b** could be reduced, the proportion of (-)-**269a** might increase to a point where it would crystallise preferentially instead. The mother liquors were therefore returned to the 50 L reactor, and distillation of solvent out of the vessel was continued. The solution was allowed to cool and stir overnight and a third crop of crystals, yield 273 g, were isolated and found to be of a similar composition to the second crystallisation. A fourth cycle of heating the mother liquors and removing solvent, cooling and precipitating gave a fourth crop of 139 g, which now contained no *myo*-inositol at all (the composition of the mother liquors being almost 100% water by this stage, and *myo*-inositol being extremely soluble in water) but a mixture of (-)-**269a**, **269b**, **269c**, and somewhat more of **269d** than had been obtained in the previous crystallisations. This would be expected, as the previous crystallisations favoured **269b** and **269c**, and to a lesser degree (-)-**269a**, and hence **269d** had become more concentrated in the mother liquors. Since **269d** did not precipitate out when the solvent was richer in acetone, this could also indicate that it is more soluble in acetone than (-)-**269a**, **269b** and **269c**.

After the fourth crystallisation, the time available in LT9 was almost complete. Thus the final mother liquors were concentrated from about 20 L to a slurry of about 5 L volume. The same was done with the first mother liquors (which had been set aside), in order to make the material more manageable on the laboratory scale. All further work was carried out in the laboratory.

Figure 7.14. Composition of the slurry of the fourth mother liquors.



When a portion of the final slurry of the fourth mother liquors was filtered, it was found that the solids contained a small amount of *myo*-inositol and all four diastereomers (-)-**269a** and **269b-d** (figure 7.14 above). The mother liquors from this filtration, when reduced to dryness, contained nearly 100% *myo*-inositol, which is very soluble in water. In effect, a fifth precipitation/crystallisation had been conducted, in which all of the camphor acetal diastereomers (-)-**269a** and **269b-d** precipitated due to the fact that they are essentially insoluble in water. The compositional analysis of this portion was extrapolated to give the total mass composition of the fourth mother liquor slurry; this is presented in figure 7.14. The total dry weight of the fourth mother liquors was 321 g.

Mass Balance Analysis for the Crystallisation Sequence

As may be apparent from the previous discussion, none of the parts collected during the series of crystallisations was significantly enriched in the desired diastereomer, (-)-**269a**. In an attempt to understand the fate of (-)-**269a**, an overall mass balance analysis was done. This mass balance is presented in table 7.2. Included are the main crystallisation products, and two portions that were removed during the sequence (the test solution removed from the second

Table 7.2. Mass balance over all parts of the crystallisation sequence.

	<i>Myo</i> - (g)	(-)- 269a (g)	269b/c (g)	269d (g)	Total mass (g)
1st ml slurry*	334	43	156	85	618
Sols from 1st ml**	0	3	31	0	34
Test 2nd cryst	22	27	33	10	92
2nd cryst	17	112	411	10	550
3rd cryst	11	58	194	10	273
4th cryst	3	5	90	41	139
4th ml slurry	247	24	29	21	321
Total isolated	633	271	945	177	2026
Crude product composition	287	729	941	250	2210

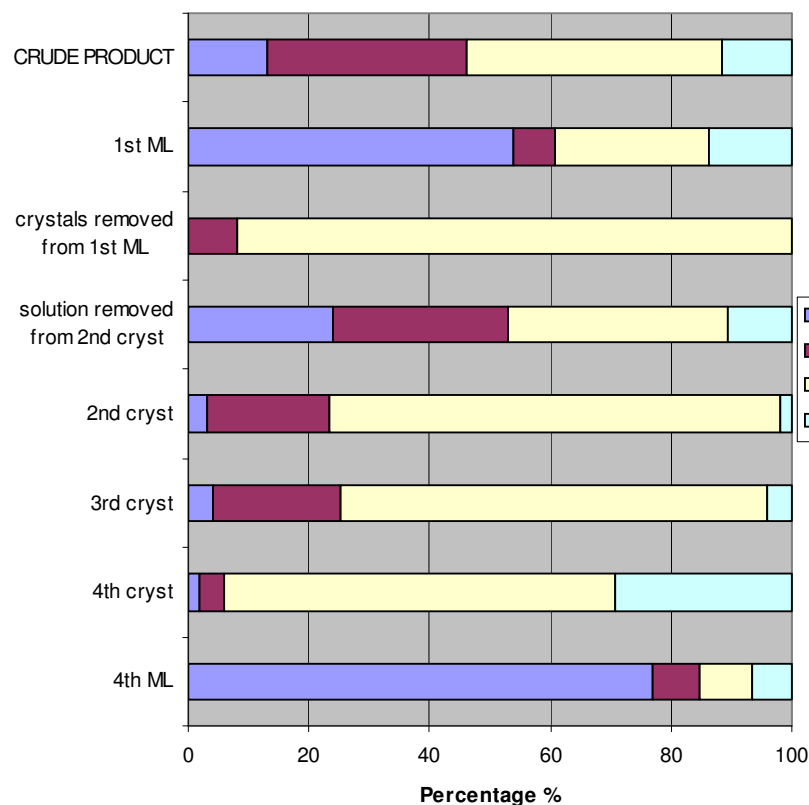
* The composition of the dry material when all solvents removed from the 1st mother liquor under reduced pressure.

**Crystalline solids removed by filtration from the first mother liquors after they had been set aside for several days (and before the reduction to a slurry).

crystallisation, and the solids that were filtered from the first mother liquor after it had been standing for several days but before it was reduced to a slurry). All the figures in the table represent dry weights.

Analysis of the crude product indicated that before the crystallisations, there had been approximately 730 g of (-)-**269a** present. However, the total amount of (-)-**269a** over all of the parts after the crystallisation sequence was only *ca.* 270 g. This represents a loss of 460 g!! Losses of the other diastereomers were less dramatic. The combined mass of **269b** + **269c** did not change, while that of **269d** dropped from *ca.* 250 g to *ca.* 175 g. Thus, the loss of (-)-**269a** is certainly significant. There are two possible explanations for this loss; a) preferential hydrolysis of (-)-**269a**, to give *myo*-inositol, and b) that some interconversion between diastereomers was taking place. These two scenarios are discussed further below.

Figure 7.15. Percentage composition of each of the parts of the mass balance.

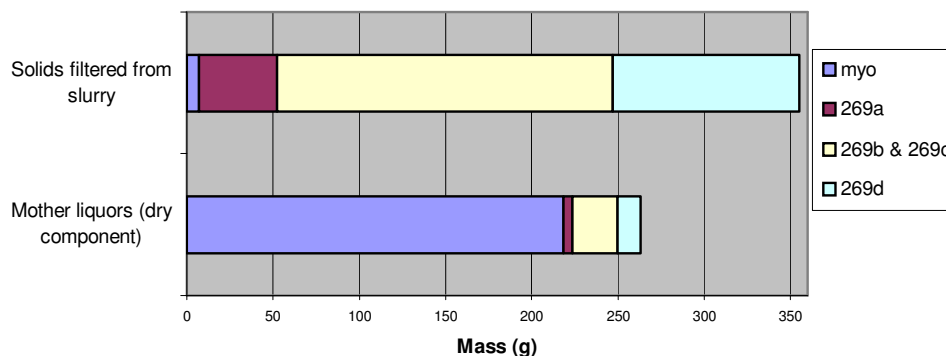


The percentage composition of each of the parts of the mass balance is shown in figure 7.15 on the previous page. This emphasises that none of the parts were enriched in the desired diastereomer, **(-)-269a**. Indeed, none of the four diastereomers were cleanly isolated in this crystallisation sequence.

Hydrolysis of the camphanylidene acetals

The total mass of crude product that went into the first crystallisation was 2210 g, while the total mass of the parts collected after the crystallisations was 2027 g. this represents an overall loss of 183 g. Some of this may be accounted for by mechanical losses during the filtrations. However, some must also be due to loss of camphor by hydrolysis of the camphor acetals. Camphor was observed subliming in the condenser of the 50 L Buchi rotary evaporator, particularly during the concentration of the first mother liquors to a slurry. The loss of camphor in this manner was not quantified. However, this observation is in agreement with the apparent significant hydrolysis during the first crystallisation discussed earlier in this section.

Figure 7.16. Composition of the slurry of the first mother liquors.



The composition of the first mother liquor slurry, analysed as the solids filtered out and the mother liquors therefrom, is shown in figure 7.16 above. It is worth noting at this point that the first mother liquors may have initially contained less *myo*-inositol and more of **(-)-269a** and **269b-d** than the analysis presented here indicates. Although the ^1H NMR taken on the day of the filtration

indicates that no significant change had occurred, a rigorous analysis of the composition of the first mother liquors was not done until after the solution had been concentrated. It is, however unlikely that hydrolysis occurred during the concentration. No further sublimation of camphor was observed when a portion of the slurry was later reduced to dryness for the mass balance analysis.

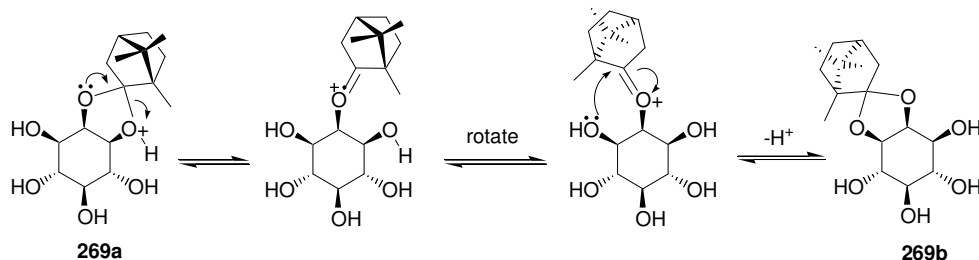
The amount of *myo*-inositol present in the crude was 420 g, which increased by 312 g over the course of the crystallisations according to this mass balance analysis. If formed from the hydrolysis of *myo*-inositol camphanylidenes acetal, 312 g (1.73 moles) of *myo*-inositol would liberate 264 g of camphor. Therefore camphor loss by hydrolysis and sublimation could account for a large part of the 183 g of mass lost in the overall mass balance analysis. The amount of all the camphanylidenes acetals ((-)-**269a** and **269b-d**) lost from the total mass is 529 g (1.68 moles). This is in good agreement with the increase in the number of moles of *myo*-inositol present.

Why (-)-**269a** might be hydrolysed in preference to the other camphor acetals is not clear. However it is likely that if hydrolysis did occur, it would be while the acetal was dissolved. Since **269b/269c** were being precipitated out preferentially, they spent less time in solution (and a smaller proportion of their mass was resubmitted to the next cycle of crystallisation each time). This means that (-)-**269a** (and **269d**, which also suffered a mass loss) simply spent more time in conditions that might cause hydrolysis. Alternatively, if the hydrolysis of (-)-**269a** was occurring more rapidly than hydrolysis of the other diastereomers under these conditions, then even if it was relatively slow, it would keep the proportion of (-)-**269a** relative to the other diastereomers down and hence inhibit the crystallisation of (-)-**269a**.

Interconversion of diastereomers

Although the mass balance supports an overall loss of (-)-**269a** by hydrolysis, it is notable that the major impurity **269b** is the diastereomer that is available from an acetal migration of (-)-**269a**, as shown in scheme 7.2 (of course, all of the diastereomers (-)-**269a** and **269b-d** may be interconverted by

this type of mechanism). It is possible that, as **269b** precipitated out of solution, some (-)-**269a** was converted to **269b** by this mechanism, with the equilibrium being driven by the decrease in concentration of **269b** as it precipitated out. Better data about the levels of **269b** would be necessary to prove this, as from the available data it is not possible to determine whether the total amount of **269b** has increased. If hydrolysis of **269b** was also occurring during the crystallisation sequence, this would further complicate the situation.



Scheme 7.2. Acid-catalysed interconversion between **269a** and **269b**.

7.6 Conclusions

Although a successful large-scale preparation of (-)-**269a** was not achieved during the course of the work presented in this chapter, several positive outcomes of the work were identified:

- The 50 L reactor was considered ‘commissioned’ at the end of the work. It had been demonstrated to perform well and to be suitable for carrying out the requisite operations.
- The preparation of the L-camphor dimethyl acetal reagent in two steps from borneol was successfully carried out. Of particular note, it was demonstrated that the cooling available in the 50 L reactor was sufficient to control the exotherm of the borneol oxidation step.
- The single crystal XRD structures of (-)-**269a**, **269b** and **269c** were all obtained. None of these had been previously published. This also allowed definitive assignment of the NMR spectra of the diastereomeric impurities that are seen in the preparation of **269a**.

The results obtained in the attempt to prepare 1D-*myo*-inositol-1,2-L-camphanylidene acetal were probably related to the quality of the DMSO, and the lack of inert atmosphere in the reactor. Some time after this work was completed, the synthesis of (-)-**269a** was repeated at Industrial Research, using a slightly higher quality DMSO from a different supplier for the third stage and conducting the reaction under inert atmosphere. With these modifications, 600 g of (-)-**269a** were successfully prepared, and subsequently used in the production of a target compound requested by a client. This confirms the usefulness of the process development work described here, particularly the crystallisation procedure, which performed very well on scale. A yield of slightly less than 30% of good quality pure crystalline product was obtained from *myo*-inositol, equal to the best yields typically obtained on laboratory scale.

Chapter Eight

Experimental Section

8.1 General

Unless otherwise stated, the following conditions apply: All reactions were performed under argon in oven-dried glassware using standard syringe techniques. Diethyl ether and THF were distilled from sodium and benzophenone. Dichloromethane, triethylamine, acetonitrile and methanol were distilled from calcium hydride. Diisopropylamine and pyridine were distilled from sodium hydroxide. Toluene was distilled from sodium. Anhydrous *N,N*-dimethylformamide (DMF) and dimethylsulfoxide (DMSO) were purchased from Aldrich Chemical company and used without further purification. All other reagents were of commercial quality and distilled prior to use if necessary. Reaction progress was monitored using aluminium backed t.l.c. plates pre-coated with silica UV254 and visualised by either UV radiation (254 nm), ceric ammonium molybdate dip, anisaldehyde dip, or an iodine tank. Purification of products via flash column chromatography was conducted using a column packed with silica gel 60 (220-240 mesh) with the solvent systems as indicated. Optical rotations were measured using a Perkin-Elmer 241 polarimeter. ^1H and ^{13}C spectra were recorded on either a Varian Inova NMR spectrometer or a Bruker Advance NMR spectrometer, at 300 and 75 MHz respectively. Spectra were referenced to solvent peaks (^1H – residual CHCl_3 or DMSO or acetone, ^{13}C – CDCl_3 or d_6 -DMSO or d_6 -acetone). Infrared spectra were obtained on a Biorad FTS-7 or a Bruker Tensor 27 FTIR spectrometer. High-resolution mass spectra were recorded using a Mariner electrospray time of flight spectrometer.

8.2 Experimental for Chapter Two

3-(*tert*-Butyldimethylsilyloxy)-propionitrile (137): 3-Hydroxy-propionitrile (960 μL , 1.00 g, 14 mmol) and imidazole (1.43 g, 21 mmol) were dissolved in DMF (5 mL) and then cooled to 0 °C. TBDMSCl (2.32 g, 15 mmol)

was then added, and the mixture allowed to warm to RT and stirred overnight. The mixture was then diluted with diethyl ether (80 mL), washed with sat. aq. NaHCO₃ (20 mL), water (20 mL), and brine (20 mL), dried over anhydrous MgSO₄, and the solvent removed under reduced pressure. Flash column chromatography (1:10 EtOAc:petroleumether) gave the TBDMS-protected nitrile **137** as a colourless oil, 2.50 g (97%). ¹H NMR (300 MHz, CDCl₃) δ 3.84 (t, 2 H, *J* = 6.2 Hz), 2.54 (t, 2 H, *J* = 6.2 Hz), 0.90 (s, 9 H), 0.10 (s, 6 H) ppm. ¹³C NMR (75 MHz, CDCl₃) δ 118.1, 58.5, 25.7, 21.7, 18.1, -5.5 ppm. IR (neat) 2956, 2931, 2859, 2253, 1427, 1256, 1116, 914, 838, 779, 722 cm⁻¹. HRMS (ESI) calcd. for C₉H₂₀NOSi [M + H⁺] 186.1314, found 186.1543.

3-(tert-Butyldiphenylsilyloxy)-propionitrile (14): 3-Hydroxy-propionitrile (868 μL, 904 mg, 12.7 mmol) and imidazole (1.96 g, 28.8 mmol) were dissolved in DMF (4.5 mL) and then cooled to 0 °C. TBDPSCl (3.0 mL, 3.17 g, 11.5 mmol) was then added and the mixture allowed to warm slowly to RT. After stirring at RT for two days, the mixture was diluted with diethyl ether (80 mL), washed with sat. aq. NaHCO₃ (30 mL), water (30 mL), and brine (20 mL), and then dried over anhydrous MgSO₄. The solvent was removed under reduced pressure to yield a colourless oil. Purification by flash column chromatography (1:20 EtOAc:petroleumether) gave the nitrile **14** as a colourless oil, 3.21 g (90%, based on the limiting reagent TBDPSCl). ¹H NMR (300 MHz, CDCl₃) δ 7.68 (m, 4 H), 7.44 (m, 6 H), 3.85 (t, 2 H, *J* = 6.4 Hz), 2.55 (t, 2 H, *J* = 6.4 Hz), 1.09 (s, 9 H) ppm. ¹³C NMR (75 MHz, CDCl₃) δ 135.5, 132.6, 130.0, 127.9, 117.9, 59.0, 26.6, 21.4, 19.1 ppm. IR (neat) 3071, 2931, 2857, 2252, 1427, 1104, 914, 821, 733, 700 cm⁻¹. HRMS (ESI) calcd. for C₁₉H₂₇N₂OSi [M + NH₄⁺] 327.1887, found 327.1904.

3-Tetrahydropyranyloxy-propionitrile (146): A mixture of 3-hydroxy-propionitrile (1 mL, 1.04 g, 14.6 mmol) and 3,4-dihydro-2-*H*-pyran (1.47 mL, 1.36 g, 16.1 mmol) was stirred at 30 °C. AlCl₃·6H₂O was then added and stirring continued at 30 °C for 2 h, after which time the mixture was filtered through a short silica plug which was then washed with 1:5 EtOAc:petroleum ether (100 mL). The solvent was removed under reduced pressure to yield the crude product. ¹H NMR indicated 80% conversion to the product. Flash column

chromatography (1:10 EtOAc:petroleumether) gave the tetrahydropyranyl ether **146** as a colourless oil, 1.48 g (an isolated yield of 65%). ^1H NMR (300 MHz, CDCl_3) δ 4.67 (m, 1 H), 3.97-3.82 (m, 2 H), 3.69-3.61 (m, 1 H), 3.58-3.50 (m, 1 H), 2.64 (m, 2 H), 1.87-1.50 (m, 6 H) ppm. ^{13}C NMR (75 MHz, CDCl_3) δ 117.9, 98.6, 61.9, 61.8, 30.1, 25.1, 18.8 (2 C) ppm. IR (neat) 2942, 2873, 2251, 1352, 1122, 1065, 1032, 917, 847, 813 cm^{-1} . HRMS (ESI) calcd. for $\text{C}_{18}\text{H}_{17}\text{O}_2\text{N}_2$ [$\text{M} + \text{NH}_4^+$] 173.1285, found 173.1285.

3-(*para*-Methoxybenzyloxy)-propionitrile (147): A solution of 3-hydroxypropionitrile (150 μL , 156 mg, 2.21 mmol) and KO^tBu (1 M in THF, 1.63 mL, 1.63 mmol) in DMF was cooled to 0 $^\circ\text{C}$. PMBCl (200 μL , 231 mg, 1.48 mmol) was then added and the mixture stirred for 1 h at that temperature, then warmed to RT and stirred for a further 4 h. The mixture was quenched with 5% aq. HCl, and extracted with diethyl ether (three times 50 mL). The combined organic portions were washed with water (50 mL) and brine (50 mL) and then dried over anhydrous MgSO_4 . The solvent was removed under reduced pressure to yield a colourless oil. Purification by flash column chromatography (1:20 EtOAc:petroleumether) gave *para*-methoxybenzyl ether **147** as a colourless oil, 110 mg (40%). ^1H NMR (300 MHz, CDCl_3) δ 7.29 (d, 2 H, $J = 8.5$ Hz), 6.90 (d, 2 H, $J = 8.6$ Hz), 4.52 (s, 2 H), 3.82 (s, 3 H), 3.66 (t, 2 H, $J = 6.4$ Hz), 2.61 (t, 2 H, $J = 6.5$ Hz) ppm. ^{13}C NMR (75 MHz, CDCl_3) δ 159.5, 129.4, 129.2, 117.8, 114.1, 73.0, 64.2, 55.3, 18.9 ppm. IR (neat) 3000.4, 2859, 2252, 1611, 1512, 1245, 1172, 1102, 1006, 908, 818, 730 cm^{-1} . HRMS (ESI) calcd. for $\text{C}_{11}\text{H}_{17}\text{O}_2\text{N}$ [$\text{M} + \text{NH}_4^+$] 209.1285, found 209.1285.

6-(*tert*-Butyldimethylsilyloxy)-hex-1-en-4-one (138): The nitrile **137** (500 mg, 2.7 mmol) was dissolved in THF (60 mL) under argon and then allylmagnesium chloride (2 M solution in Et_2O , 4.05 mL, 8.1 mmol) was added dropwise. The mixture was stirred overnight at RT, and then poured onto an ice/water mixture (50 mL) to which had been added 5 drops of glacial acetic acid. This was stirred for 0.5 h, after which time the aqueous mixture was extracted with diethyl ether (three times 50 mL). The combined organic fractions were then washed with 5% aq. NaHCO_3 (20 mL) and brine (20 mL), and then dried over anhydrous MgSO_4 . The solvent was removed under reduced pressure

to yield an orange oil which was promptly purified by gradient flash column chromatography (petroleum ether – 1:20 EtOAc:petroleum ether) to yield **138** as a colourless oil, 230 mg (38%). ¹H NMR (300 MHz, CDCl₃) δ 6.01-5.87 (m, 1 H), 5.22-5.11 (m, 2 H), 3.90 (t, 2 H, *J* = 6 Hz), 3.24 (d, 2 H, *J* = 7 Hz), 2.67 (t, 2 H, *J* = 6 Hz), 0.91 (s, 9 H), 0.08 (s, 6 H) ppm. ¹³C NMR (75 MHz, CDCl₃) δ 207.7, 130.4, 118.8, 58.8, 48.6, 45.1, 25.8, 18.2, -5.5 ppm. IR (neat) 2956, 2930, 2858, 1716, 1472, 1256, 1097, 836, 778 cm⁻¹. HRMS (ESI) calcd. for C₁₂H₂₅O₂Si [M + H⁺] 229.1624, found 229.1728.

***E*-6-(*tert*-Butyldimethylsilyloxy)-hex-2-en-4-one (143).** Isolated as a byproduct in the preparation of **138** in yields of 5 – 40%. ¹H NMR (300 MHz, CDCl₃) δ 6.89 (dq, 1 H, *J* = 14, 7 Hz), 6.70 (d, 1 H *J* = 14 Hz), 3.96 (t, 2 H, *J* = 6 Hz), 2.78 (t, 2 H, *J* = 6 Hz), 1.93 (d, 3 H, *J* = 7 Hz), 1.89 (s, 9 H), 0.08 (s, 6 H) ppm. ¹³C NMR (75 MHz, CDCl₃) δ 199.2, 143.3, 135.6, 133.5, 132.5, 129.7, 127.7, 60.0, 42.6, 26.7, 19.1, 18.3 ppm. IR (neat) 2955, 2930, 2858, 1673, 1633, 1471, 1390, 1255, 1095, 971, 834, 778 cm⁻¹.

6-(*tert*-Butyldiphenylsilyloxy)-hex-1-en-4-one (16): The nitrile **14** (1.57 g, 5.07 mmol) was dissolved in THF (60 mL) under argon and then allylmagnesium chloride (2 M solution in Et₂O, 7.6 mL, 15.2 mmol) was added dropwise. The mixture was heated to reflux for 3 h. The mixture was then cooled and poured onto an ice/water mixture (100 mL) to which had been added 10 drops of glacial acetic acid. This was stirred for 1 h, after which time the aqueous mixture was extracted with diethyl ether (three times 100 mL). The combined organic fractions were then washed with 5% aq. NaHCO₃ (50 mL) and brine (50 mL), and then dried over anhydrous MgSO₄. The solvents were removed under reduced pressure to yield an orange oil which was promptly filtered through a short silica plug to give the crude product. Purification by flash column chromatography (1:50 EtOAc:petroleum ether) gave **16** as a colourless oil, 943 mg (53%). ¹H NMR (300 MHz, CDCl₃) δ 7.69 (m, 4 H), 7.4 (m, 6 H), 6.04-5.88 (m, 1 H), 5.25-5.12 (m, 2 H), 3.97 (t, 2 H, *J* = 6.2 Hz), 3.27 (d, 2 H, *J* = 6.8 Hz), 2.69 (t, 2 H, *J* = 6.2 Hz), 1.07 (s, 9 H) ppm. ¹³C NMR (75 MHz, CDCl₃) δ 207.6, 135.5, 133.3, 130.4, 129.7, 127.7, 118.9, 59.6, 48.5, 44.9, 26.7, 19.1 ppm. HRMS (ESI) calcd. for C₂₂H₂₈NaO₂Si [M + Na⁺] 375.1756, found 375.2170.

The isomeric product **144** was also isolated, as a colourless oil, 350 mg (20%): ***E*-6-(*tert*-Butyldiphenylsilyloxy)-hex-2-en-4-one (144)**. ^1H NMR (300 MHz, CDCl_3) δ 7.68-7.63 (m, 4 H), 7.44-7.34 (m, 6 H), 6.82 (dq, 1 H, $J = 15.9$, 6.8 Hz), 6.14 (dq, 1 H $J = 15.9$, 1.7 Hz), 3.97 (t, 2 H, $J = 6.4$ Hz), 2.77 (t, 2 H, $J = 6.4$ Hz), 1.89 (dd, 3 H, $J = 6.6$, 1.5 Hz), 1.05 (s, 9 H) ppm. ^{13}C NMR (75 MHz, CDCl_3) δ 199.2, 143.3, 135.6, 133.5, 132.5, 129.7, 127.7, 60.0, 42.6, 26.7, 19.1, 18.3 ppm. IR (neat) 3050, 2930, 2857 1670, 1631, 1428, 1108, 735, 702 cm^{-1} .

Representative procedure for the conversion of ketones 138 and 16 into the alcohols 139 and 12, respectively: The ketone (1 eq.) was dissolved in THF (3.5 mL/mmol ketone). Lithium borohydride (2 M solution in Et_2O , 1.2 eq.) was then added dropwise at 0 °C. The mixture was allowed to warm slowly to RT over 3 h, and was then quenched by the addition of $\text{Na}_2\text{SO}_4 \cdot 10\text{H}_2\text{O}$ (and sometimes drops of water) until effervescence was no longer observed. Anhydrous MgSO_4 was then added, and the salts filtered off, rinsing well with diethyl ether. The solvents were then removed under reduced pressure to yield an oil which was purified by flash column chromatography (1:10 or 1:20 (depending on the levels of impurities present) EtOAc:petroleum ether) to yield the alcohol as a colourless oil.

6-(*tert*-Butyldimethylsilyloxy)-4-hydroxy-hex-1-ene (139) was prepared from **138** (230 mg, 1.01 mmol) to yield **139** (225 mg, 97%). ^1H NMR (300 MHz, CDCl_3) δ 5.86 (m, 1 H), 5.23 (m, 2 H), 3.93 (m, 2 H), 3.86 (m, 1 H), 2.26 (m, 2 H), 1.68 (m, 2 H), 0.92 (s, 9 H), 0.10 (s, 6 H) ppm. ^{13}C NMR (75 MHz, CDCl_3) δ 135.0, 117.3, 71.3, 56.3, 42.0, 37.7, 25.8, 18.1, -5.6 ppm. IR (neat) 3397, 3081, 2946, 2859, 1642, 1472, 1257, 1097, 1005, 913, 836, 776, 667 cm^{-1} . HRMS (ESI) calcd. for $\text{C}_{12}\text{H}_{27}\text{O}_2\text{Si}$ [$\text{M} + \text{H}^+$] 231.1780, found 231.1812.

6-(*tert*-Butyldiphenylsilyloxy)-4-hydroxy-hex-1-ene (12) was prepared from **16** (857 mg, 2.43 mmol) to yield **12** (694 mg, 84%). ^1H NMR (300 MHz, CDCl_3) δ 7.70 (m, 4 H), 7.41 (m, 6 H), 5.86 (m, 1 H), 5.18 (m, 1 H), 5.12 (m, 1 H), 4.00 (m, 1 H), 3.88 (m, 2 H), 3.26 (broad s, 1 H), 2.28 (m, 2 H), 1.72 (m, 2 H), 1.08 (s, 9 H) ppm. ^{13}C NMR (75 MHz, CDCl_3) δ 135.8, 135.2, 133.3, 133.2, 130.1, 128.1, 117.7, 71.2, 63.6, 42.2, 38.0, 27.1, 19.3 ppm. IR (neat) 3385, 3071, 2930, 2857, 1734, 1638, 1471, 1427, 1275, 1108, 1038, 914, 764, 748, 701 cm^{-1} . HRMS (ESI) calcd. for $\text{C}_{22}\text{H}_{31}\text{O}_2\text{Si}$ [$\text{M} + \text{H}^+$] 355.2088, found 355.2086.

6-*para*-Methoxybenzyloxy-4-hydroxy-hex-1-ene (72): Nitrile **147** (100 mg, 0.52 mmol) was dissolved in THF (6 mL) under argon and then allylmagnesium chloride (2 M solution in Et₂O, 910 μ L, 1.82 mmol) was added dropwise at 0 °C. The mixture was stirred overnight at RT, and then poured onto an ice/water mixture (10 mL) to which had been added 1 drop glacial acetic acid. This was stirred for 0.5 h, after which time the aqueous layer was separated and extracted three times with diethyl ether. The combined organic fractions were dried over anhydrous MgSO₄, and the solvent was removed under reduced pressure to yield an orange oil. This was passed through a plug of silica with 1:100 EtOAc:petroleum ether to yield 42 mg of an oil. This material was dissolved in THF (1 mL) and cooled to 0 °C. A solution of LiBH₄ (2 M in THF, 180 μ L, 0.36 mmol) was then added dropwise and the solution allowed to warm to RT over 3 h. The reaction was quenched by the addition of drops of water till effervescence was no longer observed, then dried with anhydrous MgSO₄, filtered, and solvents removed under reduced pressure. The resulting oil was purified by flash column chromatography (1:10 EtOAc:petroleum ether) to yield **72** as a colourless oil, 37 mg (30% over 2 steps from **147**). ¹H NMR (300 MHz, CDCl₃) δ 7.24 (d, 2 H, *J* = 8.3 Hz), 6.87 (d, 2 H, *J* = 8.8 Hz), 5.83 (m, 1 H), 5.10 (m, 2 H), 4.45 (s, 2 H), 3.86 (m, 1 H), 3.80 (s, 3 H), 3.65 (m, 2 H), 2.24 (t, 2 H, *J* = 6.1 Hz), 1.72 (m, 2 H) ppm. ¹³C NMR (75 MHz, CDCl₃) δ 159.2, 134.9, 130.0, 129.3, 117.5, 113.8, 72.9, 70.4, 68.6, 55.3, 41.9, 35.8 ppm. IR (neat) 3074, 2932, 2858, 1640, 1512, 1246, 1088, 1030, 913, 820 cm⁻¹. HRMS (ESI) calcd. for C₁₄H₂₁O₃ [M + H⁺] 237.1491, found 237.1477.

Representative procedure for the conversion of alcohols 139, 12 and 72 into the TES-protected alcohols 140, 148 and 73, respectively: The alcohol (1 eq.) and imidazole (2.2 eq.) were dissolved in DMF (ca. 1 mL/mmol alcohol) and then cooled to 0 °C. TESCl (1.1 eq.) was then added and the mixture allowed to warm to RT and stir at RT overnight. The mixture was then diluted with diethyl ether (ca. 50 mL/mmol alcohol), washed with sat. aq. NaHCO₃, water, and brine, dried over anhydrous MgSO₄, and the solvent removed under reduced pressure. Flash column chromatography (1:50 EtOAc:petroleum ether) gave the protected alcohol as a colourless oil in yields typically > 80%.

6-(*tert*-Butyldimethylsilyloxy)-4-(triethylsilyloxy)-hex-1-ene (140) was prepared from **139** (190 mg, 0.83 mmol) to yield **140** (240 mg, 86%). ¹H NMR (300 MHz, CDCl₃) δ 5.85 (m, 1 H), 5.17 (m, 2 H), 3.92 (m, 1 H), 3.71 (t, 2 H, *J* = 6.6 Hz), 2.25 (m, 2 H), 1.66 (m, 2 H), 0.98 (t, 9 H, *J* = 7.6 Hz), 0.91 (s, 9 H), 0.62 (q, 6 H, *J* = 7.6 Hz), 0.07 (s, 6 H) ppm. ¹³C NMR (75 MHz, CDCl₃) δ 135.1, 116.8, 68.8, 59.8, 42.2, 39.9, 25.9, 18.2, 6.9, 5.0, -5.3 ppm. IR (neat) 3073, 2954, 2877, 1651, 1464, 1255, 1096, 1006, 911, 835, 774, 741 cm⁻¹. HRMS (ESI) calcd. for C₁₈H₄₁O₂Si₂ [M + H⁺] 345.2645, found 345.2703.

6-(*tert*-Butyldiphenylsilyloxy)-4-(triethylsilyloxy)-hex-1-ene (148) was prepared from **12** (410 mg, 1.16 mmol) to yield **148** (460 mg, 85%). ¹H NMR (300 MHz, CDCl₃) δ 7.65-7.63 (m, 4 H), 7.42-7.34 (m, 6 H), 5.81 (m, 1 H), 5.12 (m, 2 H), 3.97 (m, 1 H), 3.72 (m, 2 H), 2.22 (m, 2 H), 1.69 (m, 2 H), 1.05 (s, 9 H), 0.93 (t, 9 H, *J* = 7.9 Hz), 0.59 (q, 6 H, *J* = 7.9 Hz) ppm. ¹³C NMR (75 MHz, CDCl₃) δ 135.8, 135.4, 134.2, 129.8, 129.7, 127.8, 117.1, 69.1, 61.0, 42.4, 39.9, 27.1, 19.4, 7.2, 5.2 ppm. IR (neat) 3071, 2953, 2875, 1461, 1423, 1108, 1085, 1005, 909 cm⁻¹. HRMS (ESI) calcd. for C₂₈H₄₅O₂Si₂ [M + H⁺] 469.2953, found 469.2973.

6-(*para*-Methoxybenzyloxy)-4-(triethylsilyloxy)-hex-1-ene (73) was prepared from **72** (30 mg, 0.13 mmol) to yield **73** (35 mg, 80%). ¹H NMR (300 MHz, CDCl₃) δ 7.26 (d, 2 H, *J* = 8.9 Hz), 6.88 (d, 2 H, *J* = 8.9 Hz), 5.84 (m, 1 H), 5.05 (m, 2 H), 4.46 (d, 1 H, *J* = 10.9 Hz), 4.41 (d, 1 H, *J* = 10.9 Hz), 3.94 (m, 1 H), 3.83 (s, 3 H), 3.57 (t, 2 H, *J* = 6.8 Hz), 2.26 (m, 2 H), 1.78 (m, 2 H), 0.97 (t, 6 H, *J* = 7.8 Hz), 0.63 (q, 9 H, *J* = 7.8 Hz) ppm. ¹³C NMR (75 MHz, CDCl₃) δ 159.1, 134.9, 130.6, 129.3, 117.0, 113.7, 72.6, 69.0, 66.7, 55.2, 42.4, 36.8, 6.9, 5.0 ppm.ⁱ

5-(*tert*-Butyldimethylsilyloxy)-3-(triethylsilyloxy)-pentanal (141) - ozonolysis using the IRL ozonolysis machine: Alkene **140** (175 mg, 0.51 mmol) was dissolved in CH₂Cl₂ (4 mL) and anhydrous MeOH (0.4 mL) and one drop of Sudan (III) solution (0.1% in CH₂Cl₂) was added. The solution was cooled to -78 °C, purged with argon, and then ozone was bubbled through the solution until the pink colour disappeared (ca. 15 min). The flask was then

ⁱ HRMS and IR data were not obtained for this compound when it was initially prepared, and since it was not useful to the progress of the synthesis it was not re-made.

purged with argon, and DMS (200 μ L, 169 mg, 2.72 mmol) was added. The stirred solution was kept at -78 $^{\circ}$ C for 1 h, 0 $^{\circ}$ C for 30 min, and RT for 1 h, and the solvents then removed under reduced pressure. The residue was purified by gradient flash column chromatography (1:100-1:40 EtOAc:petroleum ether) to give the aldehyde **141** as a colourless oil, 95 mg (54%). ^1H NMR (300 MHz, CDCl_3) δ 9.81 (t, 1 H, J = 2 Hz), 4.38 (m, 1 H), 3.68 (t, 2 H, J = 7.7 Hz), 2.59 (m, 2 H), 1.80 (m, 2 H), 0.98 (t, 9 H, J = 7.6 Hz), 0.91 (s, 9 H), 0.63 (q, 6 H, J = 7.6 Hz), 0.07 (s, 6 H) ppm. HRMS (ESI) calcd. for $\text{C}_{17}\text{H}_{39}\text{O}_3\text{Si}_2$ [$\text{M} + \text{H}^+$] 347.2432, found 347.2453.

Note: The optimised ozonolysis procedure using the VUW ozonolysis machine is presented later in this chapter on page 208).

Data for the byproducts of the ozonolysis (152a and 152b) discussed in section 2.1.2 of chapter 2 follows. Data for 152a as a mixture of two diastereomers: ^1H NMR (300 MHz, CDCl_3) δ 7.66 (m, 8 H), 7.40 (m, 12 H), 5.34 (m, 2 H), 5.19 (s, 1 H), 5.16 (s, 1 H), 5.08 (s, 1 H), 5.06 (s, 1 H), 4.18 (m, 2 H), 3.72 (m, 4 H), 1.90 (m, 4 H), 1.79 (m, 4 H), 1.08 (s, 18 H), 0.96 (t, 18 H, J = 7.8 Hz), 0.62 (q, 12 H, J = 7.8 Hz) ppm. HRMS (ESI) calcd. for the carboxylic acid derivative (**153a**) $\text{C}_{27}\text{H}_{42}\text{O}_4\text{Si}_2\text{Na}$ [$\text{M} + \text{Na}^+$] 509.2519, found 509.2496. **Data for 152b:** ^1H NMR (300 MHz, CDCl_3) δ 7.64 (m, 8 H), 7.60 (m, 8 H), 7.40 (m, 24 H), 5.35 (m, 2 H), 5.12 (s, 1 H), 5.11 (s, 1 H), 4.98 (s, 1 H), 4.95 (s, 1 H), 4.24 (m, 2 H), 3.62 (m, 4 H), 2.03 – 1.66 (m, 8 H), 1.09 (s, 9 H), 1.08 (s, 9 H), 1.02 (s, 9 H), 1.01 (s, 9 H) ppm. ^{13}C NMRⁱⁱ (75 MHz, CDCl_3) δ 136.2, 135.8, 134.3, 134.2, 134.0, 133.9, 130.0, 129.9, 129.8, 127.9, 127.8, 102.0, 101.8, 94.0, 93.9, 68.0, 67.9, 60.7, 39.9, 39.8, 38.6, 38.5, 27.3, 27.0, 19.7, 19.6, 19.3 ppm. HRMS (ESI) calcd. for the carboxylic acid derivative (**153b**) $\text{C}_{37}\text{H}_{46}\text{O}_4\text{Si}_2\text{Na}$ [$\text{M} + \text{Na}^+$] 633.2832, found 633.2919.

3-(tert-Butyldiphenylsilyloxy)-propanal (10): Oxalyl chloride (89 μ L, 1.02 mmol) was dissolved in CH_2Cl_2 (7 mL). Upon cooling to -78 $^{\circ}$ C, DMSO

ⁱⁱ In the ^{13}C NMR spectrum of the two diastereomers of **152b**, most of the signals show different values for the two diastereomers. Those that do not (i.e. where the signals for the two diastereomers overlap) are at 60.7 ppm, three of the *t*-butyl signals at 27.3, 27.0, and 19.3 ppm, and the phenyl signals at 136.2, 135.8, 127.9, and 127.8 ppm.

(145 μ L, 2.04 mmol) was added dropwise via syringe. Gas evolution was observed. After 15 min, a solution of 3-(*tert*-butyldiphenylsilyloxy)-propan-1-ol (synthesis follows) in CH_2Cl_2 was slowly added. The cloudy solution was stirred at $-78\text{ }^\circ\text{C}$ for 30 min, and then Et_3N (460 μ L, 3.30 mmol) was added dropwise. The resultant clear solution was stirred at $-78\text{ }^\circ\text{C}$ for 1.25 h, and was then warmed to $0\text{ }^\circ\text{C}$ and stirred for an additional 5 min. The mixture was quenched at $0\text{ }^\circ\text{C}$ with sat. aq. NaHCO_3 (4.5 mL), extracted twice with CH_2Cl_2 , and the combined extracts then washed twice with 1 M sodium bisulfite, once with brine, dried over anhydrous MgSO_4 , and the solvent removed under reduced pressure. Flash column chromatography (1:10 EtOAc:petroleum ether) gave the aldehyde **10** as a colourless oil, 215 mg (84%). ^1H NMR (300 MHz, CDCl_3) δ 9.82 (t, 1 H, $J = 2.1$ Hz), 7.67-7.62 (m, 4 H), 7.45-7.36 (m, 6 H), 4.03 (t, 2 H, $J = 6.0$ Hz), 2.61 (dt, 2 H, $J = 2.1, 6.0$ Hz) ppm. ^{13}C NMR (75 MHz, CDCl_3) δ 202.0, 135.5, 133.2, 129.8, 127.7, 58.2, 46.3, 26.7, 19.1 ppm. IR (neat) 3071, 2930, 2857, 1726, 1612, 1472, 1427, 1389, 1105, 822, 737, 700 cm^{-1} . HRMS (ESI) calcd. for $\text{C}_{19}\text{H}_{28}\text{O}_2\text{NSi}$ [$\text{M} + \text{NH}_4^+$] 330.1884, found 330.1879.

3-(*tert*-butyldiphenylsilyloxy)-propan-1-ol: 1,3-propane diol (140 μ L, 147 mg, 1.92 mmol) and imidazole (288 mg, 4.22 mmol) were dissolved in DMF (5 mL) and then cooled to $0\text{ }^\circ\text{C}$. TBDPSCl (500 μ L, 528 mg, 1.92 mmol) was then added and the mixture allowed to warm slowly to RT. After stirring at RT overnight, the mixture was diluted with Et_2O (100 mL), washed with sat. aq. NaHCO_3 (40 mL), water (40 mL), and brine (40 mL), dried over anhydrous MgSO_4 , and the solvent removed under reduced pressure. Gradient flash column chromatography (1:20-1:10 EtOAc:petroleum ether) gave the title compound as a colourless oil, 376 mg (61%). ^1H NMR (300 MHz, CDCl_3) δ 7.70-7.66 (m, 4 H), 7.42-7.36 (m, 6 H), 3.85 (t, 4 H, $J = 5.9$ Hz), 2.08 (broad s, 1 H), 1.81 (m, 2 H), 1.06 (s, 9 H) ppm. ^{13}C NMR (75 MHz, CDCl_3) δ 135.5, 133.2, 129.8, 127.8, 63.4, 62.1, 34.1, 26.8, 19.0 ppm. IR (neat) 3366, 3070, 2930, 2857, 1472, 1427, 1275, 1260, 1106, 1086, 822, 745, 700, 689 cm^{-1} . HRMS (ESI) calcd. for $\text{C}_{19}\text{H}_{27}\text{O}_2\text{Si}$ [$\text{M} + \text{H}^+$] 315.1775, found 315.1791. Also isolated was di-protected product 1,3-di-(*tert*-butyldiphenylsilyloxy)-propane, as a white solid, 370 mg (35%, based on the diol). ^1H NMR (300 MHz, CDCl_3) δ 7.68-7.62 (m, 8 H), 7.42-7.32 (m, 12 H), 3.82 (t, 4 H, $J = 5.9$ Hz), 1.60 (m, 2 H), 1.03 (s, 18 H) ppm.

^{13}C NMR (75 MHz, CDCl_3) δ 135.5, 134.0, 129.5, 127.6, 60.5, 35.5, 26.8, 19.2 ppm. IR (neat) 3070, 2929, 2856, 1471, 1427, 1104, 1084, 978, 821, 698 cm^{-1} . HRMS (ESI) calcd. for $\text{C}_{35}\text{H}_{45}\text{O}_2\text{Si}_2$ [$\text{M} + \text{H}^+$] 533.2958, found 533.3019.

(+)-*B*-allyldiisopinocampheylborane ((+)-11): A dry 250 mL 3-neck round bottomed flask (fitted with a large magnetic stir bar and a Schlenk filtration unit) was charged with $\text{BH}_3\cdot\text{SMe}_2$ (2 M in Et_2O , 25 mL, 50 mmol). The solution was cooled to 0 $^\circ\text{C}$, and (-)- α -pinene (15.9 mL, 13.6 g, 100 mmol) was added dropwise *via* syringe. The mixture was stirred at 0 $^\circ\text{C}$ for 3 h, during which time a white solid precipitated. Anhydrous THF (10 mL) was then added to the flask, and DMS and Et_2O subsequently removed under vacuum (ca. 20 mm) with vigorous stirring. When a solid white mass remained, the flask was returned to atmospheric pressure by flushing with argon. A further 10 mL THF, and 2.4 mL (2.04 g, 15 mmol) of (-)- α -pinene were then added to the flask, the slurry stirred to homogeneity and then left to stand (without stirring) at 0 $^\circ\text{C}$ for 3 days. MeOH (4 mL, 3.2 g, 100 mmol) was then added at 0 $^\circ\text{C}$ (H_2 gas was evolved). The reaction mixture was then stirred at RT for 1 h, the solvents removed under vacuum (20 mm Hg, 1 h, then 0.2 mm, 2 h), then the flask was returned to atmospheric pressure by flushing with argon. The resulting viscous oil was dissolved in anhydrous Et_2O and cooled to -78 $^\circ\text{C}$ to yield a clear pale yellow solution. Allylmagnesium bromide (2 M in Et_2O , 25 mL, 50 mmol) was then slowly added and the mixture allowed to stir for 15 min at -78 $^\circ\text{C}$. The flask was removed from the cold bath and allowed to warm slowly to RT, and stirred for an additional 30 min after reaching that temperature. White solids began to precipitate soon after warming. Solvents were removed under reduced pressure, and the residues treated with anhydrous pentane (ca. 60 mL). The precipitated magnesium salts were removed by filtration (under argon), and rinsed with a further ca. 40 mL pentane. The solvent was removed under reduced pressure to yield the *B*-allyldiisopinocampheylborane, 14.72 g (90%), which was stored neat in a freezer under argon until required for use. The viscous material was then dissolved in anhydrous Et_2O (165 mL, to give a 0.27 mmol/mL solution), and stored as a solution under argon for a period of weeks without apparent detriment to the subsequent allylation reaction. (-)-11 was prepared in an analogous manner using (+)- α -pinene.

(4-*R*)-6-(*tert*-Butyldiphenylsilyloxy)-4-hydroxy-hex-1-ene ((*R*)-12): A solution of reagent (+)-**11** in Et₂O (0.27 mmol/mL, 4.6 mL, 1.25 mmol) was cooled to -78 °C and aldehyde **10** (280 mg, 0.90 mmol) then slowly added as a solution in anhydrous Et₂O. The mixture was stirred at -78 °C for 45 min, and then quenched by the addition of MeOH (0.7 mL). The reaction mixture was then allowed to warm to RT before the addition of 2M aq. NaOH (0.7 mL) and 30% aq. H₂O₂ (0.6 mL). After stirring for 1 h, the mixture was extracted three times with Et₂O (three times 20 mL). The combined organic fractions were then washed with brine (30 mL), and dried over anhydrous MgSO₄. The solvent was removed under reduced pressure to yield an oil which was purified by flash column chromatography (1:20 EtOAc:petroleum ether) to yield pure (*R*)-**12** as a colourless oil, 161 mg (51%), and a further 65 mg (ca. 20%) of product which was not pure. ¹H NMR, ¹³C NMR, IR, and HRMS data were equivalent to those obtained for the racemic alcohol **12**.

(4-*S*)-6-(*tert*-Butyldiphenylsilyloxy)-4-hydroxy-hex-1-ene ((*S*)-12): Was prepared in an analogous manner to (*R*)-**12** but using reagent (-)-**11**. ¹H NMR, ¹³C NMR, IR, and HRMS data were equivalent to those obtained for racemic **12**.

Note: The following series of reactions to yield aldehydes (*R*)-**13** and (*R*)-**160** from (*R*)-**12**, also applies for the preparation (*S*)-**13** and (*S*)-**160** from (*S*)-**12**. Spectral data for the (*S*)-enantiomers were analogous to those obtained for the (*R*)-enantiomers.

(4-*R*)-6-(*tert*-Butyldiphenylsilyloxy)-4-triethylsilyloxy-hex-1-ene ((*R*)-148): The representative procedure given above for the preparation of **140** and **148** was followed. Hence, (*R*)-**12** (580 mg, 1.64 mmol) was converted into silyl ether (*R*)-**148** (580 mg, 75%). ¹H NMR, ¹³C NMR, IR, and HRMS data were equivalent to those obtained for the racemic silyl ether **148**.

(4-*R*)-6-(*tert*-Butyldiphenylsilyloxy)-4-(methoxymethyloxy)-1-hexene ((*R*)-158): Alcohol (*R*)-**12** (232 mg, 0.65 mmol) and *N,N*-diisopropylethylamine

(230 μ L, 170 mg, 1.31 mmol) were cooled to 0 °C. MOMCl (60 μ L, 64 mg, 0.78 mmol) was then added and the mixture allowed to warm slowly to RT. After stirring at RT overnight, the mixture was quenched with water (10 mL) and diluted with Et₂O (50 mL). The aqueous layer was separated and extracted once with Et₂O (50 mL), and the combined organic fractions then washed with brine (40 mL), dried over anhydrous MgSO₄, and the solvent removed under reduced pressure. Gradient flash column chromatography (1:20-1:10 EtOAc:petroleum ether) gave the methoxymethyl ether (**(R)**-**158**) as a colourless oil, 150 mg (60%). ¹H NMR (300 MHz, CDCl₃) δ 7.71-7.66 (m, 4 H), 7.44-7.36 (m, 6 H), 5.83 (m, 1 H), 5.10 (m, 1 H), 5.06 (m, 1 H), 4.65 (s, 2 H), 3.87 (m, 1 H), 3.78 (m, 2 H), 3.34 (s, 3 H), 2.32 (t, 2 H, *J* = 6.5 Hz), 1.80 (m, 2 H), 1.07 (s, 9 H) ppm. ¹³C NMR (75 MHz, CDCl₃) δ 135.5, 134.6, 133.8, 129.6, 127.6, 117.2, 95.7, 74.0, 60.4, 55.4, 39.2, 37.1, 26.8, 19.1 ppm. IR (neat) 3071, 2930, 2886, 2857, 1640, 1472, 1427, 1152, 1106, 1036, 915, 822, 740, 701 cm⁻¹. HRMS (ESI) calcd. for C₂₄H₃₅O₃Si [M + H⁺] 399.2355, found 399.2343.

Representative procedure for ozonolysis of alkenes 148, 158, and 159 (using the Envirozone V.T-2A ozonolysis machine): Alkene (1 equivalent) was dissolved in CH₂Cl₂ (10 mL/mmol) and anhydrous MeOH (1 mL/mmol) and cooled to -78 °C under argon. Then, ozone was bubbled through the solution for a brief period (see under individual compounds below). The flask was then purged with argon, and PPh₃ (1.5 equivalents) was added. The stirred solution was kept at - 78 °C for 30 min, and then at RT for 1 h. Solvents were then removed under reduced pressure. The residue was purified by flash column chromatography (usually 1:20 EtOAc:petroleum ether), loading the residue onto the column with 1:50 EtOAc:petroleum ether in order to precipitate the by-product, triphenylphosphine oxide (which otherwise elutes on the column close to the desired product). The aldehydes were obtained as clear oils that were reasonably stable (for a period of days) if kept under argon in the freezer.

(3-R)-5-(tert-Butyldiphenylsilyloxy)-3-triethylsilyloxy-pentanal ((R)-13) was prepared from (**(R)**-**148**) (164 mg, 0.35 mmol), with ozone bubbling for 150 seconds, to yield (**(R)**-**13**) (136 mg, 84%). ¹H NMR (300 MHz, CDCl₃) δ 9.80 (t, 1 H, *J* = 2.4 Hz), 7.66 (m, 4 H), 7.42 (m, 6 H), 4.46 (m, 1 H), 3.74 (m, 2 H), 2.54 (m, 2 H), 1.79 (m, 2 H), 1.07 (s, 9 H), 0.94 (t, 9 H, *J* = 8 Hz), 0.60 (q,

6 H, $J = 8$ Hz) ppm. ^{13}C NMR (75 MHz, CDCl_3) δ 202.2, 135.6, 135.5, 133.6, 133.5, 129.7, 129.6, 127.7, 127.6, 65.4, 60.2, 50.9, 40.4, 26.8, 19.1, 6.8, 4.8 ppm. IR (neat) 2953, 1725, 1427, 1238, 1086, 1005, 731, 700 cm^{-1} . HRMS (ESI) calcd. for $\text{C}_{27}\text{H}_{42}\text{O}_3\text{Si}_2\text{Na}$ [$\text{M} + \text{Na}^+$] 493.2565, found 493.2571.

(3-*R*)-5-(*tert*-Butyldiphenylsilyloxy)-3-(methoxymethyloxy)-pentanal ((*R*)-160) was prepared from (*R*)-158 (120 mg, 0.31 mmol), ozone bubbling for 90 seconds, to yield (*R*)-160 (100 mg, 83%). ^1H NMR (300 MHz, CDCl_3) δ 9.77 (t, 1 H, $J = 2.0$ Hz), 7.68-7.62 (m, 4 H), 7.45-7.32 (m, 6 H), 4.67 (d, 1 H, $J = 7.1$ Hz), 4.61 (d, 1 H, $J = 7.1$ Hz), 4.32 (m, 1 H), 3.76 (m, 2 H), 3.30 (s, 3 H), 2.62 (m, 2 H), 1.82 (m, 2 H), 1.05 (s, 9 H) ppm. ^{13}C NMR (75 MHz, CDCl_3) δ 201.4, 135.5, 133.5, 129.7, 127.7, 96.1, 70.7, 60.0, 55.5, 49.0, 37.6, 26.8, 19.1 ppm. HRMS (ESI) calcd. for $\text{C}_{23}\text{H}_{32}\text{O}_4\text{SiNa}$ [$\text{M} + \text{Na}^+$] 423.1968, found 423.1972.

8.3 Experimental for Chapter Three

Dihydro-3-allyloxy-4,4-dimethyl-2(3*H*)-furanone (165): To a solution of pantolactone **25** (10 g, 76.8 mmol) in DMF (80 mL) at 0 °C was slowly added a solution of KO^{*t*}Bu (8.62 g, 76.8 mmol) in THF (80 mL). The solution was stirred at 0 °C for 30 min before the addition, over 40 min, of allyl bromide (6.98 mL, 9.75 g 80.6 mmol) in THF (7 mL). The reaction mixture was warmed to RT and stirred overnight, and then quenched with water (50 mL), extracted with Et₂O (4 x 100 mL). The combined organic extracts were then washed twice with sat. aq. NaHCO₃ solution (100 mL), water (100 mL), and brine (100 mL), dried over MgSO₄ and solvents removed under reduced pressure. Purification by gradient flash column chromatography (1:20 – 1:5 EtOAc:petroleum ether) gave the allyl pantolactone **165** as a colourless oil, 11.62 g (88%). Spectral data matched those reported by Stocker.⁴⁸

2,2-Dimethyl-3-(allyloxy)butane-1,4-diol (166): LAH (3.86 g, 101.85 mmol) was suspended in THF (130 mL) and a solution of allyl pantolactone **165** (11.62 g, 67.9 mmol) in THF (65 mL) was added cautiously dropwise over 20 min. The resulting solution was then refluxed for 3 h before being cooled to 0 °C and being quenched by portionwise addition of hydrated

sodium sulphate and drops of water until effervescence was no longer apparent. Anhydrous MgSO_4 was added, and the mixture diluted with ethanol (200 mL), divided into portions, and filtered through several celite/silica gel plugs with ethanol. The solvents were removed under reduced pressure to yield 10.5 g of crude product which was purified by flash column chromatography (1:1 EtOAc:petroleum ether) to yield 8.73 g (74%) of the diol **166**. Spectral data matched those reported by Stocker.⁴⁸

1,4-Dibenzyloxy-2,2-dimethyl-3-(allyloxy)butane (167): A solution of diol **166** (8.73 g, 50 mmol) in DMF (65 mL) was added to a rapidly stirred solution of NaH (5.4 g, 225 mmol) in DMF (80 mL) at 0 °C. The mixture was stirred at that temperature for 30 min and then benzyl bromide (12.15 mL, 17.47 g, 102 mmol) was added over 30 min. The reaction mixture was then warmed to room temperature and stirred overnight before being quenched with water (200 mL) and extracted three times with Et_2O (three times 200 mL). The combined organic fractions were then washed with sat. aq. NaHCO_3 solution (200 mL), water (100 mL), and brine (150 mL), dried over MgSO_4 and the solvents removed under reduced pressure. ^1H NMR analysis of the crude product revealed the presence of the dibenzyl ether **167** and also the mono-benzylated product, which were readily separated by flash column chromatography (petroleum ether - 1:10 EtOAc:petroleum ether) to yield **167**, 10.1 g (57%) and 5.0 g (38%) of the monobenzylated product. The latter (4.98 g, 18.8 mmol) was resubmitted to the benzylation procedure described above (NaH 1.35 g, 56.4 mmol; DMF 85 mL (total); benzyl bromide 2.34 mL, 19.7 mmol; workup and flash column chromatography as above) to yield 6.42 g (96%) of **167**. The total yield of **167** was therefore 16.52 g (93%). Spectral data matched those reported by Stocker.⁴⁸

1,4-Dibenzyloxy-3,3-dimethylbutan-2-ol (168): To a solution of **167** (5 g, 14 mmol), in THF (75 mL) were added *para*-toluenesulfinic acid as its HCl salt (2.6 g, 16.8 mmol) and $\text{Pd}(\text{PPh}_3)_4$ (1 g, 0.98 mmol). After stirring for 18 h at RT, ^1H NMR analysis of an aliquot showed a significant amount of starting material was still present. A further 2 g of *para*-toluenesulfinic acid as its HCl salt and 1 g of $\text{Pd}(\text{PPh}_3)_4$ from a freshly opened bottle were added and stirring

was continued for a further 24 h. At this point the reaction was judged to be essentially complete by ^1H NMR, and so was quenched by addition of Et_3N (1 mL). Solvents were then removed under reduced pressure and the residues purified by gradient flash column chromatography (1:50 - 1:10 EtOAc:petroleum ether) to yield **168**, 3.23 g (73%). Spectral data matched those reported by Stocker.⁴⁸

1,4-Dibenzyloxy-3,3-dimethylbutan-2-one (7): To a solution of **168** (2.87 g, 9.11 mmol) in CH_2Cl_2 (46 mL) was added PDC (5.14 g, 13.6 mmol), freshly activated 3 Å molecular sieves (7.5 g) and anhydrous AcOH (0.90 mL, 15.8 mmol). The mixture was stirred at RT for 3 h and then filtered through a short celite-silica plug (washing the plug thoroughly with CH_2Cl_2). The filtrate was washed with water and brine and then dried over MgSO_4 , and solvents then removed under reduced pressure. Purification of the crude material by flash column chromatography (1:10 EtOAc:petroleum ether) gave the ketone **7** as a colourless oil, 2.34 g (82%). Spectral data matched those reported by Stocker.⁴⁸

(Z)-1,4-Dibenzyloxy-3,3-dimethyl-2-(trimethylsilyloxy)-1-butene

(169): A stirred solution of diisopropylamine (395 μL , 2.79 mmol) in THF (5 mL) was cooled to 0 °C and *n*-BuLi (1.74 mL of a 1.6 M solution in hexane, 2.79 mmol) then added. The mixture was stirred at 0 °C for 20 min and then cooled to -78 °C, at which temperature **7** (580 mg, 1.86 mmol) was added as a solution in THF (5 mL). Stirring was continued at -78 °C for 30 min during which time the solution developed a bright yellow colour. TMSCl (375 μL , 321 mg, 2.79 mmol) was added and the mixture was stirred at -78 °C for 30 min and then warmed to RT for 1 h. The reaction was quenched by the addition of water (2 mL) and then extracted 3 times with hexanes (three times 10 mL). The combined organic fractions were washed with water (5 mL) and brine (10 mL), dried over MgSO_4 , and the solvents removed under reduced pressure. Only one isomer was detectable in the ^1H NMR of the crude product, determined to be the *Z*- isomer by NOE experiments (see discussion in chapter three). Purification by flash column chromatography (1:50 EtOAc:petroleum ether, neutralised with a few drops of Et_3N) gave the silyl enol ether **169** as a colourless oil, 680 mg (95%). ^1H NMR (300 MHz, CDCl_3) δ 7.35-7.25 (m, 10 H), 5.67 (s, 1 H), 4.70 (s,

2 H), 4.51 (s, 2 H), 3.26 (s, 2 H), 1.02 (s, 6 H), 0.12 (s, 9 H) ppm. ^{13}C NMR (75 MHz, CDCl_3) δ 140.5, 139.0, 137.5, 128.3, 128.2, 127.9, 127.7, 127.4, 127.2, 76.7, 73.7, 73.1, 38.8, 23.0, 0.7 ppm. IR (neat) 2958, 2863, 1679, 1496, 1247, 1205, 1098, 1027, 843, 731 cm^{-1} .

1,4-Di(methoxymethyl)oxy-3,3-dimethylbutan-2-one (188), was prepared by Dr John Hoberg by an analogous synthesis (using MOMCl in place of BnCl) to that used for the preparation of ketone 7: ^1H NMR (300 MHz, CDCl_3) δ 4.68 (s, 2 H), 4.58 (s, 2 H), 4.52 (s, 2 H), 3.51 (s, 2 H), 3.38 (s, 3 H), 3.33 (s, 3 H), 1.18 (s, 6 H) ppm. ^{13}C NMR (75 MHz, CDCl_3) δ 209.8, 96.6, 96.3, 74.4, 69.1, 55.6, 55.4, 46.9, 21.7 (2 C) ppm. IR (neat) 2933, 1723, 1466, 1149, 1111, 1048, 912, 730 cm^{-1} . HRMS (ESI) calcd. for $\text{C}_{10}\text{H}_{24}\text{O}_5\text{N}$ [$\text{M} + \text{NH}_4^+$] 238.1649, found 238.1661.

(1S*, 2R*)-2,5-Di(benzyloxy)-4,4-dimethyl-1-hydroxy-1-phenyl-3-pentanone ((±)-170a) and **(1S*, 2S*)-2,5-Di(benzyloxy)-4,4-dimethyl-1-hydroxy-1-phenyl-3-pentanone ((±)-170b)** were prepared by the following methods A-F:

A. LDA. A stirred solution of diisopropylamine (40 μL , 29 mg, 0.30 mmol) in THF (1 mL) was cooled to -78°C and *n*-BuLi (150 μL of a 1.6 M solution in hexane, 0.30 mmol) then added. The mixture was stirred at -78°C for 15 min and then **7** (80 mg, 0.25 mmol) was added as a solution in THF (ca. 1 mL). Stirring was continued at -78°C for 50 min during which time the solution developed a bright yellow colour. Then, benzaldehyde (60 μL , 63 mg, 0.50 mmol) was added. After 70 minutes stirring at -78°C , although TLC analysis did not indicate complete conversion, it appeared that by-products were beginning to form and so the reaction was quenched by the addition of aq. NH_4Cl and diluted with Et_2O (20 mL). The phases were separated and the aqueous phase extracted a further two times with Et_2O (two times 10 mL). The combined organic fractions were then washed with water (10 mL) and brine (10 mL), dried over MgSO_4 , and the solvents removed under reduced pressure. Purification of the crude material by flash column chromatography (1:10 – 1:5

EtOAc:petroleum ether) gave a mixture of (\pm)-**170a** and (\pm)-**170b** as a colourless oil, 68 mg (65%), *syn:anti* ratio 14:1.

B. LiTMP. A stirred solution of LiTMP (101 μ L, 0.60 mmol) in THF (1.5 mL) was cooled to -78 $^{\circ}$ C and *n*-BuLi (300 μ L of a 2 M solution in hexane, 0.60 mmol) then added. The mixture was stirred at -78 $^{\circ}$ C for 15 min and then **7** (170 mg, 0.54 mmol) was added as a solution in THF (ca. 1 mL). Stirring was continued at -78 $^{\circ}$ C for 1 h during which time the solution developed a bright yellow colour. Then, benzaldehyde (110 μ L, 115 mg, 1.08 mmol) was added. After 90 minutes stirring at -78 $^{\circ}$ C, the reaction was quenched by the addition of aq. NH_4Cl (10 mL) and diluted with Et_2O (20 mL). The phases were separated and the aqueous phase extracted a further two times with Et_2O (two times 10 mL). The combined organic fractions were then washed with water (10 mL) and brine (10 mL), dried over MgSO_4 , and the solvents removed under reduced pressure. Purification of the crude material by gradient flash column chromatography (1:10 – 1:5 EtOAc:petroleum ether) gave a mixture of (\pm)-**170a** and (\pm)-**170b** as a colourless oil, 125 mg (55%), *syn:anti* ratio 13:1.

C. Cy_2BOTf . A solution of **7** (210 mg, 0.67 mmol) and Et_3N (224 μ L, 1.61 mmol) in CH_2Cl_2 (3.5 mL) was cooled to -78 $^{\circ}$ C. A solution of Cy_2BOTf in hexane (3 mL of a 0.5 M solution, 1.48 mmol) was then slowly added. The resultant solution was stirred at -78 $^{\circ}$ C for 30 min before the addition of benzaldehyde (81 μ L, 85 mg, 0.80 mmol). After stirring at -78 $^{\circ}$ C for 30 min, the solution was warmed to RT and stirred for a further h before being quenched by the addition of pH 7 buffer solution (2 mL), 30% aq. H_2O_2 (2 mL) and MeOH (2.5 mL). The mixture was stirred at RT overnight, after which time water (15 mL) was added and the solution then extracted three times with CH_2Cl_2 (three times 20 mL). The combined organic fractions were then washed with water (20 mL) and brine (20 mL), dried over MgSO_4 , and the solvents removed under reduced pressure. Purification of the crude material by gradient flash column chromatography (1:10 – 1:5 EtOAc:petroleum ether) gave a mixture of (\pm)-**170a** and (\pm)-**170b** as a colourless oil, 168 mg (60%), *syn:anti* ratio > 20:1. Several columns were required to free the product from the cyclohexanol by-product, which has an R_f very close to that of **170**.

D. LDA then Ti(OiPr)₄. A stirred solution of diisopropylamine (90 μ L, 0.62 mmol) in THF (1 mL) was cooled to 0 °C and *n*-BuLi (375 μ L of a 1.6 M solution in hexane, 0.60 mmol) then added. The mixture was stirred at 0 °C for 10 min and then cooled to –78 °C, at which temperature **7** (170 mg, 0.54 mmol) was added as a solution in THF (ca. 1 mL). Stirring was continued at –78 °C for 30 min and then freshly distilled Ti(OiPr)₄ (180 μ L, 173 mg, 0.60 mmol) was added. The temperature was increased to –40 °C for 30 min. Then, benzaldehyde (82 μ L, 86 mg, 0.81 mmol) was added and the solution allowed to warm slowly to RT over 2.5 h. The reaction was quenched by the addition of aq. NH₄Cl (2 mL) and diluted with Et₂O (10 mL). The phases were separated and the aqueous phase extracted two times with Et₂O (two times 10 mL). The combined organic fractions were then washed with water (5 mL) and brine (10 mL), dried over MgSO₄, and the solvents removed under reduced pressure. Purification of the crude material by gradient flash column chromatography (1:20 – 1:10 EtOAc:petroleum ether) gave a mixture of (\pm)-**170a** and (\pm)-**170b** as a colourless oil, 132 mg (59%), *syn:anti* ratio 4:1.

E. Cy₂BCl. A solution of Cy₂BCl (230 mg, 0.93 mmol) in Et₂O (5 mL) was cooled to 0 °C and then treated with Et₃N (138 μ L, 100 mg, 0.99 mmol), followed by addition of a solution of the ketone **7** (192 mg, 0.62 mmol) in Et₂O (2 mL). The mixture was stirred for 20 min at 0 °C, after which time the white suspension was cooled to –78 °C. Benzaldehyde (126 μ L, 132 mg, 1.24 mmol) was then added and the mixture stirred at –78 °C for 5 h. The reaction was then quenched by the addition of 2 mL of a 6:1 mixture of MeOH : pH 7 buffer solution, and then 30% aq. H₂O₂ (0.6 mL). The mixture was stirred at RT overnight, and then water (10 mL) was added and the solution extracted 3 times with Et₂O (three times 20 mL). The combined organic fractions were then washed with water (20 mL) and brine (20 mL), dried over MgSO₄, and the solvents removed under reduced pressure. Purification of the crude material by gradient flash column chromatography (1:10 – 1:5 EtOAc:petroleum ether) and removal of the last traces of the cyclohexanol by-product using a hi-vacuum pump gave a mixture of (\pm)-**170a** and (\pm)-**170b** as a colourless oil, 110 mg (42%), *syn:anti* ratio 1:4.

F. TiCl₄. To a solution of benzaldehyde (52 μ L, 54 mg, 0.51 mmol) in CH₂Cl₂ (1 mL) at -78 °C was added freshly distilled TiCl₄ (56 μ L, 97 mg, 0.51 mmol). The resultant mobile slurry was stirred for 10 min before the addition of enol silane **169** (197 mg, 0.51 mmol) as a solution in CH₂Cl₂ (1 mL). The reaction was then stirred at -78 °C for 1 h, at which time TLC analysis showed that no more **169** was present. The reaction was then quenched by the addition of aq. NH₄Cl (5 mL) and diluted with CH₂Cl₂ (10 mL). The phases were separated and the aqueous phase extracted a further two times with CH₂Cl₂ (two times 10 mL). The combined organic fractions were then washed with water (5 mL) and brine (5 mL), dried over MgSO₄, and the solvents removed under reduced pressure. Purification by flash column chromatography (1:10 – 1:5 EtOAc:petroleum ether) gave a mixture of (\pm)-**170a** and (\pm)-**170b** as a colourless oil, 70 mg (33%), *syn:anti* ratio 1:3, plus 95 mg (60% recovery) of the ketone **7**.

(1S*, 2R*)-2,5-Di(benzyloxy)-4,4-dimethyl-1-hydroxy-1-phenyl-3-pentanone ((\pm)-170a): ¹H NMR (300 MHz, CDCl₃) δ 7.35-7.22 and 7.08-7.02 (m, 10 H), 5.06 (dd, 1 H, *J* = 4.2, 5.4 Hz), 4.58 (d, 1 H, *J* = 4.2 Hz), 4.51 (d, 1 H, *J* = 11.7 Hz), 4.46 (s, 2 H), 4.23 (d, 1 H, *J* = 11.7 Hz), 3.47 (d, 1 H, *J* = 8.8 Hz), 3.40 (d, 1 H, *J* = 8.8 Hz), 3.22 (d, 1 H, *J* = 5.4 Hz, *OH*), 1.10 (s, 3 H), 1.04 (s, 3 H) ppm. ¹³C NMR (75 MHz, CDCl₃) δ 213.1, 140.4, 138.0, 137.6, 128.7, 128.6, 128.5 (2 C), 128.3, 128.1, 128.0, 127.5, 127.0, 83.3, 77.5, 73.8, 73.5, 72.4, 48.7, 22.2, 22.1 ppm. IR (neat) 3444, 2859, 1701, 1495, 1360, 1095, 1027, 910, 697 cm⁻¹. HRMS (ESI) calcd. for C₂₇H₃₀O₄Na [M + Na⁺] 441.2036, found 441.2041.

(1S*, 2S*)-2,5-Di(benzyloxy)-4,4-dimethyl-1-hydroxy-1-phenyl-3-pentanone ((\pm)-170b): ¹H NMR (300 MHz, CDCl₃) δ 7.40-7.20 and 7.01-6.85 (m, 10 H), 4.97 (d, 1 H, *J* = 7.3 Hz), 4.48 (s, 2 H), 4.43 (d, 1 H, *J* = 7.3 Hz), 4.29 (d, 1 H, *J* = 11.5 Hz), 4.07 (d, 1 H, *J* = 11.5 Hz), 3.49 (d, 2 H, *J* = 1.0 Hz), 1.15 (s, 3 H), 1.14 (s, 3 H) ppm. ¹³C NMR (75 MHz, CDCl₃) δ 214.9, 140.9, 137.5, 137.2, 128.4, 128.2, 128.0, 127.8 (2 C), 127.7, 127.2, 82.3, 77.4, 74.6, 73.5, 72.3, 48.7, 22.1, 22.0 ppm. IR (neat) 3445, 3063, 3031, 2860, 1703, 1602, 1495, 1362,

1205, 1093, 1026, 909, 712, 695 cm^{-1} . HRMS (ESI) calcd. for $\text{C}_{27}\text{H}_{30}\text{O}_4\text{Na}$ $[\text{M} + \text{Na}^+]$ 441.2036, found 441.2047.

Representative procedure for LDA aldol reactions between ketone 7 or 188 and aldehydes 13, 140, or 160: A stirred solution of diisopropylamine (1.1 eq) in THF (3 mL per mmol of ketone) was cooled to $-78\text{ }^\circ\text{C}$ and *n*-BuLi (2 M solution in hexane, 1.1 eq) then added. The mixture was stirred at $-78\text{ }^\circ\text{C}$ for 5 min, at $0\text{ }^\circ\text{C}$ for 15 min, and then cooled back to $-78\text{ }^\circ\text{C}$ before addition of the ketone (1 eq.) as a solution in THF (ca. 1 mL per mmol). Stirring was continued at $-78\text{ }^\circ\text{C}$ for 50 min, during which time the solution developed a bright yellow colour. Then the aldehyde (0.5-1.5 eq.) was added as a solution in THF (ca. 1 mL per mmol). After 60 minutes stirring at $-78\text{ }^\circ\text{C}$, the reaction was quenched by the addition of aq. NH_4Cl and diluted with Et_2O . The phases were separated and the aqueous phase extracted a further two times with Et_2O . The combined organic fractions were then washed with water and brine, dried over MgSO_4 , and the solvents removed under reduced pressure. Products were purified by column chromatography using the solvent systems indicated.

(4*S,5*R**)-1,4-Di(benzyloxy)-9-(*tert*-butyldiphenylsilyloxy)-5-hydroxy-7-(triethylsilyloxy)-2,2-dimethyl-nonan-3-one (28c/28d):** An aldol reaction was performed using the representative aldol procedure, between ketone 7 (150 mg, 0.48 mmol) and aldehyde (\pm)-13 (180 mg, 0.38 mmol). Purification of the crude material by flash column chromatography (1:10 EtOAc:petroleum ether) gave an unidentified diastereomer of 28 (28c or 28d) as a colourless oil, 60 mg (20%). Only one diastereomer was isolated, but retrospective inspection of the crude ^1H NMR suggested that other diastereomers had also been formed (the other diastereomers were not isolated cleanly and, due to the inexperience of the author at the time, inadvertently discarded!). Also isolated were the elimination product 176, 30 mg (23%), and unreacted 13 20 mg (11%). Data for the isolated diastereomer of 28: ^1H NMR (300 MHz, CDCl_3) δ 7.67 (m, 4 H), 7.42-7.20 (m, 16 H), 4.60 (d, 1 H, $J = 11.7\text{ Hz}$), 4.47 (s, 2 H), 4.31 (m, 1 H), 4.26 (d, 1 H, $J = 11.7\text{ Hz}$), 4.20 (m, 2 H), 3.69 (m, 2 H), 3.57 (d, 1 H, $J = 9.0\text{ Hz}$), 3.47 (d, 1 H, $J = 9.0\text{ Hz}$), 2.72 (broad s, 1 H), 1.90-1.65 (m, 3 H), 1.43 (m, 1 H), 1.23 (s, 3 H), 1.19 (s, 3 H), 1.05 (s, 9 H), 0.93 (t, 9 H, $J = 7.9\text{ Hz}$), 0.59 (q, 6 H, $J = 7.9\text{ Hz}$)

ppm. ^{13}C NMR (75 MHz, CDCl_3) δ 213.0, 138.2, 138.0, 135.8, 134.1, 134.0, 129.9, 129.8, 128.6, 128.5, 128.3, 127.8, 127.9, 83.0, 78.3, 73.7, 72.1, 68.1, 67.2, 60.8, 48.3, 40.8, 40.7, 27.1, 22.6, 22.4, 19.4, 7.2, 5.2 ppm. HRMS (ESI) calcd. for $\text{C}_{47}\text{H}_{67}\text{O}_6\text{Si}$ [$\text{M} + \text{H}^+$] 783.4471, found 783.4503.

Data for 5-(*tert*-Butyldiphenylsilyloxy)-pent-2-en-1-al (176): ^1H NMR (300 MHz, CDCl_3) δ 9.48 (d, 1 H, $J = 8.1$ Hz), 7.65 (m, 4 H), 7.40 (m, 6 H), 6.85 (dt, 1 H, $J = 15.6, 6.9$ Hz), 6.15 (m, 1 H), 3.83 (t, 2 H, $J = 6.1$ Hz), 2.55 (m, 2 H), 1.05 (s, 9 H) ppm. ^{13}C NMR (75 MHz, CDCl_3) δ 194.1, 155.6, 135.5, 134.4, 133.4, 129.8, 127.7, 61.9, 35.9, 26.8, 19.2 ppm. IR (neat) 1691, 1471, 1427, 1389, 1104, 1007, 822, 733, 700 cm^{-1} . HRMS (ESI) calcd. for $\text{C}_{21}\text{H}_{30}\text{NO}_2\text{Si}$ [$\text{M} + \text{NH}_4^+$] 356.2046, found 356.2072.

(4*S,5*R**)-1,4-Di(benzyloxy)-9-(*tert*-butyldiphenylsilyloxy)-5,7-di(hydroxy)-2,2-dimethyl-nonan-3-one (181):** A solution of **28** (one diastereomer, 50 mg, 0.06 mmol) in MeOH (2 mL) was cooled to 0 °C and catalytic *p*TsOH (5 mg, 0.02 mmol) was then added. The mixture was stirred for 20 min at 0 °C and then solid NaHCO_3 (50 mg, 0.60 mmol) was added. The mixture was concentrated under reduced pressure and the residue purified by column chromatography (1:10-1:1 EtOAc:petroleum ether) to yield the diol **181** (32 mg, 82%). ^1H NMR (300 MHz, CDCl_3) δ 7.66-7.22 (m, 20 H), 4.64 (d, 1 H, $J = 11.7$ Hz), 4.49 (s, 2 H), 4.47 (d, 1 H, $J = 3.2$ Hz), 4.28 (d, 1 H, $J = 11.7$ Hz), 4.24 (m, 1 H), 3.83 (m, 2 H), 3.68 (m, 1 H), 3.49 (d, 1 H, $J = 8.8$ Hz), 3.54 (d, 1 H, $J = 8.8$ Hz), 3.24 (broad s, 1 H), 2.95 (broad s, 1 H), 1.86-1.46 (m, 4 H), 1.27 (s, 3 H), 1.22 (s, 3 H), 1.06 (s, 9 H) ppm. ^{13}C NMR (75 MHz, CDCl_3) δ 213.4, 135.8, 135.7, 130.1, 128.7, 128.6, 128.4, 128.1 (2 C), 128.0, 127.9, 81.6, 78.1, 73.7, 72.1, 71.3, 71.2, 63.3, 48.5, 40.1, 38.9, 27.0, 22.7, 22.5, 19.3 ppm. HRMS (ESI) calcd. for $\text{C}_{41}\text{H}_{52}\text{NaO}_6\text{Si}$ [$\text{M} + \text{Na}^+$] 691.3425, found 691.3453.

(4*S,5*R**,7*S*)-1,4-Di(benzyloxy)-9-(*tert*-butyldiphenylsilyloxy)-5-hydroxy-7-(methoxymethyloxy)-2,2-dimethyl-nonan-3-one (178a/b):** An aldol reaction was performed using the representative aldol procedure above, between ketone **7** (110 mg, 0.35 mmol) and aldehyde (*S*)-**160** (50 mg, 0.12 mmol). Purification of the crude material by flash column chromatography (1:10-1:5 EtOAc:petroleum ether) gave the title compound (R_f 0.35, 1:5

EtOAc:petroleum ether), as a 1:1 mixture of two diastereomeric *syn*- aldol products, as a colourless oil, 50 mg (56%). Data for the mixed diastereomers: ¹H NMR (300 MHz, CDCl₃) δ 7.70 (m, 8 H), 7.45-7.22 (m, 32 H), 4.66-4.56 (m, 6 H), 4.48 (s, 2 H), 4.47 (s, 2 H), 4.39 (d, 1 H, *J* = 3.2 Hz), 4.34 (d, 1 H, *J* = 2.7 Hz), 4.30 (d, 1 H, *J* = 4.4 Hz), 4.26 (d, 1 H, *J* = 4.6 Hz), 4.23 (m, 1 H), 4.14 (m, 1 H), 4.01 (m, 1 H), 3.90 (m, 1 H), 3.75 (m, 4 H), 3.60-3.48 (m, 4 H), 3.31 (s, 3 H), 3.30 (s, 3 H), 2.83 (d, 1 H, *J* = 6.6 Hz, *OH*), 2.72 (d, 1 H, *J* = 7.1 Hz, *OH*), 1.90-1.70 (m, 7 H), 1.54 (m, 1 H), 1.26 (s, 3 H), 1.24 (s, 3 H), 1.21 (s, 6 H), 1.07 (s, 18 H) ppm. ¹³C NMR (75 MHz, CDCl₃) δ 213.1, 212.8, 138.1, 137.9, 135.8, 134.1, 134.0, 129.9, 128.7, 128.6, 128.3, 128.2, 128.1, 128.0, 127.9, 96.9, 95.9, 82.9, 82.3, 78.2, 78.1, 73.8, 73.7, 73.6, 72.2, 72.1, 69.4, 67.9, 60.7, 60.6, 55.9, 55.8, 48.4, 48.3, 39.7, 38.7, 38.4, 37.7, 27.1, 22.6 (2 C),ⁱⁱⁱ 22.5, 22.4, 19.4 ppm. HRMS (ESI) calcd. for C₄₃H₅₇O₇Si [M + H⁺] 713.3874, found 713.3871.

(7*S*)-1,4-Di(benzyloxy)-7,9-di(*tert*-butyldiphenylsilyloxy)-2,2-dimethyl-non-4-en-3-one (179): A stirred solution of diisopropylamine (65 μL, 47 mg, 0.46 mmol) in THF (1 mL) was cooled to 0 °C and *n*-BuLi (275 μL of a 1.6 M solution in hexane, 0.44 mmol) then added. The mixture was stirred at 0 °C for 10 min and then cooled to –78 °C, at which temperature ketone **7** (125 mg, 0.40 mmol) was added as a solution in THF (ca. 1 mL). Stirring was continued at –78 °C for 30 min and then freshly distilled Ti(O*i*Pr)₄ (130 μL, 125 mg, 0.44 mmol) was added. The temperature was increased to –40 °C for 30 min. Then, aldehyde (**S**)-**161** (160 mg, 0.27 mmol) was added and the solution warmed slowly to RT over 2.5 h. The reaction was quenched by the addition of aq. NH₄Cl (2 mL) and diluted with Et₂O (10 mL). The phases were separated and the aqueous phase extracted with Et₂O (two times 10 mL). The combined organic fractions were then washed with water (5 mL) and brine (10 mL), dried over MgSO₄, and the solvents removed under reduced pressure. Purification of the crude material by flash column chromatography (1:20 – 1:10 EtOAc:petroleum ether) gave the eliminated aldol product **179** (98 mg, 40%), along with ketone **7**

ⁱⁱⁱ The signal at 22.6 ppm is attributed to the overlapping *gem*-dimethyl groups of one diastereomer of **178**, whereas for the other diastereomer the *gem*-dimethyl groups are not equivalent and their signals appear at 22.5 and 22.4 ppm. Overlapping peaks also occur for the TBDPS and Bn groups of the two diastereomers of **178**; however these are not noted in the peak listing.

(70 mg, 56%) and the eliminated aldehyde **176** (45 mg, 50%). Data for **179**: ^1H NMR (300 MHz, CDCl_3) δ 7.65-7.20 (m, 30 H), 5.92 (t, 1 H, $J = 9$ Hz), 4.55 (s, 2 H), 4.41 (s, 2 H), 4.10 (m, 1 H), 3.62 (m, 2 H), 3.53 (s, 2 H), 2.32 (m, 2 H), 1.78 (m, 1 H), 1.61 (m, 1 H), 1.19 (s, 6 H), 0.99 (s, 9 H), 0.93 (s, 9 H) ppm. HRMS (ESI) calcd. for $\text{C}_{57}\text{H}_{69}\text{O}_2\text{Si}_2$ $[\text{M} + \text{H}^+]$ 782.4187, found 782.4182.

(4*S,5*R**,7*S*)-1,4,7-Tri(methoxymethoxy)-9-(*tert*-butyldiphenylsilyloxy)-5-acetyloxy-2,2-dimethyl-nonan-3-one (190a and 190b)**: An aldol reaction between ketone **7** (60 mg, 0.24 mmol) and aldehyde (*S*)-**160** (65 mg, 0.16 mmol) was performed using the representative LDA aldol procedure above. The crude aldol product was purified by column chromatography (1:3-1:1 EtOAc:petroleum ether) to yield 38 mg (0.06 mmol, 38%) of **189** as a mixture of diastereomers. The mixture was dissolved in pyridine (0.2 mL) and acetic anhydride (0.2 mL) was then added at 0 °C. The solution was warmed to RT and stirred overnight, and then quenched with water (5 mL). The mixture was extracted with diethyl ether (two times 20 mL), and the combined organic portions then washed with brine (5 mL), dried over anhydrous MgSO_4 , and evaporated under reduced pressure. Column chromatography (1:10-1:3 EtOAc:petroleum ether) allowed the separation of two diastereomers of **190**, the first eluting (in 1:3 EtOAc:petroleum ether) at R_f 0.31 (17 mg, 43%). ^1H NMR (300 MHz, CDCl_3) δ 7.68 (m, 4 H), 7.40 (m, 6 H), 5.49 (m, 1 H), 4.68 (m, 1 H), 4.62-4.49 (m, 6 H), 3.75 (m, 3 H), 3.51 (s, 2 H), 3.34 (s, 3 H), 3.31 (s, 3 H), 3.30 (s, 3 H), 2.18-1.62 (m, 4 H), 2.03 (s, 3 H), 1.28 (s, 3 H), 1.19 (s, 3 H), 1.04 (s, 9 H) ppm. ^{13}C NMR (75 MHz, CDCl_3) δ 210.5, 170.7, 135.5 (4 C), 133.6 (2 C), 129.6 (2 C), 127.7 (4 C), 96.6, 96.4, 95.9, 77.6, 74.6, 72.1, 69.3, 60.1, 56.0, 55.8, 55.3, 48.1, 38.0, 37.3, 26.7 (3 C), 21.5, 21.4, 20.9, 19.1 ppm. IR (neat) 2931, 2889, 1739, 1715, 1472, 1371, 1238, 1150, 1108, 1034, 918, 734, 703 cm^{-1} . The second diastereomer, eluting at R_f 0.25 (15 mg, 37%). ^1H NMR (300 MHz, CDCl_3) δ 7.64 (m, 4 H), 7.39 (m, 6 H), 5.46 (dt, 1 H, $J = 2.2, 6.5$ Hz), 4.73 (d, 1 H, $J = 2.2$ Hz), 4.63-4.50 (m, 6 H), 3.85 (m, 1 H), 3.74 (m, 2 H), 3.51 (s, 2 H), 3.33 (s, 3 H), 3.32 (s, 3 H), 3.31 (s, 3 H), 2.18-1.92 (m, 2 H), 2.02 (s, 3 H), 1.88-1.65 (m, 2 H), 1.27 (s, 3 H), 1.19 (s, 3 H), 1.04 (s, 9 H) ppm. ^{13}C NMR (75 MHz, CDCl_3) δ 210.4, 170.3, 135.5 (4 C), 133.7 (2 C), 129.6 (2 C), 127.7 (4 C), 96.6, 96.1, 95.8, 77.2, 74.7, 71.9, 69.2, 60.1, 56.2, 55.6, 55.3, 48.1, 37.2, 36.1, 26.8 (3

C), 21.6 (2 C), 21.0, 19.1 ppm. IR (neat) 2931, 2888, 1738, 1715, 1472, 1237, 1149, 1108, 1030, 916, 733, 702 cm^{-1} . HRMS (ESI) calcd. for $\text{C}_{35}\text{H}_{58}\text{NO}_{10}\text{Si}$ [$\text{M} + \text{NH}^+$] 680.3830, found 680.3800.

(S)-6-(4-(*Tert*-butyldiphenylsilyloxy)-2-hydroxybutyl)-3,3-dimethyl-2,3-dihydropyran-4-one (194): A solution of **190** (one diastereomer, 14 mg, 0.02 mmol) in 0.2 mL of 0.5% (v/v) H_2SO_4 in AcOH was stirred for 30 minutes at RT. The solution was diluted with toluene and solid NaHCO_3 (50 mg) was added and stirred for 15 minutes. Then the solvents were removed under reduced pressure and the residue subjected to column chromatography (1:10-1:3 EtOAc:petroleum ether) to yield 3 mg (35%) of **194**. IR (neat) 3450, 2958, 2929, 1767, 1436, 1428, 1111, 1006, 740, 702 cm^{-1} . HRMS (ESI) calcd. for $\text{C}_{27}\text{H}_{37}\text{O}_4\text{Si}$ [$\text{M} + \text{H}^+$] 453.2461, found 453.2465.

Experimental for Chapter Five

Cyclohexanone dimethyl acetal (275): A solution of cyclohexanone (20 mL, 18.9 g, 193 mmol), $\text{HC}(\text{OMe})_3$ (52 mL, 466 mmol), and $\text{pTsOH} \cdot \text{H}_2\text{O}$ (670 mg, 3.22 mmol) in MeOH (50 mL) was stirred at RT overnight, after which time ^1H NMR analysis showed > 95% conversion to the acetal product. The reaction was then diluted with Et_2O (200 mL), and quenched with 5% NaHCO_3 . The layers were separated and the aqueous portion extracted once with Et_2O (200 mL), then the combined organic fractions were washed with water and brine (100 mL each), dried with anhydrous MgSO_4 , and the solvents and by-products removed in-vacuo to yield a pale yellow liquid. This crude product was distilled under vacuum (approximately 20 mbar, 35 $^\circ\text{C}$) to yield 27 mL (27.8 g, 92%) of the product **275** as a clear colourless liquid, used directly in the next reaction.

1L-1,2:3,4-di-*O*-cyclohexylidene-5-*O*-methyl-*chiro*-inositol (274) and 1L-1,2-*O*-cyclohexylidene-5-*O*-methyl-*chiro*-inositol (276): To a stirred suspension of quebrachitol (50 g, 0.25 mol) in DMF (400 mL) and dimethoxycyclohexane (320 mL, 2.06 mol), under argon, was added $\text{pTsOH} \cdot \text{H}_2\text{O}$ (8.0 g, 0.04 mol) at room temperature. The mixture was then heated to 85 $^\circ\text{C}$ and

stirred for 18 h, after which time ^1H NMR analysis of an aliquot of the reaction mixture showed a 70:30 ratio of **274** to **276**. Heating to 105°C for 4.5 h increased this to a steady 75:25 ratio. The reaction was then cooled, treated with Et_3N (7 mL; 0.05 mol), and diluted with EtOAc (1 L). The solution was washed with three times 500 mL H_2O , and the combined H_2O washings were extracted with ether (two times 300 mL). The combined organic fractions were washed with brine (100 mL), dried with anhydrous MgSO_4 , and the solvents removed in-vacuo to yield a yellow solid, which was recrystallised from petroleum ether (ca. 500 mL) to yield **274** as white crystals (45.5 g, 50%). Two further crystallisations from petroleum ether gave a total yield of 64.8 g (71%). m.p. 117-119 °C, lit.¹³⁰ 117-119 °C. $[\alpha]_{\text{D}} = -18$ (c 0.1, CH_2Cl_2), lit.¹³⁰ -18 (c 0.1, CH_2Cl_2). ^1H NMR (300 MHz, CDCl_3) δ 3.80-4.24 (m, 3 H), 3.71-3.56 (m, 3 H), 3.56 (s, 3 H), 2.80 (broad s, 1 H) 1.76-1.32 (m, 20 H) ppm. ^{13}C NMR (75 MHz, CDCl_3) δ 112.7, 110.6, 79.3, 79.0, 78.3, 76.4, 75.9, 69.5, 58.2, 38.0, 36.7, 34.9, 25.2, 24.1, 23.9, 23.8, 23.7 ppm. IR (neat) 3499, 2940, 1468, 1336, 1098, 1040, 973, 902, 769, 648 cm^{-1} . HRMS (ESI) calcd. for $\text{C}_{19}\text{H}_{31}\text{O}_6$ $[\text{M} + \text{H}^+]$ 355.2115, found 355.2106.

The aqueous washings from the extraction of **274** were reduced under high vacuum to yield 34 g of an orange oil, which was dissolved in a minimum amount of H_2O and then extracted with EtOAc (three times 200 mL). The combined EtOAc portions were dried with anhydrous MgSO_4 , and the solvent volume reduced under vacuum (water aspirator) to ca. 35 mL. Standing overnight gave one crop of crystals which were washed with petroleum ether to yield **276** as pale yellow crystals, 6.6 g (9%). ^1H NMR (300 MHz, CDCl_3) δ 4.4 (dd, 1 H, $J = 3.0, 3.2$ Hz), 4.3 (dd, 1 H, $J = 5.4, 2.9$ Hz), 4.16 (dd, 1 H, $J = 7.3, 5.9$ Hz), 3.75 (dd, 1 H, $J = 9.0, 8.8$ Hz), 3.63 (dd, 1 H, $J = 9.6, 7.6$ Hz), 3.38 (dd, 1 H, $J = 8.8, 3.2$ Hz), 3.53 (s, 3 H), 2.70 (broad s, 3 H), 1.72-1.32 (m, 10 H) ppm. ^{13}C NMR (75 MHz, CDCl_3) δ 110.3, 81.8, 78.3, 76.5, 76.3, 70.7, 66.6, 58.4, 38.1, 35.1, 25.2, 24.2, 23.9 ppm. IR (neat) 3498, 2935, 2861, 1276, 1148, 1098, 1040, 940, 647 cm^{-1} . HRMS (ESI) calcd. for $\text{C}_{13}\text{H}_{23}\text{O}_6$ $[\text{M} + \text{H}^+]$ 275.1495, found 275.1499.

1L-1,2:3,4-Di-*O*-cyclohexylidene-*chiro*-inositol (282): Dicyclohexylidene quebrachitol (**274**, 1.00 g, 2.82 mmol) was dissolved in anhydrous MeCN (25 mL) and cooled to 0°C. Pyridine (2.3 mL, 28.2 mmol), *n*-Bu₄NI (7.0 g, 19.0 mmol) and AlCl₃ (3.8 g, 28.2 mmol) were then added in that order. The mixture was heated to 62°C overnight, cooled to RT, quenched by careful addition of water (60 mL) and extracted with CH₂Cl₂ (three times 60 mL). The organic fractions were combined and washed with brine, dried over MgSO₄ and the solvents removed under reduced pressure to yield a white solid which was subsequently re-dissolved in a minimum amount of CH₂Cl₂. Diethyl ether (ca. 100 mL) was added to the solution and the resulting white precipitate removed by vacuum filtration. The filtrate was reduced in-vacuo to yield an oil which was purified by flash chromatography (EtOAc:petroleum ether, 1:10 – 1:3) to give 624 mg (65%) of **282** as a white solid. ¹H NMR (300 MHz, CDCl₃) δ 4.39 (m, 2 H), 4.19 (m, 1 H), 4.13 (m, 1 H), 3.78 – 3.63 (m, 2 H), 2.77 (d, 1 H, *J* = 2.9 Hz), 2.73 (d, 1 H, *J* = 2.4 Hz), 1.85 – 1.36 (m, 20 H) ppm. ¹³C NMR (75 MHz, CDCl₃) δ 113.1, 110.9, 78.7, 78.1, 77.3, 75.9, 71.0, 70.1, 38.0, 36.7 (2 C), 34.8, 25.2, 25.1, 24.2, 23.9, 23.8, 23.7 ppm. [α]_D = -18 (*c* 0.1, CH₂Cl₂). IR (neat) 3460, 2937, 2857, 1368, 1270, 1095, 1046, 909, 730 cm⁻¹. HRMS (ESI) calcd. for C₁₈H₂₉O₆ [M + H⁺] 341.1959, found 341.1973.

Data for the isomer of 282, 1L-1,2:5,6-Di-*O*-cyclohexylidene-*chiro*-inositol (283): ¹H NMR (300 MHz, CDCl₃) δ 4.41 (dd, 2 H, *J* = 4.9, 2.0 Hz), 4.17 (dd, 2 H, *J* = 7.1, 2.7 Hz), 3.55 (dd, 2 H, *J* = 5.2, 2.5 Hz), 2.87 (broad s, 2 H), 1.84 – 1.36 (m, 20 H) ppm. ¹³C NMR (75 MHz, CDCl₃) δ 110.4, 78.4, 75.9, 72.9, 37.8, 34.7, 25.2, 24.2, 23.8 ppm. IR (neat) 3450, 3400, 2937, 2856, 1363, 1231, 1089, 1042, 931, 909, 730 cm⁻¹. HRMS (ESI) calcd. for C₁₈H₂₉O₆ [M + H⁺] 341.1959, found 341.1960.

1L-1-*O*-Benzoyl-3,4:5,6-di-*O*-cyclohexylidene-2-*O*-methyl-*chiro*-inositol (278): Benzoyl chloride (260 μL, 2.32 mmol) and DMAP (7 mg, 0.06 mmol) were added to a solution of **274** (412 mg, 1.16 mmol) in CH₂Cl₂ (5.5 mL) and Et₃N (645 μL, 4.66 mmol) at 0 °C under argon, and then stirred for 5 days at RT. Water (10 mL) was then added and the mixture extracted three times with CH₂Cl₂ (50 mL each). The combined organic fractions were washed with brine

(20 mL), dried over MgSO₄ and the solvents removed under reduced pressure to yield an orange oil which was purified by flash chromatography (EtOAc:petroleum ether 1:15) to yield **278** as a white solid, 522 mg (98%). m.p. 79-81 °C. $[\alpha]_D = -8.3^\circ$ (*c* 0.1, CH₂Cl₂). ¹H NMR (300 MHz, CDCl₃) δ 8.04 (m, 2 H), 7.59 (m, 1 H), 7.46 (m, 2 H), 5.82 (dd, 1 H, *J* = 3.7, 3.2 Hz), 4.42 (m, 2 H), 3.90-3.68 (m, 3 H), 3.46 (s, 3 H), 1.85-1.35 (m, 20 H) ppm. ¹³C NMR (75 MHz, CDCl₃) δ 165.5, 133.3, 129.9, 129.5, 128.4, 112.6, 111.0, 79.2, 77.9, 76.4, 76.0, 75.7, 70.0, 58.2, 37.9, 36.5, 36.3, 34.8, 25.0, 24.9, 23.9, 23.6 (2 C), 23.5 ppm. IR (neat) 2936, 2860, 1724, 1450, 1269, 1107, 1070, 908, 731 cm⁻¹. HRMS (ESI) calcd. for C₂₆H₃₅O₇ [M + H⁺] 459.2377, found 459.2383.

1L-1-*O*-para-toluenesulfonyl-3,4:5,6-di-*O*-cyclohexylidene-2-*O*-methyl-*chiro*-inositol (211): *para*-Toluenesulfonyl chloride (285 mg, 1.50 mmol) and DMAP (2 mg, 0.01 mmol) were added to a stirred solution of **274** (105 mg, 0.30 mmol) in CH₂Cl₂ (1 mL) and Et₃N (1 mL) at RT under argon, and then heated to reflux overnight. The reaction mixture was diluted with EtOAc (30 mL), washed with 5% aqueous HCl (10 mL), water (10 mL) and brine (10 mL), dried over MgSO₄, and reduced *in-vacuo*. The resulting red coloured residue was purified by flash column chromatography (EtOAc:petroleum ether 1:15) to yield **211** as a white solid, 120 mg (79%). m.p. 126-128 °C, lit.¹³⁰ 128-129 °C. $[\alpha]_D = -13^\circ$ (*c* 0.1, CH₂Cl₂), lit.¹³⁰ -12° (*c* 0.73, CHCl₃). ¹H NMR (300 MHz, CDCl₃) δ 7.83 (d, 2 H, *J* = 8.8 Hz), 7.42 (d, 2 H, *J* = 8.8 Hz), 4.97 (dd, 1 H, *J* = 3.8, 3.6 Hz), 4.35 (m, 2 H), 3.68-3.50 (m, 3 H), 3.27 (s, 3 H), 2.41 (s, 3 H), 1.82-1.30 (m, 20 H) ppm.

Representative procedure for the conversion of 276, 274, 278, 211, and 303 into the butane diacetal derivatives 293, 293, 300, 301, and 304 respectively: To a stirred solution of the starting material (1 eq) and camphor-sulfonic acid (2.5 mol%) in MeOH under argon were added HC(OMe)₃ (3.7 eq.) and butanedione (1.2 eq.). The resulting clear yellow solution was heated to reflux for 5 h, cooled to RT, treated with 1 drop Et₃N per mmol of starting material, and reduced *in-vacuo* to yield a gelatinous material. Unless otherwise indicated, addition of a small amount of acetone induced the formation of fine

white needle-like crystals, which were collected by filtration to yield the BDA derivatives in yields of 10 to 45%.

1L-(2'S,3'S)-2-O-Methyl-4,5-O-(2',3'-dimethoxybutane-2',3'-diyl)-chiro-inositol (293) was prepared from both quebrachitol monocyclohexylidene acetal (**276**) (2.85 g, 10.4 mmol) to yield 1.21 g (38%) of **293**, and from quebrachitol dicyclohexylidene acetal (**274**) (645 mg, 1.82 mmol) to yield 250 mg (45%) of **293**. m. p. 188-190 °C. $[\alpha]_D = +135^\circ$ (*c* 0.1, CH₂Cl₂). ¹H NMR (300 MHz, CDCl₃) δ 4.23 (dd, 1 H, *J* = 3.2, 3.0 Hz), 4.12 (m, 1 H), 3.94 – 3.86 (m, 3 H), 3.53 (s, 3 H), 3.47 (m, 1 H), 3.28 (s, 3 H), 3.25 (s, 3 H), 2.42 (broad s, 3 H), 1.33 (s, 3 H), 1.32 (s, 3 H) ppm. ¹³C NMR (75 MHz, CDCl₃) δ 99.9, 99.2, 81.6, 70.1, 70.0, 68.1, 67.9, 67.5, 58.2, 48.1, 48.0, 17.7, 17.6 ppm. IR (neat) 3468, 3347, 2928, 1463, 1376, 1212, 1129, 1049, 1031, 925, 670 cm⁻¹. HRMS (ESI) calcd. for C₁₃H₂₈O₈N [M + NH₄⁺] 326.1809, found 326.1813.

1L-(2'S,3'S)-1-O-Benzoyl-2-O-methyl-4,5-O-(2',3'-dimethoxybutane-2',3'-diyl)-chiro-inositol (300) was prepared from **278** (42 mg, 0.09 mmol) to yield **300** (17 mg, 44%). ¹H NMR (300 MHz, CDCl₃) δ 8.04 – 8.00 (m, 2 H), 7.62 – 7.53 (m, 1 H), 7.48 – 7.42 (m, 2 H), 5.79 (dd, 1 H, *J* = 3.5, 3.2 Hz), 4.12 (m, 1 H), 4.06 – 4.01 (m, 3 H), 3.95 (m, 1 H), 3.65 (dd, 1 H, *J* = 5.0 Hz), 3.45 (s, 3 H), 3.34, (s, 3 H), 3.24 (s, 3 H), 2.86 (broad s, 1 H), 2.70 (broad s, 1 H), 1.40 (s, 3 H), 1.35 (s, 3 H) ppm. ¹³C NMR (75 MHz, CDCl₃) δ 165.2, 133.3, 129.8, 129.4, 128.5, 100.1, 99.3, 80.0, 70.1, 68.9, 68.3, 68.1, 68.0, 58.1, 48.1, 48.0, 17.7, 17.5 ppm. IR (neat) 3446, 2930, 1707, 1267, 1108, 1128, 923, 881, 844, 711 cm⁻¹. HRMS (ESI) calcd. for C₂₀H₃₂O₉N [M + NH₄⁺] 430.2096, found 430.2072.

1L-(2'S,3'S)-1-O-*para*-toluenesulfonyl-2-O-methyl-4,5-O-(2',3'-dimethoxybutane-2',3'-diyl)-chiro-inositol (301) was prepared from **211** (115 mg, 0.23 mmol) to yield 40 mg (38%) of **301** as a white solid. m.p. 187-189 °C. ¹H NMR (300 MHz, CDCl₃) δ 7.82 (d, 2 H, *J* = 8.3 Hz), 7.33 (d, 2 H, *J* = 8.3 Hz), 4.96 (dd, 1 H, *J* = 3.4, 3.1 Hz), 4.96 (dd, 1 H, *J* = 3.6, 2.5 Hz), 3.89 – 3.78 (m, 3 H), 3.44 (dd, 1 H, *J* = 9.1, 3.1 Hz), 3.27 (s, 3 H), 3.23 (s, 3 H), 3.13 (s, 3 H), 2.45 (s, 3 H), 1.32 (s, 3 H), 1.31 (s, 3 H) ppm. ¹³C NMR (75 MHz, CDCl₃)

δ 145.3, 133.3, 129.6, 128.0, 100.1, 99.3, 79.1, 74.9, 69.4, 69.0, 68.0, 67.1, 57.8, 48.0, 47.9, 21.6, 17.6, 17.5 ppm. IR (neat) 3464, 2952, 1367, 1177, 1136, 1113, 1035, 891, 683, 556 cm^{-1} . HRMS (ESI) calcd. for $\text{C}_{24}\text{H}_{34}\text{O}_{10}\text{SN}$ [$\text{M} + \text{NH}_4^+$] 480.1903, found 480.1944.

1L-(2'S,3'S)-1-O-Benzoyl-2-O-*tert*-butyldiphenylsilyloxy-4,5-O-(2',3'-dimethoxybutane-2',3'-diyl)-*chiro*-inositol (304) was prepared from **303** (see below), (250 mg, 0.37 mmol, containing 20% of the isomer **315**) to yield **304** (60 mg, 30% from **303**) isolated by flash column chromatography (EtOAc:petroleum ether 1:5) as an oil. ^1H NMR (300 MHz, CDCl_3) δ 8.18 (m, 2 H), 7.64-7.22 (m, 13 H), 5.28 (dd, 1 H, $J = 3.4, 3.5$ Hz), 4.22-4.08 (m, 2 H), 3.99 (m, 1 H), 3.80 (m, 2 H), 3.22 (s, 3 H), 3.15 (s, 3 H), 1.32 (s, 3 H), 1.27 (s, 3 H), 0.97 (s, 9 H) ppm. ^{13}C NMR (75 MHz, CDCl_3) δ 165.3, 136.0, 135.6, 133.8, 133.3, 132.8, 129.8, 129.7, 128.5, 127.7, 127.6, 99.9, 99.2, 73.3, 72.5, 71.6, 68.6, 68.0, 67.9, 48.0, 47.9, 26.7, 19.3, 17.7, 17.5 ppm. IR (neat) 3481, 3071, 2932, 2857, 1723, 1266, 1132, 1108, 1029, 735, 701 cm^{-1} . HRMS (ESI) calcd. for $\text{C}_{35}\text{H}_{48}\text{O}_9\text{SiN}$ [$\text{M} + \text{NH}_4^+$] 654.3093, found 654.3066.

1L-(2'S,3'S)-1,2,3,6-Tetra-O-methyl-4,5-O-(2',3'-dimethoxybutane-2',3'-diyl)-*chiro*-inositol (297): To a solution of **293** (320 mg, 1.04 mmol) in DMF (4.5 mL) at 0 °C was added NaH (80% in mineral oil, 140 mg, 4.68 mmol). After stirring the suspension for 10 min, MeI (970 μL , 2.21 g, 15.6 mmol) was added and the solution allowed to warm to RT. After stirring at RT for 18 h, the reaction was quenched with water (5 mL), and then extracted 3 times with Et_2O (three times 10 mL). The combined organic fractions were washed with sat. aq. NaHCO_3 (10 mL) and brine (10 mL), dried over MgSO_4 and the solvents removed under reduced pressure. The residues were purified by flash column chromatography (EtOAc:petroleum ether 1:3 – 1:1) to yield **297** as a colourless oil, 254 mg (70%). ^1H NMR (300 MHz, CDCl_3) δ 3.88 – 3.84 (m, 2 H), 3.2 (dd, 1 H, $J = 3.7, 3.0$ Hz), 3.62 (s, 3 H), 3.61 (m, 1 H), 3.50 (s, 3 H), 3.47 (s, 3 H), 3.44 (m, 1 H), 3.43 (s, 3 H), 3.33 (dd, 1 H, $J = 9.5, 3.0$ Hz), 3.28 (s, 3 H), 3.24 (s, 3 H), 1.30 (s, 6 H) ppm. ^{13}C NMR (75 MHz, CDCl_3) δ 99.5, 98.7, 81.0, 80.4, 76.4, 76.3, 69.8, 67.9, 60.9, 59.1, 59.0, 58.6, 47.7, 47.6, 17.8, 17.6 ppm. IR (neat)

2932, 2831, 1445, 1372, 1110, 1093, 1038, 967, 882, 729 cm^{-1} . HRMS (ESI) calcd. for $\text{C}_{16}\text{H}_{34}\text{O}_8\text{N}$ $[\text{M} + \text{NH}_4^+]$ 368.2279, found 368.2293.

1L-1,2,3,6-Tetra-*O*-methyl-*chiro*-inositol (298): A solution of **297** (150 mg) in 3 mL of MeOH and 0.3 mL of conc. HCl was heated to 50 °C for 48 h, during which time a yellow colour developed. The solution was then cooled to RT and diluted with MeOH before solid NaHCO_3 was added until effervescence was no longer observed. Solvents were then removed under reduced pressure and the residues purified by gradient flash column chromatography (MeOH: CH_2Cl_2 , 1:50 – 1:10) to yield **298** as an oil, 83 mg (82%). ^1H NMR (300 MHz, CDCl_3) δ 3.77 – 3.72 (m, 2 H), 3.67 (dd, 1 H, J = 3.7, 3.2), 3.60 (s, 3 H), 3.55 (dd, 1 H, J = 9.2, 1.5 Hz), 3.48 (s, 3 H), 3.47 (s, 3 H), 3.46 (s, 3 H), 3.38 – 3.27 (m, 2 H), 2.78 (broad s, 2 H) ppm. ^{13}C NMR (75 MHz, CDCl_3) δ 82.2, 81.2, 77.9, 75.4, 73.4, 71.2, 60.8, 59.2, 59.0, 58.4 ppm. IR (neat) 3443, 2930, 2828, 1445, 1369, 1191, 1135, 1090, 1048, 957 cm^{-1} . HRMS (ESI) calcd. for $\text{C}_{10}\text{H}_{21}\text{O}_6$ $[\text{M} + \text{H}^+]$ 237.1333, found 237.1341.

1L-(2'S,3'S)-1,3,6-Tri-*O*-acetyl-2-*O*-methyl-4,5-*O*-(2',3'-dimethoxybutane-2',3'-diyl)-*chiro*-inositol (299): A solution of **293** (83 mg) in 0.85 mL of pyridine was cooled 0 °C and acetic anhydride (152 μL , 1.62 mmol) was added. The solution was then warmed to RT and stirred for 18 h. Water (5 mL) was then added, and the mixture extracted with Et_2O (three times 40 mL). The combined organic fractions were washed with water and brine, dried over MgSO_4 , solvents removed under reduced pressure and the residues purified by flash column chromatography (EtOAc :petroleum ether 1:3) to yield **299** as an oil, 92 mg (78%). $[\alpha]_{\text{D}} = +82.0^\circ$ (c 0.12, CH_2Cl_2). ^1H NMR (300 MHz, CDCl_3) δ 5.43 (dd, 1 H, J = 3.7, 2.8 Hz), 5.26 (dd, 1 H, J = 9.8, 9.5 Hz), 5.20 (dd, 1 H, J = 3.4, 3.4 Hz), 4.20 – 3.88 (m, 2 H), 3.44 (dd, 1 H, J = 9.8, 3.4 Hz), 3.34 (s, 3 H), 3.22 (s, 3 H), 3.21 (s, 3 H), 2.14 (s, 3 H), 2.11 (s, 3 H), 2.10 (s, 3 H), 1.25 (s, 3 H), 1.23 (s, 3 H) ppm. ^{13}C NMR (75 MHz, CDCl_3) δ 169.7, 169.2, 169.1, 99.8, 99.1, 78.3, 70.7, 68.4, 66.8, 65.9 (2 C), 58.4, 47.9, 47.4, 20.9 (3 C), 17.5, 17.4 ppm. IR (neat) 2949, 2834, 1751, 1370, 1132, 1112, 1035, 915, 730 cm^{-1} . HRMS (ESI) calcd. for $\text{C}_{19}\text{H}_{34}\text{O}_{11}\text{N}$ $[\text{M} + \text{NH}_4^+]$ 452.2126, found 452.2114.

1L-3,4:5,6-Di-*O*-cyclohexylidene-1,2-di-*O*-methyl-*chiro*-inositol (308):

To a solution of **274** (460 mg, 1.30 mmol) in anhydrous DMF (6 mL) at 0 °C was added NaH (80% in mineral oil, 60 mg, 1.95 mmol). The resulting suspension was stirred for 30 min after which time methyl iodide (405 µL, 923 mg, 6.5 mmol) was added. The solution was then warmed to RT and allowed to stir overnight. Water (10 mL) was then added to quench the reaction, and the mixture was extracted twice with Et₂O (two times 20 mL). The combined organic fractions were then washed with 5% NaHCO₃ (5 mL), water (5 mL), and brine (5 mL), dried over MgSO₄ and the solvents removed under reduced pressure. The residues were purified by flash column chromatography (EtOAc:petroleum ether 1:10 - 1:5) to yield **308** as an oil which solidified upon standing, 450 mg (94%). $[\alpha]_D = -50^\circ$ (*c* 0.18, CH₂Cl₂). ¹H NMR (300 MHz, CDCl₃) δ 4.39 – 4.26 (m, 2 H), 3.83 (dd, 1 H, *J* = 4.1, 3.8 Hz), 3.74 – 3.68 (m, 2 H), 3.59 (dd, 1 H, *J* = 8.0, 1.5 Hz), 3.54 (s, 3 H), 3.52 (s, 3 H), 1.84 – 1.32 (m, 20 H) ppm. ¹³C NMR (75 MHz, CDCl₃) δ 112.0, 110.4, 79.0, 78.6, 78.2, 76.2, 76.1, 75.6, 59.5, 57.8, 37.6, 36.3, 36.2, 34.5, 24.8 (2 C), 23.7, 23.5, 23.4, 23.3 ppm. $[\alpha]_D = -50$ (*c* 0.18, CH₂Cl₂). IR (neat) 2934, 2860, 1449, 1279, 1100, 907, 830, 727 cm⁻¹. HRMS (ESI) calcd. for C₂₀H₃₃O₆ [M + H⁺] 369.2272, found 369.2267.

1L-1,2-Di-*O*-methyl-*chiro*-inositol (305): A solution of **308** (250 mg, 0.68 mmol) was stirred overnight at RT under air in 3 mL 10% aq. HCl in MeOH. After this time, solid NaHCO₃ was added until effervescence was no longer observed, and the solvents then removed under reduced pressure. The residues were purified by flash column chromatography (MeOH:CH₂Cl₂ 1:6) to yield **305**, 120 mg (71%), as an oil which crystallised upon standing. m.p. 138-140 °C, lit.¹⁸¹ 141.5-142.5 °C. $[\alpha]_D = -56^\circ$ (*c* 0.06, MeOH), lit.¹⁸¹ -52.1° (*c* 0.98, MeOH). ¹H NMR (300 MHz, DMSO) δ 4.86 (d, 1 H, *J* = 3.9 Hz), 4.60 (d, 1 H, *J* = 4.2 Hz), 4.55 (d, 1 H, *J* = 3.7 Hz), 4.45 (d, 1 H, *J* = 4.7 Hz), 3.80 (m, 1 H), 3.53 (m, 1 H), 3.30 (s, 3 H), 3.29 (s, 3 H), 3.26 (m, 3 H), 3.15 (dd, 1 H, *J* = 9.3, 2.7 Hz) ppm. ¹³C NMR (75 MHz, DMSO) δ 81.3, 78.6, 73.5, 72.7, 71.0, 69.1, 58.9, 57.7 ppm. IR (neat) 1340, 2932, 2854, 1448, 1365, 1278, 1105, 1026, 927, 907 cm⁻¹. HRMS (ESI) calcd. for C₈H₁₇O₆ [M + H⁺] 209.1019, found 209.1009.

1L-1-*O*-Benzoyl-5,6-*O*-cyclohexylidene-2-*O*-methyl-*chiro*-inositol

(279): To a solution of **278** (30 mg, 0.07 mmol) in acetone (1 mL) at RT under air was added pTsOH (1 mg, 0.005 mmol). The solution was stirred for 2 h at RT, after which time solid NaHCO₃ (10 mg) was added, and the solvents removed under reduced pressure. The residues were purified by flash column chromatography (EtOAc:petroleum ether 1:1) to yield **279**, 18 mg (72%) as an oil. ¹H NMR (300 MHz, CDCl₃) δ 8.02 (m, 2 H), 7.59 (m, 1 H), 7.46 (m, 2 H), 6.00 (m, 1 H), 4.31 (dd, 1 H, *J* = 5.3, 2.9 Hz), 4.26 (m, 1 H), 3.89 (m, 1 H), 3.77 (dd, 1 H, *J* = 7.1, 7.8 Hz), 3.53 (dd, 1 H, *J* = 9.3, 2.9 Hz), 3.48 (s, 3 H), 1.80-1.30 (m, 10 H) ppm. ¹³C NMR (75 MHz, CDCl₃) δ 165.2, 133.5, 129.8, 129.3, 128.5, 110.8, 79.4, 78.3, 76.1, 74.6, 70.7, 66.7, 58.2, 37.9, 35.1, 24.8, 23.9, 23.6 ppm. IR (neat) 3335, 2934, 1721, 1451, 1265, 1249, 1093, 1068, 1023, 707 cm⁻¹. HRMS (ESI) calcd. for C₂₀H₂₇O₇ [M + H⁺] 379.1757, found 379.1762.

1L-1-*O*-Benzoyl-2-*O*-methyl-*chiro*-inositol (306): To a solution of **278** (80 mg, 0.18 mmol) in acetone (1 mL) at RT under air was added a catalytic amount of pTsOH (3.5 mg, 0.02 mmol). The solution was stirred at RT for 3 days, after which time TLC analysis showed approximately equal amounts of **279** and **306** present. Two drops of aqueous HCl were added and the reaction stirred for a further 2 days, after which time TLC analysis showed essentially complete conversion to **306**. Solid NaHCO₃ (50 mg) was added, and the solvents removed under reduced pressure. The residues were purified by flash column chromatography (MeOH:CH₂Cl₂ 1:10) to yield **306**, 46 mg (88%) as a crystalline solid. m.p. 144-149 °C, lit.¹⁸² 143-144 °C. [α]_D = -48° (*c* 0.06, MeOH or acetone), lit.¹⁸² +50.1° (*c* 1.01, MeOH). ¹H NMR (300 MHz, (CD₃)₂CO) δ 8.00 (m, 2 H), 7.64 (m, 1 H), 7.51 (m, 2 H), 5.63 (m, 1 H), 4.65 (d, 1 H, *J* = 3.4 Hz), 4.32 (broad s, 1 H), 4.24 (broad s, 1 H), 4.15 (broad s, 1 H), 4.06 (m, 1 H), 3.66 (m, 3 H), 3.47 (dd, 1 H, *J* = 9.5, 3.2 Hz), 3.38 (s, 3 H) ppm. ¹³C NMR (75 MHz, (CD₃)₂CO) δ 165.6, 133.9, 130.8, 130.2, 129.3, 80.5, 74.1, 73.8, 72.4, 70.6, 70.5, 58.1 ppm. IR (neat) 3336, 2928, 1699, 1450, 1178, 1096, 1070, 1025, 751, 708 cm⁻¹. HRMS (ESI) calcd. for C₁₄H₁₉O₇ [M + H⁺] 299.1125, found 299.1133.

1L-1,2:3,4-Di-*O*-cyclohexylidene-5-*O*-(*tert*-butyldimethylsilyloxy)-*chiro*-inositol (309) and 1L-1,2:3,4-Di-*O*-cyclohexylidene-6-*O*-(*tert*-butyldimethylsilyloxy)-*chiro*-inositol (310): To a solution of the diol **282** (130 mg, 0.38 mmol) in DMF (650 μ L) at 0 °C were added imidazole (52 mg, 0.76 mmol) and TBDMSCl (63 mg, 0.42 mmol). The solution was then allowed to warm to RT and stir overnight, after which it was diluted with Et₂O (50 mL), washed with sat. aq. NaHCO₃ (10 mL), water (10 mL) and brine (10 mL), dried over MgSO₄, and the solvents removed under reduced pressure. The product was isolated by flash column chromatography (EtOAc:petroleum ether 1:5) as an oil, 130 mg (75%, as a mixture of **309** and **310** in a 2:1 ratio).^{iv} The mixture was used directly in the next reaction without further purification.

1L-1-*O*-methyl-3,4:5,6-di-*O*-cyclohexylidene-2-*O*-(*tert*-butyldimethylsilyloxy)-*chiro*-inositol (316): To a solution of a mixture of **309** and **310** from the above reaction (220 mg, 0.48 mmol) in DMF (2 mL) was added NaH (80% in mineral oil, 25 mg, 0.72 mmol). The suspension was stirred for 10 min, after which time methyl iodide (150 μ L, 342 mg, 2.40 mmol) was added. The solution was warmed to RT and allowed to stir for 20 h. Water (10 mL) was then added to quench the reaction, and the mixture was extracted three times with Et₂O (three times 20 mL). The combined organic fractions were washed with 5% NaHCO₃ (20 mL), water (10 mL), and brine (20 mL), dried over MgSO₄ and the solvents removed under reduced pressure. The residues were purified by flash column chromatography (EtOAc:petroleum ether 1:20) to yield 101 mg (45%) of **316** as an oil. ¹H NMR (300 MHz, CDCl₃) δ 4.32 – 4.25 (m, 2 H), 4.60 (dd, 1 H J = 9.0, 4.2 Hz), 3.68 – 3.60 (m, 2 H), 3.53 (s, 3 H), 3.49 (m, 1 H), 1.70 – 1.30 (m, 20 H), 0.93 (s, 9 H), 0.17 (s, 3 H), 0.14 (s, 3 H) ppm. ¹³C NMR (75 MHz, CDCl₃) δ 111.6, 110.3, 81.3, 79.3, 77.1, 76.9, 76.4, 75.9, 71.6, 60.6, 37.9, 36.8, 36.0, 34.9, 25.8 (3 C), 25.1, 25.0, 23.9, 23.8, 23.6, 23.5, 18.4, -

^{iv} Benzoylation of a portion of the product mixture to give a mixture of **313** and **314** simplified the determination of the regioisomeric ratio. Downfield shift of the signal attributed to the proton next to the OBz group was observed. In the ¹H NMR of the product mixture, a doublet of doublets at 5.58 ppm ($J_{\text{eq-eq}}$ = 4.9, $J_{\text{ax-eq}}$ = 3.5 Hz) was attributed to the equatorial proton vicinal to the OBz group in the major product **313**, and a doublet of doublets at 5.41 ppm ($J_{\text{ax-ax}}$ = 9.6, $J_{\text{ax-eq}}$ = 4.4 Hz) was attributed to the axial proton vicinal to the OBz group in the regioisomeric product (**314**). The 2:1 ratio of **313:314** (and hence 2:1 ratio of **309:310**) was obtained from the ratio of the integrals of those two signals.

4.5, -5.0 ppm. IR (neat) 2933, 2856, 1449, 1366, 1252, 1104, 907, 837, 778, 731 cm^{-1} . HRMS (ESI) calcd. for $\text{C}_{25}\text{H}_{45}\text{O}_6\text{Si}$ [$\text{M} + \text{H}^+$] 469.2979, found 469.2973.

1L-1-*O*-Methyl-*chiro*-inositol (307): The fully protected *chiro*-inositol derivative **316** (45 mg, 0.1 mmol) was dissolved in 2 mL of 10% HCl in methanol and stirred at RT for 4 h. Solvents were then removed under reduced pressure and the residue purified by gradient flash column chromatography ($\text{MeOH}:\text{CH}_2\text{Cl}_2$ 1:3 – 1:2) to yield **307** (17 mg, 89%). $[\alpha]_{\text{D}} = -57^\circ$ (c 0.05, D_2O), lit.¹⁸³ for the enantiomer, 1D-1-*O*-methyl-*chiro*-inositol: $[\alpha]_{\text{D}} = +59^\circ$ (c 1.3, D_2O). ^1H NMR (300 MHz, DMSO) δ 4.76 (d, 1 H, $J = 3.9$ Hz), 4.49 (d, 1 H, $J = 4.1$ Hz), 4.47 (d, 1 H, $J = 3.9$ Hz), 4.41 (d, 1 H, $J = 3.9$ Hz), 4.39 (d, 1 H, $J = 3.4$ Hz), 3.77 (dd, 1 H, $J = 6.7, 3.4$ Hz), 3.53 – 3.43 (m, 1 H), 3.33 – 3.16 (m, 4 H), 3.32 (s, 3 H) ppm. ^{13}C NMR (75 MHz, DMSO) δ 82.9, 73.5, 73.3, 71.2, 70.8, 69.4, 59.2 ppm. HRMS (ESI) calcd. for $\text{C}_7\text{H}_{18}\text{O}_6\text{N}$ [$\text{M} + \text{NH}_4^+$] 212.1129, found 212.1126.

1L-1,2:3,4-Di-*O*-cyclohexylidene-5-*O*-(*tert*-butyldiphenylsilyloxy)-*chiro*-inositol (311) and 1L-1,2:3,4-di-*O*-cyclohexylidene-6-*O*-(*tert*-butyldiphenylsilyloxy)-*chiro*-inositol (312): To a solution of the diol **282** (110 mg, 0.35 mmol) in DMF (2 mL) at 0 °C were added imidazole (70 mg, 0.77 mmol) and TBDPSCl (100 μL , 0.39 mmol). The solution was then allowed to warm to RT and stir overnight, after which it was diluted with Et_2O , washed with sat. aq. NaHCO_3 , water and brine, dried over MgSO_4 , and the solvents removed under reduced pressure. The product was isolated by flash column chromatography ($\text{EtOAc}:\text{petroleum ether}$ 1:10) as an oil, 165 mg (88% as a mixture of **311** and **312** in a 5:1 ratio).^v Further column chromatography ($\text{EtOAc}:\text{petroleum ether}$ 1:50-1:10) isolated 66 mg (35%) of essentially pure **311** as an oil. ^1H NMR (300 MHz, CDCl_3) δ 7.74-7.69 (m, 4 H), 7.48-7.36 (m, 6 H), 4.37-4.27 (m, 2 H), 4.11 (dd, 1 H, $J = 9.3, 4.6$ Hz), 4.02 (dd, 1 H, $J = 4.4, 2.9$

^v Benzoylation of a portion of the product mixture to give a mixture of **303** and **315**, again was used to simplify determination of the regioisomeric ratio. The ^1H NMR spectrum of the benzoylated product mixture showed a doublet of doublets at 5.45 ppm ($J_{\text{eq-eq}} = 3.9$, $J_{\text{ax-eq}} = 3.8$ Hz) which was attributed to the equatorial proton vicinal to the OBz group in the major product **303**, and a doublet of doublets at 5.36 ppm ($J_{\text{ax-ax}} = 10.2$, $J_{\text{ax-eq}} = 3.9$ Hz) attributed to the axial proton vicinal to the OBz group in **315**. The ratio of products **303** and **315** (and hence of **311** and **312**) was found to be ca. 5:1; significantly better than the analogous TBDMS analogue.

Hz), 3.78 (dd, 1 H, $J = 9.8, 9.7$ Hz), 3.38 (dd, 1 H, $J = 10.2, 8.4$ Hz), 3.01 (broad s, 1 H), 1.64-1.26 (m, 20 H), 1.12 (s, 9 H) ppm. ^{13}C NMR (75 MHz, CDCl_3) δ 136.2, 135.7, 133.1, 132.5, 130.0, 129.9, 127.8, 127.4, 111.9, 110.0, 79.1, 78.1, 76.0, 75.7, 72.6, 71.1, 37.8, 36.6, 36.0, 34.7, 26.9, 25.0, 24.9, 23.8, 23.7, 23.5 (2 C), 19.4 ppm. IR (neat) 3071, 2932, 2857, 1730, 1448, 1104, 934, 820, 737 cm^{-1} . HRMS (ESI) calcd. for $\text{C}_{34}\text{H}_{47}\text{O}_6\text{Si}$ $[\text{M} + \text{H}^+]$ 579.3136, found 579.3116.

Experimental for Chapter Six

(-)-1,3,3-trimethyl-2-norbornanone dimethyl acetal (321):

(-)-Fenchone ((-)-1,3,3-trimethyl-2-norbornanone) (10 g, 0.066 mol) was dissolved in MeOH (10 mL) and trimethyl orthoformate (30 mL, 29 g, 0.274 mol) at RT under an inert atmosphere. To the solution was added pTsOH. H_2O (680 mg, 0.003 mol), and the reaction was then stirred at RT for 3 days. Solid NaHCO_3 (820 mg, 0.009 mol) was added and the mixture stirred for 30 min. Diethyl ether (200 mL) and water (80 mL) were then added, and after vigorous stirring the layers were separated. The ether part was washed with brine, dried over anhydrous MgSO_4 and concentrated under vacuum. The residue was purified by flash column chromatography (petroleum ether) to yield the product **321** as an oil which solidified upon standing, 3.62 g (28%). m. p. 107-109 $^\circ\text{C}$. $[\alpha]_{\text{D}} = +20^\circ$ (c 0.15, CH_2Cl_2). ^1H NMR (300 MHz, CDCl_3) δ 3.25 (s, 3 H), 3.23 (s, 3 H), 1.83 (m, 2 H), 1.67 (m, 2 H), 1.60 (m, 1 H), 1.38 (m, 2 H), 1.19 (s, 3 H), 1.10 (s, 3 H), 0.97 (s, 3 H) ppm. ^{13}C NMR (75 MHz, CDCl_3) δ 108.4, 51.9, 51.8, 51.6, 49.8, 48.0, 42.8, 30.2, 26.0, 25.1, 23.1, 18.7 ppm. IR (neat) 2931, 2831, 1468, 1267, 1171, 1139, 1123, 1056, 1011, 739 cm^{-1} . HRMS (ESI) calcd. for $\text{C}_{12}\text{H}_{23}\text{O}_2$ $[\text{M} + \text{H}^+]$ 199.1698, found 199.1695.

(±)-2-Norbornanone dimethyl acetal (322): To a solution of (±)-norcamphor ((±)-2-norbornanone) (21.8 g, 0.20 mol) in anhydrous MeOH (44 mL) were added trimethyl orthoformate (66 mL, 64.02 g, 0.60 mol) and pTsOH. H_2O (2.07 g, 0.01 mol), at RT under argon. The mixture was stirred for 18 h during which time a deep purple colour developed. Solid NaHCO_3 (4 g) was added and the mixture stirred for 10 min, during which time the colour changed

to a pale brown. The mixture was then diluted with diethyl ether (150 mL) and water (100 mL), vigorously mixed, and the aqueous and organic parts separated. The aqueous layer was extracted with further diethyl ether (two times 50 mL) and the combined organic fractions then washed with water and brine, dried over MgSO_4 , and reduced in-vacuo. The crude product was purified by kugelrohr short-path distillation to yield 25.06 g (82%) of **322** as a clear, colourless liquid. ^1H NMR (300 MHz, CDCl_3) δ 3.15 (s, 3 H), 3.12 (s, 3 H), 2.32 (m, 1 H), 2.21 (m, 1 H), 1.73 (m, 1 H), 1.62 (m, 1 H), 1.58 – 1.48 (m, 2 H), 1.36 (m, 1 H), 1.25 (m, 1 H), 1.22 – 1.12 (m, 2 H) ppm. ^{13}C NMR (75 MHz, CDCl_3) δ 110.5, 50.0, 47.5, 43.1, 41.2, 37.2, 35.9, 28.5, 21.9 ppm. IR (neat) 2945, 2828, 1453, 1331, 1174, 1133, 1103, 1048, 965, 871, 847 cm^{-1} . HRMS (ESI) calcd. for $\text{C}_9\text{H}_{12}\text{O}_2$ [$\text{M} + \text{H}^+$] 157.1229, found 157.1232.

(\pm)-1,2-*O*-((\pm)-2-norbornylidene)-*myo*-inositol (323**). Method A:** To a suspension of *myo*-inositol (4.0 g, 22.2 mmol) in anhydrous DMSO (44 mL) were added **322** (7.86 g, 50 mmol) and sulphuric acid (0.22 mL, 0.40 g, 4.1 mmol). The mixture was heated to 70 °C for 3 h, to give a clear, very pale yellow solution. This solution was cooled and neutralised with triethylamine (1.5 mL) and then concentrated under vacuum (< 5 mbar) to a weight of ca. 13 g. The residue was dissolved in CHCl_3 (51 mL) and then MeOH (5.1 mL), H_2O (1.0 mL) and pTsOH (15 mg) were added. The resulting slurry was stirred at RT overnight and then filtered. The solid was washed with CHCl_3 (three times 5 mL) and air-dried to yield 4.86 g (80%) of mixed diastereomers of **323**.

Method B: To a suspension of *myo*-inositol (2.7 g, 14.7 mmol) in anhydrous DMSO (29 mL) were added **322** (5.2 g, 33 mmol) and sulphuric acid (0.16 mL, 0.26 g, 2.7 mmol). The mixture was heated to 70 °C for 3 h, to give a clear, very pale yellow solution. This solution was cooled and neutralised with triethylamine (1.0 mL) and then concentrated under vacuum (ca. 20 mbar) to remove the volatile solvents, to a weight of ca. 40 g. The residue was dissolved in toluene (130 mL) and then washed with water (10 mL) and brine (20 mL). The combined aqueous fractions were then extracted with toluene (two times 20 mL), and all the toluene parts finally combined and washed with brine (30 mL), dried over anhydrous MgSO_4 and concentrated under vacuum to a weight of 4.1 g. The residue was dissolved in CHCl_3 (33 mL), MeOH (3.3 mL), H_2O (0.66 mL) and

pTsOH (10 mg). The resulting solution was stirred at RT overnight, during which time a precipitate developed. The solid was filtered off, washed with CHCl₃ (three times 5 mL) and air-dried to yield 4.04 g (30%) of mixed diastereomers of **323**.

Data for the mixed diastereomers of 323 (see discussion): ¹H NMR (300 MHz, *d*₆-DMSO)^{vi} δ 4.93-4.65 (m, 4 H), 3.94 (m, 1 H), 3.72 (m, 1 H), 3.45 (m, 1 H), 3.25 (m, 1 H), 3.20 (m, 1 H), 2.90 (m, 1 H), 2.20, 2.14, 2.02, and 1.78-1.15 (multiplets, total 10 H) ppm. ¹³C NMR (75 MHz, *d*₆-DMSO)^{vii} δ 116.6, 116.0, 79.9, 79.5, 78.2, 77.8, 75.1, 74.7, 74.6, 74.5, 73.4, 72.9, 70.5, 70.4, 45.4, 45.0, 44.9, 44.2, 37.5, 37.2, 35.4, 35.3, 28.2, 28.0, 21.6, 21.2 ppm. HRMS (ESI) calcd. for C₁₃H₂₁O₆ [M + H⁺] 273.1333, found 273.1331.

(±)-1,2-*O*-((±)-2-norbornylidene)-3,4,5,6-tetra-*O*-acetyl-*myo*-inositol (per-acetylated **323):** Recrystallised **323** (24 mg, 0.09 mmol of a ca. 2:1 ratio of two diastereomers) was dissolved in pyridine (100 µL) and acetic anhydride (100 µL) and stirred at RT for 18 h. The reaction mixture was then diluted with diethyl ether and water and agitated vigorously. The layers were then separated and the organic part washed with brine, dried over anhydrous MgSO₄ and concentrated under vacuum, and then azeotroped with toluene to remove residual pyridine. The product was purified by flash column chromatography (EtOAc:petroleum ether 1:3) to yield the tetra-acetylated products as an oil, 28 mg (72%), containing two inseparable diastereomers in a ca. 2:1 ratio. ¹H NMR (300 MHz, CDCl₃)^{viii} δ 5.51 (m, 1 H), 5.20 (m, 2 H), 5.03 (m, 1 H), 4.32 (m, 1 H), 4.14 (m, 1 H), 2.27 (m, 1 H), 2.14, (s, 3 H), 2.09 (s, 3 H), 2.08 (s, 3 H), 2.03 (s, 3 H), 2.02, (s, 3 H), 2.01 (s, 3 H), 1.70-1.20 (m, 6 H) ppm. ¹³C NMR (75

^{vi} Signals for the two diastereomers of **323** present in the mixture overlap; integrals are reported as if for ONE diastereomer/molecule.

^{vii} Signals for the two diastereomers are reported together; it was not possible to assign signals to the separate diastereomers. Molecule **323** contains 13 carbons; 26 signals are reported.

^{viii} Signals from the two diastereomers overlap in the inositol and nor-camphor regions. Integrations are given for ONE molecule of per-acetylated **323**. The signals for the acetate methyl groups partially overlap; six acetate signals are reported, although each molecule of per-acetylated **323** has only four acetate groups.

MHz, CDCl₃)^{ix} δ 170.5, 170.1, 169.8, 119.3(A), 118.9(B), 76.3(B), 75.8(A), 74.3(A), 73.9(B), 72.8(A), 72.4(B), 71.5, 70.0, 69.6(A), 69.5(B), 45.3(A), 44.7(B), 44.5(A), 44.3(B), 38.1(B), 37.9(A), 36.0(A), 35.9(B), 28.4(A), 28.2(B), 22.2(A), 21.7(B), 21.2, 21.1, 21.0, 20.9 ppm.

Experimental for Chapter Seven

Scaleup campaign stage 1; preparation of (1S)-(-)-camphor:
(-)-Borneol (5.02 kg, 32.54 mol) and glacial acetic acid (15.0 L) were charged to the 50 L reactor and stirred at 15 °C until the borneol was completely dissolved. Aqueous sodium hypochlorite (16.66 L of a 15% solution) was then slowly added over 2.5 h (this is equivalent to an addition rate of ca. 30 mL per minute). The temperature of the solution was maintained at 25 °C (\pm 5 °C) during the addition period, and the solution was stirred at 15 °C for a further h after completion of the addition. At this time a positive potassium iodide-starch test was obtained. Saturated aqueous sodium bisulfite solution (2.0 L) was then added, after which addition the solution colour changed from yellow to white and the starch test was negative. The mixture was removed from the reaction vessel and poured over an ice-brine mixture (50 L). The resulting white solid was isolated by filtration (10 L Buchi flasks / 24 cm filters) and washed with saturated aqueous sodium carbonate and water (ca. 10 L each). The solid product was pressed dry and then charged manually to the 50 L reactor and dissolved in petroleum ether (20 L). The aqueous layer was removed and the organic layer washed with brine in the 50 L reactor. The petroleum ether was evaporated under reduced pressure in the 50 L Buchi to yield a white solid, which was dissolved in toluene (5 L) and the toluene then removed under reduced pressure to yield the product, 4.55 kg (92%). ¹H and ¹³C NMR were analogous to the previously reported values and to those obtained for an authentic sample.

^{ix} Signals for two diastereomers are listed together, denoted A and B (the configuration of the diastereomers A and B was not determined). Signals for A were approximately two times stronger than those for B. Where neither A or B is indicated, signals were overlapping.

Scaleup campaign stage 2; preparation of (1S)-(-)-camphor dimethyl acetal ((-)-268): The (-)-camphor (4.55 kg, 29.89 mol) from stage 1, trimethyl orthoformate (17.5 L, 16.98 kg, 159.84 mol) and methanol (4.5 L) were charged to the 50 L reactor and stirred at 20 °C under an inert atmosphere until the camphor was dissolved (ca. 10 min). Concentrated sulphuric acid (44 mL, 81 g, 0.83 mol) was then added and the mixture stirred at 20 °C overnight. Solid sodium methoxide (110 g, 2.11 mol) was then charged to the reactor (pH paper used to check the solution is neutral) and the mixture reduced in the 50 L Buchi to a volume of approximately 6 L. Toluene (12 L) was then added to the solution and the resulting precipitate removed by filtration (10 L Buchi/24 cm filter). The filtrate was transferred to a clean 50 L Buchi flask and the majority of the toluene removed under vacuum to give crude (-)-268, 6.40 kg (¹H and ¹³C NMR matched previously reported values). The product, still containing toluene, was used directly in stage 3.

Scaleup campaign stage 3; preparation of 1D-(6'-S)-1,2-O-(L-1',7',7'-trimethyl[2',2',1']bicyclohept-6'-ylidene)-myo-inositol ((-)-269a): *Myo*-inositol (2.40 kg, 13.32 mol) was charged to the 50 L reactor. The crude (-)-268 (5.92 kg, 29.86 mol, based on 100% yield in stage 2) was then dissolved in DMSO (7.5 L) and transferred to the reactor. The mixture was stirred rapidly and sulphuric acid (131 mL, 241 g, 2.46 mol) added. Then the mixture was heated to 70 °C for 3 h, during which time the solution turned an unexpected and unpleasant brown-black colour. The mixture was cooled, triethylamine (885 mL, 643 g, 6.33 mol) added, and the solution removed from the reactor (using ca. 2 L of methanol to rinse the vessel). Undissolved solids (ca. 300 g) were filtered out, and the solution then transferred to the 50 L Buchi, where the excess methanol and trimethyl orthoformate and finally ca. 4 L of DMSO were removed under vacuum at 90 °C (± 5 °C) (this brought the weight down to less than the critical 12.6 kg – see discussion in chapter seven). The residue was largely dissolved in CHCl₃ (38.5 L) and transferred back to the 50 L reactor (some undissolved material was present). After the transfer, methanol (3.90 L), water (775 mL) and pTsOH.H₂O (8.9 g) were added to the reactor and the mixture stirred over the weekend at 20 °C. A mobile slurry formed, which was neutralised with

triethylamine (290 mL) and the precipitate filtered off in two portions (using two 10 L Buchi/24 cm filters). Approximately 10 L of CHCl₃ was used to rinse the slurry out of the reactor and wash the filter cakes, and then each cake was slurried with 4 L of CHCl₃ and refiltered. This was repeated and the product was air-dried for 3 days to give 2.26 kg (54%) of a pale tan coloured solid. The composition of this solid was an unexpected mixture of the diastereomers **(-)-269a**, **269b**, **269c**, **269d**, and unreacted *myo*-inositol, which were partially separated by successive crystallisations (see the discussion in chapter seven).

Data for (-)-269a: m.p. 244-47 °C; lit.¹⁷¹ 231-232 °C and lit.¹⁶⁹ 260-262 °C. $[\alpha]_D = -38^\circ$ (*c* 0.2, acetone:water 1:1); $[\alpha]_D = -44.2^\circ$ (*c* 1.0, py); lit.¹⁶⁹ -44.0° (*c* 1.0, py). ¹H NMR (300 MHz, *d*₆-DMSO)^x δ 4.84-4.68 (m, 4 H), 4.06 (m, 1 H), 3.64 (m, 1 H), 3.48 (m, 1 H), 3.30-3.18 (m, 2 H), 2.90 (m, 1 H), 1.98-1.82 (m, 2 H), 1.64 (m, 2 H), 1.38 (m, 1 H), 1.29 (m, 1 H), 1.11 (m, 1 H), 0.94 (s, 3 H), 0.80 (s, 3 H), 0.74 (s, 3 H) ppm. ¹³C NMR (75 MHz, *d*₆-DMSO) δ 116.3, 77.0, 76.4, 75.9, 74.1, 72.1, 70.0, 51.1, 47.6, 45.3, 44.6, 29.2, 26.9, 20.6, 20.4, 9.8 ppm. IR (KBr disc) 3370, 2952, 1453, 1359, 1375, 1317, 1148, 1122, 1106, 1024, 986, 893, 727 cm⁻¹. Anal. calcd. for C₁₆H₂₆O₆: C, 61.13; H, 8.34; O, 30.54; found: C, 61.22; H, 8.41.

Data for the co-crystals of 1D-(6'-S)-2,3-O-(L-1',7',7'-trimethyl[2',2',1']bicyclohept-6'-ylidene)-*myo*-inositol (269b) and 1D-(6'-R)-2,3-O-(L-1',7',7'-trimethyl[2',2',1']bicyclohept-6'-ylidene)-*myo*-inositol (269c): m.p. 238-241 °C. $[\alpha]_D = +40^\circ$ (*c* 0.1, acetone:water 1:1); ¹H NMR (300 MHz, *d*₆-DMSO)^{xi} δ 4.96-4.68 (m, 4 H), 3.94 (m, 1 H), 3.76 (m, 1 H), 3.84 (m, 1 H), 3.26 (m, 2 H), 2.87 (1 H), 1.97 (m, 1 H), 1.82 (m, 1 H), 1.68-1.48 and 1.34-1.04 (multiplets, 5 H), 0.94 (s, 3 H), 0.79 (s, 3 H, **269b** only), 0.78 (s, 3 H), 0.72 (s, 3 H, **269c** only) ppm. IR (KBr disc) 3444, 2947, 1451, 1390, 1370, 1311, 1121, 1023, 968, 887, 848, 725 cm⁻¹. Anal. calcd. for C₁₆H₂₆O₆ + 3H₂O: C, 52.16; H, 8.75; O, 39.08; found: C, 52.54; H, 8.71.

Data for 269b: ¹³C NMR (75 MHz, *d*₆-DMSO) δ 116.3, 78.6, 78.0, 73.7, 73.0, 71.9, 70.1, 53.1, 47.3, 46.4, 44.5, 28.2, 26.6, 20.4, 20.3, 9.8 ppm.

^x Literature NMR data¹⁶⁹ was reported in D₂O.

^{xi} Signals in the ¹H NMR spectrum overlap for **269b** and **269c** in all cases except for one of the methyl singlets, which were assigned based on their relative integrals.

Data for 269c: ^{13}C NMR (75 MHz, d_6 -DMSO) δ 116.7, 78.5, 75.6, 74.7, 74.0, 72.1 69.9, 51.0, 47.7, 45.6, 44.5, 29.2, 26.5, 20.6, 20.2, 10.8 ppm.

Data for 1D-(6'-*R*)-1,2-*O*-(L-1',7',7'-trimethyl[2',2',1']bicyclohept-6'-ylidene)-*myo*-inositol (269d): ^1H NMR (300 MHz, d_6 -DMSO): Inositol ring proton signals, differentiable from the other three isomers appear at δ 4.01 and 3.82 ppm. ^{13}C NMR (75 MHz, d_6 -DMSO): The acetal C appears at δ 116.8 ppm.

Recovery of (-)-L-camphor: The CHCl_3 , MeOH, and H_2O filtrates from the initial crude product filtration were returned to the 50 L reactor and washed with water (20 L) and 10% brine (20 L) and the organic part then reduced in the 50 L Buchi to yield 1.80 kg of a brown solid. Water (10 L) was added to the solid and left for 3 days, and the resulting pale tan solid was collected by filtration, washed with distilled water, air-dried for 48 h and then dried in a desiccator to yield approximately 1.20 kg of crude L-camphor as a pale tan solid.

References

1. West, L. M.; Northcote, P. T.; Battershill, C. N. *J. Org. Chem.* **2000**, *65*, 445-449.
2. Cancer Society of New Zealand, <http://www.cancernz.org.nz> (oct **2004**).
3. NZ Health Information service, <http://www.nzhis.govt.nz> (oct **2004**).
4. Hood, K. A.; West, L. M.; Rouwé, B.; Northcote, P. T.; Berridge, M. V.; Wakefield, St. J.; Miller, J. H. *Cancer Research*, **2002**, *62*, 3356-3360.
5. Hood, K. A.; West, L. M.; Rouwé, B.; Northcote, P. T.; Berridge, M. V.; Wakefield, St. J.; Miller, J. H. *Anti-Cancer Drug Design*, **2001**, *16*, 155-166.
6. Gaitanos, T. N.; Buey, R. M.; Diaz, J. F.; Northcote, P. T.; Teesdale-Spittle, P.; Andreu, J. M.; Miller, J. H. *Cancer Research*, **2004**, *64*, 5063-5067.
7. The U.S National Cancer Institute's Surveillance, Epidemiology and End Results (SEER) Program, <http://training.seer.cancer.gov> (oct **2004**).
8. Nicolau, K. C.; Roschangar, F.; Vourloumis, D. *Angew. Chem. Int. Ed. Engl.* **1998**, *37*, 2014-2045.
9. McKean, P. G.; Vaughn, S.; Gull, K. *J. Cell Science*, **2001**, *114*, 2723-2733.
10. Nogales, E.; Wolf, S. G.; Downing, K. H. *Nature*, **1998**, *391*, 199-202.
11. Nogales, E. *Ann. Rev. Biochem.* **2000**, *69*, 277-302.
12. a) Mitchison, T.; Kirschener, M. W. *Nature*, **1984**, *312*, 237-242. b) Kirschener, M. W.; Mitchison, T. *Cell*, **1986**, *45*, 329-342. c) Kirschener, M. W.; Mitchison, T. *Nature*, **1986**, *324*, 621-622.
13. Timashiff, S.; Andreu, J.; Gorbunoff, M.; Medranot, F.; Prakash, V. *Cell. Pharmacol.* **1993**, *1*, S27-S33. b) Toso, R. J.; Jordan, M. A.; Farrell, K. W.; Matsumoto, B.; Wilson, L. *Biochemistry*, **1993**, *32*, 1285-1293.
14. a) Natale, R. B.; *Semin. Oncol.* **1997**, *24*, 29-37. b) Sackett, D. L.; *Pharmacol. Ther.* **1993**, *59*, 163-228.
15. Hamel, E. *Pharmacol. Ther.* **1992**, *51*, 31-51.
16. Combeau, C.; Provost, J.; Lancelin, F.; Tournoux, Y.; Prod'homme, F.; Herman, F.; Lavelle, F.; Leboul, J.; Vuilhorgne, M. *Molecular Pharmacology*, **2000**, *57*, 533-563.
17. Wani, M. C.; Taylor, H. L.; Wall, M. E.; Coggon, P.; McPhail, A. T. *J. Am. Chem. Soc.* **1971**, *93*, 2325-2327.
18. a) Denis, J. N.; Greene, A. E.; Guénard, D.; Gueritte-Voegelein, F.; Mangatal, L.; Potier, P. *J. Am. Chem. Soc.* **1998**, *110*, 5917-5919. b) Mangatal, L.; Adeline, M. T.; Guénard, D.; Gueritte-Voegelein, F.; Potier, P. *Tetrahedron*, **1989**, *45*, 4177-4190. c) Barasoain, I.; de Ines, C.; Diaz, F. *et al. Proc. Am. Assoc. Cancer Res.* **1991**, *32*, 329. d) Fromes, Y.; Gounon, P.; Bissery, M. C. *Proc. Am. Assoc. Cancer Res.* **1992**, *33*, 511.

19. a) Schiff, P. B.; Horwitz, S. B. *Proc. Natl. Acad. Sci. USA*, **1980**, 77, 1561. b) Dustin, P. *Microtubules*, 2nd Edition, Springer-Verlag, Berlin, **1984**, 484.
20. Abal, M.; Andreu, J. M.; Barrasoain, I. *Curr. Cancer Drug Targets*, **2003**, 3, 193.
21. Trielli, M. O.; Andreassen, P. R.; Lacroix, F. B.; Margolis, R. L. *J. Cell Biol.* **1996**, 135, 689.
22. Höfle, G.; Bedorf, N.; Gerth, K.; Reichenbach, H. (GBF), DE-B 4138042, **1993** [*Chem. Abstr.* **1993**, 120, 52841].
23. Bollag, D. M.; McQueeney, P.A.; Zhu, J.; Hensens, O.; Koupal, L.; Liesch, J.; Goetz, M.; Lazarides, E.; Woods, C. M. *Cancer Res.* **1995**, 55, 2325-2333.
24. Kowalski, R. J.; Giannakakou, P.; Hamel, E. *J. Biol. Chem.* **1997**, 272, 2534-2541.
25. Nicolau, K. C.; Ritzén, A.; Namoto, K. *Chem. Comm.* **2001**, 1523.
26. Gunasekera, S. P.; Gunaserka, M.; Longley, R. E.; Schulte, G. K. *J. Org. Chem.* **1990**, 55, 4912-4915.
27. a) ter Haar, E.; Kowalski, R. J.; Hamel, E.; Lin, C. M.; Longley, R. E.; Gunasekera, S. P.; Rosenkranz, H. S.; Day, B. W. *Biochemistry*, **1996**, 35, 243-250. b) Kowalski, R. J.; Giannakakou, P.; Gunasekera, S. P.; Longley, R. E.; Day, B. W.; Hamel, E. *Molecular Pharmacology*, **1997**, 52, 613-622.
28. Fenical, W.; Jensen, P. R.; Lindel, T.; US-A 5473057, **1995**. b) Lindel, T.; Jensen, P. R.; Fenical, W.; Long, H. B.; Casazza, A. M.; Carboni, J.; Fairchild, C. R. *J. Am. Chem. Soc.* **1997**, 119, 8744-8745.
29. a) D'Ambrosio, M.; Guerriero, A.; Pietra, F. *Helv. Chim. Acta* **1987**, 70, 2019-2027. b) D'Ambrosio, M.; Guerriero, A.; Pietra, F. *Helv. Chim. Acta* **1988**, 71, 964-976.
30. a) Mooberry, S. L.; Tien, G.; Hernandez, A. H.; Plubrukarn, A.; Davidson, B. S. *Cancer Research*, **1999**, 59, 653-660. b) Pryor, D. E.; O'Brate, A.; Bilcer, G.; Díaz, J. F.; Wang, Y.; Wang, Y.; Kabaki, M.; Jung, M. K.; Andreu, J. M.; Ghosh, A. K.; Giannakakou, P.; Hamel, E. *Biochemistry*, **2002**, 41, 9109-9115.
31. Perry, N. B.; Blunt, J. W.; Munro, H. G. *J. Am. Chem. Soc.* **1988**, 110, 4850-4851.
32. Perry, N. B.; Blunt, J. W.; Munro, H. G.; Thompson, A. M. *J. Org. Chem.* **1990**, 55, 223-227.
33. Northcote, P. T.; Blunt, J. W.; Munro, H. G. *Tetrahedron Lett.* **1991**, 32, 6411-6414.
34. Liao, X.; Wu, Y.; De Brabander, J. K.; *Angew. Chem. Int. Ed. Engl.* **2003**, 42, 1648-1652.
35. Horwitz, S. B. *Trends Pharmacol. Sci.* **1992**, 13, 134.
36. Giannakakou, P.; Sackett, D. L.; Kang, Y. K.; Zhan, Z.; Buters, J. T. M.; Fojo, T.; Poruchynsky, M. S. *J. Biol. Chem.* **1997**, 272, 17118.
37. Brown, H. C.; Ramachandran, P. V. *Pure & Appl. Chem.* **1991**, 63, 307-316.
38. Brown, H.C.; Jadhav, P. K. *J. Am. Chem. Soc.* **1983**, 105, 2092-2093.

39. Brown, H.C.; Desai, M. C.; Jadhav, P. K. *J. Org. Chem.* **1982**, *47*, 5065-5069.
40. Smith, A. B. III; Safonov, I. G.; Corbett, R. M. *J. Am. Chem. Soc.* **2001**, *123*, 12426-12427.
41. Martin, T.A. *et. al. J. Med. Chem.* **1969**, *12*, 1950-1953.
42. Soai, K.; Niwa, S.; Kobayashi, T. *J. Chem. Soc. Chem. Comm.* **1987**, 801-802.
43. Kitamura, M.; Tokunaga, M.; Ohkuma, T.; Nyori, R. *Tetrahedron Lett.* **1991**, *32*, 4163-4166.
44. Itsuno, S.; Yokoi, A.; Kuroda, S. *Synlett.* **1999**, *12*, 1987-1989.
45. Shi-Qi, P.; Winterfeldt, E. *Liebigs Ann. Chem.* **1989**, 1045-1047.
46. Erker, G.; Riedel, M.; Koch, S.; Jödicke, T.; Würthwein, E-U. *J. Org. Chem.* **1995**, *60*, 5284-5290.
47. Blaise, E. E.; *C. R. Hebd. Seances Acad. Sci.* **1901**, *132*, 478.
48. Stocker, B. L. *PhD Thesis*, Victoria University of Wellington, **2004**.
49. a) Takai, K.; Heathcock, C. H.; *J. Org. Chem.* **1985**, *50*, 3247-3251. b) Adam, W.; Arias Encarnacion, L. A. *Synthesis*, **1979**, 338-390. c) Davies, S. G.; Middlemiss, D.; Naylor, A.; Wills, M. *Tetrahedron Lett.* **1989**, *30*, 2971-2974.
50. Zimmerman, H. E.; Traxler, M. D. *J. Am. Chem. Soc.* **1957**, *79*, 1920-1923.
51. Procter, G. *Asymmetric Synthesis*, Oxford University Press, **1996**, pg 69-73 and 204-205.
52. a) Mukaiyama, T.; Banno, K.; Narasaka, K. *J. Am. Chem. Soc.* **1974**, *96*, 7503-7509. b) Mukaiyama, T. *Angew. Chem. Int. Ed. Engl.* **1977**, *16*, 817-826.
53. Heathcock, C. H.; Davidsen, S. K.; Hug, K. T.; Flippin, L. A. *J. Org. Chem.* **1986**, *51*, 3027-3037.
54. Mori, I.; Ishihara, K.; Heathcock, C. H. *J. Org. Chem.* **1990**, *55*, 1114-1117.
55. a) Reetz, M. T. *Angew. Chem. Int. Ed. Engl.* **1984**, *23*, 556-569. b) Masamune, S.; Ellingboe, J. W.; Choy, W. *J. Am. Chem. Soc.* **1982**, *104*, 5526-5528.
56. a) Hanessian, S.; Pougny, J.-R.; Boessenkool, I. K. *Tetrahedron*, **1984**, *40*, 1289-1301. b) Wood, A. J.; Holt, D. J.; Dominguez, M.-C.; Jenkins, P. R. *J. Org. Chem.* **1998**, *63*, 8522-8529.
57. Stocker, B. L.; Teesdale-Spittle, P.; Hoberg, J. O. *Eur. J. Org. Chem.* **2004**, 330-336.
58. Xu, Z., Johannes, C. W., Hour, A. F., La, D. S., Cogan, D. A., Hofilena, G. E., Hoveyda, A. H. *J. Am. Chem. Soc.* **1997**, *119*, 10302-10316.
59. a) Evans, D. A.; Bartroli, J.; Shih, T. L. *J. Am. Chem. Soc.* **1981**, *103*, 2127-2129. b) Evans, D. A.; Rieger, D. L.; Bilodeau, M. T.; Urpi, F. *J. Am. Chem. Soc.* **1991**, *113*, 1047-1049. c) Keck, G. E.; Palani, A.; McHardy, S. F. *J. Org. Chem.* **1994**, *59*, 3113-3122. d) Crimmins, M. T.; King, B. W.; Tabet, E. A.; Chaudhary, K. *J. Org. Chem.* **2001**, *66*, 894-902.

60. Hoye, T. R.; Dellaria Jr. J. F.; Kurth, M. J. *J. Am. Chem. Soc.* **1982**, *104*, 6704.
61. Mancuso, A. J.; Huang, S.-L.; Swern, D. *J. Org. Chem.* **1978**, *43*, 2480.
62. Evans, D. A.; Hoveyda, A. H. *J. Am. Chem. Soc.* **1990**, *112*, 6447-6449.
63. Inanaga, J.; Hirata, K.; Saeki, H.; Katsuki, T.; Yamaguchi, M. *Bull. Chem. Soc. Jpn.* **1979**, *52*, 1989-1993.
64. Paterson, I.; Di Francesco, M. E.; Kühn, T. *Org. Lett.* **2003**, *5*, 599-602.
65. Ghosh, A. K.; Kim, J.-H. *Tetrahedron Lett.* **2003**, *44*, 3967-3969.
66. Ghosh, A. K.; Kim, J.-H. *Tetrahedron Lett.* **2003**, *44*, 7659-7661.
67. Taylor, R. E.; Jin, M. *Org. Lett.* **2003**, *5*, 4959-4961.
68. Gurjar, M. K.; Pedduri, Y.; Ramana, C. V.; Puranik, V. G.; Gonnade, R. G. *Tetrahedron Lett.* **2004**, *45*, 387-390.
69. Liu, B.; Zhou, W.-S. *Org. Lett.* **2004**, *6*, 71-74.
70. Engers, D. W.; Bassindale, M. J.; Pagenkopf, B. L. *Org. Lett.* **2004**, *6*, 663-666.
71. Weiberth, F. J.; Hall, S. S. *J. Org. Chem.* **1987**, *52*, 3901-3904.
72. Hanessian, S.; Lavalley, P. *Can. J. Chem.* **1975**, *53*, 2975-2977.
73. Ireland, R. E.; Obrecht, D. M. *Helv. Chim. Acta*, **1986**, *69*, 1273-1281.
74. Armstrong, A.; Brackenridge, I.; Jackson, R. F. W.; Kirk, J. M. *Tetrahedron Lett.* **1988**, *29*, 2483-2486.
75. Namboodiri, V. V.; Varma, R. S. *Tetrahedron Lett.* **2002**, *43*, 1143-1146.
76. a) Greene, T. W.; Wuts, P. G. M., *Protective Groups in Organic Synthesis*, John Wiley & Sons, 3rd Edition, **1999**, pg 49-52; b) 86-88; c) 122-123; d) 29-32; e) 25-26.
77. Nelson, T. D.; Crouch, R. D. *Synthesis*, **1996**, 1031-1069.
78. Bellassoued, M.; Gaudemar, M. *J. Organometallic Chem.* **1974**, *81*, 139-144.
79. Moyer, M. P.; Feldman, P. L.; Rapoport, H. *J. Org. Chem.*, **1985**, *50*, 5223-5230.
80. Hannick, S. M.; Kishi, Y. *J. Org. Chem.* **1983**, *48*, 3833-3835.
81. Lee, A. S.-Y.; Cheng, R.-Y. *Tetrahedron Lett.* **1997**, *38*, 443-446.
82. Johnson, D. V.; Fischer, R.; Griengl H. *Tetrahedron*, **2000**, *56*, 9289-9295.
83. Gauthier Jr., D. R.; Carreira, E. M. *Angew. Chem. Int. Ed. Engl.* **1996**, *35*, 2363-65.
84. Kleschick, W. A.; Buse, C. T.; Heathcock, C. H.; *J. Am. Chem. Soc.* **1977**, *99*, 247.
85. House, H. O.; Crumrine, D. S.; Teranishi, A. Y.; Olmsted, H. D. *J. Am. Chem. Soc.* **1973**, *95*, 3310-3324.
86. a) Heng, K. K.; Simpson, J.; Smith, R. A. J.; Robinson, W. T. *J. Org. Chem.* **1981**, *46*, 2932-2934; b) Heathcock, C. H.; Pirrung, M. C.; Sohn, J. E. *J. Org. Chem.* **1979**, *44*, 4294-4299.
87. Hall, P. L.; Gilchrist, J. H.; Collum, D. B. *J. Am. Chem. Soc.* **1991**, *113*, 9571-9574.

88. a) Carey, F. A., Sundberg, R. J., *Advanced Organic Chemistry, Part B: Reactions and Synthesis*, 4th edition, **2001**, Kluwer Academic/Plenum Publishers, pg 74; b) pg 88-89; c) pg 71; d) pg 74.
89. Bernardi, A.; Marchionni, C.; Novo, B.; Karamfilova, K.; Potenza, D.; Scolastico, C.; Roversi, P. *Tetrahedron*, **1996**, 52, 3497-3508.
90. *Lewis Acid Reagents*, editor: Yamamoto, H.; in *The Practical Approach in Chemistry Series*, series editor: Harwood, L. M.; Moody, C. I, Oxford Univ. Press, **1999**.
91. Andrews, D. M.; Carey, S. J.; Chaignot, H.; Coomber, B. A.; Gray, N. M.; Hind, L.; Jones, P. S.; Mills, G.; Robinson, J. E.; Slater, M. J. *Org. Lett.* **2002**, 4, 4475-4478.
92. Mukaiyama, T.; Inoue, T. *Chem. Lett.* **1976**, 559.
93. Inoue, T.; Mukaiyama, T. *Bull. Chem. Soc. Jpn.* **1980**, 53, 174.
94. a) Brown, H. C.; Dhar, R. K.; Bakshi, R. K.; Pandiarajan, P. K.; Singaram, B. *J. Am. Chem. Soc.* **1989**, 111, 3441-3442. b) Brown, H. C.; Dhar, R. K.; Ganesan, K.; Singaram, B. *J. Org. Chem.* **1992**, 57, 499-504. c) Brown, H. C.; Dhar, R. K.; Ganesan, K.; Singaram, B. *J. Org. Chem.* **1992**, 57, 2716-2721. d) Brown, H. C.; Ganesan, K.; Dhar, R. K. *J. Org. Chem.* **1993**, 58, 147-153.
95. Goodman, J. M.; Paterson, I. *Tetrahedron Lett.* **1992**, 33, 7223-7226.
96. Rotulo-Sims, D.; Prunet, J. *Org. Lett.* **2002**, 4, 4701-4704.
97. Greene, A. E.; Drian, C. L.; Crabbe, P. *J. Am. Chem. Soc.* **1980**, 102, 7583.
98. Earle, M. J.; Fairhurst, R. A.; Giles, R. G.; Heaney, H. *Synlett*, **1991**, 728.
99. Prehm, P. *Carbohydrate Res.* **1980**, 78, 372-374.
100. Stork, G.; Takahashi, T. *J. Am. Chem. Soc.* **1977**, 99, 1275-1276.
101. Hall, D. G.; Deslongchamps, P. *J. Org. Chem.* **1995**, 60, 7796.
102. Laforge, F. B. *J. Am. Chem. Soc.* **1933**, 55, 3040.
103. Addo, J. K. **2004**, personal communication.
104. Gulab, S. A. and Turner, E. **2005**, personal communications.
105. Scherer, J. *Justus Liebigs Ann. Chem.* **1850**, 73, 322-328.
106. IUPAC Nomenclature of cyclitols, *Biochem. J.* **1976**, 153, 23-31.
107. Billington, D. C. *Chem. Soc. Rev.* **1989**, 18, 83-122.
108. Angyal, S. J.; Anderson, L. *Advances in Carbohydr. Chem.* **1967**, 135-191.
109. Painter, G. F.; Falshaw, A. *J. Chem. Soc. Perkin Trans. 1*, **2000**, 1157-1159.
110. Examples of synthetic preparations of the unnatural inositols: a) *epi*-inositol: Takahashi, H.; Kittaka, h.; Ikegami, S. *J. Org. Chem.* **2001**, 66(8), 2705-2716 (also other isomers, incl. *allo*- and *cis*-); Carless, H. A. J.; Busia, K.; Oak, O. Z. *Synlett*. **1993**, 9, 672-674 (also other isomers, incl. *allo*-). b) *allo*-inositol: Desjardins, M.; Brammer, L. E. Jr.; Hudlicky, T. *Carbohydr. Res.* **1997**, 304(1), 39-42. c) *cis*-inositol: Angyal, S. J.; Hickman, R. J.; *Carbohydr. Res.* **1971**, 20, 97-104; Chung, S.-

- K.; Kwon, Y.-U. *Bioorganic and Medicinal Chemistry Letters*, **1999**, 9, 2135-2140 (also other isomers including. *epi*- and *allo*-).
111. Potter, B. V. L.; Lampe, D. *Angew. Chem. Int. Ed. Engl.* **1995**, 34, 1933-1972.
 112. Brockerhoff, H. B.; Ballou, C. E. *J. Biol. Chem.* **1961**, 236, 1907-1911.
 113. Michell, R. H. *Biochim. Biophys. Acta*, 1975, 415, 81-147.
 114. Streb, H.; Irvine, F.; Berridge, M. J.; Schulz, I. *Nature*, **1991**, 351, 33-39.
 115. Batty, I. H.; Nahorski, S. R.; Irvine, R. F. *Biochem. J.* **1985**, 232, 211-215.
 116. Ferguson, M. A. J.; Homans, S. W.; Dwek, R. A.; Rademacher, T. W. *Science*, **1988**, 239, 753-757.
 117. Homans, S. W.; Ferguson, M. A. J.; Dwek, R. A.; Rademacher, T. W.; Anand, R.; Williams, A. F. *Nature (London)*, **1988**, 333, 269-272.
 118. Roberts, W. L.; Santikarn, S.; Reinholt, V. N.; Rosenberry, T. L. *J. Biol. Chem.*, **1988**, 263, 18776-18784.
 119. Saltiel, A. R.; Fox, J. A.; Sherline, P.; Cuatrecasas, P. *Science*, **1986**, 233, 967-972.
 120. McConville, M. J.; Ferguson, M. A. J. *Biochem. J.* **1993**, 294, 305-324.
 121. Kinoshita, T.; Ohishi, K.; Takeda, J. *J. Biochem.* **1997**, 122, 251-257.
 122. a) Murakata, C.; Ogawa, T. *Carbohydr. Res.* **1992**, 235, 95-114; b) Murakata, C.; Ogawa, T. *Carbohydr. Res.* **1992**, 234, 75-91.
 123. Baeschlin, D. K.; Chaperon, A. R.; Green, L. G.; Hahn, M. G.; Ince, S. J.; Ley, S. V. *Chem. Eur. J.* **2000**, 6(1), 172-186.
 124. Basu, J. *Current Science*, **2004**, 86(1), 103-110.
 125. Ballou, C. E.; Vilkas, E.; Lee, Y. C. *J. Biol. Chem.* **1963**, 238, 69-76.
 126. Lee, Y. C.; Ballou, C. E. *Biochemistry*, **1965**, 4, 1395-1404.
 127. Severn, W. B.; Furneaux, R. H. Falshaw, R.; Atkinson, P. H. *Carbohydr. Res.* **1998**, 308, 397-408.
 128. Severn, W.B. **2001**, personal communication.
 129. a) Gilleron, M.; Nigou, J.; Cahuzac, B.; Puzo, G. *J. Mol. Biol.* **1999**, 285, 2147-2160; b) Nigou, J.; Gilleron, M.; Puzo, G. *Biochimie*, **2003**, 85, 153-166.
 130. Mercier, D.; Barnett, J. E. G.; Gero, S. D. *Tetrahedron*, **1969**, 25, 5681-5687.
 131. Angyal, S. J.; Irving, G. C.; Rutherford, D.; Tate, M. E. *J. Chem. Soc.* **1965**, 6662-6664.
 132. Ling, L.; Ozaki, S. *Carbohydr. Res.* **1994**, 256, 49-58.
 133. Akiyama, T.; Takechi, N.; Shima, H.; Ozaki, S. *Chem. Lett*, **1990**, 1433-1436.
 134. Akiyama, T.; Takechi, N. Shima, H; Ozaki, S. *Chem. Lett*, **1990**, 1881-1884.
 135. Akiyama, T.; Takechi, N.; Ozaki, S. *Bull. Chem. Soc. Japan*, **1992**, 65, 366-372.
 136. Tanret, C. *C. R. Hebed. Seances Acad. Sci.* **1889**, 109, 908.
 137. van Alphen, J. *J Ind. Eng. Chem.* **1951**, 43, 141.

138. Angyal, S. J.; Hoskinson, R. M. *Methods Carbohydr. Chem.* **1963**, 2, 87.
139. Akiyama, T.; Shima, H.; Ozaki, S. *Tetrahedron Lett.* **1991**, 32, 5593-5596.
140. Akiyama, T.; Shima, H.; Ohnari, M.; Okazaki T.; Ozaki, S. *Bull. Chem. Soc. Japan*, **1993**, 66, 3760-3767.
141. Barton, D. H. R.; Bath, S.; Billington, D. C.; Gero, S. D.; Quiclet-Sire, B.; Samadi, M. *J. Chem. Soc. Perkin Trans. 1*, **1995**, 1551-1558.
142. Kiddle, J. K. *Chem. Rev.* **1995**, 95, 2189-2202.
143. Angyal, S. J. *Carbohydr. Res.* **1980**, 80, 203-206.
144. Miethchen, R.; Pundt, T.; Michalik, M. *Tetrahedron Lett.* **2005**, 46, 831-833.
145. de Almeida, M. V.; Figueiredo, R. M.; dos Santos, H. F.; da Silva, A. D.; de Almeida, W. B. *Tetrahedron Lett.* **2001**, 42, 2767-2769.
146. Falshaw, A.; Hart, J. B.; Tyler, P. T. *Carbohydr. Res.* **2000**, 329, 301-308.
147. Akiyama, T.; Takechi, N.; Ozaki, S. *Tetrahedron Lett.* **1990**, 31, 1433-1434.
148. Liu, C.; Nahorski, S. R.; Potter, B. V. L. *Carbohydr. Res.* **1992**, 234, 107-115.
149. Fauq, A. H.; Zaidi, J. H.; Wilcox, R. A.; Varvel, G.; Nahorski, S. R.; Kozikowski, A. P.; Erneux, C. *Tetrahedron Lett.* **1996**, 37, 1917-1920.
150. Liu, C.; Al-Hafidh, J.; Westwick, J.; Potter, B. V. L. *Bioorganic and Medicinal Chem.* **1994**, 2, 253-257.
151. Kozikowski, A. P.; Powis, G.; Gallegos, A.; Tückmantel, W. *Bioorganic and Medicinal Chem. Lett.* **1993**, 3, 1323-1326.
152. Hu, Y.; Meuillet, E. J.; Qiao, L.; Berggren, M. M.; Powis, G.; Kozikowski, A. P. *Tetrahedron Lett.* **2000**, 41, 7415-7418.
153. a) Blum, C.; Karlsson, S.; Schlewer, G.; Spiess, B.; Rehnberg, N. *Tetrahedron Lett.* **1995**, 36, 7239-7242; b) Blum, C.; Rehnberg, N.; Spiess, B.; Schlewer, G. *Carbohydr. Res.* **1997**, 302, 163-168.
154. a) Takahashi, H.; Kittaka, H.; Ikegami, S. *J. Org. Chem.* **2001**, 66, 2705-2716. b) Takahashi, H.; Kittaka, H.; Ikegami, S. *Tetrahedron Lett.* **1998**, 39, 9707-9710. c) Cleophax, J.; Dubreuil, D.; Gero, S. D.; Loupy, A.; Vieira de Almeida, M.; Da Silva, A. D.; Vass, G.; Bischoff, E.; Perzborn, E.; Hecker, G.; Lockhoff, O. *Bioorganic & Medicinal Chem. Lett.* **1995**, 8, 831-834. d) Dubreuil, D.; Cleophax, J.; Vieira de Almeida, M.; Verre-Sebrié, C.; Liaigre, J.; Vass, G.; Gero, S. D. *Tetrahedron*, **1997**, 53, 16747-16766.
155. Nguyen, B. V.; York, C.; Hudlicky, T. *Tetrahedron*, **1997**, 53, 8807-8814. b) Hudlicky, T.; Restrepo-Sánchez, N.; Kary, P. D.; Jamarillo-Gómez, L. M. *Carbohydr. Res.* **2000**, 324, 200-203. c) Brammer Jr. L. E.; Hudlicky, T. *Tetrahedron: Asymmetry*, **1998**, 9, 2011-2014.

156. Watanabe, Y.; Ogasawara, T.; Nakahira, H.; Matsuki, T.; Ozaki, S. *Tetrahedron Lett.* **1988**, 29, 5259-5262.
157. Ozaki, S.; Watanabe, Y.; Ogasawara, T.; Hirata, M.; Kanematsu, T. *Carbohydr. Res.* **1992**, 234, 189-206.
158. Liu, Y-C.; Chen, C-S. *Tetrahedron Lett.* **1989**, 30, 1617-1620.
159. Mayer, T. G.; Schmidt, R. R. *Eur. J. Org. Chem.* **1999**, 1153-1165.
160. Desai, T.; Gigg, J.; Gigg, R.; Martín-Zamora, E.; Schetz, N. *Carbohydr. Res.* **1994**, 258, 135-144.
161. Garrett, S. W.; Liu, C., Riley, A. M.; Potter, B. V. L. *J. Chem. Soc. Perkin Trans. 1*, **1998**, 367-368.
162. Innes, J. E.; Edwards, P. J.; Ley, S. V. *J. Chem. Soc. Perkin Trans. 1*, **1997**, 795-796.
163. Horne, G.; Potter, B. V. L. *Eur. J. Chem.* **2001**, 7, 80-87.
164. Ozaki, S.; Watanabe, Y.; Ogasawara, T.; Kondo, Y.; Shiotani, N.; Nishii, H.; Matsuki, T. *Tetrahedron Lett.* **1986**, 27, 3157-3160.
165. Sureshan, K. M.; Yamasaki, T.; Hayashi, M.; Watanabe, Y. *Tetrahedron: Asymm.* **2003**, 14, 1771-1774.
166. Chung, S-K.; Ryu, Y. *Carbohydr. Res.* **1994**, 258, 145-167.
167. Bruzik, K. S.; Salamończyk, G. M. *Carbohydr. Res.* **1989**, 195, 67-73.
168. Pietrusiewicz, K. M.; Salamończyk, G. M.; Bruzik, K. S. *Tetrahedron*, **1992**, 48, 5523-5542.
169. Lindberg, J.; Öhberg, L.; Garegg, P. J.; Konradsson, P. *Tetrahedron*, **2002**, 58, 1387-1389.
170. Takahashi, Y.; Nakayama, H.; Katagiri, K.; Ichikawa, K.; Ito, N.; Takita, T.; Takouchi, T.; Mikaye, T. *Tetrahedron Lett.* **2001**, 42, 1053-1056.
171. Bruzik, K. S.; Tsai, M.-D. *J. Am. Chem. Soc.* **1992**, 114, 6361-6374.
172. Pietrusiewicz, K. M., Salamończyk, G. M. *Tetrahedron Lett.* **1991**, 32, 4031-4032.
173. Paulsen, H.; von Deyn, W.; Röben, W. *Liebigs. Ann. Chem.* **1984**, 433-449.
174. Cousins, G. S.; Falshaw, A.; Hoberg, J. O. *Carbohydr. Res.* **2003**, 338, 995-998.
175. Akiyama, T.; Takechi, N.; Ozaki, S. *Bull. Chem. Soc. Japan*, **1990**, 31, 1433-1434.
176. Cousins, G. S. *PhD Thesis*, Victoria University of Wellington, **2003**.
177. a) Clarke, P. A.; Holton, R. A.; Kayaleh, N. E. *Tetrahedron Lett.* **2000**, 41, 2687-2690. b) Clarke, P. A.; Kayaleh, N. E.; Smith, M. A.; Baker, J. R.; Bird, S. J.; Chan, C. *J. Org. Chem.* **2002**, 67, 5226-5231.
178. Montchamp, J.-L.; Tian, F.; Hart, M. E.; Frost, J. W. *J. Org. Chem.* **1996**, 61, 3897-3899.
179. Hense, A.; Ley, S. V.; Osborn, H. M. I.; Owen, D. R.; Poisson, J.-F.; Warriner, S. L.; Wesson, K. E. *J. Chem. Soc. Perkin Trans. 1*, **1997**, 2023-2031.

180. Marwood; Riley; Jenkins; Potter, B. *J. Chem. Soc. Perkin Trans. I*, **2000**, 1935-1947.
181. Angyal, S. J.; Gallagher, R. T.; Pojer, P. M. *Aust. J. Chem.* **1976**, *29*, 219-22.
182. Miethchen, R.; Nietzel, K.; Weise, K.; Michalik, M.; Reinke, H.; Faltin, F. *Eur. J. Org. Chem.* **2004**, 2010-2018.
183. Jaramillo, C.; Chiara, J.-L.; Martín-Lomas, M. *J. Org. Chem.* **1994**, *59*, 3135-3141.
184. Jin, J. H.; Seyfang, A. *Microbiology*, **2003**, *149*, 3371-3381.
185. Mongan, T. P.; Ganapasam, S. Hobbs, S. B.; Seyfang, A. *Molecular and Biochemical Parasitology*, **2004**, *135*, 133-141.
186. Seyfang, A. **2004**, personal communication – manuscript to be submitted for publication.
187. a) Martínez, A. G.; Vilar, E. T.; Fraile, A. G.; de la Moya Cerero, S.; Maroto, B. L. *Tetrahedron: Asymm.* **2003**, *14*, 1959-1963; b) Martínez, A. G.; Vilar, E. T.; Fraile, A. G.; de la Moya Cerero, S.; Maroto, B. L. *Tetrahedron Lett.* **2002**, *43*, 1183-1185; c) Martínez, A. G.; Vilar, E. T.; Fraile, A. G.; de la Moya Cerero, S.; Maroto, B. L. *Tetrahedron: Asymm.* **2000**, *11*, 4437-4440; d) Maroto, B. L.; de la Moya Cerero, S.; Martínez, A. G.; Fraile, A. G.; Vilar, E. T. *Tetrahedron: Asymm.* **2000**, *11*, 3059-3062.
188. a) Bentz, H.; Subramanian, L. R.; Hanack, M.; Martínez, A. G.; Marin, M. G.; Perez-Ossorio, R. *Tetrahedron Lett.* **1977**, 9-12; b) Martínez, A. G.; Vilar, E. T.; Fraile, A. G.; Franco, C. R.; Salvador, J. S.; Subramanian, L. R.; Hanack, M.; *Synthesis*, **1987**, 321-323.
189. Satterwhite, D. M.; Croteau, R. B. *Journal of Chromatography*, **1987**, *407*, 243-252.
190. a) Dauben, W. G.; Gerdes, J. M.; Look, G. C. *Synthesis*, **1986**, 532-535; b) Dauben, W. G.; Gerdes, J. M.; Look, G. C. *J. Org. Chem.* **1986**, *51*, 4964-4970.
191. Stevens, R. V.; Chapman, K. T.; Weller, H. N. *J. Org. Chem.* **1980**, *45*, 2030-2032.